Host response in relation to tuberculosis susceptibility, transmission and outcome

Arjan van Laarhoven

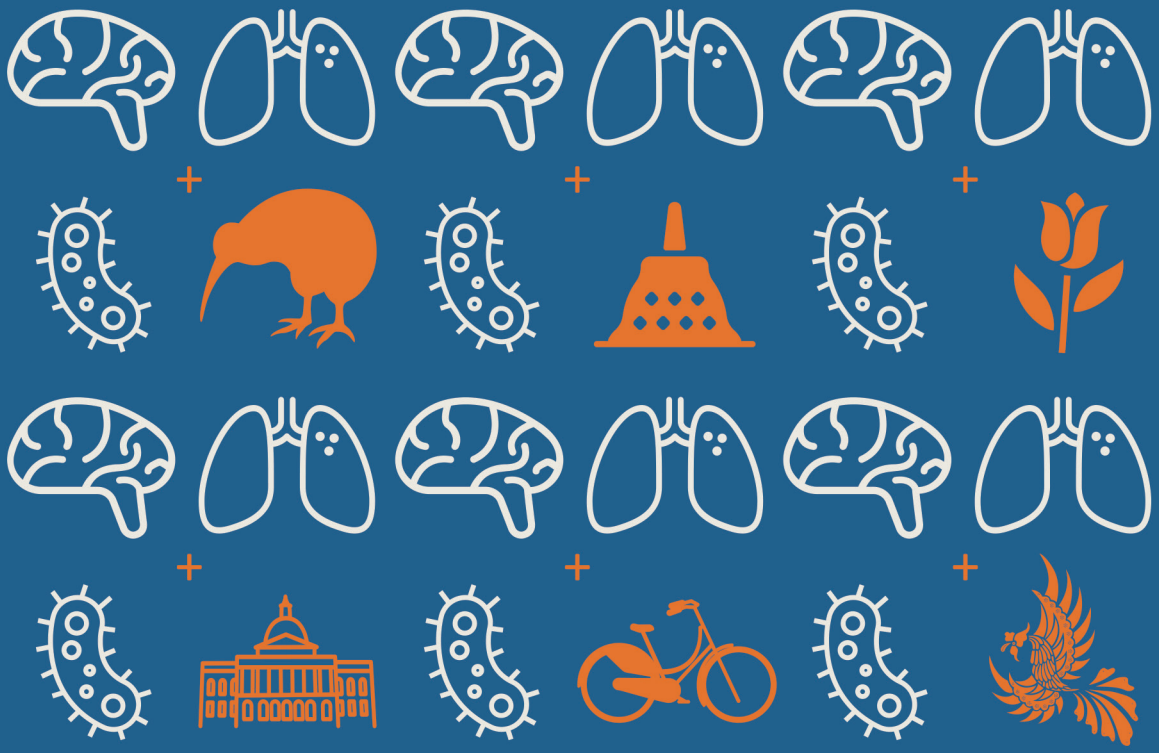

ISBN
978-94-028-1030-1

Cover concept
Suzanne van Dorp

Design/lay-out
Promotie In Zicht, Arnhem

Print
Ipskamp Printing, Enschede

Online availability
This thesis including its online supplement is available in the Radboud Repository at http://repository.ubn.ru.nl/handle/2066/190507

Host response in relation to tuberculosis susceptibility, transmission and outcome

Proefschrift

ter verkrijging van de graad van doctor
aan de Radboud Universiteit Nijmegen
op gezag van de rector magnificus prof. dr. J.H.J.M. van Krieken,
volgens besluit van het college van decanen
in het openbaar te verdedigen op vrijdag 25 mei 2018
om 10.30 uur precies

door

Arjan van Laarhoven
geboren op 23 november 1984
te Nijmegen

Promotoren
prof. dr. R. van Crevel
prof. dr. M.G. Netea

Manuscriptcommissie
prof. dr. R.W. Sauerwein *(voorzitter)*
prof. dr. I. Joosten
prof. dr. J.T. van Dissel *(Leids Universitair Medisch Centrum)*

Contents

1

General introduction

Tuberculosis: an overview

Tuberculosis is caused by *Mycobacterium tuberculosis*, which is spread through the air by coughing tuberculosis patients. Some individual's lung mucosa and alveolar macrophages can prevent a persistent infection after inhalation of bacteria. In others, macrophages digest the bacteria and present parts of it to helper T cells. These will stimulate the macrophages to kill the bacteria. T cells recruit more macrophages, which get infected by a proportion of bacteria that survive macrophage killing. Tuberculosis' unique feature is the subsequent formation of a granuloma, which creates a niche for bacterial persistence. In most individuals, a standstill ('latency') eventually arises in the granuloma with bacteria contained in macrophages, surrounded by T cells. One-fourth of the world's population is estimated to have a latent tuberculosis infection[1]. When immunity is weakened by advanced age, HIV co-infection, immunosuppressive therapies or other, yet unknown mechanisms, pulmonary disease can develop after which patients become contagious to others. Only one out of ten infected individuals develops pulmonary tuberculosis at some point during life, but given the estimated 1.7 billion latently infected individuals, this still leads to 10.4 million new cases and 1.7 million deaths globally each year[2].

Although knowledge on immunology in response to *M. tuberculosis* has vastly expanded over the past decades, this has hardly translated to effective strategies to prevent or treat tuberculosis. One reason may be that we need to study the immunology of tuberculosis in its specific context, as much as possible linking epidemiology, clinical manifestations and laboratory sciences. That is what I aimed for in this thesis, focussing on specific aspects of the pathophysiology of tuberculosis: susceptibility, transmission and outcome.

Persistence of *M. tuberculosis* in hunter-gatherer times

Some individuals are more susceptible to tuberculosis than others. To understand differences in susceptibility, the first topic of this thesis, it is important to realise that mankind and *M. tuberculosis* have had a long-lasting interaction. Tuberculosis is an endemic disease in most parts of the world, with very different epidemiology compared to present epidemics as Zika and Ebola, or pox and plague in the past. These other pathogens cause disease directly in a large proportion of the exposed population and across ages, in contrast to the long latency of *M. tuberculosis*. This unique pattern can be understood because of its co-existence with mankind since hunter-gatherer times. Humans then lived in small groups with infrequent encounters outside of the group. In these circumstances, bacteria are most likely to be selected when they combine a high rate of infection with late breakthrough-to-disease, preferably in individuals after the reproductive

age. *M. tuberculosis* uses the granuloma to persist[3] during this period of 'waiting', called 'latency', before active disease occurs. Indeed during its evolution, *M. tuberculosis* conserved genes that encode for proteins that can be recognized by T cells[4], suggesting this to be beneficial for the bacterium. Indeed, the T cells initiated granuloma formation does not only help containing *M. tuberculosis*, but also protects it from an effective host response[3].

It is now estimated that *M. tuberculosis* evolved around 70,000[5] years ago from the genus Mycobacteria, whose members otherwise persist in soil and water and rarely infect humans. Humans are the primary host of *M. tuberculosis*, from which *M. bovis* diverged, which causes tuberculosis in cows and sporadically infects humans[6]. The other members of the *M. tuberculosis* complex are also found in humans but more frequently in animals: goats (*M. caprae*), rodents (*M. microti*), oryx (*M. orygis*) and even seals (*M. pinnipidi*)[7]. All are slow-growing bacteria that have the special feature of retaining their staining in an acid environment, which is why they are called 'acid fast'. It is possible that the relationship between *M. tuberculosis* and early *Homo sapiens* was mutually beneficial, at least as long as the infection stayed latent. In this hypothesized symbiosis, the bacterium provided vitamins and essential amino acids that have allowed human brain development[8]. Although the exact driving mechanisms and consequences are not yet known, it is clear that *M. tuberculosis* and man have a relationship that dates back a long time and co-evolved to their present state.

Transmission of *M. tuberculosis* in modern times

Tuberculosis can only remain endemic if *M. tuberculosis* can spread from one individual to the next individual. When the first humans migrated from East to West Africa, *M. tuberculosis* migrated with them and established two genetically ancient *M. africanum* lineages that still exist and are part of the *M. tuberculosis* complex. *M. africanum* strains transmit equally well, but take a longer time to cause active disease compared to modern strains[9]. The two *M. africanum* and five *M. tuberculosis* lineages identified so far, are all still found in Africa. From East-Africa, *M. tuberculosis* also co-migrated with man to the Arabian Peninsula and further to Europe and Asia[5]. From an evolutionary perspective, all the lineages that evolved after migration out-of-Africa are considered 'modern' based on genetic markers. Most other continents are dominated by the lineage that was introduced by the founding human population, although later migration made the picture less homogenous[10]. In Asia, the founder lineage is the East-Asian lineage, of which the Beijing genotype family is especially successful. Within the Beijing family, some members are evolutionary more

'modern' than others and these outcompete the relatively more 'ancient' strains[11]. Possible explanations for this include better transmission of modern Beijing strains, and therefore more latent infections for each coughing patient, or faster progression to disease of an infected individual. Both are suitable strategies in these areas with a high population density. From a mycobacterial perspective, a different strategy may be needed in a country with high population density, but low prevalence of latent tuberculosis and low incidence of active tuberculosis, such as the Netherlands. In both high and low endemic countries it is likely that the interplay between *M. tuberculosis* and the human immune response is important in tuberculosis transmission. This interaction is the topic of one of the studies in this thesis.

Tuberculosis phenotypes

Infection with *M. tuberculosis* can follow many different scenarios. This thesis investigates some of most extreme outcomes after exposure to *M. tuberculosis* resulting from mycobacterial-human interplay (**figure 1.1**). In an unknown proportion of exposed individuals, 'early clearance' occurs, i.e. the first lines of defence, mucosa and macrophages, eliminate the bacteria before a T-cell response occurs[12]. In others, a persistent infection develops called 'latent tuberculosis infection' or 'latency', which has a 5-15% life-time risk for progression to 'active disease'[2], highest in the first years after infection[14]. Risk factors for active disease are infection at a younger age, patients with HIV, and those who received anti-TNF-α treatment[15]. Active disease manifests in the majority of patients as a pulmonary infection: 'pulmonary tuberculosis', or

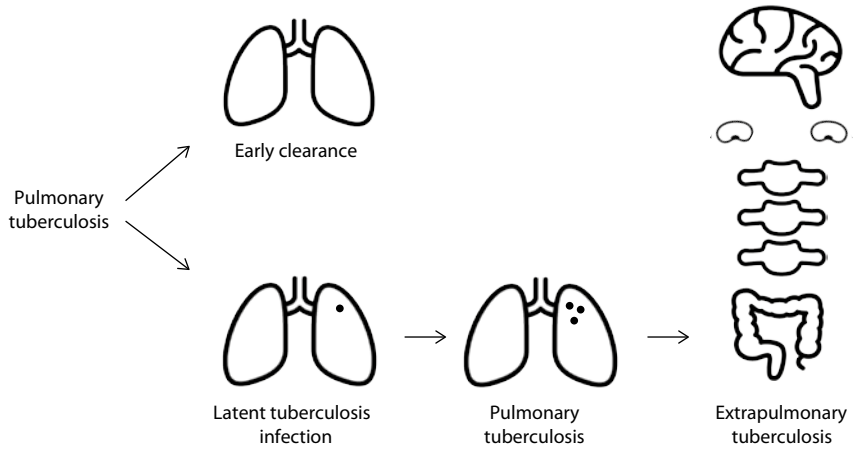

Figure 1.1 The different tuberculosis immune phenotypes.

'consumption' in layman terms. Extrapulmonary tuberculosis can manifest itself in most sides of the body, but most prevalent locations are brain (tuberculous meningitis), lymph nodes (tuberculous cervical lymphadenitis or 'scrofula'), bones and especially the spine (spinal tuberculosis or 'Pott's disease'), and bowel (intestinal tuberculosis). In some cases the infection widely disseminates and mycobacteria can be found in the blood, liver and spleen. This is called 'miliary tuberculosis'. Lastly, also without miliary tuberculosis, bacteria can spread to the brain through a disrupted blood-brain barrier, possibly in infected monocytes[16]. Then so-called Rich foci are established, which can give rise to meningitis later[17]. This tuberculous meningitis has a subacute course with symptoms developing over weeks, from headache and drowsiness to severe disease with cranial nerve palsies and paresis, eventually leading to coma[18].

Host-pathogen interaction

The delicate balance between mycobacterium and human host defence is governed by a complex interaction of cell types and receptors (**figure 1.2**). Many innate cell receptors recognize *M. tuberculosis,* including Toll-like receptors, C-type lectins and NOD-like receptors[19]. Antigen-presenting cells such as macrophages load mycobacterial peptides on their Major Histocompatibility Complex class II molecules, which allows recognition by $CD4^+$ T cells. Macrophages, possibly alveolar epithelial cells and certainly T cells then produce a wide range of messenger molecules called cytokines. Of these, IFN-γ stimulates macrophage killing and TNF-α is crucial to maintain granuloma integrity[20]. Granuloma disruption and subsequent development of active disease occurs when immunity is still immature as in small children, or when immunity wanes during life by age, malnutrition, or immune deficiencies caused by HIV co-infection or immune modulating agents such as corticosteroids and TNF-α inhibitory molecules. Naturally, at each disease stage, different host defence mechanisms and different *M. tuberculosis* virulence factors may be involved. For instance, susceptibility to initial infection might be caused by macrophage factors[12], whereas breakthrough to pulmonary disease might be prevented by the CD4 T-cell response. When disease is established, the neutrophil inflammatory response can cause tissue damage when not adequately governed by T cells, and this in turn may facilitate bacterial spread[20]. Clear definition of the host phenotype is therefore paramount for successful study of the host-pathogen interaction.

The extent to which there is human genetic variation in the risk of tuberculosis infection and progression to disease is unknown. An in-vitro study suggests that the *M. tuberculosis*-induced cytokine response is largely genetically determined[21], but only few genetic loci potentially contributing to susceptibility have been reported[22] and these have not yet been replicated. The genetic risk for active disease has been studied more extensively but still, only few loci have been reproduced, each locus only marginally contributing to increased risk[23]. Explanations for this limited success of genetic studies include differences in linkage disequilibrium across human populations for these loci, and different *M. tuberculosis* strains infecting these populations[24]. A confounding factor in the current studies are inadequate phenotyping of the healthy control populations, which often have unknown infection status. Moreover, lack of data on the degree of exposure of the controls leaves the possibility that some of them were simply not infected. When control populations are well chosen and clinical covariates are taken into account, a useful contribution of genetics is expected.

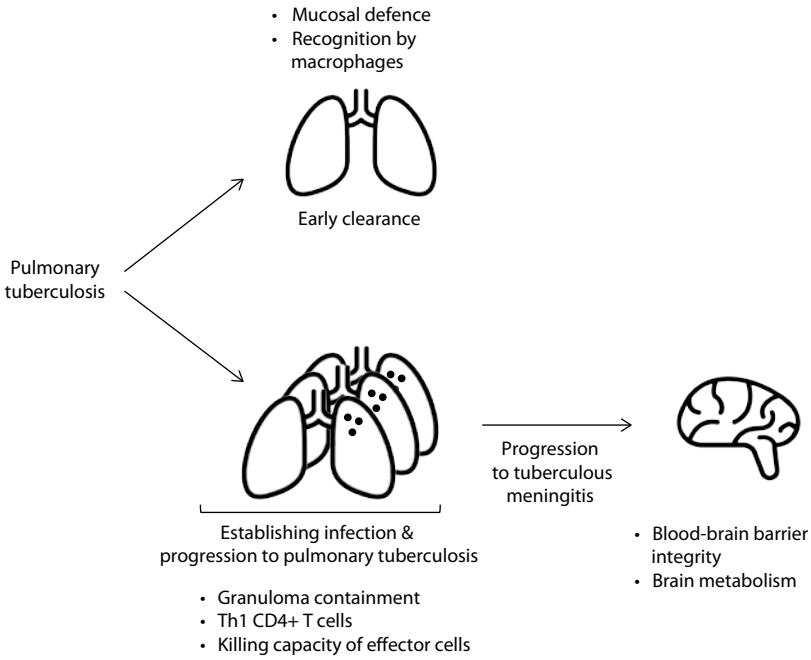

Figure 1.2 The different biological processes hypothesized to be important at different stages of disease.

Host response in relation to outcome of tuberculous meningitis

The immune system is critical in tuberculosis, but its specific role, that may be beneficial or detrimental, depends on the stage or specific disease 'phenotype'. Tuberculous meningitis is the most severe manifestation of tuberculosis, and its risk is increased with HIV-infection[25] and young age[14]. This implies a malfunctioning or immature immune system to be important in tuberculous meningitis susceptibility. Tuberculous meningitis leaves 30-50% of patients disabled or dead[25,26] and has a complex pathogenesis that is not well understood. Good outcome is dependent on a correct and swift diagnosis of the disease[27], which often remains unrecognized at first presentation (Ganiem et al., unpublished data). Other important factors are adequate supportive nutrition, oxygenation and blood pressure[28] and adequate antibiotic concentrations[29,30].

This thesis focuses on how the immune system is important for the outcome of tuberculous meningitis. Mortality of tuberculous meningitis, like susceptibility for tuberculous meningitis, is linked to HIV-infection[25], which implies that adequate immunity, i.e. $CD4^+$ T cells, is important to combat infection. On the other hand, uncontrolled inflammation is thought to cause damage[16] and it is not yet known which cells cause this inflammation. Hektoen described 'giant cells' (fused epithelioid macrophages) in the brain of a previous tuberculous meningitis sufferer already in 1898[31] but it was not until 1972 that cerebrospinal fluid (CSF) leukocytes were systematically analysed microscopically[32]. Later, flow cytometry and ex-vivo expansion techniques have been used to acquire further knowledge on CSF leukocytes in tuberculous meningitis (summarised in **text box 1.1**).

CSF is routinely obtained through lumbar puncture to test for the presence of mycobacteria and to determine the leukocyte count and glucose and protein concentration for diagnostic purposes. Inflammatory mediators such as cytokines and metabolites can be studied later in the remaining material from routine diagnostic tests. CSF contains waste products from the brain, leukocytes and bacteria. Studies of circulating cytokines show an increase in concentration compared to controls, with persistence up until a year after diagnosis. A positive correlation to severity is found in HIV-positive tuberculous meningitis patients, while in HIV-negative tuberculous meningitis patients this relationship is often absent (see **text box 1.2**). Only one study compared cytokine according to HIV-status and found higher levels of TNF-α, IL-1β, IL-2, IL-5, IL-6, IL-10 and IL-12p70 for HIV-positive patients[43]. The strong inflammatory response in tuberculous meningitis has led to the idea of adding treatment to modulate the host inflammatory response to antibiotic therapy. Examples of this so-called adjunctive host-directed therapy are the use of corticosteroids, which reduces

Text box 1.1 Cerebrospinal fluid (CSF) leukocytes

- **T cells** present in CSF consist of at least CD4+, CD8+ and γδT cells[33] and are more vulnerable to mitogen-induced cell death compared to blood T cells[33]. They are antigen-specific as shown by clonal expansion in response to *M. tuberculosis* purified protein derivate[34]. Numbers of antigen-specific T cells have not been compared in CSF and blood, but incorporation of thymidine by antigen-specific lymphocytes is higher in CSF than blood[35]. Although specificity of IFN-γ produced *ex vivo* by antigen-specific T cells is higher for CSF than blood, sensitivity is lower[36-38]. Concluding, T cells compartmentalise to CSF, and an unknown proportion of those T cells are *M. tuberculosis* antigen specific.
- **B cells** are present in CSF and show antigen-specificity, as shown by an ex-vivo anti-purified protein derivate IgG antibody response[39], but these have not been well studied.
- **NK cells** are present[33] but have not been studied in detail.
- **Monocytes** and **macrophages** have been described in CSF of tuberculous meningitis patients, but not been studied in detail[32].
- **Neutrophils** commonly form 10-30% [26,40] and sometimes up to 50% [41] of CSF cells. In HIV-positive patients they are associated with tuberculous meningitis immune reconstitution inflammatory syndrome[42].

mortality especially in HIV-negative patients with milder disease[44] and aspirin, which might show a survival benefit[45] although this requires further study. One may hypothesize that host-directed therapy needs to be targeted. For instance, corticosteroids may be beneficial in one patient, but harmful in another. However, previous trials have not taken the immune response in individual patients into account. This thesis aims to provide a more detailed description of the immune response in tuberculous meningitis and to examine its relation to patient survival. I think that such insights are necessary to improve the design of future host-directed trials.

Text box 1.2 Circulating immune mediators in CSF of patients with tuberculous meningitis

- **TNF-α** levels approximate 43 pg/mL (geometric mean of four studies, including 204 patients[42,46-49]) and are comparable levels to patients with bacterial meningitis[50], and persist up to 16 months[51]. Higher TNF-α correlates with severity in HIV-positive patients[43,52] while in HIV-negative patients a positive[49] or no association[43,48] is seen.
- **IFN-γ** levels approximate 99 pg/mL (geometric mean of five studies including 287 patients[42,46,49,53,54]) are higher than in bacterial meningitis[53] and persist up to 8 months[51]. High IFN-γ after one month relate to intracranial granuloma at that moment[54]. Higher IFN-γ correlates with disease severity in HIV-positive[43,52] and HIV-negative[43,49] tuberculous meningitis patients.
- **IL-1β** levels are low and often below the limit of detection (geometric mean of three studies including 158 patients is 2 pg/mL[42,48,49]). Levels are comparable to viral and bacterial meningitis[50]. Higher IL-1β correlates with disease severity in HIV-positive[43,52] patients, while in HIV-negative patients a positive[49] or no association[43,48] is seen.
- **IL-2** levels approximate 2 pg/mL (geometric mean of two studies, including 200 patients[49,53]) and are higher than in bacterial meningitis[53]. IL-2 relates correlates positively to disease severity in HIV-positive patients[43], while in HIV-negative patients both a positive[49] and no association[43] is seen.
- **IL-4**, **IL-5**, **IL-12p70** and **IL-13** were measured in only one study. The first three correlate with disease severity in HIV-positive tuberculous meningitis patients[43].
- **IL-6** levels approximate 249 pg/mL (geometric mean of three studies, including 174 patients[42,48,49]). IL-6 relates correlates with disease severity in HIV-positive patients[43], while in HIV-negative patients both a positive[49] or no association[43] is seen.
- **IL-8** shows levels comparable to bacterial meningitis[55] and higher than aseptic meningitis or control patients in whom meningitis was excluded[56] in children. Only one study in adults quantified levels of IL-8, averaging 501 pg/mL (n = 16)[48].
- **IL-10** levels approximate 23.2 pg/mL (geometric mean of four studies, including 133 patients[42,48,53,54]) and persist up to months[51]. Studies comparing IL-10 levels used mixed control groups and IL-10 in tuberculous meningitis is lower than in bacterial meningitis and patients in whom meningitis was excluded[53] and higher than in syphilitic meningitis and bacterial meningitis[57].

Aim and scope of the thesis

This thesis aims at *better understanding of factors determining tuberculosis susceptibility, transmission and outcome*. An integrative approach was used, combining patient studies with genetics and in-vitro experimental models (see **text box 1.3** for a concise summary of materials). The thesis consists of two parts (graphically summarised in **figure 1.3**). The first part focuses on susceptibility to tuberculosis and on transmission of *M. tuberculosis*, combining mycobacterial genotyping with experimental models or host genetics. The second part of the thesis addresses factors that influence outcome of tuberculous meningitis, using a systematic analysis of clinical parameters, CSF metabolites and inflammatory markers**.** This may ultimately lead to rational design of immunomodulatory therapy for the individual patient.

Tuberculosis susceptibility and transmission

This part combines in-vitro studies with molecular epidemiological studies of human host and *M. tuberculosis.* As mentioned before, C-type lectin receptors are among the many human receptors that recognize *M. tuberculosis*. The recently described CLEC4D, present on human monocytes and neutrophils, recognizes the mycobacterial component trehalose 6,6-dimycolate (TDM). In **chapter 2**, we first used an experimental *M. tuberculosis* mouse infection model because it allowed investigating the role of *clec4d* in curtailing early infection,

Text box 1.3 Materials and data sources used in this thesis

- Peripheral blood mononuclear cells and neutrophils of healthy, Dutch volunteers, collected by blood bank in Nijmegen, the Netherlands
- *M. tuberculosis* strains collected together with their clinical information by the National Institute for Public Health and the Environment, the Netherlands
- Patient clinical characteristics and materials collected in the Hasan Sadikin Hospital in Bandung, Indonesia. Established in 1923, this is the tertiary referral hospital for the province of West Java (43 million inhabitants), linked to the Medical Faculty of the Universitas Padjadjaran. Its joint tuberculosis-HIV Working Group, together with Radboud university medical center, studied tuberculosis diagnostics[25,58], pharmacology[29,59] and human[60] and mycobacterial[61] genetics, establishing a research infra-structure that enabled much of the research in this thesis.

but also later pathology. Then, in human studies, we examined whether tuberculosis infection and disease influence *CLEC4D* expression, and if genetic variation in *CLEC4D* is associated in human pulmonary tuberculosis.

Besides genetic variation of the human host, genetic variation of *M. tuberculosis* may also be relevant to the outcome of infection. In the next two chapters, we examined if evolutionary more successful strains of *M. tuberculosis* evoke a different immune response that might explain their success. We stimulated leukocytes from healthy volunteers with *M. tuberculosis* lysate, which of course is different from natural infection with live mycobacteria that encounter lung epithelium and macrophages, but which has the advantage of a high level of standardisation. We used peripheral blood mononuclear cells that contain monocytes and lymphocytes, both of which are important in mycobacterial clearance. In **chapter 3**, we compared the response to modern versus ancient strain groups of the 'Beijing' family of the East Asian *M. tuberculosis* lineage. We investigated if the immune response helped explaining the success of the modern Beijing strains, which have a high and increasing prevalence. We compared different groups of strains within this rather specific branch of the

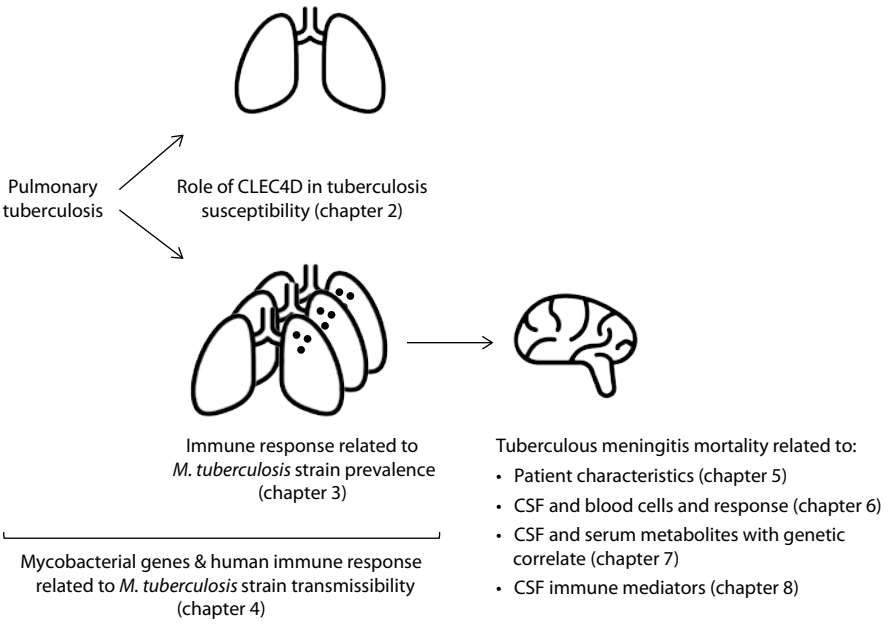

Figure 1.3 A schematic overview of the topics addressed in this thesis.

phylogenetic tree of *M. tuberculosis*, as they are in evolutionary 'competition' in high endemic settings in East Asia. In **chapter 4** we first identified individual *M. tuberculosis* strains that had shown high or very low transmissibility in the Netherlands. We could then search for mycobacterial genetic factors explaining these differences in transmissibility, and examined whether strains with and without these genetic factors yielded different immune responses in leukocytes of healthy volunteers.

Outcome in tuberculous meningitis

Most immunological studies in tuberculosis have addressed the question why some individuals are more susceptible than others, few have studied why some patients survive and others die from the disease. The second part of the thesis focuses on tuberculous meningitis, the most deadly manifestation of tuberculosis, linking patient studies and laboratory sciences. Mortality in tuberculous meningitis is known to be associated with HIV-infection and more advanced disease presentation. Systematically collected data on other patient characteristics predicting a worse outcome were lacking. In **chapter 5** we therefore examined prospectively collected clinical parameters, blood and cerebrospinal fluid (CSF) measurements in a large number of tuberculous meningitis patients, and used sensitivity analyses restricted to culture positive patients as clinical diagnosis is not 100% specific.

The immune system clearly plays an important role in outcome of tuberculous meningitis. Therefore In the next chapter we examined the immune profile of tuberculous meningitis patients in more depth. It is thought that better host-directed therapy, adjunctive to antibiotics, can contribute to reducing mortality. A one-size-fits-all approach is not likely to be successful as patients may have very different immune responses. We therefore asked whether it is possible to distinguish 'immune phenotypes' in **chapter 6**. To add to routinely collected data as analysed in the previous chapter, we optimised flow cytometry to study innate leukocyte cell types and activation in blood and CSF, and used ex-vivo whole blood cytokine assays. The results were compared with pulmonary tuberculosis patients and healthy controls.

It is generally thought that damaging inflammation contributes to mortality of tuberculous meningitis. Cellular metabolism is known to underlie inflammation, but it has not been studied systematically in tuberculous meningitis. In **chapter 7**, we examined which aminoacids and lipids differentiate tuberculous meningitis patients from control subjects, and surviving from non-surviving patients. We therefore measured more than 400 metabolites in blood and CSF of tuberculous

meningitis patients. We chose a platform that required only a small volume of sample to measure a large number of amino acids, sugars, vitamins and lipids, including relevant inflammatory lipid mediators. With this large number of metabolites relative to the number of patients, there is a high chance of false positive findings. We therefore confirmed the most promising result in an independent group of patients. We then searched for genetic determinants of the concentration of relevant metabolites, and examined if they could predict survival in an independent group of patients, as this would support a causal role for altered cerebral metabolism in outcome of tuberculous meningitis. In **chapter 8**, we used a similar approach, this time focusing on inflammatory proteins in the CSF. We used a very sensitive technique on a pre-defined panel of almost 100 proteins and also tested which inflammatory proteins correlated with markers of CSF inflammation, brain damage or blood-CSF barrier disruption. We then searched for a genetic signature of prognostic proteins and tested whether this genetic signature predicted mortality in a different group of patients.
In **chapter 9** the findings of this thesis are summarised and discussed.

Part 1

Tuberculosis susceptibility and transmission

amor tussisque non celatur

(often attributed to Ovid, but most probably added to Desiderius Erasmus' *Adagia* by his secretary Gilbert Cousin. Source: Heinrich Bebel's *Proverbia Germanica*, ed. 1879*)*

2

The C-Type lectin receptor CLECSF8/CLEC4D is a key component of anti-mycobacterial immunity

Gillian J Wilson*, Mohlopheni J. Marakalala*, Jennifer C. Hoving*, Arjan van Laarhoven*, Rebecca A. Drummond, Bernhard Kerscher, Roanne Keeton, Esther van de Vosse, Tom H.M. Ottenhoff, Theo S. Plantinga, Bachti Alisjahbana, Dhirendra Govender, Gurdyal S. Besra, Mihai G. Netea, Delyth M. Reid, Janet A. Willment, Muazzam Jacobs, Sho Yamasaki, Reinout van Crevel and Gordon D. Brown

* Equal contribution

Cell Host and Microbe. 2015;17(2):252–9.

Abstract

Rationale
The interaction of microbes with pattern recognition receptors (PRRs) is essential for protective immunity. While many PRRs that recognize mycobacteria have been identified, none is essentially required for host defence in vivo. The recently discovered C-type lectin CLEC4D (CLECSF8, MCL) recognizes the important mycobacterial compound trehalose 6,6-dimycolate (TDM). This study explores its role in mouse and man.

Methods
Wild-type and Clec4d$^{-/-}$ C57BL/6 mice were challenged intratracheally with *M. bovis* BCG, *M. tuberculosis* strain H37Rv and unrelated microorganisms after which mice were evaluated for weight loss, bacterial burden and survival. Flow cytometry was performed on blood and bronchio-alveolar lavage fluid from lungs. Cytokine levels were measured using the Bio-Plex Pro Mouse 23-Plex kit. In-vitro binding experiments were performed using green fluorescent protein (GPF)-expression BCG. Genotype assignation by Sequenom was performed on a cohort of pulmonary tuberculosis patients from Indonesia (n=1032) with age and gender-matched controls (n=952).

Findings
Clec4d$^{-/-}$ mice exhibited higher bacterial burdens and increased mortality upon *M. tuberculosis* infection. Additionally, Clec4d deficiency was associated with exacerbated pulmonary inflammation, characterized by enhanced neutrophil recruitment. Clec4d$^{-/-}$ mice showed reduced mycobacterial uptake by pulmonary leukocytes, but infection with opsonized bacteria could restore this phagocytic defect as well as decrease bacterial burdens. Notably, a *CLEC4D* polymorphism identified in humans was associated with an increased susceptibility to pulmonary tuberculosis.

Interpretation
CLEC4D plays a non-redundant role in anti-mycobacterial immunity in mouse and in man.

Introduction

Tuberculosis caused by *M. tuberculosis* is one of the leading causes of infectious disease-related death worldwide. Mycobacterial recognition by innate immune cells is mediated by several pattern recognition receptors (PRRs), including members of the Toll like receptor, NOD-like receptor, and the C-type lectin receptor family. These receptors activate inflammatory reactions that are essential for controlling the infection. Indeed, these early innate responses determine the outcome of disease and deficiencies in the major signalling adaptors downstream of these receptors, including MyD88 and Card9, render mice extremely susceptible to mycobacterial infection. Yet, despite convincing evidence from in-vitro studies, no single PRR has yet been found to play a non-redundant role in anti-mycobacterial immunity *in vivo*[62]. This has given rise to the assumption that recognition of *M. tuberculosis* involves multiple redundant interactions with numerous PRRs.

While the susceptibility of the MyD88-deficient mice to tuberculosis has been ascribed to defects in IL-1 receptor signalling[63], the receptor(s) involved in the Card9-deficient phenotype have not been fully defined. Card9 is an essential component of the intracellular signalling pathway utilized by CLRs, and loss of this molecule leads to neutrophil-mediated pulmonary inflammation and rapid death in infected mice[64]. Three CLRs that utilize this pathway, Dectin-1, Mincle and Dectin-2, have been described to recognise *M. tuberculosis* or its components. Dectin-1 was found to play a role in dendritic cell IL-12 production in response to mycobacteria *in vitro*, however loss of this receptor did not alter susceptibility to infection *in vivo*[62]. Mincle recognises trehalose 6,6′-dimycolate (TDM or cord factor) and was found to mediate robust responses to this mycobacterial cell wall glycolipid both *in vitro* and *in vivo*[65,66]. However, the role of Mincle *in vivo* is controversial, with some studies describing no clear role for this receptor during mycobacterial infection[67,68]. Dectin-2 induces pro- and antiinflammatory cytokines in response to mannose-capped lipoarabinomannan and knockout mice infected with *M. avium* presented with altered lung pathology at early time points during infection[69]. However, the importance of Dectin-2 during infection with *M. tuberculosis* is still unknown.

We recently identified another CLR (CLEC4D or CLECSF8) and have shown that it also recognises TDM[70,71]. CLEC4D is a member of the "Dectin-2 cluster" of CLRs and consists of a single extracellular C-type lectin-like domain, a stalk and transmembrane region and a short cytoplasmic tail. The receptor is expressed by peripheral blood neutrophils, monocytes and various subsets of dendritic

cells[70]. CLEC4D can associate with FcRγ chain to trigger intracellular signalling, inducing phagocytosis, the respiratory burst and the release of proinflammatory cytokines[70,71]. Moreover, like Mincle, Clec4d can drive both innate and adaptive immunity in response to TDM[71]. In this study, we have explored the role of Clec4d *in vivo* and have discovered that this CLR plays a non-redundant role in anti-mycobacterial immunity.

Methods

Animals

10 to 12 week old C57BL/6, Clec4d$^{-/-}$ [70], and OT.II mice were obtained from specific pathogen free facilities at the University of Aberdeen (UoA) and University of Cape Town (UCT). Animal experiments were performed using age and sex matched mice and conformed to the animal care and welfare protocols approved by the UoA (project licence 60/4007) and UCT (011/027 and 012/031).

Strains, growth conditions and infections

M. tuberculosis strain H37Rv or Beijing and *M. bovis* Bacille Calmette-Guérin (BCG) strain Pasteur were grown on Middlebrook 7H10 agar plates containing 10% ADC (BD), or Middlebrook 7H9 broth containing 10% ADC and 0.05% Tween 80 (Sigma). Green fluorescent protein (GFP)-expressing *M. bovis* BCG was cultured in the presence of 10 μg/mL Kanamycin (Sigma). 100 colony-forming units (CFU) of *M. tuberculosis* H37Rv were administered using an inhalation exposure system (Terre Haute, IN). For intratracheal inoculations, 5 x 10^5 CFU *M. tuberculosis* or *M. bovis* BCG were administered to the caudal oropharynx of anesthetized mice. In some experiments, *M. bovis* BCG was opsonized with anti-BCG antiserum (Alpha diagnostics) before intratracheal challenge. Organs were homogenised in PBS containing 0.05% Triton X-100 and complete mini-EDTA-free protease inhibitors (Roche). Bacterial burdens determined by plating onto Middlebrook 7H10 agar.

Flow cytometric analysis of lung cells

Cells were obtained from the lung by bronchio-alveolar lavage with PBS containing 5 mM EDTA (Gibco), or by enzymatic digest with DNase (Sigma-Aldrich) and liberase (Roche). Digested tissue was passed through 70 μm and 40 μm nylon filters and erythrocytes lysed in Pharm lyse solution (BD). The following antibodies were used: CD45.2, Ly6G, CD11c, CD11b, Siglec F, CD3, CD4, CD8, CD19, Vα2, CD45.1, CD62L, CD44, CD69, CD25, IFN-γ, and F4/80 (BD or Abd Serotec). FACS was performed using an LSRII, Fortessa or FACSAria (BD)

and analysed using FlowJo 7.6.4. Alveolar macrophages were defined as CD11c^{+} SiglecF^{+}, neutrophils as CD11b^{+} Ly6G^{high}, and macrophages as CD11b^{high} F4/80^{+}.

Cytokine assays

Tissue homogenates (above) were centrifuged to remove debris and supernatant stored at -80 °C. Cytokine levels were measured using the Bio-Plex Pro Mouse 23-Plex kit (Bio-Rad) or by ELISA (BD OptEIA and R&D Systems). Cytokine levels of tissue homogenates were normalized to sample protein concentrations.

Reporter cell analysis

Reporter cell analysis with NFAT-GFP expressing T hybridoma cells, co-transfected with mCLEC4D and Fcγ, was performed as described previously[71].

BCG binding experiments

For in-vivo binding experiments, 1.5 x 10^6 CFU GFP-expressing *M. bovis* BCG were administered intratracheally and bronchio-alveolar lavage cells isolated after 4 h and analysed by FACS. For in-vitro binding experiments, BCG-GFP was added to thioglycollate elicited macrophages (10:1) or neutrophils (1:1). In some experiments, TDM was added at 1 μg/mL. Cells were harvested, stained for CD45 and GFP-positivity (indicating bacterial association) ascertained by FACS.

Human CLEC4D Expression Analyses

Publicly available micro-array data sets from the Gene Expression Omnibus (GEO) were analysed for the transcript of *CLEC4D* in six cohorts. Expression in whole blood of HIV-negative pulmonary tuberculosis cases was compared to expression in healthy controls or latently infected individuals from the same setting with a Mann-Whitney U test. In order to display the expression of the different cohorts in one graph, data were log-transformed and then normalised by subtracting each value with the mean value of the controls of the respective cohort, divided by the standard deviation of the controls. The United Kingdom cohort in the study of Berry et al., included data on follow-up, and on cell subsets (CD4^{+} cells, CD8^{+} cells, monocytes and neutrophils). The cohorts used were (country; patients; GEO accession number; assay; probe):

- United Kingdom and South-Africa[72]; adult pulmonary tuberculosis cases; GSE19491; Illumina Human HT-12 V3 BeadChip; ILMN_1808979.
- Germany[73]; adult pulmonary tuberculosis cases; GSE34608; Agilent 4 × 44-k human expression arrays; A_23_P25235.
- Indonesia[74]; adult pulmonary tuberculosis cases; GSE56153; Illumina HumanRef-8 V3 BeadChip; ILMN_1808979.

- Malawi and Kenya[75]: paediatric tuberculosis cases; GSE39941; HumanHT-12 v.4 Expression BeadChip; ILMN_1808979.

For quantitative trait locus (eQTL) analysis of *CLEC4D* expression in whole blood, we used data available from a meta-analysis of >5000 individuals (online available at http://genenetwork.nl/bloodeqtlbrowser[76]) and the Genotype-Tissue Expression (GTEx) consortium[77], which currently includes 168 individuals (online available at http://www.gtexportal.org/).

Selection of SNPs investigated

Using Haploview version 4.2[78] we accessed the publicly available HapMap Version 3 Release 2 to select single nucleotide polymorphisms (SNPs) for testing. As no data are available for the Indonesian population specifically, we based our selection on the data for the Han-Chinese (CHB) and Japanese (JPT) population. For *CLEC4D*, three SNPs tagged all the predicted haplotypes with frequencies of > 0.05 (See **supplementary figure 2.3** and **table 2.1**). In the current cohort, based on a disease prevalence of 262/100,000 (WHO Global tuberculosis report 2012), the power of detecting an allele that has a relative risk of 1.5 to disease, is 87% with a nominal significance of 0.05 (http://www.sph.umich.edu/csg/abecasis/cats/tour1.html).

Subject recruitment and Ethics statement

We made use of cohort of pulmonary tuberculosis patients in Indonesia. We previously recruited 1135 consecutive pulmonary tuberculosis patients diagnosed in two outpatient clinics and two hospitals in Jakarta and Bandung (Indonesia) from January 2001 to December 2006, for a series of genetic studies examining host susceptibility to tuberculosis ([79] and references therein). Diagnosis of pulmonary tuberculosis was done according to WHO criteria by clinical presentation and chest radiograph examination, followed by confirmation with microscopic detection of acid-fast bacilli in ZN-stained sputum smears and positive culture of *M. tuberculosis* on 3% Ogawa medium. Patients with confirmed diagnosis of extrapulmonary tuberculosis (n=93) and HIV-positive subjects (n=10) were excluded. During the same period, 1000 age and gender matched genetically unrelated community control subjects were selected; those with symptoms or chest X-rays suggesting possible active tuberculosis (n=48) were excluded from further analysis. Sample collection and genotype analysis is described in the **supplementary methods**. All individuals recruited had signed a written informed consent. The study protocol was approved by the review boards of the University of Indonesia, the Eijkman Institute for Molecular Biology, and the Medical Ethical Committee Arnhem-Nijmegen.

Statistical analysis

Data were analysed using GraphPad Prism 5.04. Unpaired *t* test or non-parametric Mann-Whitney was applied for comparison of groups, as appropriate, and the Wilcoxon sign rank test for paired follow-up data. For genotyping analysis the Hardy-Weinberg equilibrium was checked for each SNP using the *p*rogram *HWE Version 1.10* (Rockefeller University, New York). Significance was indicated by $p<0.05$.

Results

Clec4d is required for resistance to mycobacterial infection *in vivo*

We previously characterized the effect of Clec4d deficiency but did not identify a role for this receptor *in vivo* despite extensive analysis[70]. However, during these experiments we noticed that subcutaneous immunisation with Complete Freund's Adjuvant reproducibly led to ulceration at the injection site in more than 50% of the Clec4d-deficient mice, an effect which was not apparent in the wild-type mice (**figure 2.1A** and data not shown). Given that the major immune-stimulating component of Complete Freund's Adjuvant is *M. tuberculosis*, and that Clec4d can recognise TDM[71], we investigated whether this receptor was required for anti-mycobacterial immunity *in vivo*.

We first determined whether the loss of Clec4d would influence the survival of mice during infection with live mycobacteria. In order to explore this possibility, wild-type and Clec4d$^{-/-}$ mice were challenged intratracheally with the attenuated vaccine strain *M. bovis* BCG and survival of the animals was monitored over time. Notably, in contrast to the wild-type mice, the Clec4d$^{-/-}$ mice gained less weight (**figure 2.1B**) and more than 10% of these animals succumbed to infection between 6 and 14 weeks (**figure 2.1C**). Importantly, knockout mice aerosol infected with *M. tuberculosis* H37Rv also gained less weight and 20% of these animals succumbed to the infection within 6 weeks (**figure 2.1D** and data not shown). Longer-term experiments did not reveal any further reduction in survival of the Clec4d-deficient mice, compared to wild-type animals (data not shown).

Zhu and colleagues have recently suggested that Clec4d is also required for control of systemic infection with *Candida albicans*[80], but only after low dose infection. These results are in contrast to previous observations from several laboratories including our own[70], and repeated experiments using high and low doses of *C. albicans* failed to demonstrate any role for Clec4d in controlling this

fungal pathogen (**supplementary figure 2.1A**). Clec4d has also been implicated in immunity to *Klebsiella pneumoniae*[81], but as with *Candida*, we observed no differences in mortality or weight loss in the knockout mice following intratracheal infection with this organism (**supplementary figure 2.1B** and data not shown). Importantly, *K. pneumoniae* and *C. albicans* both failed to stimulate GFP expression in Clec4d-expressing reporter cells[71], whereas these cells robustly induced GFP in response to BCG (**figure 1E**).

Thus, these data identify Clec4d as a pattern recognition receptor with a non-redundant role in anti-mycobacterial immunity *in vivo*.

Clec4d is not required for adaptive responses to mycobacteria

Purified ligands of many C-type lectins receptors, including Clec4d[71], can act as adjuvants and direct the development of adaptive immunity, but the role of these receptors in driving responses to intact microorganisms is less clear. Notably, acquired immunity to mycobacteria was unaffected by the loss of the major CLR intracellular signalling adaptor Card9 [64]. Nevertheless, we investigated the possibility that this receptor may be capable of modulating adaptive immunity using Complete Freund's Adjuvant. However, no differences were observed in the Clec4d$^{-/-}$ mice in terms of the number, division or activation of antigen-specific CD4^{+} T-cells in the draining lymph nodes at the two time points that were examined post immunization (**supplementary figures 2.1C-F** and data not shown). The knockout mice also developed normal antigen-specific immunoglobulin responses (**supplementary figure 2.1G**). There were no defects in CD4/CD8 T-cell ratios in the lungs during mycobacterial infection (**supplementary figure 2.1H**). Clec4d$^{-/-}$ mice also displayed normal delayed-type hypersensitivity (**supplementary figure 2.1I**) and mycobacterial-specific T-cell recall responses (**supplementary figure 2.1J**), following BCG vaccination. Thus, deficiency of Clec4d does not influence the development of acquired immunity to mycobacteria.

Clec4d is involved in controlling bacterial burdens, cytokine production and granuloma formation *in vivo*

To examine how deficiency of Clec4d was affecting anti-mycobacterial immunity, we characterised the lungs of wild-type and Clec4d$^{-/-}$ mice following aerosol infection with *M. tuberculosis* H37Rv. At early time points after infection, we did not detect any difference in bacterial burdens, but by 4 months we observed moderately increased burdens in the infected knockout mice (~0.50 log; **figure 2.2A**). These increased bacterial burdens could be observed directly in Ziehl-Neelsen stained tissue sections (**supplementary figure 2.2A**), and analysis

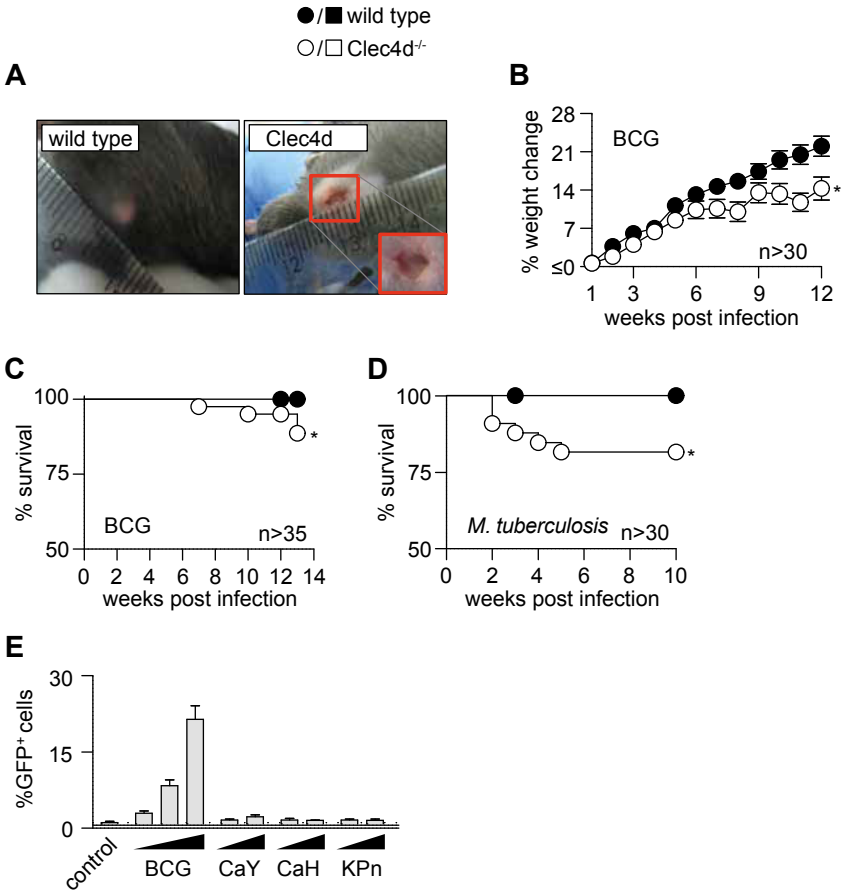

Figure 2.1 Clec4d$^{-/-}$ is required for resistance to mycobacterial infection *in vivo*.

(A) Ulceration in Clec4d$^{-/-}$ but not wild-type mice at the site of injection with Complete Freund's Adjuvant. Change in weight (B; mean ± SEM) and survival curve (C) of Clec4d$^{-/-}$ and wild-type mice following intratracheal infection with $5x10^5$ *M. bovis* BCG. (D) Survival of wild-type and Clec4d$^{-/-}$ mice following aerosol infection with 100 CFU *M. tuberculosis* H37Rv. (E; mean ± SD) Analysis of green fluorescent protein (GFP) expression in Clec4d-expressing reporter cells following stimulation with BCG (MOI: 1, 5, 15), *C. albicans* yeast (CaY; MOI: 5, 50) or hyphae (CaH; MOI: 5, 50), and *K. pneumoniae* (KPn, MOI: 5, 50), as indicated. Values in (B - D) are pooled data from at least two experiments, while the data in (E) is from one representative experiment. *, $p<0.05$. See also supplementary figure 2.1.

of the lungs of mice infected with *M. tuberculosis* revealed larger inflammatory lesions in the Clec4d$^{-/-}$ mice at later time points (**figure 2.2B** and **supplementary 2.2B**). Similarly, increased bacterial burdens were also observed in BCG-infected knockout mice at later time points (**figure 2.2C**), and cellular analysis of digested lung tissue at 3 months post infection revealed significantly more CD11b^{+}Ly6G^{high} neutrophils and CD11b^{+}F4/80^{+} macrophages in the Clec4d$^{-/-}$ mice (**figure 2.2D**). Strikingly, Clec4d$^{-/-}$ mice most affected by infection, as determined by less than 10% weight gain, had the highest numbers of neutrophils in their lung, even when compared to wild-type mice with a similar phenotype (**figure 2.2E**). Consistent with the increased cellular infiltrates, there were significantly higher levels of inflammatory cytokines including TNF-α, IFN-γ and G-CSF, in the lungs of the knockout mice (**figure 2.2F**). There were no differences in IL-10 levels in the Clec4d$^{-/-}$ mice.

To gain further insights, we next characterised pulmonary inflammation 48 hour following the administration of a high dose of mycobacteria. Similar to the later time points, flow cytometry analysis and histology revealed a significant increase in neutrophils in the lungs of Clec4d$^{-/-}$ mice infected with either BCG, *M. tuberculosis* H37Rv or the more pathogenic *M. tuberculosis* Beijing (**figure 2.2G** and **supplementary 2.2C**). The cellular inflammatory response to *M. tuberculosis* H37Rv was accompanied by increased levels of many pro-inflammatory cytokines and chemokines, but also increased levels of IL-10 (**figure 2.2H**). There were no differences in CFU recovered from wild-type and knockout mice at this early time point (**supplementary figure 2.2D**). Therefore we conclude that deficiency of Clec4d results in higher mycobacterial burdens and increased pulmonary inflammation, which is predominantly neutrophilic.

Clec4d is required for mycobacterial uptake

We have previously shown that intracellular signalling from Clec4d can trigger particle phagocytosis[70,71], and therefore examined the possibility that the phenotype of the Clec4d$^{-/-}$ mice was stemming from a defect in mycobacterial uptake and clearance by leukocytes. For these experiments, we infected mice with a GFP-expressing strain of *M. bovis* BCG and then characterised bacterial association with pulmonary CD45^{+} myeloid cells four hours after challenge. Notably, while the total number of pulmonary leukocytes was similar in both groups of mice at this early time-point (**supplementary figure 2.2E**), we observed significantly less mycobacterial-association with leukocytes isolated from the Clec4d$^{-/-}$ mice, as determined by GFP-positivity (**figure 2.3A**). Characterisation of these cells demonstrated defective mycobacterial association with all major pulmonary leukocyte subsets, including CD11c^{+}SiglecF^{+} alveolar macrophages,

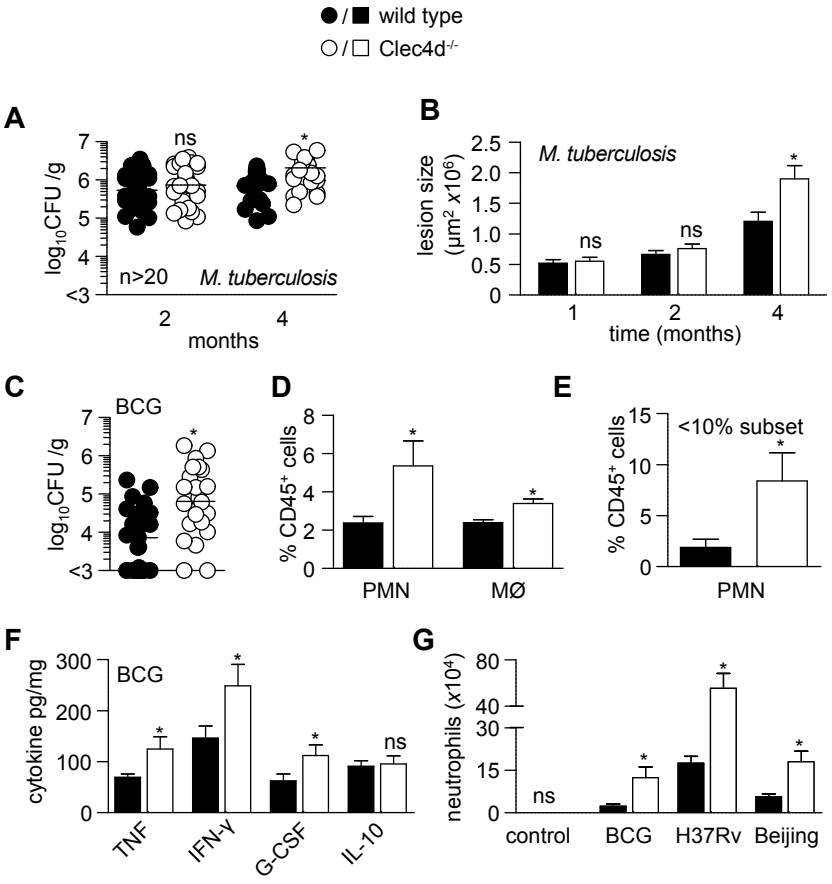

Figure 2.2 Clec4d$^{-/-}$-deficiency results in exacerbated pulmonary inflammation with increased accumulation of neutrophils and higher bacterial burdens.

(A) Pulmonary bacterial burdens in wild-type or Clec4d$^{-/-}$ mice following aerosol infection with 100 colony forming units (CFU) *M. tuberculosis* H37Rv. (B) Pulmonary inflammatory lesion size over time. Pulmonary bacterial burdens (C) and leukocyte composition (D) in wild-type or Clec4d$^{-/-}$ mice 3 months following intratracheal infection with $5x10^5$ *M. bovis* BCG. (E) Neutrophil levels in wild-type (n=3) and Clec4d$^{-/-}$ animals (n=8) that show the greatest change in body weight (<10%). (F) Pulmonary cytokine levels in 3 month *M. bovis* BCG infected animals. (G) Pulmonary leukocyte composition in wild-type or Clec4d$^{-/-}$ mice 48 h after intratracheal infection with *M. bovis* BCG, *M. tuberculosis* H37Rv or Beijing, as indicated. (H) Bronchio-alveolar lavage cytokine levels in mice at 48 h after infection with *M. tuberculosis* H37Rv. Shown are pooled data (mean ± SEM). *, $p<0.05$. ns =, not significant. See also supplementary figure 2.2.

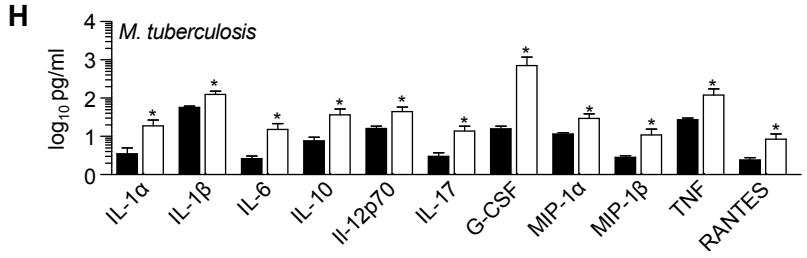

Figure 2.2 Continued.

CD11b^{+}Ly6G^{high} neutrophils and CD11b^{+}F4/80^{+} macrophages (**figure 2.3B**). Consistent with this observation, there were increased levels of non-cell associated mycobacteria in the lungs of the Clec4d$^{-/-}$ mice (**supplementary figure 2.2F**).

To demonstrate that the defect was solely due to loss of recognition by Clec4d, we opsonized the bacteria with anti-BCG antibodies, prior to infection, and observed that association of the bacteria with leukocytes was fully restored in Clec4d$^{-/-}$ mice *in vivo* (**figure 2.3C**). Unlike with unopsonized bacteria (**figure 2.2G**), there was no difference in cellular inflammation at 48 hour in the knockout mice when challenged with opsonized bacteria (**figure 2.3D**). Importantly, opsonisation rescued the phenotype of the knockout mice even out to 3 months, in terms of weight gain (**supplementary figure 2.2G**), survival (**supplementary figure 2.2H**), pulmonary neutrophil influx (**figure 2.3E**) and bacterial burdens (**figure 2.3F**).

We could also demonstrate defective mycobacterial association with Clec4d$^{-/-}$ thioglycollate-elicited macrophages (**figure 2.3G**) and neutrophils (**figure 2.3H**) *in vitro*. Clec4d-deficiency specifically affected mycobacterial binding to leukocytes, but not phagocytosis, as the levels of ingestion of bacteria that were cell-bound was equivalent to wild-type cells (**supplementary figure 2.2I**). Importantly, bacterial binding to knockout macrophages could be restored following opsonisation, and was specific for mycobacteria as loss of Clec4d had no effect on association of the unrelated particle zymosan (**figure 2.3G**). Moreover, we could show that TDM inhibited the binding of unopsonized mycobacteria with wild-type thioglycollate-elicited macrophages *in vitro*, but had no effect on bacterial binding to cells isolated from the knockout mice (**figure 2.3I**). TDM had no effect on the association of zymosan with macrophages isolated from either strain of mice (**supplementary figure 2.2J**). Thus, we conclude that the phenotype of the Clec4d$^{-/-}$ mice stems from defective mycobacterial recognition by leukocytes.

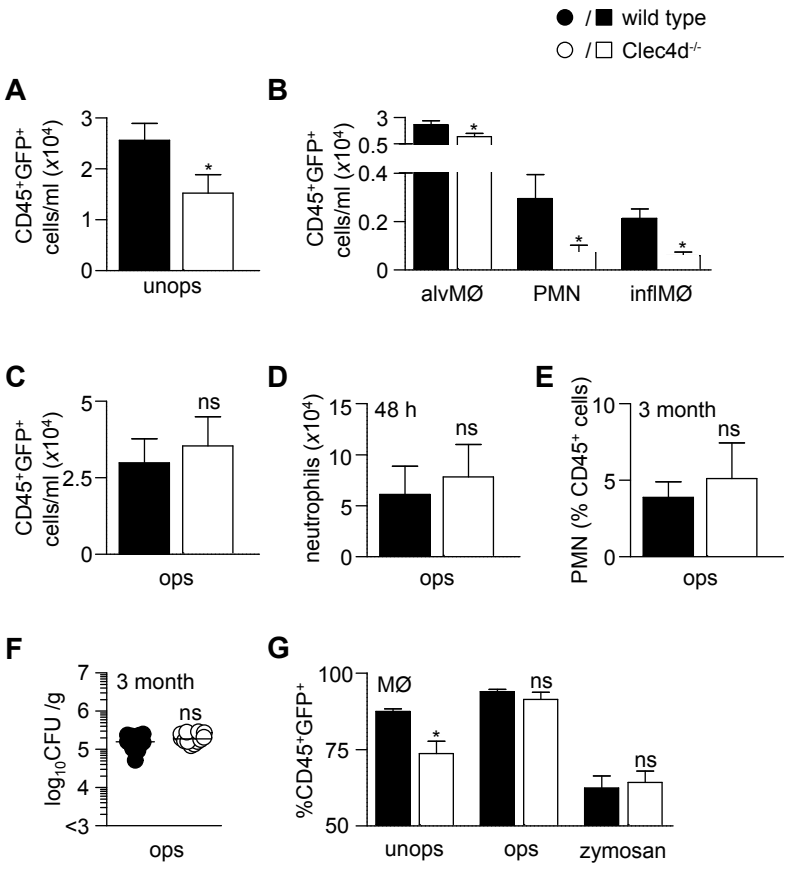

Figure 2.3 Clec4d$^{-/-}$ is required for mycobacterial binding.

Total green fluorescent protein (GFP)$^{+}$ CD45^{+} cells (A) or particular cell types (B), as indicated, in the lungs of wild-type or Clec4d$^{-/-}$ mice 4 h after infection with GFP- expressing *M. bovis* BCG (n>14). Total GFP^{+} CD45^{+} cells (C) and numbers of neutrophils (D) in bronchio-alveolar lavage isolated from wild-type or Clec4d$^{-/-}$ mice after infection with opsonized *M. bovis* BCG at 4 and 48 h, respectively (n>10). Numbers of neutrophils (E) and bacterial burdens (F) in the lungs of wild-type or Clec4d$^{-/-}$ mice 3 months after infection with opsonized *M. bovis* BCG (n=12). In-vitro binding of unopsonized (unops) and opsonized (ops) GFP-expressing *M. bovis* BCG, or zymosan, to (G) thioglycollate-elicited macrophages or (H) neutrophils. (I) Effect of trehalose 6,6-dimycolate (TDM) on *in vitro* binding of GFP^{+}BCG to thioglycollate-elicited macrophages isolated from wild-type or Clec4d$^{-/-}$ mice. Shown are pooled data (mean ± SEM) from at least two independent experiments. *, $p<0.05$. See also supplementary figure 2.2.

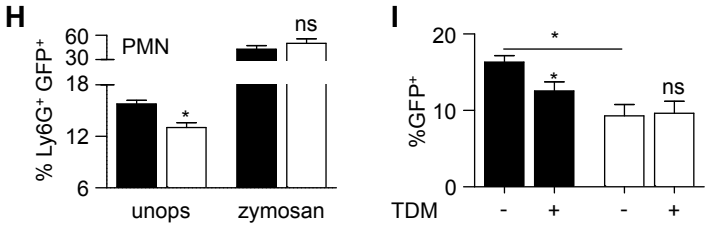

Figure 2.3 Continued.

Polymorphisms of human *CLEC4D* cause susceptibility to tuberculosis

To determine whether CLEC4D may also be important for human anti-mycobacterial immunity, we examined publicly available micro-array data sets for effects of tuberculosis on the expression of this CLR. Expression of *CLEC4D* in whole blood was strongly upregulated in HIV-negative patients with pulmonary tuberculosis compared to controls in five out of six cohorts from various geographic areas (**supplementary figure 2.3A**). In mice, we observed similar increases in Clec4d expression on leukocytes during pulmonary infection (**supplementary figure 2.3B**). In the United Kingdom tuberculosis cohort, expression data were also available for uninfected (tuberculin skin test negative) and latently infected (tuberculin skin test positive) controls; there was no difference in *CLEC4D* expression between these two groups (**supplementary figure 2.3C**). Initiation of treatment in pulmonary tuberculosis patients led to normalization of *CLEC4D* expression over time (**supplementary figure 2.3D**). The highest levels of expression of the receptor were observed in monocytes and neutrophils in peripheral blood, consistent with our earlier observations[70], and pulmonary tuberculosis was associated with significantly increased levels of expression on circulating neutrophils compared to healthy controls (**supplementary figure 2.3E**). These differences cannot be explained by differences in leukocyte numbers, as absolute and relative neutrophil counts did not differ between active tuberculosis patients and controls[72].

As the expression of *CLEC4D* correlated with pulmonary tuberculosis, and as we had identified a role for this receptor in anti-mycobacterial immunity in mice, we then determined whether polymorphisms of this CLR had an influence on susceptibility to tuberculosis in humans. We genotyped three *CLEC4D* SNPs in a total of 1032 confirmed pulmonary tuberculosis patients and 955 age- and gender-matched community controls from an Indonesian cohort collected in Jakarta and Bandung, West-Java. These SNPs were chosen as together they covered all haplotypes with a frequency of >5%, as described in the HapMap

database for Japanese and Han-Chinese populations (**table 2.1** and **supplementary figure 2.3F**). However, we found that the minor allele frequencies of the three *CLEC4D* SNPs were lower in the control Indonesian subjects (**table 2.2)** than those described in the HapMap database.

Table 2.1 The *CLEC4D* SNPs selected for analysis

SNP	alleles	Minor allele frequency for the JPT & CHB population	Type
rs4883165	T / G	0.076	5'upstream of gene
rs4304840	A / G	0.129	nonsynonymous (Ser32Gly; transmembrane)
rs4486677	T / G	0.062	in intron 2

JPT = Japanese; CHB = Han-Chinese

Of the three polymorphisms, the combined GA and GG genotypes of the non-synonymous SNP rs4304840, were significantly associated with disease with an odds ratio of 1.33 with a 95% confidence interval of 1.02–1.73 (**supplementary figure 2.3F** and **table 2.2**). As the number of patients with the GG genotype was small, it seems likely that the G allele confers susceptibility in a dominant fashion. The functional relevance of the rs4304840 polymorphism is further demonstrated in available expression quantitative trait locus (eQTL) data, where we found the G allele to be significantly associated ($p<10^{-4}$) with altered *CLEC4D* expression (data not shown). The intronic SNP rs4486677, which showed a high degree of linkage disequilibrium with rs4304840 in HapMap, had a similar odds ratio, which bordered significance (**supplementary figure 2.3F** and **table 2.2**). Haplotype analyses showed that the haplotypes with GG/GA alleles for rs4304840 had similar odds ratio's (OR), irrespective of the rs4486677 allele (data not shown). The SNP rs4883165, which is located 12 kb upstream of the *CLEC4D* gene, was not associated with disease. In conclusion, the GG and GA genotypes for *CLEC4D* rs4304840 are associated with susceptibility to pulmonary tuberculosis, irrespective of the genotype for the SNP rs4486677.

The rs4304840 polymorphism causes a non-synonymous change (Ser32Gly) in the transmembrane region of the protein. This change could influence the association of this CLR with the Fcγ adaptor and affect the ability of this receptor to be transported to the cell surface[62]. To explore this, we generated constructs

Table 2.2 Distribution of polymorphism allele and genotype frequencies in tuberculosis cases and controls

SNP	Allele or genotype	Frequency in cases (%)	Frequency in controls (%)	p	OR (95% CI)	OR (95% CI)
rs4883165	T	1896 (94.8%)	1814 (95.0%)			
	G	104 (5.2%)	96 (5.0%)			
	TT	898 (89.8%)	861 (90.2%)	0.805	TT vs. TG & GG:	TT & TG vs. GG:
	TG	100 (10.0%)	92 (9.6%)		0.96 (0.72–1.29)	1.05 (0.15–7.45)
	GG	2 (0.2%)	2 (0.2%)			
rs4304840	A	1844 (92.3%)	1795 (94.0%)			
	G	154 (7.7%)	115 (6.0%)			
	AA	849 (84.9%)	843 (88.3%)	**0.037**	AA vs. GA & GG:	AA & GA vs. GG:
	GA	146 (14.6%)	109 (11.4%)		1.33 (1.02–1.73)	1.28 (0.28–5.72)
	GG	4 (0.4%)	3 (0.3%)			
rs4486677	T	1927 (96.7%)	1859 (97.5%)			
	G	65 (3.3%)	47 (2.5%)			
	TT	931 (93.5%)	906 (95.1%)	0.136	TT vs. TG:	TT & TG vs. GG:
	TG	65 (6.5%)	47 (4.9%)		1.35 (0.92–1.99)	n/a
	GG	0	0			

SNP = single nucleotide polymorphism; OR = odds ratio

for both wild-type and mutated CLEC4D and transfected them into fibroblasts. These experiments revealed that while both wild-type and mutated proteins were expressed at equivalent levels in transfected cells, there was a significant reduction in the surface expression of the mutated protein (**supplementary figure 2.3G**). Thus the rs4304840 polymorphism reduces surface expression of CLEC4D.

Discussion

C-type lectin receptors (CLRs) have key functions in host defence and although they are best known as PRRs for fungi, there is growing evidence that CLRs are also involved in host responses to mycobacteria[62]. The most compelling data comes from analysis of mice deficient in a central CLR-signalling adaptor, Card9, which were extremely susceptible to mycobacterial infection[64]. Yet despite the identification of several CLRs capable of mycobacterial recognition, all have been found to be dispensable during infection with *M. tuberculosis in vivo*[62]. In this report, we identify the CLR Clec4d as the first PRR to have a non-redundant role in anti-mycobacterial immunity.

Loss of Clec4d led to exacerbated pulmonary inflammation, characterised by enhanced neutrophil recruitment and increased mycobacterial burdens, but had no effect on the development of adaptive immunity. This phenotype resembles that of the Card9$^{-/-}$ mice, however, these animals presented with greater pathology and all of the animals died shortly after infection; a severity that was linked to defects in IL-10 production[64]. Similar profound phenotypes have also been observed in mice lacking other essential immune components, such as IFN-γ. In contrast, fewer Clec4d$^{-/-}$ mice succumbed to mycobacterial infection and there was no loss of IL-10. This suggests that the levels of IL-10 were protecting the majority of the infected Clec4d$^{-/-}$ mice from lethal pathology, despite the enhanced inflammation and bacterial burdens that was present in their lungs.

This difference in phenotype raises the question about the relationship between Clec4d and Card9. Card9 is downstream of several PRRs implicated in mycobacterial recognition, including C-type lectin receptors, NOD-like receptors and Toll like receptors and deficiency of this adaptor is likely to affect all of these pathways. Yet mouse models have not revealed a clear role for any of the PRRs so far identified[82]. Although Clec4d has not formally been shown to require Card9, it triggers intracellular signalling via the Fcγ chain and Syk

kinase, and therefore must utilize this pathway[70,71]. Clec4d also associates and functionally interacts with Dectin-2[80] and Mincle[83], both of which have also been implicated in anti-mycobacterial immunity[65,69]. In fact, Clec4d stimulation is required for Mincle expression, at least in response to TDM[71]. However we detected expression of both Dectin-2 and Mincle during mycobacterial infection in the Clec4d$^{-/-}$ mice (data not shown). Interestingly, expression of Clec4d with Fcγ alone was insufficient to mediate mycobacterial binding in transfected fibroblasts, suggesting that its ability to associate with these other receptors is an important component of its function (data not shown). Thus, despite the fact that these and other receptors are involved in mycobacterial recognition (mediating the IL-10 response discussed above, for example), Clec4d deficiency recapitulates the major components of the Card9$^{-/-}$ phenotype.

In both the Card9$^{-/-}$[64] and Clec4d$^{-/-}$ mice, pulmonary pathology was associated with an accumulation of neutrophils and higher levels of neutrophil-associated cytokines, such as G-CSF. Indeed, depletion of either neutrophils or G-CSF reduced inflammation and prolonged survival of the Card9$^{-/-}$ mice[64]. However, the involvement of neutrophils during tuberculosis is still controversial, with evidence for both protective and non-protective roles during infection. In humans, infected neutrophils were found to predominate in the lungs of patients with active pulmonary tuberculosis and a neutrophil-driven transcriptional signature in blood was shown to correlate with disease severity[72]. Interestingly, even though lessening the clinical disease, depletion of neutrophils in the Card9$^{-/-}$ mice did not affect bacterial burdens in the lung, demonstrating that these granulocytes were the major drivers of pathology and were not directly contributing to protective host responses[64]. Indeed, the ability of neutrophils to actually kill mycobacteria is also controversial[84].

In humans, we show that neutrophils have the highest levels of CLEC4D expression[70]. Importantly, we have identified the association of a polymorphism (rs4304840) in this receptor with increased susceptibility to pulmonary tuberculosis in an Indonesian cohort. This polymorphism causes a non-synonymous change (Ser32Gly) in the transmembrane region of the protein that substantially reduces its expression at the cell surface. Genetic variations in several PRRs have been shown to influence mycobacterial disease susceptibility, severity and/or outcome, but many of these observations have not been confirmed in other cohorts. Moreover, the effects of these PRR polymorphisms are also dependent on bacterial genotype[85]. However, the involvement of Clec4d does not appear to be strain specific, at least in our animal models (**figure 2G**). Moreover, based on *M. tuberculosis* spoligotyping, we did not find any difference

in allele frequency for rs4304840 (the non-synonymous SNP that showed an association with disease) between the cases infected by a Beijing strain (n=182) versus those infected by other strains (n=379) (p=.371, data not shown). It will be nevertheless important to validate our observations in additional patient cohorts and determine the effect, if any, of *CLEC4D* polymorphisms in other disease phenotypes, such as meningeal and paediatric tuberculosis.

Interestingly, the few families with mutations in Card9 have not been associated with an increased susceptibility to tuberculosis[62]. While the underlying reasons for this are unclear, the intact adaptive responses[64] may mediate protection due to successful vaccination of these patients in endemic areas. Another possible mitigating factor is the inability of human neutrophils to express IL-10[86], one of the major defects causing the pathology in the Card9$^{-/-}$ mice[64]. This suggests that the cellular functions of Card9 may differ in humans and mice during mycobacterial infection.

Neutrophils can internalize mycobacteria[84] and we found that Clec4d-deficiency resulted in defective mycobacterial association with these and several other leukocyte populations in the lung. Defective mycobacterial clearance in the Clec4d-deficient mice led to increased levels of extracellular bacteria, exacerbating neutrophilic pulmonary inflammatory responses. In a small subset of infected knockout mice, these deregulated responses ultimately led to death. Restoring mycobacterial leukocyte association through antibody opsonisation completely rescued the Clec4d-deficient phenotype both *in vitro* and *in vivo*.
In addition to mycobacteria, Clec4d has been implicated in immunity to *Candida albicans*[80] and *Klebsiella pneumoniae*[81]. Yet we found no defect in resistance to infection with either of these pathogens. The role of Clec4d in immunity to *C. albicans* is arguably the most controversial, as previous experiments[70,83] and the data shown here failed to show any role for this CLR in the control of this fungal pathogen. The underlying reasons for these disparate results remain to be determined.

Overall, our data show that mycobacterial recognition is the primary function of CLEC4D. Importantly, a polymorphism of CLEC4D causing reduced surface expression associates with increased susceptibility to pulmonary tuberculosis in humans. In conclusion, CLEC4D is a non-redundant component of anti-mycobacterial immunity.

Acknowledgements
We would like to thank S. Hardison, P. Redelinghuys, J. Taylor, C. Wallace, A. Richmond, S. Hadebe, A. Plato, F. Abbass, L. Fick, N. Allie, R. Wilkinson, K. Wilkinson, S. Cooper, D. Lang and V. Kumar for reagents and assistance, and the animal facility staff for the care of our animals.

Author contributions
GJW and JCH performed experiments with BCG. MJM and JCH performed experiments with *M. tuberculosis*. AvL analysed the human data.

Supplementary methods

Infections

Mice were challenged intratracheally with 600 CFU *K. pneumonia* strain 32. Intravenous infection with low ($2x10^4$ CFU) and high ($2x10^5$ CFU) doses of *Candida albicans* SC5314 was carried out as described previously (Vautier et al., 2012). *C. albicans* hyphae were induced in 20% FCS in PBS for 3-5 h at 37°C.

Histology

Lungs were prepared for histology by fixing the large left lobe in 10% phosphate-buffered formalin and then embedding in paraffin. 5 μm-thick sections were stained with haematoxylin and eosin (H&E) for evaluation of pathologic changes and Ziehl-Neelsen for *M. tuberculosis* detection. The sizes of all inflammatory lesions per section in infected mouse lungs were determined by automated morphometric analysis using a Nikon microscope eclipse 90i and the software NIS-Elements BR 3.1 (Nikon), as described previously[87].

Adoptive Transfer

OT.II donor mice were culled and the lymph nodes and spleens were removed, disaggregated through 70 μM filters and white cells counted by trypan blue exclusion. $CD4^+$ cells were purified from single-cell suspensions by depleting irrelevant populations using biotin-antibody cocktail and anti-biotin micro-beads (Miltenyi Biotech). The purified $CD4^+$ cells were stained with 5 μM CFSE for 5 to 8 min at room temperature with continual rotation, and CFSE labelling was subsequently quenched by washing 2-3 times in 10% FCS in PBS. $CFSE^+CD4^+$ OT.II cells were checked by FACS for labelling efficiency and purity, which was routinely >80%. $CFSE^+CD4^+$ OT.II cells were then injected intravenously into gender-matched recipient mice (3 to 5 x 10^6 cells per recipient) of the same background strain as the donors (C57BL/6). Mice were immunised 1 h following the adoptive transfer, with 50 μg purified ovalbumin (Hyglos GmBH) emulsified in Complete Freund's Adjuvant (Difco), delivered as 2 subcutaneous injections in the hind legs. Mice were sacrificed 4 and 8 days post-immunisation for analysis by flow cytometry. Inguinal (draining) lymph nodes were removed, made into single cell suspensions and processed for FACS, as described above standard methods. OT.II cells were defined as $CD4^+V\alpha2^+CD45.1^+$.

Immunoglobulin Assays

Mice were immunised with 100 μg NP-KLH (Biosearch Technologies) emulsified in Complete Freund's Adjuvant (Difco) delivered as three sub-cutaneous

injections. Animals were sacrificed 10 days later, and anti-NP antibodies in the serum were measured by ELISA using specific secondary antibodies conjugated to HRP (Cambridge Biosciences).

BCG vaccination, DTH and recall responses

Mice were subcutaneously inoculated with 10^6 CFU *M. bovis* BCG strain Pasteur as previously described[64]. At 4 weeks after vaccination, BCG-vaccinated and control mice were intradermally challenged with 2 μg purified protein derivate into the footpad. Footpad swelling was recorded 48 h after challenge using a dial gauge caliper. For recall responses, mice were infected intratracheally with 5 x 10^5 CFU BCG. Draining lymph nodes were isolated after 2 weeks, disaggregated and plated at 5 x 10^5 cells per well in 96 well plates. Cells were then stimulated for 3 days with media only or with a French-pressed BCG lysate. Cytokines were measured in the supernatant by ELISA (BD OptEIA).

Phagocytosis assays

Phagocytosis was measured using our previously published methodology[88]. In brief, thioglycollate elicited macrophages were incubated with BCG-GFP (10:1) or zymosan at 4 °C for 1 h to allow binding, washed and incubated at 37°C 5% for 3 h to allow uptake. Extracellular BCG-GFP was stained with primary anti-BCG rabbit antiserum (Alpha diagnostics) and secondary APC-conjugated goat anti-rabbit IgG (Life Technologies). Surface-bound FITC-labelled Zymosan was stained with biotinylated Fc-Dectin-1[89] and streptavidin-APC (Invitrogen). Phagocytosis was defined as the percentage of GFP^+ or $FITC^+$ cells with internalised (APC^-) particles. Samples kept at 4^0C to prevent internalization were used as controls.

Generation of Cell lines

Generation of the pFBneo retroviral vector containing the full length hCLEC4D open reading frame fused to an HA-tag was described previously[70]. The S32G SNP (rs4304840) was introduced by a two-step PCR protocol. Firstly, the sequences downstream and upstream of the S32G SNP were amplified separately from pFB_hCLEC4D using a vector specific and SNP-encoding primers (pFB-neo (5′-GCCAGGTTTCCGGGCCCTCAC-3′) and hCLEC4D_S32G_F (5′-TAGTTTTC-ATCTTACTTCTCGGTGTCTGTTTTATTGCAAG-3′); pFB-retro (5′-GGCTGC-CGA-CCCCGGGGGTGG-3′) and hCLEC4D_S32G_R (5′- CTTGCAATAAAACA-GACACCGAGAAGTAAGATGAAAACTA-3′). The original pFBneo_hCLEC4D template was digested with DpnI followed by fusion and amplification of the two PCR products using the vector specific primers. The PCR product was cloned into pFBneo_HA and the fidelity confirmed by sequencing.

NIH 3T3 cell lines stably co-expressing FcRγ with wild-type hCLEC4D-HA, hCLEC4D_S32G-HA or empty vector control were generated by retroviral transduction as described previously[90]. All cell lines were generated twice and used as non-clonal populations to reduce founder effects.

Receptor expression was assessed by flow cytometry as described in the main text. Briefly, cells were blocked in FACS wash (PBS, 5 mM EDTA, 0.5% BSA, 2 mM NaN_3) containing 5% heat-inactivated rabbit serum, followed by staining with an anti-HA antibody (HA.11, clone 16B12, Covance) for 1 h at 4°C. Cells were washed twice and stained with a goat-anti-mouse PE secondary antibody (Jackson) for 30 min at 4°C. After three additional washes, cells were fixed in 1% paraformaldehyde and analysed on a BD LSRII flow cytometer. To assess the total cellular CLEC4D content, cells were fixed in 1% paraformaldehyde followed by permeabilisation with 0.5% saponin prior to assessing receptor expression, as described above. To calculate relative expression, mean fluorescence intensities (MFI) of all samples were normalised by subtracting their respective control background MFI. Subsequently, the MFI of each cell population was divided by the average MFI of wild-type hCLEC4D expressing cells and expressed as a percentage. Data points plotted represent the means of independent experiments.

Sample collection and genotype analysis

Peripheral blood samples were obtained by venepuncture. Genotyping was performed as described previously[79]. In brief, genomic DNA was isolated from EDTA blood of patients and control subjects using standard methods. 5 ng of DNA was used for genotyping with multiplex assays designed using Mass ARRAY Designer Software (Sequenom) and genotypes were determined using Sequenom MALDI-TOF MS according to manufacturer's instructions (Sequenom Inc., San Diego, CA, USA). Briefly, the SNP region was amplified by a locus-specific PCR reaction. After amplification a single base extension from a primer adjacent to the SNP was performed to introduce mass differences between alleles. This was followed by salt removal and product spotting onto a target chip with 384 patches containing matrix. MALDI-TOF MS was then used to detect mass differences and genotypes were assigned real-time using Typer 4 software (Sequenom Inc. San Diego, CA, USA). As quality control, 5% of samples were genotyped in duplicate and each 384-well plate also contained at least 8 positive and 8 negative controls, no inconsistencies were observed. For quality control purposes the genotype of at least two samples for each homozygous genotype were confirmed by sequencing using Sanger method.

Supplementary figures

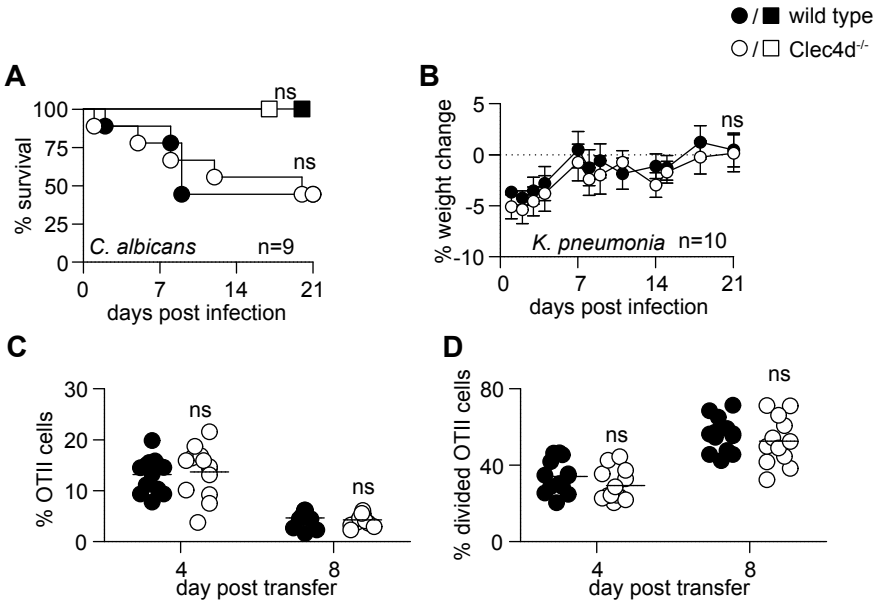

Supplementary figure 2.1 Clec4d$^{-/-}$ is required for resistance to mycobacterial infection but does not impair adaptive immunity.

Related to Figure 2.1. (A) Survival of wild-type and Clec4d$^{-/-}$ following systemic infection with a high ($2x10^5$, circles) and a low ($2x10^4$, squares) dose of *Candida albicans* SC5314. (B) Change in weight of wild-type versus Clec4d$^{-/-}$ mice following intratracheal infection with 600 CFU *Klebsiella pneumoniae* strain 32. Characterization of the frequency (C), division (D), activation (E) and differentiation (F) of adoptively transferred OT.II T-cells in the draining lymph nodes of wild-type and Clec4d$^{-/-}$ animals immunized with Ovalbumin and Complete Freund's Adjuvant. (G) Immunoglobulin responses in the serum of wild-type and Clec4d$^{-/-}$ animals immunized with NP-KLH and Complete Freund's Adjuvant. (H) CD4$^+$ and CD8$^+$ T-cell populations in the lungs of wild-type and Clec4d$^{-/-}$ mice 4 months after infection with $5x10^5$ *M. bovis* BCG. (I) DTH responses in the footpad of wild-type and Clec4d$^{-/-}$ mice 4 weeks after subcutaneous. BCG vaccination. (J) IFN-γ recall responses following a 3-day BCG stimulation of lymph-node cells isolated from mice two weeks after infection. No cytokine response was obtained following stimulation of cells isolated from naïve animals (not shown). Values shown are from a representative experiment, except for (C, D, H - J) which are data from two pooled experiments. Each symbol (C to G) represents one mouse, and the data shown are the mean ± SD. *, $p<0.05$; ns, not significant.

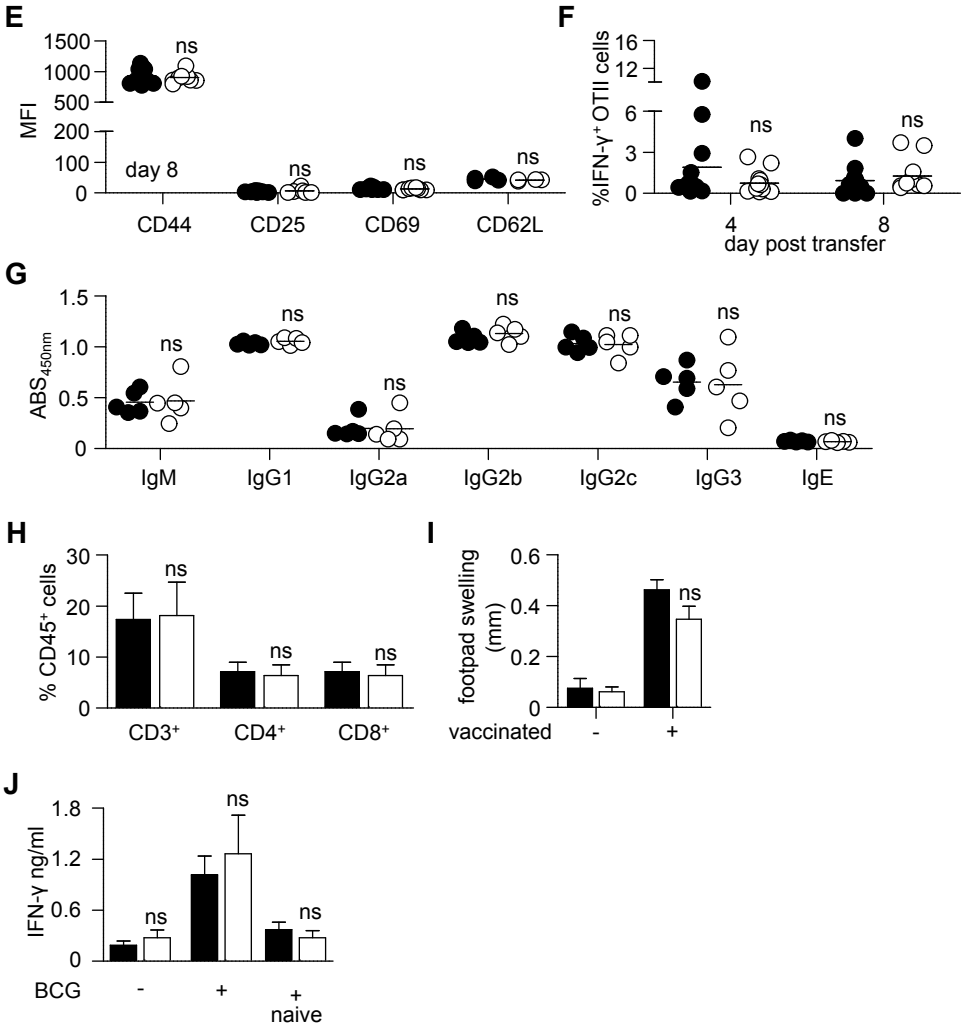

Supplementary figure 2.1 Continued.

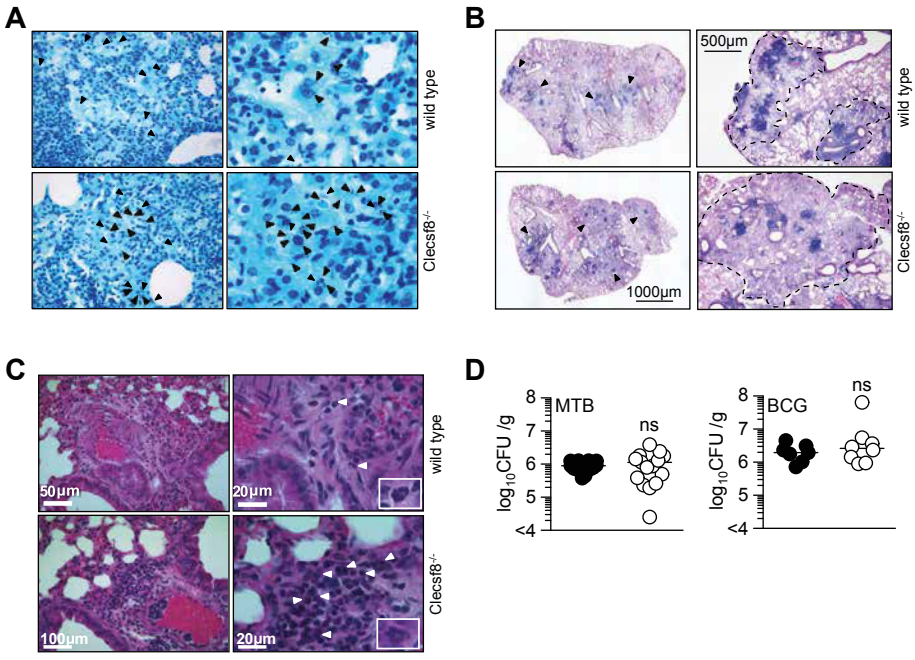

Supplementary figure 2.2 Clec4d$^{-/-}$-deficiency results in higher bacterial burdens and exacerbated pulmonary inflammation.

Related to figure 2.2 and figure 2.3. (A) Ziehl-Neelsen stained lung sections from wild-type and Clec4d$^{-/-}$ mice after 4 months of infection with *M. tuberculosis* H37Rv. Mycobacteria are indicated with arrows. (B) Inflammatory lesion size 4 months after infection with *M. tuberculosis* H37Rv in H&E stained lung sections. (C) H&E stained lung sections at 48 hour showing accumulation of neutrophils (indicated with white arrows) after intratracheal infection with a high dose (5x10^5) *M. tuberculosis* H37Rv. (D) Mycobacterial burdens in mice 48 h after intratracheal infection with 5 x 10^5 CFU *M. tuberculosis* H37Rv or *M. bovis* BCG, as indicated. (E) Numbers of CD45$^+$ cells 4 h after intratracheal inoculation of 1.5 x 10^6 CFU *M. bovis* BCG. (F) Gating strategy (control mouse shown for clarity) and percentage of non-cell associated mycobacteria (as detected in the green gate) in the lung 4 h after intratracheal inoculation of 1.5 x 10^6 CFU green fluorescent protein (GFP) $^+$ *M. bovis* BCG. (G) Percentage weight change in mice 12 weeks after infection with opsonised *M. bovis* BCG. (H) Survival curve mice following intratracheal infection with 5*x*10^5 CFU of opsonised *M. bovis* BCG. (I) Gating strategy for flow cytometric assessment of levels of internalization of unopsonized BCG or zymosan bound to thioglycollate-elicited macrophages. Percentage internalized was defined as the percentage of APC$^-$ (αBCG$^-$) GFP$^+$ or APC$^-$ (FcDectin-1$^-$) FITC$^+$ cells versus total GFP$^+$ or FITC$^+$ cells. (J) Effect of trehalose 6,6-dimycolate (TDM) on *in vitro* binding of FITC$^+$ zymosan to isolated from wild-type or Clec4d$^{-/-}$ mice. Shown in (D - I) are pooled data (mean ± SEM) from two independent experiments. *, $p<0.05$.

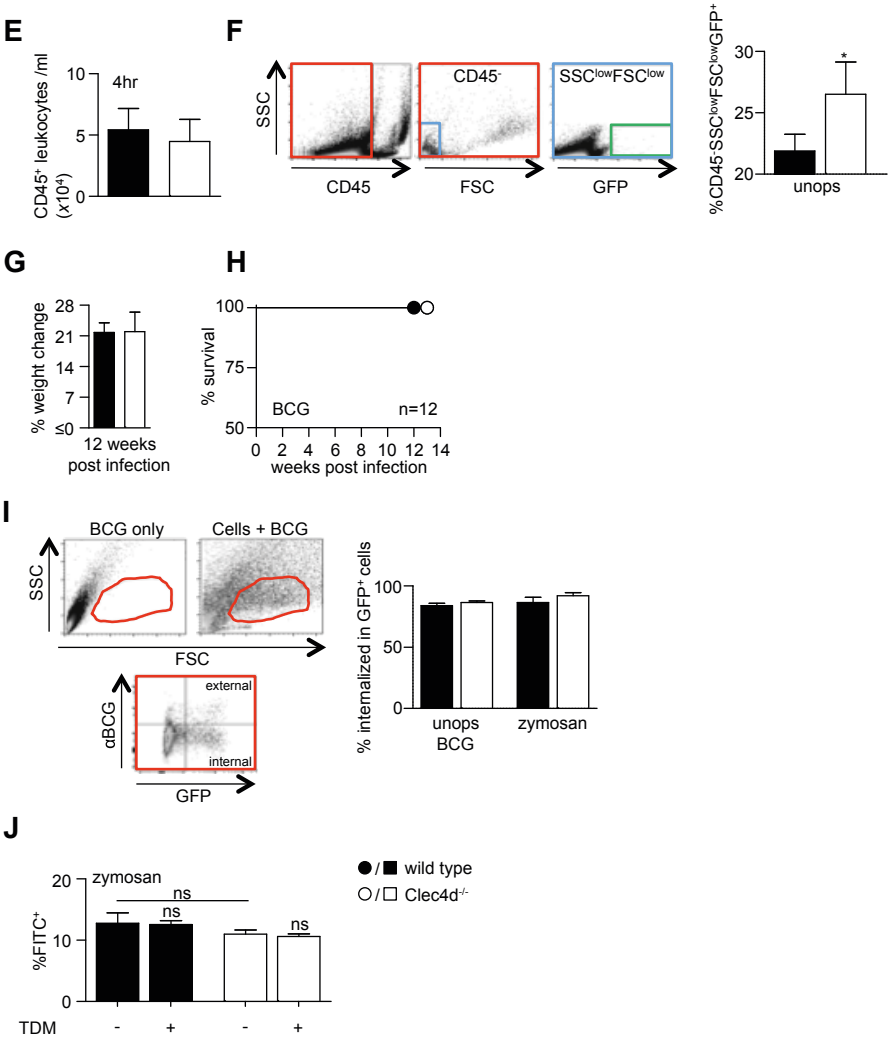

Supplementary figure 2.2 Continued.

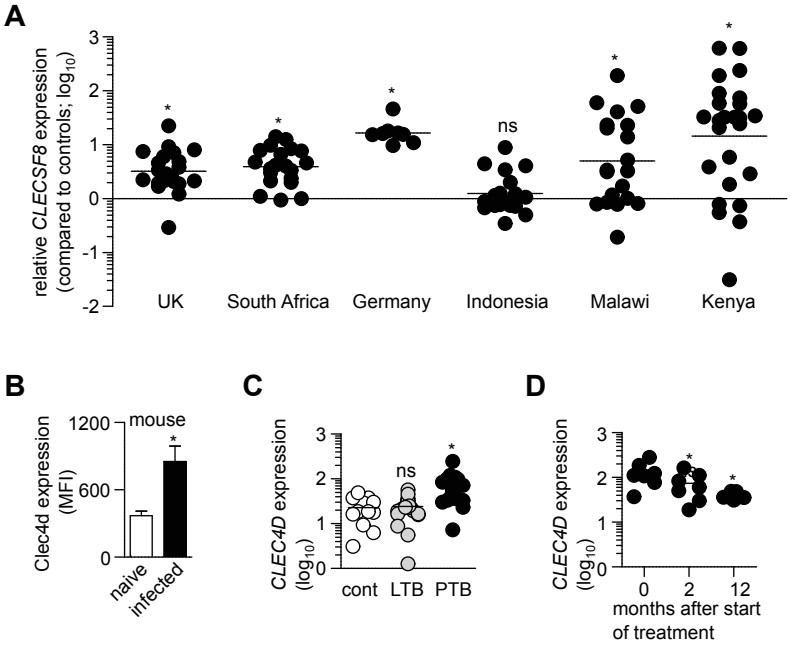

Supplementary figure 2.3 Expression and polymorphisms of CLEC4D.

(A) Relative expression of *CLEC4D* in whole blood in patients with active pulmonary tuberculosis of six cohorts, compared to the controls from the respective cohorts. (B) Clec4d expression on mouse $CD45^+$ leukocytes isolated from the lung 48 hour after BCG infection. (C) Expression of *CLEC4D* in whole blood in tuberculin skin test negative healthy control subjects (cont) from the United Kingdom (UK), individuals with latent tuberculosis infection (LTB), and patients with active pulmonary tuberculosis (PTB). Pulmonary tuberculosis and control data is the same as UK cohort data in (A). (D) Expression of *CLEC4D* over time in pulmonary tuberculosis patients following initiation of tuberculosis treatment. (E) Expression of *CLEC4D* in $CD4^+$ and $CD8^+$ cells, monocytes and neutrophils of patients and healthy controls in the UK. *, $p<0.05$. (F) Linkage disequilibrium plot of the *CLEC4D* gene region and 15kb upstream. SNPs with a prevalence of > 0.05 are shown with their linkage disequilibrium, based on data from the Han-Chinese (CHB) and Japanese (JPT) populations in HapMap. The figure was generated with Haploview and then redrawn. Bright red indicates high level of linkage. The three SNPs that were investigated in this study (shown in bold) collectively tag the haplotypes that occur with a frequency of > 0.05 in CHB + JPT populations. (G) Example flow cytometry plots (left) and pooled analysis (right) of total and surface expression of mutated CLEC4D, relative to the wild type receptor in NIH3T3 cells expressing the Fcγ chain. Each cell line was independently generated and tested twice. *, $p<0.05$; ns, not significant.

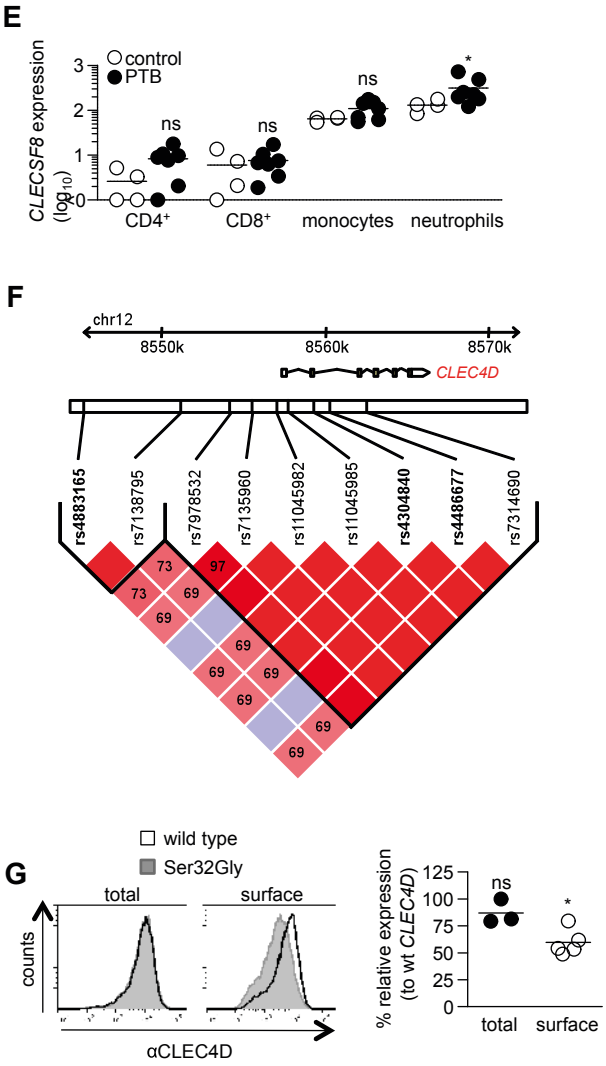

Supplementary figure 2.3 Continued.

3

Low induction of proinflammatory cytokines parallels evolutionary success of modern *M. tuberculosis* Beijing strains

Arjan van Laarhoven, Jornt J Mandemakers, Johanneke Kleinnijenhuis, Mimount Enaimi, Ekta Lachmandas, Leo AB Joosten, Tom HM Ottenhoff, Mihai G Netea, Dick van Soolingen, Reinout van Crevel

Infection and Immunity. 2013;81(10):3750–6.

Abstract

Rationale
One of the most widespread clades of *M. tuberculosis* worldwide, the Beijing genotype family, consists of ancient (atypical) and modern (typical) strains. Modern Beijing strains outcompete ancient strains in terms of prevalence, while reserving a higher degree of genetic conservation. We hypothesize that their selective advantage lies in eliciting a different host immune response.

Materials
Bead-disrupted lysates of different *M. tuberculosis* strains of the modern (n=7) or ancient (n=7) Beijing genotype, and the Euro-American lineage (n=6) were used for induction of ex-vivo cytokine production in peripheral blood mononuclear cells (PBMCs) from 10 healthy individuals. Hierarchical clustering and multivariate regression analyses were used to study possible differences in production of nine cytokines.

Findings
Modern and ancient *M. tuberculosis* Beijing genotypes induced different cytokine signatures. Overall induction of IL-1β, IFN-γ, and IL-22 was 38 to 40% lower after stimulation with modern Beijing strains (corrected p values of <0.0001, 0.0288, and 0.0002, respectively). Euro-American reactivation strains induced 2-fold more TNF-α production than both types of Beijing strains.

Interpretation
The reduction in proinflammatory cytokine response possibly contributes to the evolutionary success of modern Beijing strains.

Introduction

DNA fingerprinting has greatly facilitated the study of the molecular epidemiology of tuberculosis, while disclosing the phylogeny of the *M. tuberculosis* complex. The first genotype family described was the Beijing clade[91], later recognized as the most important part of the East Asian lineage[92]. Strains of the widespread Beijing family are of particular interest due to their established association with drug-resistance, increased virulence in animal models, and association with infection of younger patients[93], the last of which points to an increased relative reproductive fitness[94].

The vast majority of circulating Beijing strains is thought to belong to a conserved type genetically, as was first described based on insertion sequence 6110 restriction fragment length polymorphism (IS6110-RFLP)[95] and recently confirmed by whole genome sequencing[96]. These so-called 'modern' Beijing strains represent 65-95% of Beijing strains in most areas, including China[97], Russia[98], Taiwan[99], South-Africa[100], Europe[97] and the United States[101]. Modern Beijing strains were first named 'typical' by the presence of a typical pattern of one or two copies of IS6110 in the NTF chromosomal region. In contrast, this insertion was found absent in the 'atypical' or ancient Beijing strains. These strains seem in fact to be representing a genetically diverse group[96]. It is only in Japan and South-Korea that the ancient strains are still highly prevalent, although they form a declining majority[102,103].

The high prevalence and degree of genetic conservation of modern Beijing strains suggest they possess a selective advantage over ancient Beijing strains and other *M. tuberculosis* genotypes. Drug resistance has most likely occurred on several independent occasions[104] and cannot be linked definitely to one of the strain subtypes[105,106]. One possible explanation for their success is that modern Beijing strains induce a different, less effective, host immune response compared to ancient Beijing strains. Although several studies have reported differences in immune responses after infection by Beijing genotype strains, none has performed an extensive comparison of immune responses induced by modern and ancient Beijing strains. The aim of our study therefore was to examine if the epidemiological success of modern *M. tuberculosis* Beijing strains is paralleled by a distinctive cytokine production profile. Our strain selection comprised a widespread geographic area and also included Euro-American strains isolated from endogenous reactivation cases in the Netherlands. We identified differences in innate immune response between modern and ancient *M. tuberculosis* Beijing strains that may help to explain their evolutionary success.

Methods

M. tuberculosis strains

Twenty *M. tuberculosis* strains were selected from the reference database of clinical isolates of the Dutch National Institute for Public Health and the Environment (RIVM) in Bilthoven. Fourteen had been spoligotyped previously as Beijing strains. Using IS6110 PCR in NTF, these strains were further subdivided as modern (n=7) or ancient (n=7) Beijing strains[107]. A third group consisted of six strains isolated from elderly (>70 years of age) Dutch tuberculosis patients. On basis of IS*6110* restriction fragment length polymorphism (RFLP) typing that has ben applied routinely to all tuberculosis cases in the Netherlands, all six had unique profiles and are assumed to represent endogenous reactivation from remote infections decades ago. Spoligotyping designated these strains to the Haarlem and T spoligotypes of the Euro-American lineage (**figure 3.1**). All strains were grown in Middlebrook 7H9 medium in one batch for three weeks. Ancient Beijing strains grew to a median OD of 0.47 (range 0.32-0.61), modern Beijing strains to a median OD of 0.43 (0.32-0.57) while the Euro-American reactivation strains grew less efficient and reached a median OD of 0.27 (0.15-0.55). Then strains were washed two times in PBS, heat-killed and then disrupted using a bead beater, after which concentration was measured using a bicinchoninic acid (BCA) protein assay to standardise the concentration used in the immunological experiments.

Stimulation experiment with human peripheral blood mononuclear cells

Peripheral blood mononuclear cells (PBMCs) were isolated from buffy coats purchased from the Sanquin Blood bank Nijmegen. The healthy volunteers gave their written informed consent for the use of their blood for scientific purposes, as approved by the Ethics Committee of Radboud University Medical Centre, Nijmegen, The Netherlands. Donations occurred anonymously and therefore no tuberculosis skin test or interferon-gamma release assay could be performed, but the present incidence of tuberculosis in the indigenous Dutch population is extremely low (4/100,000/year) and BCG-vaccination is not part of the routine vaccination program. Isolation was performed using Ficoll-Paque, involving separation by density gradient followed by three wash steps in PBS and resuspension in RPMI 1640 supplemented with Glutamax, pyruvate and gentamicin. Subsequently, 100 μL of 5x10^6/mL PBMC's and 50μL of stimulus at 4 times the designated final concentrations were added in duplicate to a 96-well round-bottom plate, together with 50 μL of RPMI, or human pooled serum in case of a 7-day stimulation. Heat-killed *Candida* hyphae were used as a positive

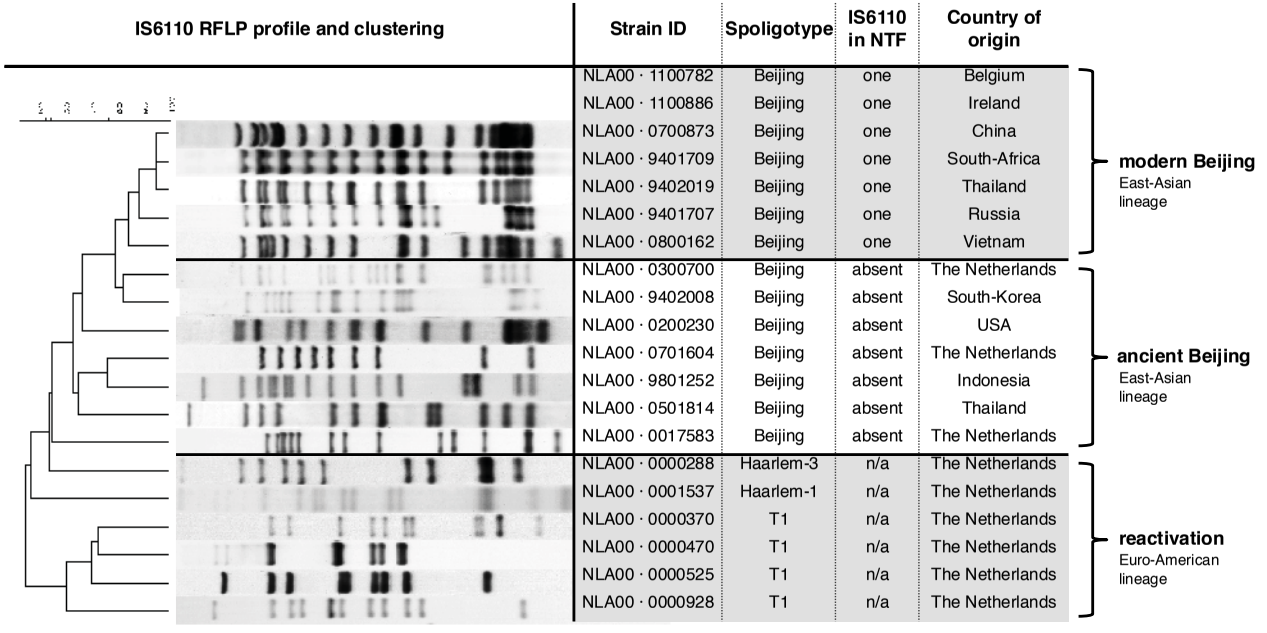

Figure 3.1 The selection of M. tuberculosis strains with genetic markers and country of origin.

IS6110 Restricted Fragment Length Patterns (RFLP) is shown with clustering, as well as typing by spoligotyping and determination of the presence of IS6110 in NTF. Note: all reactivation strains were isolated from Dutch patients over 70 years of age.

control. The plates were incubated for 24 h, 48 h or seven days at 37°C in a 5% CO_2 environment, after which they were spun at 700 g for 8 minutes. Supernatants were collected and stored at -20°C. Preliminary studies were performed using two modern and two ancient strains grown in a different batch, to define a dose-response and select the most appropriate stimulatory concentration of bead-disrupted *M. tuberculosis*, based on signatures of all cytokines tested. Afterwards, five experiments, involving two healthy volunteers each, were performed with the selection of twenty strains. Enzyme-linked Immuno-absorbence Assays (ELISA's) were performed batch-wise, following the manufacturer's protocols to measure cytokines in supernatants. The length of stimulation for the different cytokines was based on previous experiments: IL-1β, IL-1Ra, TGF-β and TNF-α (R&D Systems, Minneapolis, after 24h stimulation); IL-6 (Sanquin, Amsterdam, 24h); IFN-γ and IL-10 (Sanquin, 48 h); and IL-17 and IL-22 (R&D Systems, 7 days).

Data analysis and statistics

Hierarchical clustering analysis was performed to investigate whether modern and ancient Beijing strains induced a different cytokine signature. Data points for 20 strains times 10 donors per cytokine were ln transformed and then normalized by subtracting each value from the mean response per cytokine per donor and dividing this value by the standard deviation. This resulted in a table with standardised donor-response per cytokine in rows and different strains in columns. Using Pearson correlation a distance measure was calculated on which clustering was performed with weighted-pair group method using average linkages (WPGMA) as the linkage method, using the freeware program J Express 2012 [108].

Multivariate regression on the ln-transformed cytokine data was used to determine the contribution of the individual cytokines to the difference between the strain groups. In the multivariate regression, groups were compared based on their genetic classification, unbiased for results of the clustering hierarchy, to test the hypothesis that modern Beijing strains, on average, induced a different immune response. Fixed factors were strain type (modern Beijing, ancient Beijing or Euro-American reactivation) and donor, the latter to correct for donor variability. For the nine cytokines, predicted means of strain types and difference between those means with the respective confidence intervals were calculated with Stata MP, version 12.1. Differences with confidence intervals were plotted in a radar graph on a logarithmic axis. Reported p values and confidence intervals were Bonferroni-adjusted to correct for multiple comparisons. For clarification, relative percentages of differences were added to the radar graph

and for the reported table values were transformed as an exponent of *e* to obtain the prediction of the mean in pg/mL.

Results

Strains

All strains were fully susceptible to all first-line antituberculosis drugs. See **figure 3.1** for other characteristics. Using a standardized stimulation model with bead-disrupted M. tuberculosis and isolated PBMCs, we first explored concentrations of 0.1, 1.0 en 10 μg/mL *M. tuberculosis* looking for a single concentration associated with reasonable induction of all cytokines evaluated. We chose a final concentration of 5 μg/mL as this was expected to most clearly show differences between groups for all cytokines of interest. Production of TNF-α, IL-1β, IL-6, IL-10, IL-17 and IFN-γ using PBMCs from 4 donors was almost identical when different concentrations of a H37Rv control strain that was grown in two different laboratories (the Dutch National Tuberculosis Reference Centre and Leiden University Medical Centre, **supplementary figure 3.1**) were used.

Cytokine signature

The hierarchical clustering of cytokine signatures revealed different clusters of strains that grossly followed the distinction in modern versus ancient Beijing strains and the Euro-American reactivation strains. This study aimed explicitly to explore differences between groups of strains that have shown important epidemiological differences in terms of recent spread and genetic heterogeneity. Indeed, the ancient Beijing strains clustered separately from the epidemiologically more successful and genetically more conserved modern Beijing strains. In the hierarchical clustering, this group of modern Beijing strains was divided in two groups, one of which also harboured one Euro-American reactivation strains, while the other Euro-American strains clustered as a fourth cluster (**figure 3.2**). Multivariate regression was applied on the groups of strains as they were defined based on their genetics and statistically significant differences in cytokine responses were found between modern Beijing strains and the other two groups for IL-1β, IL-1 receptor antagonist (IL-1Ra), IFN-γ and IL-22.

Individual cytokines

The most striking difference in cytokine production was observed for induction of IL-1β, which is essential in protective host defence against *M. tuberculosis* (**figure 3.3A and table 3.1**). Overall, modern Beijing strains induced significantly

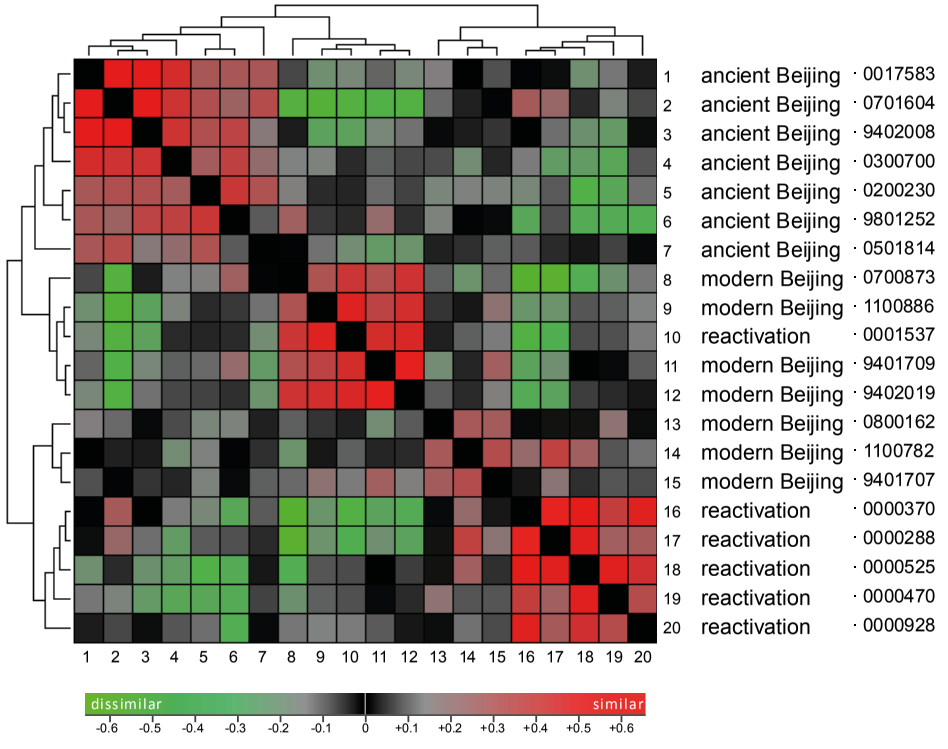

Figure 3.2 Hierarchical clustering of modern and ancient Beijing strains and Euro-American reactivation strains.

The figure shows clustering of the virtual distance between the different *M. tuberculosis strains* based on the cytokines they induce in peripheral blood mononuclear cells (PBMCs). The distance matrix shows similarity (in red) and dissimilarity (green) between cytokine signatures of the respective strains. Analysis was performed on the Ln-transformed and normalised data with open source 'J Express' software [108] (see text for further details).

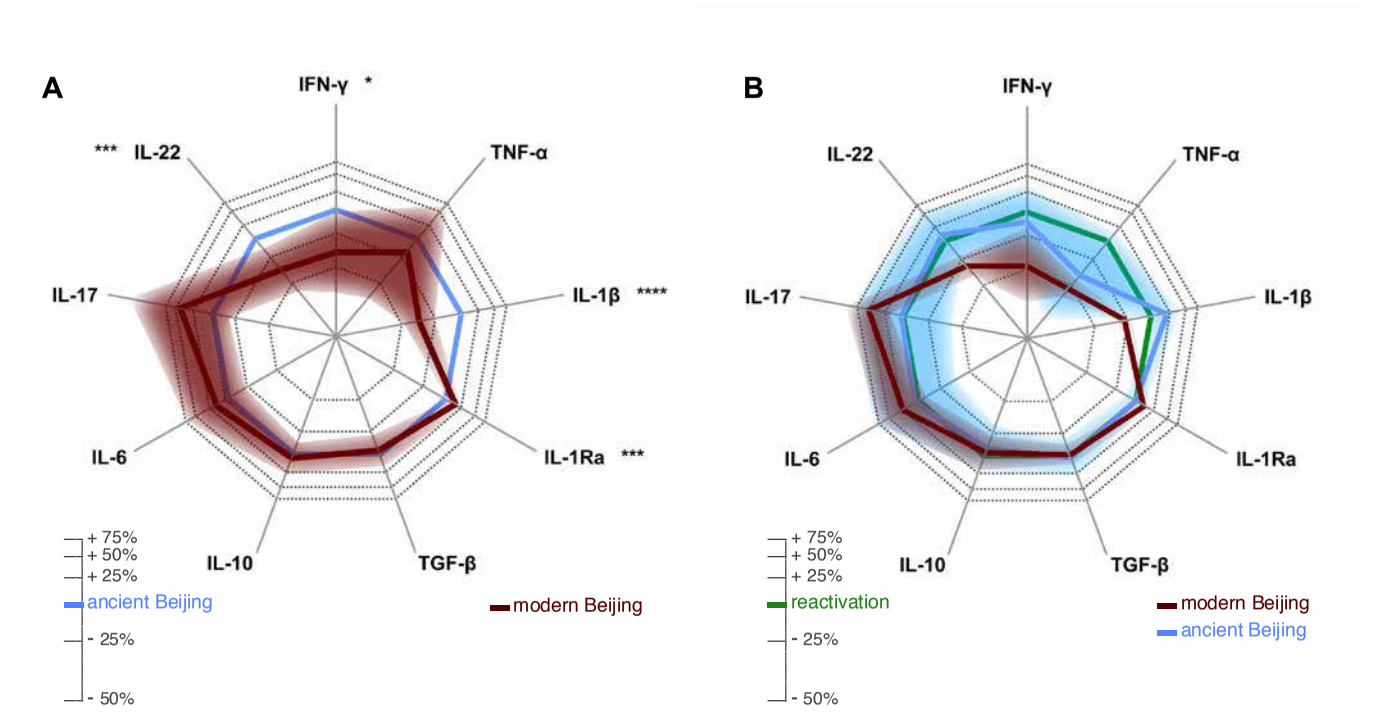

Figure 3.3 Differences in cytokine response.

(A) Differences in cytokine response after stimulation with modern (red) and ancient (blue) Beijing strains. (B) Beijing strains compared to Euro-American reactivation strains (green). Relative cytokine responses were calculated by multivariate regression. The shaded areas show the confidence intervals, which were Bonferroni-adjusted to take into account the multiple comparisons made. Axis is on ln-scale; corresponding percentages are shown in the legend; a lower response is indicated by projection towards the centre of the figure. Asterisks indicate the Bonferroni-corrected significance of the differences are indicated by * $p<0.05$, *** $p<0.001$ or **** $p<0.0001$.

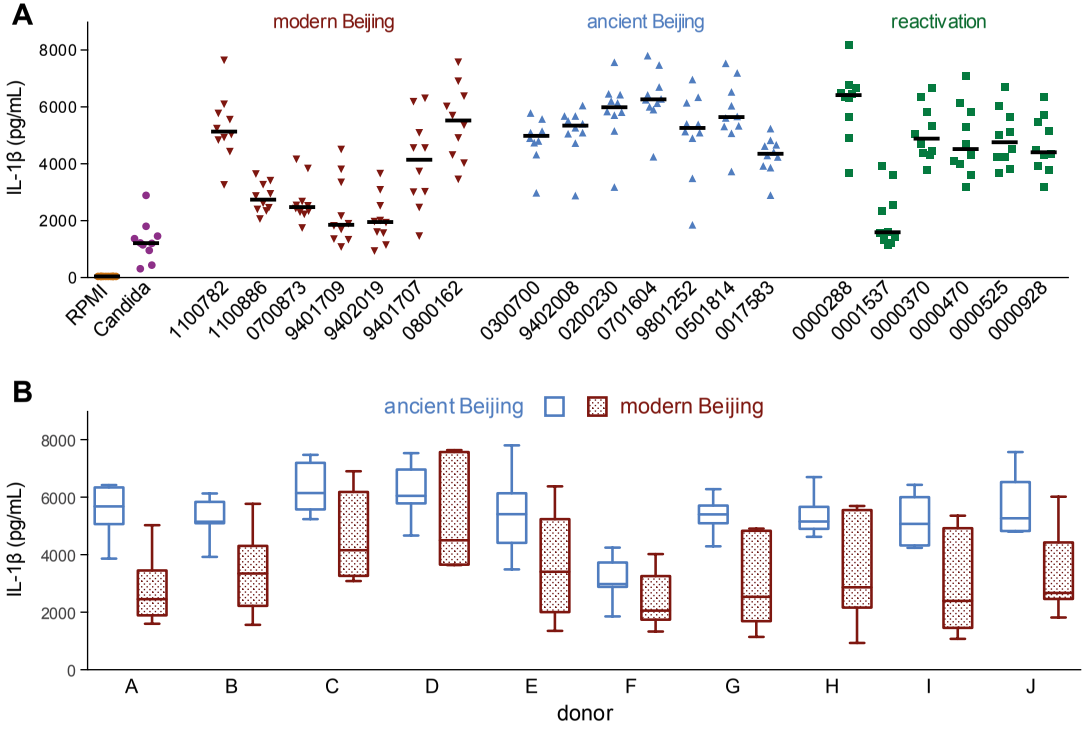

Figure 3.4 IL-1β response of ten healthy donors to modern and ancient Beijing and to Euro-American reactivation strains.

A) strain-associated differences in cytokine production. B) donor-associated differences in cytokine production for modern and ancient Beijing strains, for all ten donors individually.

lower IL-1β concentrations after 24h compared to ancient Beijing strains (estimated mean 3,115 versus 5,184 pg/mL, p<0.0001), and reactivation strains (4,250 pg/mL) (**figure 3.3B**). Moreover, compared to ancient Beijing strains, modern Beijing strains induced significantly more IL-1Ra (5,094 versus 4,501, p=0.0001). Because IL-1Ra antagonizes the effect of IL-1β, this will further deplete the biologically active fraction of IL-1β after stimulation with modern Beijing strains. Production of all cytokines, including IL-1β and IL-1Ra, showed considerable in-between-strain and in-between-donor variability (**figure 3.4A** and **supplementary figure 3.2**). However, at the level of the individual donors, the amount of IL-1β was consistently lower and that of IL-1Ra consistently larger for modern compared to ancient Beijing strains in cells from all 10 donors (**figure 3.4B and supplementary figure 3.3**).

Modern Beijing strains also induced lower production of IFN-γ (48 hour) compared to the more ancient Beijing strains (48 versus 80 pg/mL, p=0.002). TNF-α production (24 hour) was slightly lower for modern compared to ancient Beijing strains (300 and 365 pg/mL, not significant) and interestingly, both groups induced much less TNF-α than the Euro-American reactivation strains (623 pg/mL, non-significant for ancient Beijing strains after Bonferroni correction, p<0.0001 for modern Beijing strains). IL-22 (7 days) was significantly lower in modern Beijing strains compared to ancient Beijing strains (662 versus 1061 pg/mL, p=0.0002). Conversely, induction of IL-17 (7 days) was higher in modern Beijing strains compared to ancient Beijing strains (160 pg/mL versus 106 pg/mL, not significant) and the reactivation strains (103 pg/mL, p<0.0001) (**figure 3.3B**). No significant differences were found for production of IL-6 (24 hour), TGF-β (24 hour) and IL-10 (48 hour).

Table 3.1 Cytokine induction in modern and ancient Beijing strains and Euro-American reactivation strains

Cytokine	Length of stimulation	**Predicted mean** (95% CI) (pg/mL)		
		Modern Beijing strains	Ancient Beijing strains	Euro-American reactivation strains
IFN-γ	48 h	48 (40–57)	80 (67–95)	90 (76–107)
TNF-α	24 h	300 (252–357)	365 (272–490)	623 (535–725)
IL-1β	24 h	3,115 (2,954–3,285)	5,184 (4,823–5,572)	4,250 (4,082–4,424)
IL-1Ra	24 h	5,094 (4,971–5,220)	4,501 (4,329–4,681)	4,531 (4,333–4,738)
TGF-β	24 h	2,175 (2,067–2,289)	2,264 (2,080–2,465)	2,219 (2,062–2,388)
IL-10	48 h	193 (180–207)	181 (166–198)	201 (181–224)
IL-6	24 h	6,590 (5,962–7,284)	5,610 (4,641–6,782)	5,283 (4,373–6,383)
IL-17	7 days	160 (137–186)	106 (83–136)	103 (88–122)
IL-22	7 days	662 (618–711)	1,061 (914–1,231)	963 (860–1,079)

Data were calculated by multivariate regression on ln-transformed data. The outcomes were transformed back from ln-transformed data to show predicted means in pg/mL. The Bonferroni correction was applied to the *P* values to account for the multiple comparisons made. CI = confidence interval.

Discussion

In our in-vitro model, heat-killed and bead-disrupted lysates of modern ("typical") *M. tuberculosis* Beijing strains induced a clearly different cytokine signature in freshly isolated PBMCs compared to ancient ("atypical") Beijing strains. Overall, modern Beijing strains induced considerably lower production of IL-1β, IFN-γ and IL-22, and moderately higher production of IL-1Ra and IL-17. Interestingly, stimulation with Euro-American reactivation strains from elderly patients resembled stimulation with ancient Beijing strains, except for TNF-α. Euro-American reactivation strains induced twofold higher TNF-α than both type of Beijing strains, which may represent a possible explanation why infections with these strains only appear in these patients under circumstances of waning immunity.

% Difference for modern Beijing vs ancient Beijing strains	p	% Difference for modern Beijing vs Euro- American reactivation strains		% Difference for ancient Beijing vs Euro- American reactivation strains	
- 40%	0.0288	- 47%	< 0.0001	- 12%	1
- 18%	1	- 52%	< 0.0001	- 41%	0.3136
- 40%	< 0.0001	- 27%	< 0.0001	+ 22%	0.0036
+ 13%	0.0001	+ 12%	0.0010	- 1%	1
- 4%	1	- 2%	1	+ 2%	1
+ 6%	1	- 4%	1	- 10%	1
+ 17%	1	+ 25%	0.7859	+ 6%	1
+ 51%	0.7123	+ 54%	< 0.0001	+ 2%	1
- 38%	0.0002	- 31%	< 0.0001	+ 10%	1

We hypothesize that the lower induction of proinflammatory cytokines may help explain the increased spread of modern Beijing strains across the globe. The presence of an IS6110 in the NTF chromosomal region is used traditionally to distinguish modern from ancient Beijing strains. Deletions that occurred after the insertion of IS6110 are used to further type the group of modern Beijing strains, but so far, there are insufficient epidemiological data to define a genetic subgroup within the modern Beijing strains that is driving its success. For this reason we decided to compare the group of modern Beijing strains as a whole to the other groups.

A striking observation in the present data is that the ancient Beijing strains, which are considered as genetically heterogeneous[96], showed a rather uniform cytokine response, and also that only four out of seven genetically modern Beijing genotype strains showed the distinctive low-inflammatory response. The modern strains that showed the lowest induction of proinflammatory cytokines may share specific properties that enable them to counteract or subvert effective host responses, and one could thus hypothesize that an even narrower

subgroup within the modern Beijing strains is in fact responsible for its global emergence. In future epidemiological and experimental studies, mutations and deletions that occurred subsequently to the insertion of IS6110 in NTF in the evolution of modern Beijing strains will have to be assessed to define this group more specifically.

The most striking difference in our study was the almost two-fold lower IL-1β production induced in PBMCs by modern compared to ancient Beijing strains. For IL-1Ra the opposite was found, further limiting the activity of IL-1β after stimulation with modern Beijing strains. IL-1β is increasingly recognized as an important cytokine involved in host defence against *M. tuberculosis.* IL-1β restricts mycobacterial growth in murine models, and IL-1β knockout mice are highly susceptible to mycobacteria. In humans, polymorphisms in IL-1β or IL-1R are associated with increased tuberculosis susceptibility and progression[109].

Modern *M. tuberculosis* Beijing strains also induced lower production of IFN-γ, which has a well-established role in protection against mycobacterial infections, including tuberculosis[110,111]. Apart from lymphocytes, innate immune cells (NK, NKT cells and γδT cells) also contribute to the production of IFN-γ in response to mycobacteria[109,112]. TNF-α production was strikingly lower in response to both types of Beijing strains compared to the Euro-American strains isolated from patients with reactivation tuberculosis. This is of specific interest because of the swift reactivation of tuberculosis after TNF-α blocking therapy[113]. TNF-α has a paramount role in granuloma formation and maintenance[114] and contributes importantly to the balance of pro- and anti-inflammatory cytokines that determines the success of mycobacterial control[115].

IL-17, which was induced in higher amounts by modern Beijing strains, especially when compared to Euro-American reactivation strains, may act as a double edged sword: it facilitates the formation of mature granuloma, but in excess leads to enhanced neutrophil recruitment and concurrent lung tissue damage[116]. Interestingly, a zebrafish model shows that in the early phase granuloma formation IL-17 also facilitates bacterial spread[117], which makes a high IL-17 concentration possibly favourable to the bacteria[112]. In contrast, IL-22 production was lower in modern Beijing strains. IL-22 is produced in the lung and has been found in bronchoalveolar lavage fluid[118]. In general, it provides the crosstalk between immune cells that produce IL-22 but lack the receptor and nonimmune cells – e.g. lung epithelium cells – that do express the IL-22 receptor. Activation of the IL-22 receptor on these cells leads to upregulation of several chemokines in the lung[119]. Lower production of IL-22 as found in modern Beijing strains

might thus lead to lower expression of chemokines, possibly favouring outgrowth of *M. tuberculosis*. However, a definitive role of IL-22 in human tuberculosis still has to be confirmed: in a mouse model of tuberculosis the neutralisation of IL-22 did not increase the bacterial burden in the lungs[116].

In recent years a number of studies have examined whether *M. tuberculosis* from different genetic backgrounds induce strain-specific differences in cytokine production. In the global phylogeny of *M. tuberculosis*, evolutionary modern strains – bearing the TbD1 deletion, as all Euro-American and Beijing strains do – generally have a tendency towards inducing a lower cytokine response, as recently comprehensively shown in a macrophage infection model by Portevin et al.[120]. Other studies, using small numbers of strains from a wide range of lineages, show the existence of clear but ill-reproducible differences (extensively reviewed by Coscolla et al.[121]). However, it is likely that most of the evolution of *M. tuberculosis* occurs within its main lineages and our study is the first with a comprehensive assessment of immune stimulatory capacity of intralineage strains. These lineages show a distinctive geographical pattern[10] and may adapt to and shape the specific host population they encounter.

Few studies have examined cytokine production in multiple strains within one of the most successful lineages of *M. tuberculosis*, the Beijing genotype. Wang et al. found lower a TNF-α induction for Beijing strains compared to H37Rv and a trend towards lower TNF-α concentration after stimulation with two ancient Beijing strains[122]. In two macrophage infection models, one Beijing isolate appeared more immunogenic than H37Rv, with higher mRNA expression for IL-1β, TNF-α[123] and IFN-γ[124]. Krishnan et al. found less TNF-α induction with the Beijing outbreak strain HN878 but variable results for other Beijing strains[125]. Kato-Maeda et al. compared Beijing strains with different ability to cause secondary disease in humans on their pathogenicity in guinea pigs. Strains were characterized using genetic Regions of Difference. Interestingly, guinea pigs appeared to be most susceptible to ancient Beijing strains (RD207-). In line with our study, the authors of this study found that strains in modern sublineages RD142- and RD150- induced less TNF-α mRNA. Expression of IFN-γ mRNA varied among the modern sublineages and IL-1β was not measured[126].

To our knowledge, the present study is the first that specifically examines the successful sub-branch of modern strains within *M. tuberculosis* Beijing strains. There are, however, a few limitations to this study. To maximise standardisation, we used a model in which freshly isolated PBMCs were stimulated with heat-killed bead-disrupted lysates. Although these lysates, stored in many

similar aliquots, produce highly reproducible cytokine patterns, they of course lack some of the lipid structures present in the *M. tuberculosis* cell wall. In addition, the use of PBMCs may not fully reflect the response of resident tissue macrophages, although it is not logical to expect that the differences in cytokine profiles we have found would be reversed in macrophages, which are related to circulating monocytes. An alternative approach would have been to infect macrophages with live mycobacteria. This interesting model has the disadvantage of less reproducibility and absence of lymphocytes. Also, differences in growth kinetics or mycobacterial gene-expression under specific conditions may by itself lead to differences in cytokine induction. Yet another model would be to measure circulating cytokines in patients infected with different genotype strains, though possibilities are limited by differences in disease status, the high variety of genotype groups that hinder sound statistical analysis as well as the fact that plasma cytokine concentrations are generally low in tuberculosis patients. An Ethiopian study designed this way hinted at a lower induction of IL-4 in patients infected with Euro-American strains compared to East-African Indian strains[127].

As a strong point, our study design and approach to analyse the results are thorough and innovative. We used 10 donors and 20 different strains belonging to three subgroups (modern and ancient Beijing strains as well as tuberculosis reactivation strains). This approach provided enough statistical power to detect meaningful differences despite variation between donors and different strains within one subgroup, as was clearly the case for modern Beijing strains. Hierarchical clustering, which so far is mostly used for gene expression datasets, was used to analyse cytokine signatures. Radar graphs were used to graphically represent cytokine-specific differences between groups of the three groups of *M. tuberculosis* strains.

We conclude that modern Beijing strains show lower induction of IL-1β, IFN-γ and IL-22 and higher IL-1Ra *in vitro* compared to ancient Beijing strains and Euro-American reactivation strains. This differential immune induction might contribute to the epidemiological success of the modern *M. tuberculosis* Beijing strains.

Acknowledgements
The authors thank Cor Jacobs, Jessica de Beer, Tridia van der Laan, Arnout Mulder and Louis Wilson for technical help and Jochem Dijkstra for graphical design of the radar graphs. The authors are most grateful to all collaborators worldwide who provided strains for typing, including Margaret Fitzgibbon of

the Irish Mycobacteria Reference Laboratory, St. James's Hospital, Dublin, Ireland and Maryse Fauville-Dufaux of Tuberculosis and Mycobacteria, Belgian Scientific Institute for Public Health, Brussels, Belgium.

Author contributions

AvL, MGN, DvS and RvC designed the study. ME cultured the *M. tuberculosis* strains. AvL, JK and EL performed immunological experiments. AvL and JJM performed the statistical analyses. LABJ and THMO contributed to the immunological concepts. AvL, MGN and RvC wrote the manuscript to which the other authors contributes.

Supplementary figures

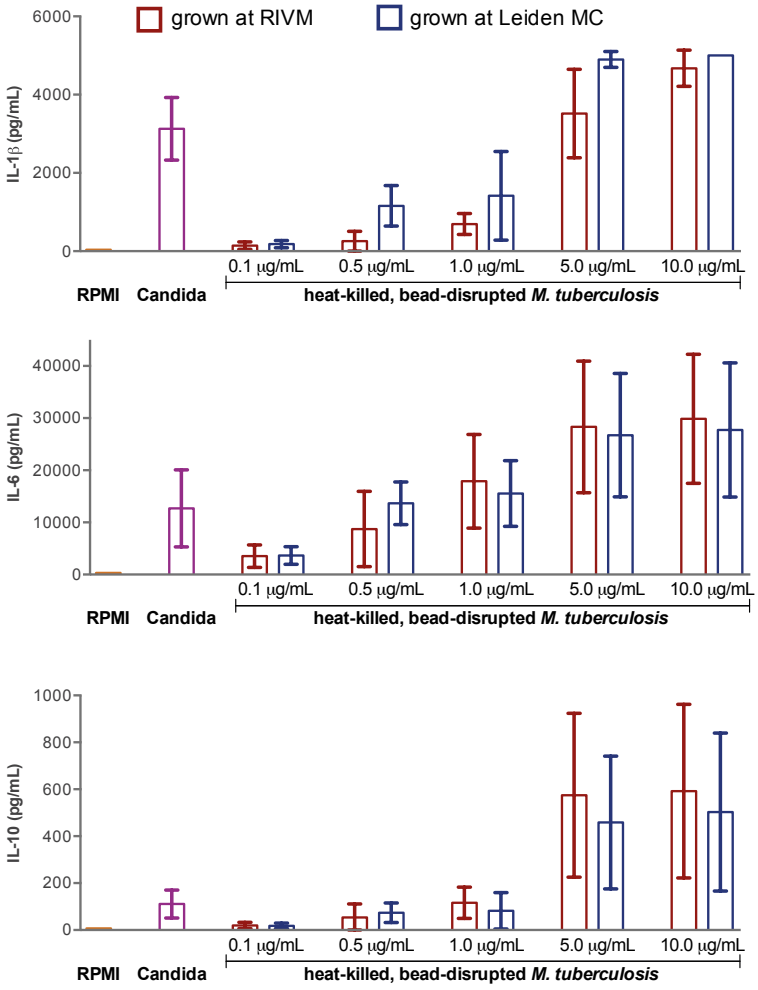

Supplementary figure 3.1

For quality control, *M. tuberculosis* H37Rv was grown in two different laboratories. Heat-killed, bead-disrupted lysates of the two stocks were used to stimulate peripheral blood mononuclear cells (PBMCs) of four donors. RPMI and heat- killed Candida hyphae ware used as controls. Below the mean and standard deviation are shown for IL-1β (after 24 h stimulation), TNF-α (24 h), IL-6 (24 h), IFN-γ (48 h), IL-10 (48 h) and IL-17 (7 days). The results are comparable for the stock from the Dutch National Tuberculosis Reference Centre (RIVM, shown in red) and Leiden University Medical Centre (LUMC, blue).

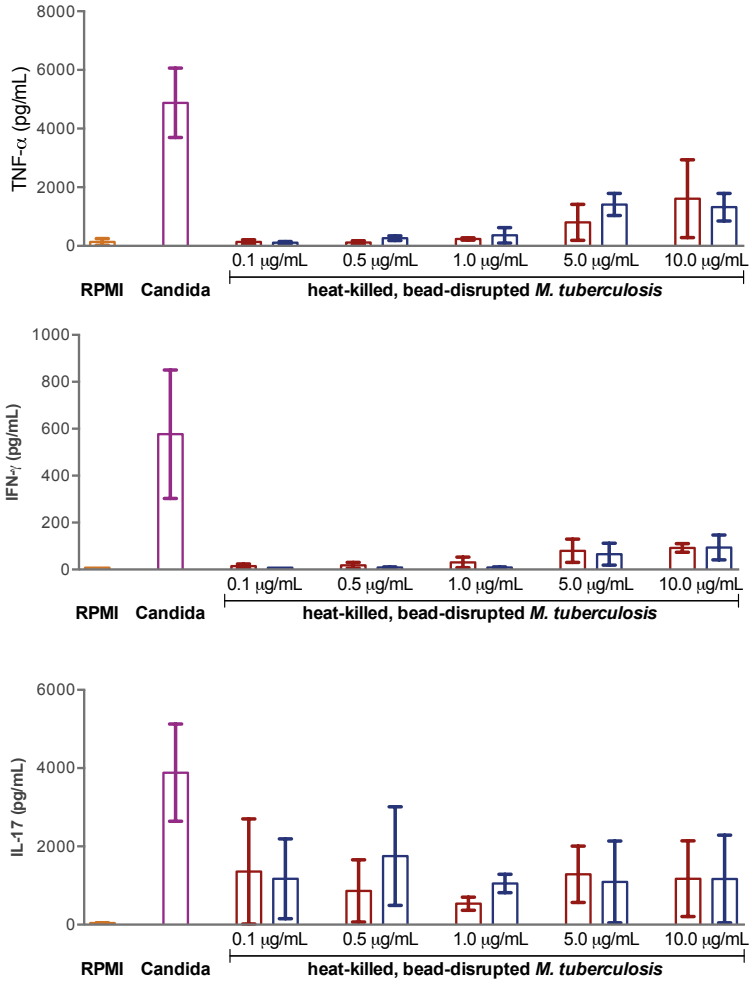
TNF-α (pg/mL)
8000
6000
4000
2000
0
0.1 μg/mL
0.5 μg/mL
1.0 μg/mL
5.0 μg/mL
10.0 μg/mL
RPMI
Candida
heat-killed, bead-disrupted *M. tuberculosis*
IFN-γ (pg/mL)
1000
800
600
400
200
0
0.1 μg/mL
0.5 μg/mL
1.0 μg/mL
5.0 μg/mL
10.0 μg/mL
RPMI
Candida
heat-killed, bead-disrupted *M. tuberculosis*
IL-17 (pg/mL)
6000
4000
2000
0
0.1 μg/mL
0.5 μg/mL
1.0 μg/mL
5.0 μg/mL
10.0 μg/mL
RPMI
Candida
heat-killed, bead-disrupted *M. tuberculosis*

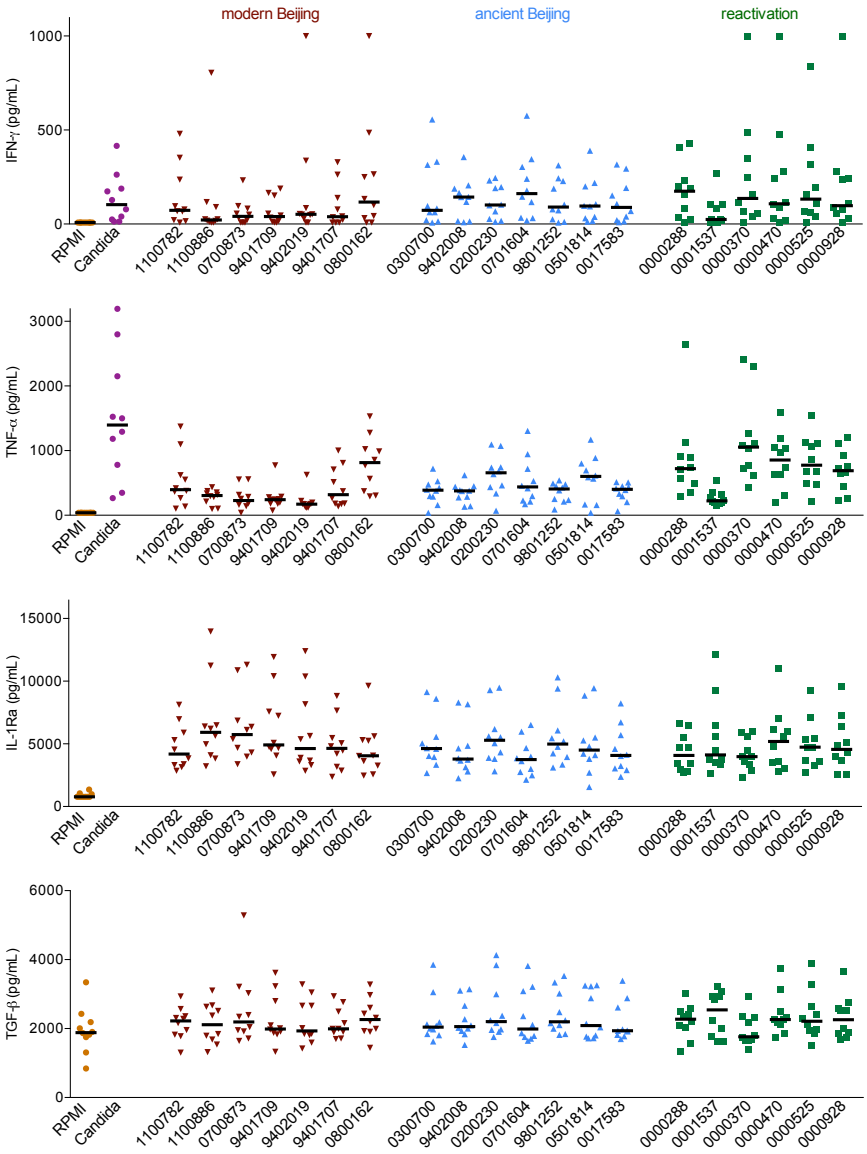

Supplementary figure 3.2 Strain-associated differences in cytokine production of ten healthy donors to 7 modern Beijing (red), 7 ancient Beijing (blue) and 6 Euro-American reactivation strains.

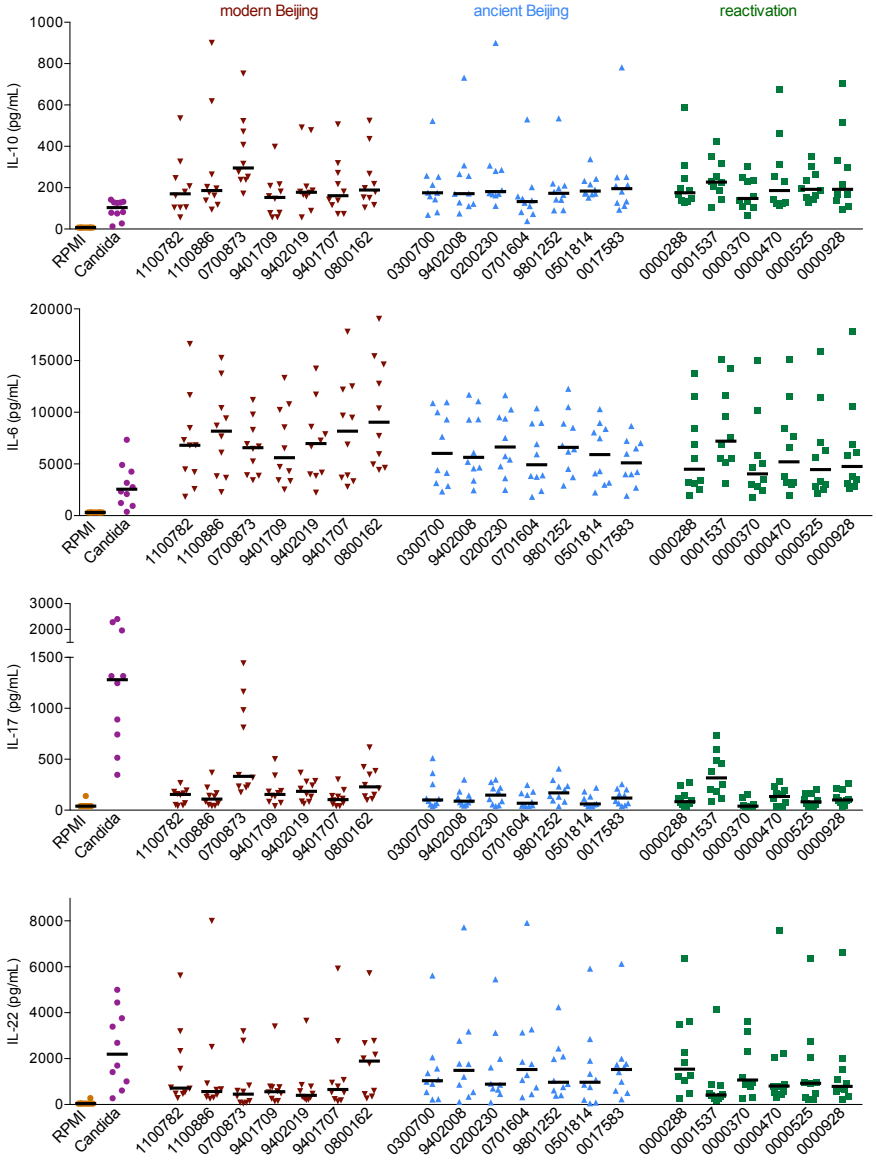
modern Beijing
ancient Beijing
reactivation
IL-10 (pg/mL)
IL-6 (pg/mL)
IL-17 (pg/mL)
IL-22 (pg/mL)
RPMI
Candida
1100782
1100886
0700873
9401709
9402019
9401707
0800162
0300700
9402008
0200230
0701604
9801252
0501814
0017583
0000288
0001537
0000370
0000470
0000525
0000928

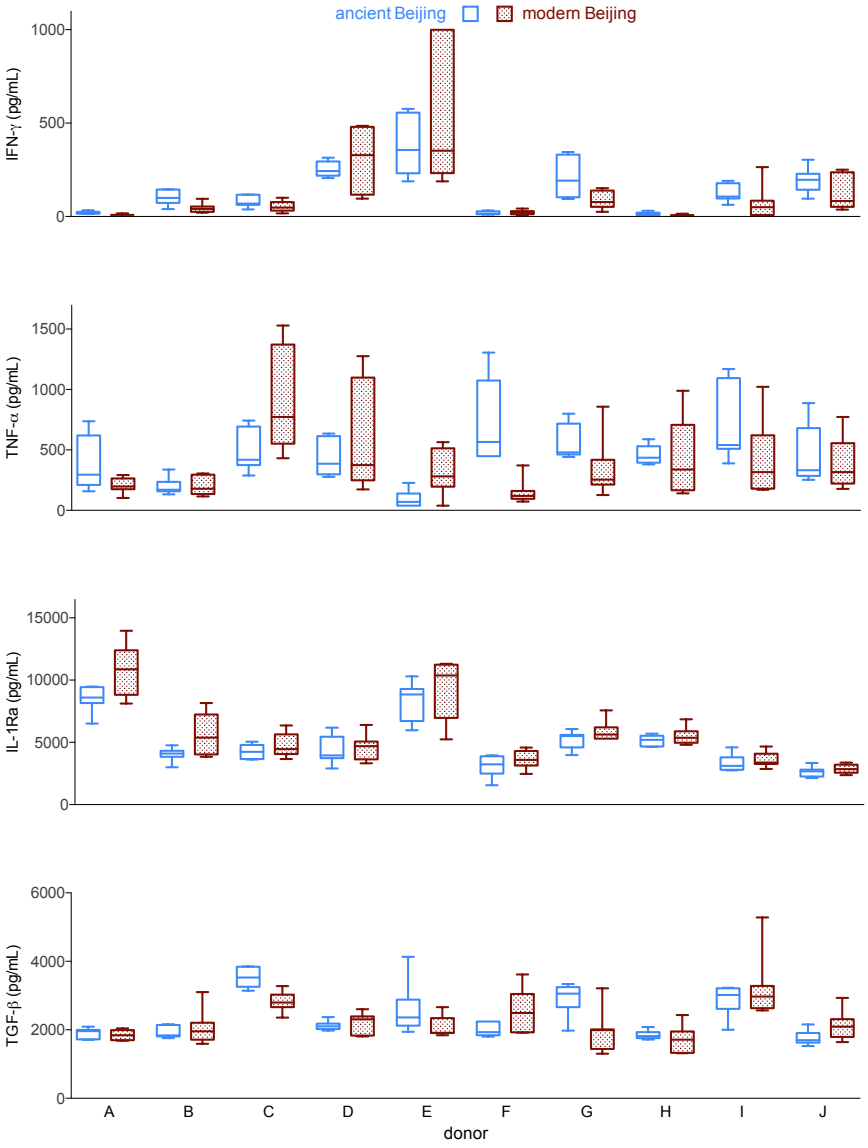

Supplementary figure 3.3 Donor-associated differences in cytokine production to modern (red) and ancient Beijing (blue) strains.

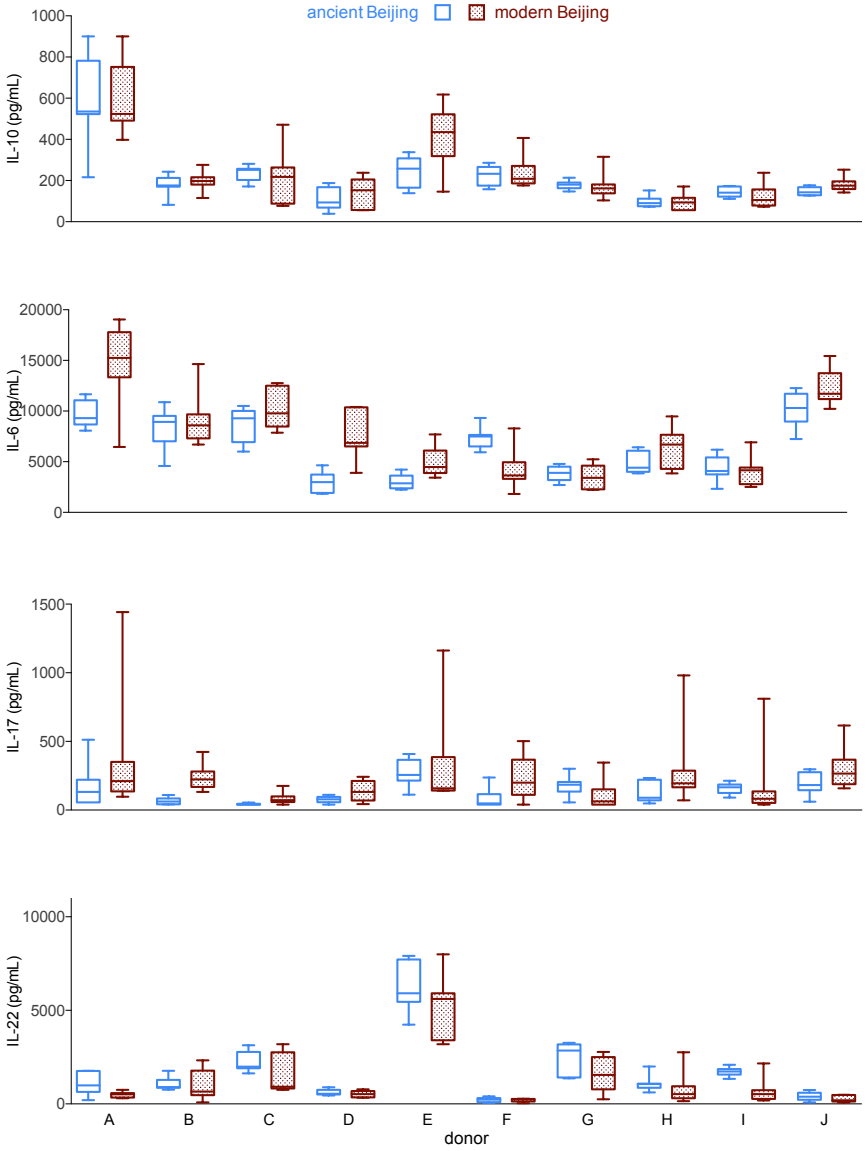
ancient Beijing
modern Beijing
IL-10 (pg/mL)
1000
800
600
400
200
0
IL-6 (pg/mL)
20000
15000
10000
5000
0
IL-17 (pg/mL)
1500
1000
500
0
IL-22 (pg/mL)
10000
5000
0
A
B
C
D
E
F
G
H
I
J
donor

4

Transmissible *M. tuberculosis* strains share genetic markers and immune phenotypes

Hanna Nebenzahl-Guimaraes[*], Arjan van Laarhoven[*], Maha R. Farhat[*], Valerie A.C.M. Koeken, Jornt J. Mandemakers, Aldert Zomer, Sacha A.F.T. van Hijum, Mihai G. Netea, Megan Murray[¶], Reinout van Crevel[¶], Dick van Soolingen[¶]

[*] Equal contribution
[¶] Equal contribution

American Journal of Respiratory and Critical Care Medicine. 2017;195(11):1519–27.

Abstract

Rationale

Successful transmission of tuberculosis depends on the interplay of human behaviour, host immune responses, and *M. tuberculosis* virulence factors. Previous studies have focused on identifying host risk factors associated with increased transmission, but the contribution of specific genetic variations in mycobacterial strains themselves are still unknown. The objective of this study is to identify mycobacterial genetic markers associated with increased transmissibility and to examine whether these markers lead to altered in-vitro immune responses.

Methods

From the comprehensive Dutch tuberculosis registry (n=10,389), a set of 100 *M. tuberculosis* strains either least or most likely to be transmitted after controlling for host factors was identified. These were subjected to whole-genome sequencing and evolutionary convergence analysis, and this analysis was repeated in an independent validation cohort (n=143). Immunological experiments were performed to measure in-vitro cytokine production and neutrophil responses to a subset of the original strains with or without the identified mutations associated with increased transmissibility.

Findings

The mycobacterial loci *espE*, *PE-PGRS56*, Rv0197, Rv2813–2814c, and Rv2815–2816c were identified as targets of convergent evolution among transmissible strains. Four of these regions could be validated in an independent set of strains, and mutations in three targets affected in-vitro monocyte and T-cell cytokine production, neutrophil reactive oxygen species release, and apoptosis.

Interpretation

The convergent evolution of *M. tuberculosis* toward enhanced transmissibility is paralleled by specific genetic markers, which are associated with altered immune responses *in vitro*.

Introduction

Transmission of pulmonary tuberculosis occurs through inhalation of small droplet nuclei containing *M. tuberculosis* bacilli that enter the lungs, evade killing by the innate immune system, and replicate intracellularly. If a series of transmission events occurs over a relatively short time, one can identify a group of patients with *M. tuberculosis* strains that are genotypically highly similar. Epidemiologists often use molecular fingerprinting to characterize the genetic similarity among a group of strains; strains that share a molecular fingerprint are described as 'clustered'[128] and are inferred to be the result of recent transmission rather than the reactivation of a previous infection.

Host factors can affect tuberculosis transmission and disease progression[129], but recent molecular epidemiologic studies have shown that *M. tuberculosis* strains also differ in their ability to cause pulmonary disease[130], their proclivity to infect contacts[131] or cause secondary cases[9,101]. This variability may reflect the strains' ability to subvert innate[122,132] and/or adaptive[133,134] immunity, or their ability to exploit the host immune system by inducing a detrimental inflammatory response[135] leading to tissue damage[126,136] and formation of cavities that enable disease spread[137]. Cytokines play a pivotal role in these events; insufficient production of proinflammatory cytokines may lead to uncontrolled mycobacterial growth, while overproduction may lead to tissue damage[20].

Phylogenetic differences in cytokine response (**chapter 3** and [120]) suggest that specific microbial genetic determinants may underlie transmission related phenotypes. Several studies have used *M. tuberculosis* mutants *in vitro* and experimental models to identify the role of a few individual genes on transmission-associated phenotypes[138]. However, further elucidation of the full spectrum of genes affecting transmission could improve our understanding of the host-pathogen relationship in tuberculosis.

We aimed to identify loci under positive selection for clustering by analysing whole *M. tuberculosis* genomes from clustered and unclustered isolates for evidence of convergence. Following the hypothesis that clustered strains have consistent genetic differences compared to unclustered ones, and that the genes or intergenic regions implicated in these differences affect the host immune response, we performed a functional validation of the newly identified targets of independent mutation (TIMs) by measuring in-vitro cytokine production and neutrophil responses.

Methods

Clinical isolates

We selected 100 mycobacterial strains with extreme phenotypes at both ends of a transmissibility spectrum. We considered strains to be highly transmissible if they came from clusters of active tuberculosis cases lacking known risk factors for being part of a cluster. Similarly, we considered strains to be minimally transmissible if they were unique (unclustered) and isolated from patients (e.g. homeless individuals with grade 3 sputum smear-positive pulmonary tuberculosis) with increased risk for clustering. To classify strains as such, we used data on host risk factors for clustering to estimate the cluster propensity to propagate (CPP), a summary measure of risk for transmission of patients belonging to a particular tuberculosis cluster[139] (**supplementary table 4.1**). This CPP was calculated for 10,389 patient isolates, with clusters defined by DNA fingerprinting[140,141]. CPP was significantly higher in clustered versus unclustered strains, although the CPP rapidly plateaus with increasing cluster size (**figure 4.1**). Because there is no basis for sample size calculation in studies associating genomic variants with transmissibility[142,143], we arbitrarily chose 100 strains for whole genome sequencing: 66 unclustered strains and 34 clustered strains. Strains for the clustered phenotype were picked at random from 56 unique cluster fingerprints (5 pairs of strains came from within the same cluster). The 100 selected strains were all drug sensitive and belonged to patients originating from 44 different countries. At least one strain from both phenotypes (clustered and unclustered) and from each the four major *M. tuberculosis* lineages was represented. In an independent dataset (n=143), we contrasted clustered and unclustered strains collected from patients of different geographical backgrounds. Most of these strains were drug resistant (**supplementary table 4.2**).

Phylogeny construction

Strains underwent whole genome sequencing and variants were called (see **Supplementary methods**). We then constructed a phylogeny on the basis of multiple-sequence alignment of the sequences, excluding single nucleotide polymorphisms (SNPs) that occurred in repetitive elements, including Pro-Glu (PE), Pro-Pro-Glu (PPE) and polymorphic GC-rich sequence (PGRS) genes.

Phylogenetic convergence test for selection

We used our previously developed method, the phylogenetic convergence test for selection, to identify genetic loci associated with clustering. For each nucleotide position in the genome, we counted the number of convergent SNPs and insertions/deletions ("Indels") in clustered and unclustered branches

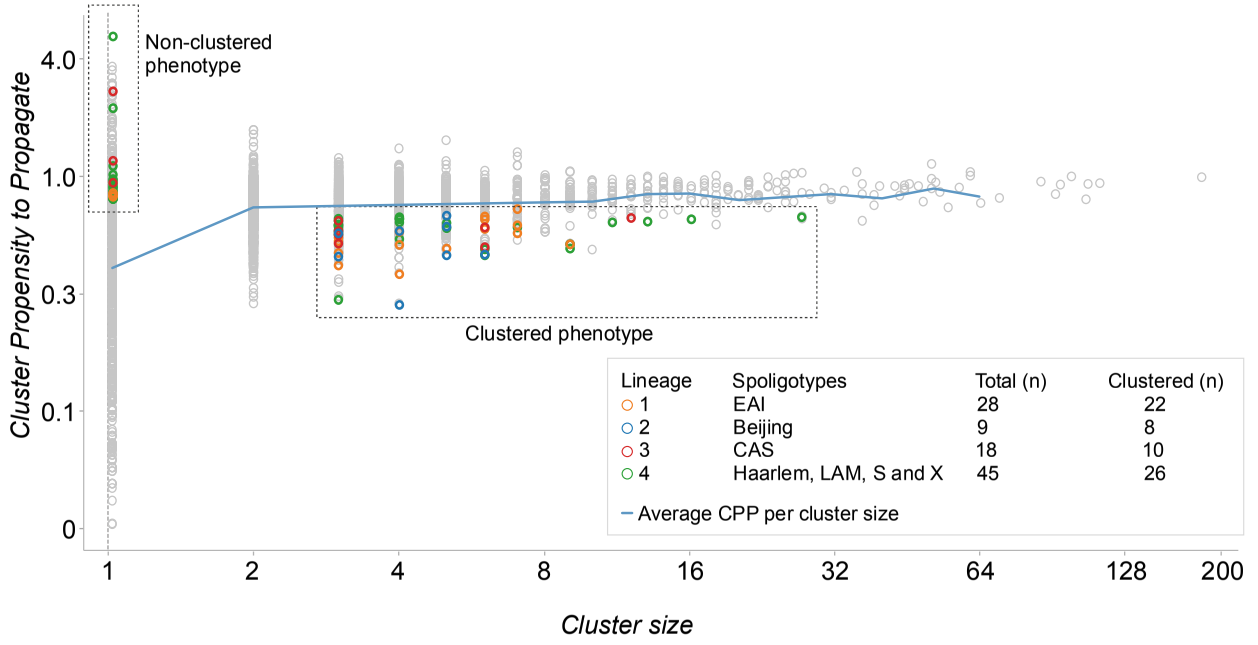

Figure 4.1 Selection of strains from clustered and unclustered phenotypes.

Grey circles represent strains from the overall National Institute for Public Health and the Environment (RIVM) dataset, whilst coloured circles denote the 100 strains selected for whole genome sequencing and the phylogenetic lineage they belong to.

respectively, counting only one strain per cluster. We therefore assessed the significance of each convergent SNP or Indel compared to the empirical background distribution using a permutation test[142].

Protein prediction

We used two protein prediction algorithms, I-Mutant v2.0 (http://folding.biofold.org/i-mutant/i-mutant2.0.html) and PolyPhen-2 (http://genetics.bwh.harvard.edu/pph2/), to predict the functional impact of the significant SNPs on protein structure and function.

Immunological experiments

Nineteen strains from the initial study were recultured, heat-killed and bead-beaten. Peripheral blood mononuclear cells (PBMCs) from 12 healthy donors were stimulated with 3 μg/mL of lysate for production of TNF-α (4 and 24 h), IL-1β, IL-1RA, IL-6 and IL-10 (24 h) and T-cell cytokines IL-17, IL-22 and IFN-γ (7 days) (see **chapter 3** for the methods. We also stimulated isolated polymorphonuclear cells (PMNs, largely consisting of neutrophils) for one hour and measured the production of reactive oxygen species (six donors) after six hours using luminal-enhanced chemiluminescence, and neutrophil apoptosis and cell death with flow cytometry (eight donors). We constructed multivariate mixed models to exploit the covariance between assays and to control for lineage effect and inter-donor variability and compared null models without assay-specific TIM indicators to full models with these indicators using Likelihood Ratio tests.

Results

Targets of independent mutations (TIMs)

The primary set of 100 selected strains included 66 clustered isolates with a low predicted CPP (mean CPP 0.75; sd=0.01) and 34 unclustered isolates with a high predicted CPP (mean CPP 1.02; sd=0.30) (**figure 4.1**). We conducted two parallel phylogenetic evolutionary convergence tests to identify either individual nucleotide positions, or genes and intergenic regions where cluster-associated mutations occur frequently along disparate locations in the phylogenetic tree (**figure 4.2**). Region-level phylogenetic evolutionary convergence tests detected three genes and two intergenic regions as statistically significant TIMs ($p<0.05$) (**table 4.1**). A total of 12 SNPs, 2 insertions and 31 deletions were found in these TIMs, including 1 SNP and 2 deletions that were also significant by the site-level phylogenetic evolutionary convergence test (**supplementary table 4.3**). TIMs in the *PE-PGRS56* gene occurred solely in clustered branches, while those in *espE*,

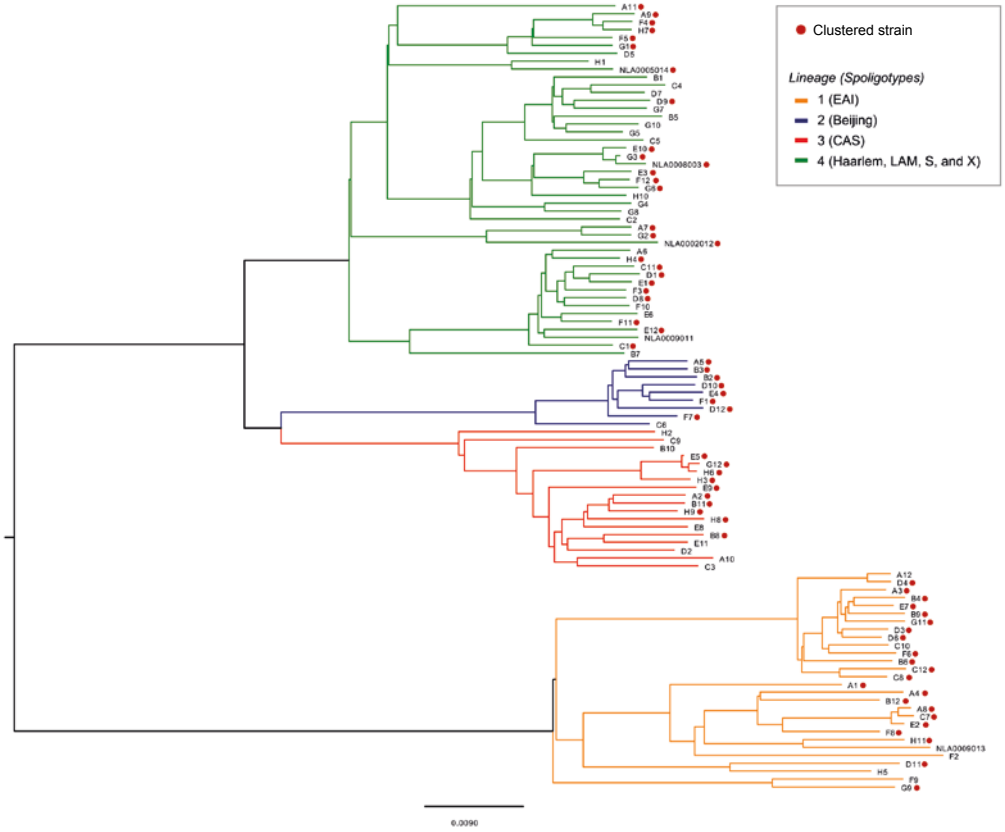

Figure 4.2 Consensus Bayesian phylogenetic tree.

Clustered strains and *M. tuberculosis* lineages are highlighted. CAS = Central Asian; EAI = East African-Indian; LAM = Latin American-Mediterranean.

Rv0197, Rv2813-2814c and Rv2815-2816c were also found in unclustered branches, but at a lower rate than in clustered branches (depicted for *espE* in **supplementary figure 4.1**).

Analysis of the validation set of 143 strains confirmed four out of five genes or intergenic regions (**table 4.1**) including Rv0197, in which the phylogenetic convergence test detected the same nonsynonymous coding site (234,477TG). The TIMs occurring in the *PE-PGRS56* gene could not be validated, because their occurrence in the original dataset was mostly restricted to lineage 1, which made up only 3.4% of the validation dataset.

Table 4.1 Significant genes or intergenic regions by the phylogenetic convergence test

	Original dataset (n=100)				Validation dataset (n=143)			
	Strains with mutations, deletions and insertions (n)				Strains with mutations, deletions and insertions (n)			
Gene/region (Rv number)	Clustering	Nonclustering	p	Lineages with cases	Clustering	Non-clustering	p	Lineages with cases
espE (Rv3864)	10	1	0.0377	1, 3, 4	10	2	0.0232	1, 3, 4
PE-PGRS56 (Rv3512)	13	0	0.0052	1, 4	1	0	1	4
unnamed (Rv0197)	20	12	0.0214	1, 2, 3, 4	26	12	0.0362	1, 2, 3, 4
unnamed (Rv2813-2814c)	20	6	0.0458	1, 3, 4	22	3	0.0001	1, 3, 4
unnamed (Rv2815-2816c)	18	4	0.0178	1, 4	22	5	0.0105	1, 4

Deleterious effect of SNP TIMs on proteins

All 12 SNPs in genes Rv0197 and *espE* are predicted to adversely affect the respective proteins (**supplementary table 4.4**), including two TIMs in Rv0197 (234,265GT and 234,477TG) that result in a STOP codon and truncation of the protein.

Association between TIMs and induction of cytokine responses

Reasoning that genetic variation associated with transmissibility might be mediated through host response we next examined in-vitro cytokine responses in strains with and without convergent changes. The distribution of TIMs across the strains is depicted in **supplementary figure 4.2** and **supplementary table 4.5**. Mutations in two of the targets we identified, *espE* and Rv2813-2814, were associated with alterations in monocyte cytokine production ($p<10^{-4}$, **table 4.2**, **figure 4.3**) in the multivariate mixed model. In the secondary analysis (see **online supplement**), mutations in *espE* were associated with decreased production of IL-10 ($p=1.7 \times 10^{-8}$, **figure 4.4A**) and TNF-α (at 4 hours, $p=8.0 \times 10^{-3}$), and mutations in Rv2813-2814c were associated with increased production of TNF-α ($p=2.5 \times 10^{-3}$), IL-1β ($p=7.7 \times 10^{-3}$) and IL-10 ($p=1.9 \times 10^{-3}$). Of the five genes or intergenic regions, only *PE-PGRS56* affected T-cell cytokine responses ($p=5.4 \times 10^{-3}$), and in our secondary analysis, this was associated with lower IFN-γ production ($p=1.6 \times 10^{-3}$, **figure 4.4B**).

Association between TIMs and response of neutrophils

We next examined the effects of TIMs on in-vitro responses of neutrophils, given their putative role in transmission and clinical manifestation of tuberculosis in the same 19 strains. In the multivariate mixed effects model, we found that Rv2813-2814c affected PMN responses ($p<10^{-4}$) with lower reactive oxygen species production ($p=4.8 \times 10^{-4}$, **Figure 4.4C**) and higher early apoptosis ($p=3.6 \times 10^{-3}$) in secondary analysis.

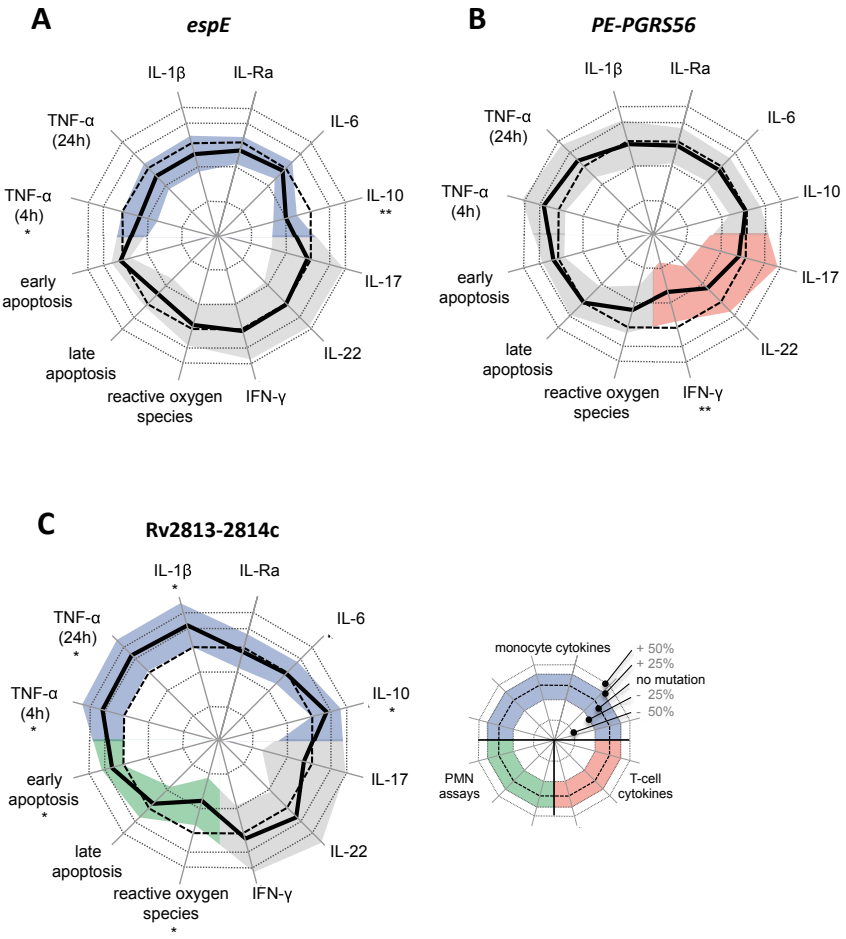

Figure 4.3 Response to *M. tuberculosis* strains with or without mutations in the three targets of independent mutation that showed an effect in the primary analysis.

Relative differences for individual assays in the secondary analysis are indicated by the difference between the thick black line (mutation present) and the thin reference line (no mutation) for each of the following targets of independent mutation that significantly influenced at least one assay group: (A) *espE*, (B) *PE-PGRS56*, or (C) Rv2813–2814c. Shaded area represents the 95% confidence interval, corrected for the fact that five genes or intergenic regions were tested for each assay. *$p<0.05/5 = 0.01$. **Significant after further correcting for number of assays per group (i.e., $p<0.05/[5 \times 6]$ for monocyte cytokines and $p<0.05/[5 \times 3]$ for T-cell cytokines and polymorphonuclear neutrophil [PMN] assays). Significance in the primary analysis is indicated by a coloured confidence interval for monocyte cytokines (blue), T-cell cytokines (red), and PMN assays (green).

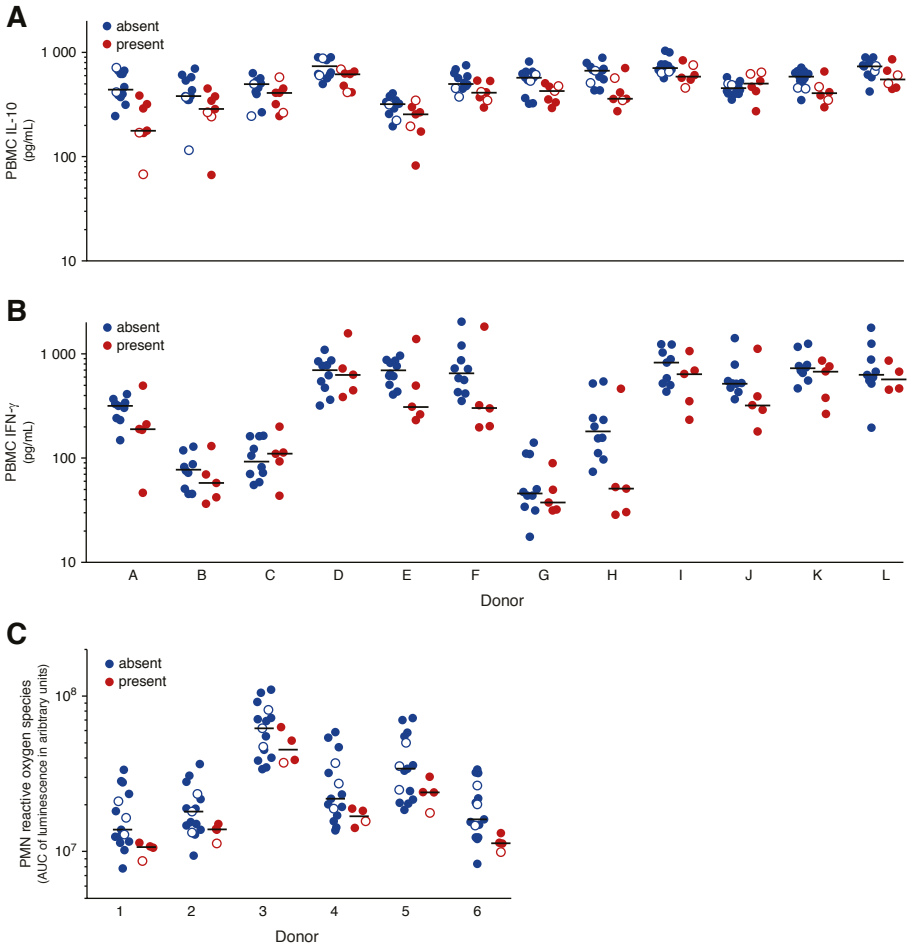

Figure 4.4 In-vitro responses of selected assays for targets of independent mutation.

Stimulation was performed with lysate of *M. tuberculosis* strains from lineage 1 (filled circles) and lineage 4 (open circles) that did not harbour (blue) or harboured (red) a mutation in (A) *espE*, (B) *PE-PGRS56*, or (C) Rv2813–2814c. Peripheral blood mononuclear cells (PBMCs) of 12 healthy donors (A–L) were stimulated. (A) IL-10 was measured after 24 hours. (B) IFN-γ was measured after 7 days. (C) Polymorphonuclear cells (PMNs) of six healthy donors (1–6) and reactive oxygen species were measured by luminol-enhanced chemiluminescence and plotted in arbitrary units of the area under the curve (AUC) of the measurement over the first hour after stimulation. Circles in A show overlap because of limited variation; only lineage 1 strain results are shown in B, because no mutations occurred in PE-PGRS56 genes in strains from lineage 4.

Table 2 Cytokine profiles and PMN responses to *M. tuberculosis* according to the presence or absence of mutations in the five TIMs.

Gene or intergenic region	monocyte cytokines (df=6)	T-cell cytokines (df=3)	PMN responses (df=3)
espE	**1.33×10^{-6}**	0.961	0.077
PE-PGRS56	0.039	**5.35×10^{-3}**	0.021
Rv0197	0.017	0.224	0.343
Rv2813-2814c	**7.47×10^{-6}**	0.309	**5.79×10^{-8}**
Rv2815-2816c	0.025	0.027	0.151

Significance (in bold) is determined at $\alpha = 0.05/5 = 0.01$, corrected for the five genes or intergenic regions tested. df = degrees of freedom. PMN = polymorphonuclear cell.

Discussion

We identified five genes and intergenic regions (*espE*, *PE-PGRS56*, Rv0197, Rv2813-14c and Rv2815-16c) as targets of independent mutation (TIMs) in clustered *M. tuberculosis* strains. We confirmed four out of five genes and intergenic regions in a second dataset despite differences in lineages and drug resistance profiles between the original and validation datasets. The TIMs we identified are predicted to alter the function of their respective proteins, and three of five identified genes or intergenic regions were associated with altered cytokine production or PMN responses, supporting the hypothesis that they confer a selective advantage for tuberculosis transmission.

Previous experimental studies have established the importance of three of the identified genes or intergenic regions, including *espE* which proved essential for *M. tuberculosis* virulence in a number of animal studies[144-146] (**supplementary table 4.6**). Further support for our findings stems from other genomic epidemiological studies. Non-synonymous SNPs – albeit different from the ones identified in this study – and a frameshift mutation in *espE* were found to be more common in *M. africanum* strains relative to H37Rv[147], and to be implied in their reduced ability to induce a CD4 T-cell ESAT-6 induced IFN-γ host response[148,149]. Similarly, a previous study identified a Large Sequence Polymorphism associated with clustering in a gene (MT1801) encoding molybdopterin oxidoreductase, which is also encoded by Rv0197[150]. In another study researchers reported that an *M. tuberculosis* strain responsible for a large outbreak in the United Kingdom harboured an insertion in position 3,121,877 of intergenic region Rv2815-2816c[151], adjacent to the 2-bp deletion in 3,121,879

observed in our own study.

Three of five genes or intergenic regions with TIMs associated with clustering of tuberculosis showed a clear and statistically significant effect on monocyte or T-cell cytokine production or PMN responses. *M. tuberculosis* strains with TIMs in *PE-PGRS56* induced lower production of IFN-γ, which is unequivocally seen as a key factor in protection against tuberculosis[20,110]. Two other TIMs were associated with altered production of the monocyte cytokines IL-10 and TNF-α which are involved in *M. tuberculosis* killing as well as damaging immunopathology, both of which may affect tuberculosis transmission[20]. In line with our previous comparison of in-vitro cytokine responses to different *M. tuberculosis* lineage strains in **chapter 3**, TNF-α and IL-6 induction in this study was higher in lineage 4 (ancient) compared to lineage 1 (modern) strains. These lineage effects may depend on strain selection, as shown by another study by Reiling et al.[152] that found opposite results. The aim of our study was not to discern lineage effects; therefore we corrected for these lineage effects in our statistical model.

With regard to neutrophils, strains harbouring cluster-associated mutations in Rv2813-2814c induced significantly lower reactive oxygen species production and early apoptosis. Neutrophils are considered protective during early infection, when they are recruited to the site of infection, phagocytose mycobacteria[84] or mycobacteria-infected macrophages[153], and resist mycobacterial growth using reactive oxygen species[153]. Children with chronic granulomatous disease have a reduced oxidative burst and are more susceptible to tuberculosis[154]. Neutrophil reactive oxygen species also correlates with apoptosis[132]. Although speculative, lower induction of reactive oxygen species production might as such contribute to disease progression and higher transmission of certain strains.

This study has several limitations. First, phenotype misclassification, most notably that of highly transmissible strains as unclustered, is a possibility among "imported" strains (those belonging to patients born outside the Netherlands: 53% versus 88% in unclustered and clustered strains, respectively). Average follow-up time however, as indicated by proxy data on 'days resided within the Netherlands' at the time of diagnosis, amongst 'imported' cases within the unclustered cohort was 3,607 days (ranging from 321 to 10,874 days). In other words, it is reassuring that, with the exception of one case (where days resided within the Netherlands was 321 days), all the remaining 'imported' cases classified as unclustered had been in the Netherlands for at least 4 years. Second the difference in drug resistance profiles and related parameters such as

treatment efficacy between the original and validation cohort of strains for the phylogenetic convergence test, could have introduced bias in measurement of the transmissibility phenotype (**supplementary table 4.2**). The fact that transmission of drug resistant strains has been widely documented[155,156] and that mathematical models have estimated the transmission cost of drug resistance to be as low as 10% [157] suggests that the overall fitness for transmission of drug resistant strains is comparable to that of sensitive strains. The possibility for epistasis indeed exists – earlier this year for example, MDR strains in China with *rpoC* compensatory mutations were found to be more likely to be clustered than their drug sensitive counterparts[158]. Future phylogenetic convergence test tests stratified by drug resistance would identify such potential (positive or negative) epistatic mutations, as has already been attempted using epidemiological tools[159]. In this study however, confirmation of four out of the five genetic markers associated with transmission in the validation dataset reduces the risk of false positive findings. Finally, the inclusion of additional key host factors that may influence disease transmissibility, such as the level of tuberculosis exposure (i.e. via prospective household contact data) and pulmonary cavitation, could improve our ability to isolate bacterial factors influencing transmissibility in the future.

Validating our findings on longitudinally collected strains from other low burden settings and at a nationwide level could further increase the significance of our results. An adequately sized and publicly available whole genome sequence dataset as described was not available at the time of our analysis. In high-burden tuberculosis settings we would expect crowding, treatment delays and host risk factors (i.e. malnutrition, uncontrolled diabetes) to be more important for transmission. These factors could be controlled for using the CPP measure. Whether the sum of all these factors acting in synergy to facilitate transmission in high burden settings translates into a reduced selective pressure for genomic adaptations in *M. tuberculosis* itself remains an interesting question.

Of note, we performed in-vitro cellular stimulations aiming to find biological support for the epidemiological associations identified through convergent evolutionary analysis, and not to identify specific effects of individual TIMs on in-vitro cellular responses. Such effects cannot be identified in this study, as multiple TIMs were present in single strains in this dataset (**supplementary table 4.5**). For this purpose, additional studies using mutagenesis or recombination-mediated genetic engineering to isolate the mutational effects should be performed. It is no surprise that no single pattern of cytokine production or PMN response was found for the five genes or intergenic regions, as *M.*

tuberculosis has different strategies to subvert or resist the host immune system or use it to its advantage.

In summary, we present evidence from an evolutionary convergence analysis that five *M. tuberculosis* genes or intergenic regions confer a selective advantage promoting the transmission of *M. tuberculosis* and/or tuberculosis disease progression, and that these genetic elements influence the response of the host to the mycobacteria. These findings serve as an important step forward in the quest for an improved understanding of the microbial genetic determinants of tuberculosis transmission.

Acknowledgments
The authors would like to thank Jessica de Beer and Arnout Mulder for culturing of mycobacterial strains; Jeroen de Keijzer for processing them; Ekta Lachmandas, Bas Blok, Mark Gresnigt and Cor Jacobs for assisting in immunological experiments; and Professor Jelle Goeman for statistical advice.

Author contributions
This study was designed and conducted by HN-G, AvL, MM, RvC and DvS; HN-G, AvL and MRF wrote the first draft of the paper, the remaining authors contributed to its final version. VACMK and AvL conducted the immunological experiments. AZ and SvH provided bioinformatics support; JJM performed the statistics on the immunological assay results. HN-G, AvL, MRF, VACMK, JJM, NMG, MM, RvC, DvS contributed to analysis and interpretation.

Supplementary methods

Background of strains

The National Institute for Public Health and the Environment (RIVM) in Bilthoven serves as a tuberculosis reference laboratory for The Netherlands. Since 1993 all clinical isolates are genotyped, using IS6110 and polymorphic GC-rich sequence (PGRS) restriction fragment length polymorphism (RFLP) until 2009, and variable number of tandem repeat (VNTR) typing from 2004 onwards. Clusters were defined as groups of patients who shared *M. tuberculosis* strains with identical RFLP or VNTR patterns or, if strains had fewer than five IS6110 copies, identical PGRS RFLP patterns[160]. DNA fingerprints of all nationwide *M. tuberculosis* complex strains and their cluster status have been stored in a database since 1993. Phylogenetic lineages were ascertained based on a combination of spoligotyping, MIRU-typing and Restriction Fragment Length Polymorphisms (RFLP)-pattern similarity, as previously described[139]. Demographic and clinical information, provided by the Netherlands Tuberculosis Register (NTR), were linked to the strains on the basis of gender, date of birth, year of diagnosis and postal code.

Validation dataset

The validation dataset contained no information on host risk factors, for which reason we compared clustered (belonging to a cluster of unique footprint and minimum size of 3, n=96) and unclustered (having a unique fingerprint and no epidemiologic links reported from contact investigation, n=47) strains. For 19 clustered strains, single end 36bp read sequencing was previously performed which made calling Indels unreliable.

Sequencing, alignment and variant calling

DNA was extracted from all strains using standard methods and was sequenced on an Illumina HiSeq 2500 instrument using reads of 50bp in length in the paired-end modus. The average genome coverage was approximately 100x. FASTQ sequence reads were generated using the Illumina Casava pipeline version 1.8.3. Initial quality assessment was based on data passing the Illumina Chastity filtering. Subsequently, reads containing adapters and/or PhiX control signal were removed using an in-house filtering protocol. A second quality assessment was based on the remaining reads using the FASTQC quality control tool version 0.10.0. The quality of the FASTQ sequences was enhanced by trimming off low-quality bases using the 'Trim sequences' option of the CLC Genomics Workbench version 6.5. The quality-filtered sequence reads were then reassembled into a number of contig sequences using the previously mentioned

software. SNPs were called against reference strain H37Rv using Breseq software (version 0.23) using a minimum threshold of 15x coverage[161]. Breseq derives a consensus score from the read Phred scores by calculating the Bayesian posterior probability of possible sample bases given the observed read bases. Specifically, it uses a haploid model with five possible base states (A,T,C,G and a gap), assuming a uniform prior probability of each state and using an empirical error model derived from the based Phred score to update the prior with each read base observation. Consensus scores averaged over the genomes assayed for the SNPs and small insertions/deletions found to be associated to transmissibility are listed in **supplementary table 4.3**. Mutations with low-quality evidence (i.e. possible mixed read alignment) or within 5 bp of an Indel (insertion or deletion) were not included. Breseq has strict criteria for calling variants and although it did call variants that occurred in repetitive regions, such as the two site-specific deletions in *PE-PGRS56* significantly associated to transmissibility, we manually inspected all of these to confirm that they were indeed high quality variants that did not fall within repetitive regions. It is worth mentioning that not every base within the Pro-Glu (PE), Pro-Pro-Glu (PPE) and polymorphic GC-rich sequence (PGRS) falls in a repetitive region and that high quality variant calls within these regions, if done carefully, is possible. All sequences have been rendered publically available through NCBI. The complete genome sequence for reference strain H37Rv was accessed from GenBank accession NC_000962.3. Raw sequences for the 200 strains from Bryant et al. are available at the European Nucleotide Archive (ENA) under accession ERP000111.

Phylogeny construction

The phylogeny was constructed on the basis of multiple-sequence alignment of the *M. tuberculosis* whole-genome sequences. The final concatenate of SNPs was used to construct phylogenetic trees using three different methods: parsimony (PHYLIP dnapars algorithm v3.68), Bayesian Markov chain Monte Carlo (MCMC) (MrBayes v3.2) and maximum-likelihood (PhyML v3.0) using the GTR model with eight categories for the gamma model. One hundred bootstrap re-samplings were performed for each tree, except for the Bayesian tree, where posterior probabilities on the branches were used as a measure of confidence. The three methods of constructing a phylogenetic tree showed fully consistent results, and the Bayesian tree was used for all subsequent analyses.

Phylogenetic convergence test for selection

The phylogenetic convergence test for selection can identify positive natural selection based on homoplasy or parallel evolution. The phylogenetic convergence test is well suited for the study of clonal pathogens such as *M.*

tuberculosis[143,162], having a higher sensitivity (and likely also specificity) than the dN/dS method[163]. The phylogenetic convergence test was conducted here as previously described[163] with two modifications: we used Carmin-sokal parsimony for reconstruction of the phenotypic states as we thought this better mirrors our assumption that transmissibility evolves unidirectionally (*i.e.* from less to more transmissible); we also performed ancestral reconstruction of Indels using FASTML and maximum-likelihood criteria[164]. We controlled for the occurrence of SNPs or INDELs in strains belonging to the same cluster (as defined by MIRU- or RFLP-typing) by counting only one strain per cluster. Some background convergence is expected owing to neutral mutation and sequence error, even without positive selection. Sites are expected to be more significant with the phylogenetic convergence test if they occur in more branches than expected (based on the pattern of distribution of mutations at other sites) or if they occur in more clustered branches than unclustered branches. As this was a permutation test based on the observed frequency distribution for all variants across the genome, a 0.05 p-value threshold was used. In parallel we ran the convergence test grouping SNPs and Indels by the gene or intergenic region in which they occurred, using the same empirical resampling strategy to assess significance.

Protein expression of genes

Publically available proteomic data from Schubert et al. confirmed the expression of Rv0197 and *espE* under logarithmic growth conditions in liquid medium[165]. Mawuenyega et al. separated lysates into cell wall, membrane and cytosolic fractions and detected PE-PGRS56 in the membrane fraction[166].

Selection of clinical isolates

Mycobacterial lineage is known to influence host immune response[167]. We therefore only selected strains from the whole genome sequence dataset belonging to lineages 1 and 4, both of which had five TIMs represented, so that lineage could be included as a factor in the statistical model. Nineteen out of twenty-one strains could be re-cultured, fifteen of lineage 1 and four of lineage 4. Fifteen of the strains were of the clustered phenotype, four unclustered. The unclustered strains had a maximum of one mutation in the genes or intergenic regions associated to increased transmissibility, whilst all clustered strains had at least one TIM in the genes of interest (range 1–5), with the exception of strain F6 which had zero. H37Rv, the most well characterized strain of *M. tuberculosis*, was added for quality control of the experiments, but not included in the analysis.

Optimal timing of harvesting mycobacterial strains and different methods for lysate preparation were compared prior to the actual experiments (**supplementary figure 4.3**). Clinical strains were cultured in Tween-albumin medium on a shaking platform to determine the growth curve, and then recultured to harvest mid-log (OD_{600} 0.6-0.8 for all strains) after a total of 5-7 passages from the clinical isolate. Strains were heat-killed, washed in phosphate buffered saline, lysed mechanically by bead-beating and divided in two aliquots. One aliquot was used for stimulation experiments and for measurement of protein concentration by the bicinchoninic acid protein assay. A second aliquot was freeze-dried to determine dry weight, and was used after resuspension for measurement of reactive oxygen species production. Protein-to-dry weight ratio did not differ substantially between isolates (**supplementary figure 4.3**).

PBMC cytokine stimulation experiments

Cytokine stimulations were done using strains with and without convergent changes using a previously established method. As described in **chapter 3** (the results of which were confirmed by others[168]), buffy coats from 12 healthy volunteers (Sanquin Blood bank, Nijmegen, the Netherlands) were used for PBMC isolation. PBMCs were stimulated in duplicate in 96-well round-bottom plates with 3 uGu/mL of selected strains in a total volume of 200 μL. Previous studies identified 24h stimulation as the optimal period for monocyte-derived cytokines[169,170]. TNF-α at 4h was added because of its early release[169] and its key role in protection from tuberculosis infection[20]. For IL-17 and IL-22, we performed dose (0.001-32 μg/mL) and time (3-10 days) response experiments to determine conditions.

After incubation at 37°C at 5% CO_2 (in the presence of 10% human pooled serum for 7 day stimulation), cytokines were measured batch-wise in supernatants using ELISA after 4h (TNF-α, using R&D Systems, Minneapolis, Minnesota, USA), 24h (TNF-α, IL-1β and IL-1Ra, R&D; IL-6 and IL-10 using Sanquin, Amsterdam, the Netherlands) or 7 days (IL-17 and IL-22, R&D; IFN-γ, Sanquin) stimulation. Stimulation of PBMCs from six donors with three batches of H37Rv showed a mean standard deviation of 0.33 for TNF-α (coefficient of variation [CV] 5.5%) and 0.45 for IL-1β (CV 6.1%).

PMN reactive oxygen species and apoptosis experiments

Polymorphonuclear cells (PMNs) were isolated from EDTA blood using Ficoll-Paque, cleared from erythrocytes by hypotonic lysis buffer (two times) and washed two times in cold PBS. Reactive oxygen species were measured for six volunteers in white 96-well flat-bottom plates using luminol-enhanced chemiluminescence (5-amino-2,3,dihydro-1,4-phtalazinedione, Sigma-Aldrich,

St. Louis, Missouri, USA). PMNs were stimulated in 240 µL at 10^6 cells/mL in 0.5% BSA HBSS with culture medium alone, zymosan (final concentration: 833 µg/mL) or the 20 different *M. tuberculosis strains* (10 µg/mL). Chemiluminescence was measured at 37°C for the next 60 min, after which the area under the curve for luminescence was calculated.

For apoptosis, PMNs of eight volunteers were stimulated for six hours with the different strains (10 µg/mL). We used IL-1β as anti-apoptotic control and cyclohexamide as positive control. Annexin V-FITC conjugate (Av, BioVision, Milpitas, California, USA) and propium iodide (PI) were added after stimulation. Annexin V stains phosphatidylserine translocating from the inner to the outer leaflet of the membrane, marking early apoptosis. PI stains nuclei from cells that are permeable, reflecting cell death, either from advanced apoptosis or necrosis[171]. Flow cytometric analysis using Cytomics FC50 was performed to distinguish Av^-/PI^- (alive) Av^+/PI^- (early apoptotic) and Av^+/PI^+ (advanced apoptotic / necrotic) populations. Optimal conditions for reactive oxygen species and apoptosis assays were defined prior to the actual experiments (**supplementary figure 4.3**).

Data analysis for immunological experiments

In the immunological experiments, the effects of 5 genetic loci (or TIM = target of independent mutation) on the immunological readout were measured in multiple experiments performed with 19 different *M. tuberculosis* strains from two mycobacterial linages (lineage 1 and 4). The experiments involved 12 different measurements and were performed with isolated 12 donors (PBMC experiments) and 6-8 other donors (PMN experiments). The experiments involved three groups of assays based on cell type and time-point: 6 early (4h and 24h) monocyte cytokines, 3 later (day 7) T-cell cytokines and 3 PMN responses.

Cytokine concentrations and reactive oxygen species area under the curve (AUCs) were Ln-transformed. Several of the outcomes were correlated and therefore a linear mixed model was appropriate for data analysis. Because the 12 assays fall into three biological groups, our primary analysis involved three separate mixed models, which were run for each of the five TIMs separately, according to this formula:

$Y_{i,j}$ = assay*$lineage_{i,j}$ + assay*$donor_{i,j}$ + assay*$TIM_{i,j}$ + random effect for $strain_i$
Y = assay outcome measure
assay * lineage = indicator for the combination of assay (6,3,3) and lineage (2)
assay * donor = indicator for the combination of assay (6,3,3) and donor (12 for PBMC, 6-8 for PMN experiments)
assay * TIM = indicator for the combination of assay (6,3,3) and TIM (1)
i = *M. tuberculosis*, j = donor observation

We took a two-step approach to conserve statistical power inspired by the inheritance procedure[172]. First, for each assay group and each TIM, we tested whether the presence of a TIM was associated with differential response by comparing null models without assay-specific TIM indicators to full models with these indicators using Likelihood Ratio tests (**table 4.2**). Second, in case a TIM gene or intergenic region was associated with differential response for a particular set of assays, we examined and discuss assay-specific effects of a TIM. Note that we reported all assay-specific results for future reference, also if the likelihood ratio test was not significant (**online supplement**). In both analyses, significance was determined at α=0.05/5, Bonferroni corrected for the five TIM. All analyses were performed using Stata MP, version 12.1. Radar graphs show the percentage change for each of the assays, plotted on a logarithmic axis.

Ethics statement

The Registration Committee of the Netherlands Tuberculosis Register approved the retrospective access to strains and provided demographic and clinical information for patients. Because the data are de-identified by name, DNA fingerprinting results from the RIVM were linked on the basis of sex, date of birth, year of diagnosis and postal code. PBMCs and PMNs were isolated from volunteers with written informed consent and approval from the Ethics Committee of Radboud University Medical Center, Nijmegen, the Netherlands.

Supplementary figures

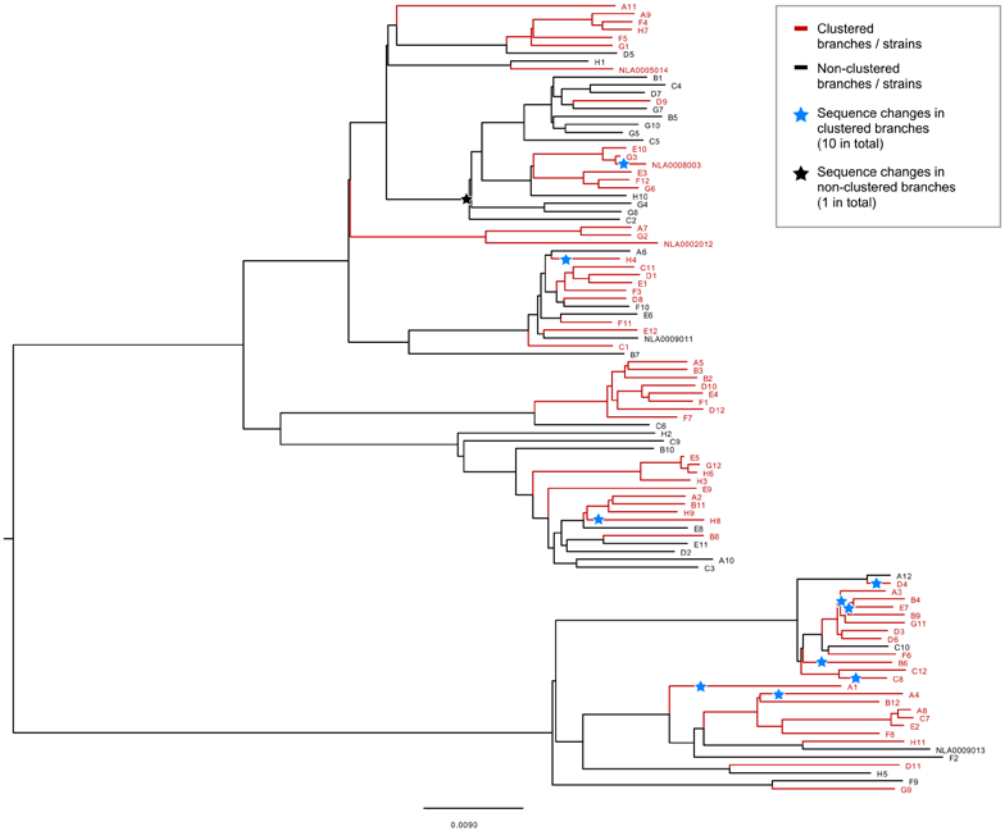

Supplementary figure 4.1 Pairwise convergence for SNPs in gene espE (Rv3864).

Branches in red represent clustered isolates, stars denote locations in the tree where TIMs associated with increased clustering occurred.

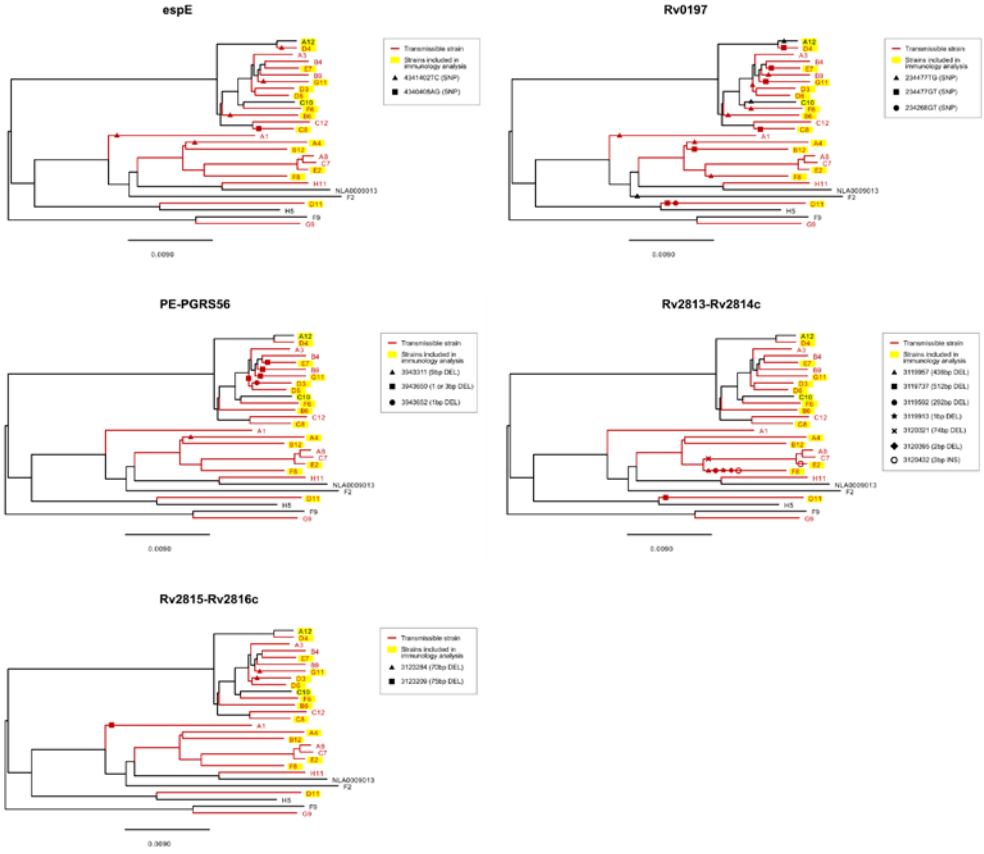

Supplementary figure 4.2 Distribution of TIMs in the five genes or intergenic regions associated to clustering across the 15 lineage 1 strains selected for functional validation studies.

Phylogenetic relationship between strains taken from the lineage 1 portion of the original Bayesian tree in Figure 4.2.

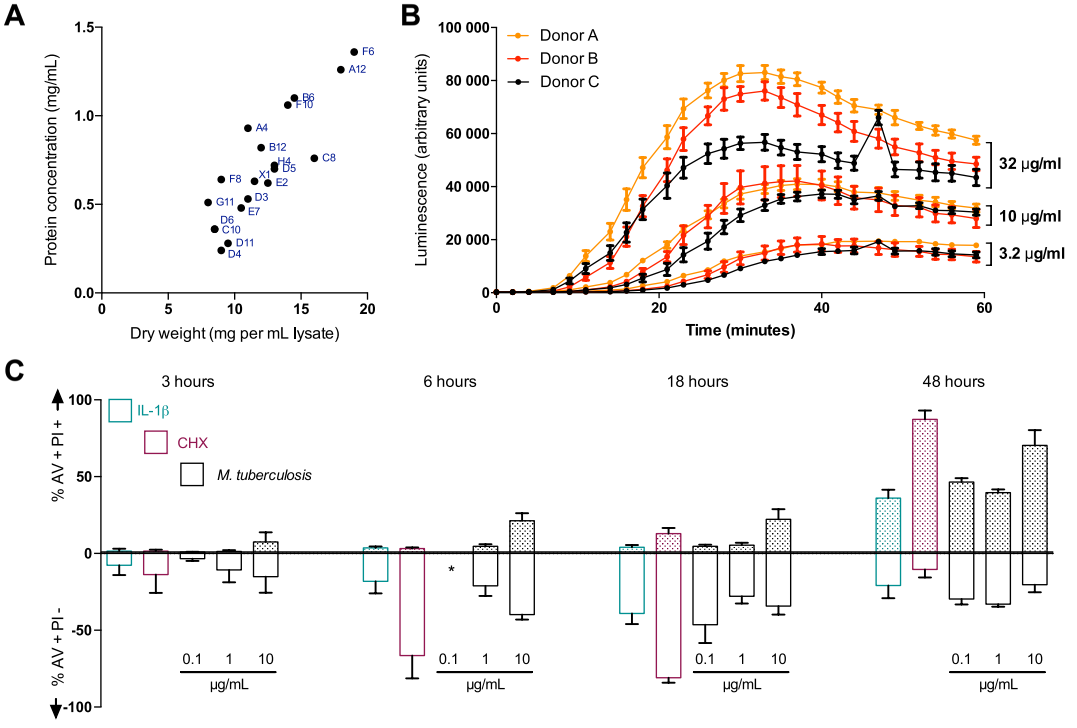

Supplementary figure 4.3 Optimising experiments for immunological assays.

(A) *M. tuberculosis* H37Rv protein concentration versus dry weight for the nineteen strains (with sequence ID) used in the immunological experiments. (B) PMN reactive oxygen production with different concentrations of H37Rv *M. tuberculosis* lysate (3.2, 10 or 32 µg/mL). (C) PMN apoptosis stimulation time and dose response optimisation after stimulation with IL-1β, cyclohexamide or H37Rv *M. tuberculosis* lysate (0.1, 1 or 10 µg/mL) at 3, 6, 18 or 48 hours. Combined results of two experiments with in total six donors. * = not measured.

Supplementary tables

Supplementary table 4.1 Summary of host risk factors taken into consideration to calculate the Patient Propensity to Propagate (PPP)*.

Category	Odds ratio	Case group	Reference
Sex	1	males	173-175
	0.87	females	
Age at diagnosis	1.05	0-15	129,173,174
	1	16-30	
	0.86	31-45	
	0.77	46-60	
	0.49	61-75	
	0.19	76-90	
	0.12	>90 years	
Disease classification	1	pulmonary	129,173,176
	0.76	extrapulmonary	
	0.90	pulmonary + extrapulmonary	
Smear-positivity	1	no	173,174,177
	1.17	yes	
Alcohol consumption	1	no	173,174,176,178
	1.29	yes	
Drug-use	1	no	173,174,176,178
	2.75	yes	
Homelessness	1	no	173,174,178
	1.58	yes	
Traveller to endemic areas	1	no	179-181
	0.58	yes	
Origin	1	native Dutch	129,173,174,176,177
	0.28	foreign-born (Asia)	
	0.76	foreign-born (Africa)	
	1.06	foreign-born (America)	
	0.43	foreign-born (Europe)	

* The geometric mean of the PPPs across the cluster was used to calculate the Cluster Propensity to Propagate (CPP). Of note: it can be argued that some of these host risk factors, such as smear positivity, may be controlled by bacterial genetic factors. Because of the likelihood of an interplay between host and bacterial factors we took the more conservative approach of including the risk factor through our CPP measure, thus decreasing the likelihood of finding a difference between the "transmissible strains" and "non transmissible strains" explained by smear positivity.

Supplementary table 4.2 Description of validation set of strains including host risk factors.

	Original dataset		Validation dataset	
	Clustered strains (n=66)	**Unclustered strains (n=34)**	**Clustered strains (n=96)**	**Unclustered strains (n=47)**
Publication source				
Farhat et al.[142]	-	-	50 (52%)	47 (100%)
Bryant et al.[182]	-	-	46 (48%)	-
Mutations called				
SNPs & Indels	66 (100%)	34 (100%)	77 (80%)	47 (100%)
SNPs only	-	-	19 (20%)	-
Lineage				
1 (EAI)	22 (34%)	6 (18%)	4 (4%)	1 (2%)
2 (Beijing)	8 (12%)	1 (3%)	21 (22%)	12 (26%)
3 (CAS)	10 (15%)	8 (23%)	3 (3%)	11 (23%)
4 (EAM)	26 (39%)	19 (56%)	62 (65%)	18 (38%)
M. bovis	-	-	1 (1%)	-
Unclassified/T	-	-	5 (5%)	5 (11%)
Patient origin				
Europe	10 (15%)	16 (47%)	12 (13%)	12 (26%)
Africa	13 (20%)	8 (23.5%)	22 (23%)	12 (26%)
Asia	40 (61%)	2 (6%)	4 (4%)	18 (38%)
The Americas	3 (4%)	8 (23.5%)	9 (9%)	1 (2%)
Unknown	-		49 (51%)	4 (8%)
Drug resistance profile				
Susceptible	66 (100%)	34 (100%)	35 (36%)	-
Mono-resistant	-	-	5 (5%)	-
MDR	-	-	36 (38%)	37 (79%)
XDR	-	-	4 (4%)	-
Unknown	-	-	16 (17%)	10 (21%)

Supplementary table 4.2 Continued.

	Original dataset		Validation dataset	
	Clustered strains (n=66)	**Unclustered strains (n=34)**	**Clustered strains (n=96)**	**Unclustered strains (n=47)**
Gender				
Male	35 (53%)	23 (68%)	NA	
Female	31 (47%)	11 (32%)		
Age at diagnosis				
0-15	-	1 (3%)	NA	
16-30	25 (38%)	13 (38%)		
31-45	12 (18%)	15 (44%)		
46-60	15 (23%)	5 (15%)		
61-75	10 (15%)	-		
76-90	4 (6%)	-		
>90 years --	-	-		
Disease classification				
Pulmonary	36 (54.5%)	27 (79%)	NA	
Extrapulmonary	20 (30%)	1 (3%)		
Pulmonary + Extrapulmonary	10 (15.5%)	6 (18%)		
Smear positivity				
No	38 (58%)	6 (18%)	NA	
Yes	28 (42%)	28 (82%)		
Alcohol consumption				
No	66 (100%)	32 (94%)	NA	
Yes	-	2 (6%)		
Drug-use				
No	65 (98%)	29 (85%)	NA	
Yes	1 (2%)	5 (15%)		

Supplementary table 4.2 Continued.

	Original dataset		Validation dataset	
	Clustered strains (n=66)	Unclustered strains (n=34)	Clustered strains (n=96)	Unclustered strains (n=47)
Homelessness				
No	66 (100%)	33 (97%)	NA	
Yes		1 (3%)		
Traveller to endemic areas				
No	63 (95%)	34 (100%)	NA	
Yes	3 (5%)	-		

NA: not available

Supplementary table 4.3 Genomic positions of SNPs and Indels associated with the clustering phenotype.

Genomic position: polymorphism	Average Score*	Mutations, deletions and insertions (N)		p-value
		In clustering strains	In non-clustering strains	
espE				
4341369: T=>G	291.3	1	0	1
4341402: C=>T	35.1	1	0	1
4341402: T=>aC	32.7	5	0	0.8
4340408: A=>G	244.7	1	0	1
4340330: G=>T	908.2	1	0	1
4341224: G=>C	266.4	1	0	1
PE-PGRS56				
3943650: Δ3bp, Δ1bp	80.9	12	0	**0.0027**
3944270: Δ9 bp	-	1	0	1
3943311: Δ9 bp	-	1	0	1
3941910: Δ9 bp	-	1	0	1

Supplementary table 4.3 Continued.

Genomic position: polymorphism	Average Score*	Mutations, deletions and insertions (N)		p-value
		In clustering strains	In non-clustering strains	
Rv0197				
234082: G=>A	314.2	1	0	1
234242: C=>T	250.3	1	0	1
234265: G=>T	502.7	1	0	1
234477: T=>G	335.9	1	1	1
234477: G=>T	301.8	16	8	**0.0179**
Rv2813-2814c				
3119737: Δ512 bp	-	1	0	1
3120432: +AGC, +AGCA	49.2	4	0	0.9998
3120031: Δ438 bp, Δ218 bp	-	12	3	0.2542
3120395: Δ2 bp	54.6	1	0	1
3119592: Δ292 bp	-	1	0	1
3120321: Δ74 bp	-	5	1	1
3119913: Δ1 bp	19.75	2	1	1
3119663: Δ221 bp, Δ74 bp	-	2	1	1
3119957: Δ438 bp	-	1	0	1
3120469: Δ1,725 bp	-	1	0	1
Rv2815-2816c				
3122774: Δ144bp	-	1	0	1
3122549: Δ72bp	-	2	1	1
3122847: Δ144bp	-	3	0	1
3123209: Δ75bp	-	1	1	1
3122122: Δ72bp, Δ350bp	-	4	0	0.9998
3121879: Δ2bp	247.6	1	1	1
3123284: Δ70bp, Δ142bp	-	8	1	0.4468

Δ = deletion; + = insertion; p-values in **bold** denote mutations significant at the site-specific level. * For SNPs and small Indels in clustering strains.

Supplementary table 4.4 Protein prediction for TIMs associated to an increased clustering phenotype.

Genomic position	Nucleotide change	Amino acid change	Protein Prediction	
			I-Mutant #	PolyPhen &
espE				
4,340,330	**T=>G**	**L21V**	Large Decrease of Stability	NA
4,340,308	A=>G	M47V	Large Decrease of Stability	NA
4,341,224	G=>C	V319L	Large Decrease of Stability	NA
4,341,369	T=>G	L367R	Large Decrease of Stability	NA
4,341,402	**T=>C**	**V378A**	Large Decrease of Stability	NA
Rv0197				
232,574	G=>T	G115V	No effect	Probably damaging
233,564	G=>T	R445L	No effect	Probably damaging
234,082	G=>A	V618M	Large Decrease of Stability	Probably damaging
234,242	C=>T	A671V	No effect	Probably damaging
234,265	G=>T	E679 (STOP)	*Prediction not possible*	*Prediction not possible*
234,268	G=>T	V680F	Large Decrease of Stability	No effect
234,477	**T=>G**	**Y749 (STOP)**	*Prediction not possible*	*Prediction not possible*

NA: No homologs of *espE* were found therefore protein prediction was not possible.
Entries in **bold** denote that backwards mutations of these polymorphisms also occurred.
I-mutant predicts free energy changes of protein stability upon a point mutation under different conditions
& PolyPhen predicts the possible impact of an amino acid substitution on the structure and function of a human protein using straightforward physical and comparative considerations.

Supplementary table 4.5 Count of TIMs in the five genes or intergenic regions associated with clustering across the 19 strains selected for functional validation studies.

		TIMs in individual genes or intergenic regions of interest (n)				
Sequencing ID	**Lineage**	**espE**	**PE-PGRS56**	**Rv0197**	**Rv2813-2814c**	**Rv2815-2816c**
Clustered						
A4	1	1	1	0	0	0
B12	1	0	0	1	0	0
B6	1	1	0	0	0	0
C8	1	1	0	1	0	0
D11	1	0	0	2	1	0
D3	1	0	2	0	0	1
D4	1	1	0	1	0	0
D6	1	0	1	0	0	0
E2	1	0	0	0	2	0
E7	1	0	1	1	0	0
F6	1	0	0	0	0	0
F8	1	0	0	0	5	0
G11	1	1	1	1	0	1
X1	4	1	0	0	0	0
H4	4	1	0	1	0	0
Non-clustered						
A12	1	0	0	0	0	0
C10	1	0	0	0	0	0
D5	4	0	0	0	1	0
F10	4	0	0	0	0	1

Supplementary table 4.6 Summary of relevant experimental findings on the functions of the five TIMs.

Gene	Experimental findings
espE codes for an ESX-1 secretion-associated protein.	Essential for survival of *M. tuberculosis* in C57BL/6J mouse macrophage[144]. Rv3616c, a homologue of espE is essential for in vivo survival of M. tuberculosis in C57BL/6J mice[145]. Homologue of Rv3864 (espE) is an Esx-1 substrate required for virulence of *M. tuberculosis* in C57BL/6J and BALB/C-SCID mice[146].
PE-PGRS56 no data on function	One of the 10 most dominant *M. tuberculosis* H37Rv proteins found within both 30- and 90-day infected guinea pig lung samples[183].
Rv0197 codes for a possible oxidoreductase.	Contains the binding motif for molybdenum cofactor, a key component in tuberculosis pathogenesis[184]. Upregulated during higB expression in M. tuberculosis H37Rv (important for bacterial survival under stress conditions encountered during infection)[185].
Rv2813-14c not coding, intergenic region.	No published data.
Rv2815-2816c contains promotor to both Rv2814c and Rv2815c	No published data.

Part 2

Outcome in tuberculous meningitis

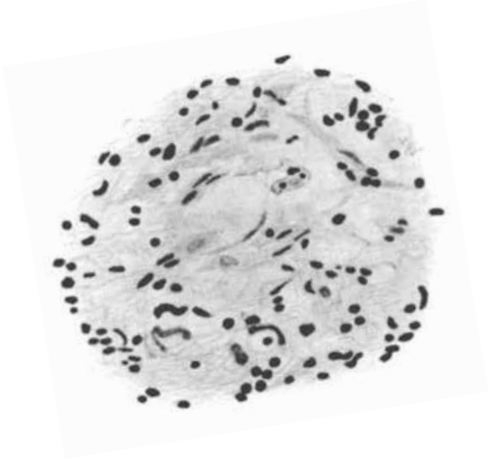

(Ludvig Hektoen. The Fate of the Giant Cells in Healing Tuberculous Tissue, as Observed in a Case of Healing Tuberculous Meningitis. *Journal of Experimental Medicine* 1898)

5

Clinical parameters, routine inflammatory markers, and *LTA4H* genotype as predictors of mortality among 608 patients with tuberculous meningitis in Indonesia

Arjan van Laarhoven* & Sofiati Dian*, Carolien Ruesen, Ela Hayati, Michelle S.M.A. Damen, Jessi Annisa, Lidya Chaidir, Mihai G. Netea, Bachti Alisjahbana, Ahmad Rizal Ganiem, Reinout van Crevel

* Equal contribution

Journal of Infectious Diseases. 2017;215(7):1029–39.

Abstract

Rationale
Damaging inflammation is thought to contribute to the high morbidity and mortality of tuberculous meningitis, but the link between inflammation and outcome remains unclear.

Methods
We performed prospective clinical and routine laboratory analyses of a cohort of adult patients with tuberculous meningitis in Indonesia. We also examined the Leukotriene A4 Hydrolase (*LTA4H*) promoter polymorphism, which predicted CSF leukocyte count and survival of Vietnamese patients with tuberculous meningitis. Patients were followed for >1 year.

Findings
We included 608 patients with tuberculous meningitis whom 67.1% had bacteriological confirmation of disease and 88.2% had severe (i.e., grade II or III) disease. One-year mortality was 43.7% and strongly associated with decreased consciousness, fever, and focal neurological signs. HIV-infection, present in 15.3% of patients, was associated with higher mortality and different CSF characteristics, compared with absence of HIV infection. Among HIV-uninfected patients, mortality was associated with higher CSF neutrophil counts (hazard ratio [HR] 1.10 per 10% increase; 95% confidence interval [CI], 1.04–1.16), low CSF to blood glucose ratio (HR 1.16 per 0.10 decrease; 95% CI, 1.04–1.30), CSF culture positivity (HR 1.37; 95% CI, 1.02–1.84), and blood neutrophilia (HR 1.06 per 10^9 neutrophils/L increase; 95% CI, 1.03–1.10). The *LTA4H* promoter polymorphism correlated with CSF mononuclear cell count but not with mortality (p=.915).

Interpretation
A strong neutrophil response and fever may contribute to or be a result of (immuno)pathology in tuberculous meningitis. Aggressive fever control might improve outcome, and more-precise characterization of CSF leukocytes could guide possible host-directed therapeutic strategies in tuberculous meningitis.

Introduction

Meningitis is the most severe manifestation of tuberculosis, resulting in death or neurological disability of more than 30% of adult patients[25,26]. Previously identified factors associated with mortality of tuberculous meningitis include disease severity at time of presentation, drug resistance, HIV infection, low CD4 cell counts among those HIV-infected, and low cerebrospinal fluid (CSF) cells and glucose level[25,26,186-188]. In addition, it has long been suggested that inflammation contributes to poor outcome of tuberculous meningitis, and adjuvant corticosteroids have shown to reduce mortality of tuberculous meningitis[44].

The exact nature of the detrimental inflammatory response in tuberculous meningitis however remains unclear. A lower CSF cell count was associated with increased mortality among tuberculous meningitis patients in Vietnam[186], but not in China[189], nor South Africa[190]. The type of CSF cells may be important. On average, 70-90% of cells in the CSF are mononuclear cells[26,40], mainly lymphocytes[32], but up to a third of patients show a predominance of neutrophils[41]. Interestingly, among HIV-infected patients in South Africa, CSF neutrophils predicted the occurrence of tuberculous meningitis immune reconstitution inflammatory syndrome (IRIS)[42]. However, in HIV-negative tuberculous meningitis patients there are no published data relating CSF neutrophils with immunopathology or mortality.

A recent study linked Leukotriene A4 Hydrolase (*LTA4H*) rs17525495 genotype to CSF leukocyte count and patient survival. LTA4H converts instable Leukotriene A4 (LTA4) to the stable proinflammatory LTB4, and Vietnamese tuberculous meningitis patients with the gain-of-function TT *LTA4H* genotype showed a higher CSF leukocyte count and better survival with adjuvant corticosteroids, while patients bearing the hypo-inflammatory CC variant showed lower CSF cell numbers and no, or even a negative effect of corticosteroids[191]. To date, no other study has examined the effect of this *LTA4H* genotype on CSF inflammatory profile and survival of tuberculous meningitis.

Adjunctive therapy is topic of intensive research in tuberculosis[192]. Corticosteroids have a proven role in tuberculous meningitis[44], while a range of other immunomodulatory drugs like thalidomide[193], anti-TNF and recombinant interferon-gamma have been used sporadically[194]. Better understanding of immune-mediate pathogenesis of tuberculous meningitis is crucial to development of more effective adjunctive therapy. Therefore, we examined clinical parameters, routine CSF and blood haematology markers, and *LTA4H* genotype in relation to patient survival.

Methods

Setting and patients

In this prospective cohort study we included all patients more than 14 years of age who presented with suspected tuberculous meningitis between October 2006 and June 2016 in a referral hospital in Bandung, Indonesia. Patients were considered suspect for tuberculous meningitis when they presented with subacute illness including headache, fever or focal neurological symptoms, irrespective of the presence or absence of pulmonary or other extrapulmonary tuberculosis. Patients underwent standardised screening that included CSF examination and chest radiography. Neurological status of tuberculous meningitis patients was classified according to modification of the British Medical Research Council (BMRC) definition as follows: grade I, normal consciousness, no neurological signs; grade II, Glasgow Coma Scale score of 11-14 or 15 with neurological signs, and grade III, Glasgow Coma Scale score ≤10 [195]. All patients were tested for HIV, retrospective HIV testing was done anonymously for those patients who died before consent was obtained or who were admitted before routine HIV testing was implemented in 2009. The study was part of the project "Optimization of diagnosis of meningitis", approved by the Ethical Committee of Hasan Sadikin Hospital/Faculty of Medicine of Universitas Padjadjaran, Bandung, Indonesia. A subset of patients in this study was included in one of three randomised clinical trials evaluating intensified antibiotic treatment, for which separate ethical approval was obtained[29,196] (clinical trials registration NCT02169882).

Microbiological testing

Microbiological diagnosis of tuberculous meningitis was done using microscopy, solid Ogawa culture and liquid commercial culture, as well as using microscopic observation drug susceptibility assay (MODS, a liquid culture)[197] after 2010. Four to 10 mL of CSF is concentrated by centrifugation at 3000 x g for 15 minutes, and CSF sediment is used for microscopy and culture. IS6110 PCR was performed retrospectively for a subset of 230 samples[58], and Gene Xpert *MTB/RIF* has been used since 2015. Drug resistance testing is otherwise not routinely available in our setting, but genotypic drug resistance was measured through whole genome sequencing in 102 patients. Further microbiological testing included CSF microscopy and culture for bacteria and fungi, and cryptococcal antigen testing for those HIV-infected. CSF real-time PCR and serological testing for *Toxoplasma gondii* was performed retrospectively for HIV-infected patients[198].

Treatment and follow-up

Tuberculous meningitis was treated with a combination of rifampicin (450 mg, corresponding to approximately 10 mg/kg), isoniazid (300 mg), ethambutol (750 mg) and pyrazinamide (1500 mg) for six months. For unconscious patients, drugs were given by nasogastric tube. As part of two published pharmacokinetic studies[29,199] and one ongoing RCT (NCT02169882), 47 patients received high-dose rifampicin, and 25 patients received moxifloxacin instead of ethambutol. Patients were given adjunctive dexamethasone, following the internationally accepted six-week tapering regimen starting at 0.3 mg/kg for grade I and 0.4 mg/kg for grade II/III tuberculous meningitis[186], and switching to an equivalent dose of oral prednisolone in case of early discharge. Patients with newly diagnosed HIV infection were started on efavirenz-based antiretroviral treatment 4–8 weeks after the start of tuberculosis treatment[200]. Patients were followed prospectively for at least one year. Field doctors or nurses made phone calls, and a social worker conducted home visits for patients not returning after hospital discharge. Death after hospital discharge was assessed by interview of family members and retrieval of patients' death certificates from local authorities.

LTA4H genotyping

Genotyping for rs17525495 *LTA4H* single nucleotide polymorphism (SNP) was performed using the TaqMan C__25593629_10 assay on the 7300 ABI real-time PCR system (Applied Biosystems, Foster City, CA). Samples with an indeterminate allele call could be assigned in a second run except for one, resulting in a final 99.8% call rate.

Case definitions

Most meningitis patients in this setting present with subacute disease, and tuberculosis is the commonest cause[25]. Tuberculous meningitis was classified as "definite" if either CSF microscopy for acid-fast bacilli, *M. tuberculosis* culture or PCR was positive. Diagnosis of cerebral toxoplasmosis was based on toxoplasma PCR or neuroimaging[198]; cryptococcal meningitis on India Ink or CrAg testing[201]; and acute bacterial meningitis on Gram-staining. Based on prior evaluation of CSF characteristics of definite and clinically suspected cases in this cohort, patients were classified as having probable tuberculous meningitis if they had a CSF to blood glucose ratio <0.5 combined with a CSF cell count ≥ 5 /μL. Patients for whom no alternative diagnosis was made and who presented with a CSF leukocyte count <5 /μL were classified as no meningitis. All remaining patients were classified as unknown diagnosis. Not all information listed in the recent consensus-based research definition for tuberculous meningitis[202] was available, and a positive score according to this definition

suggesting "probable meningitis" (≥ 10 points in the absence of neuroimaging) was found in 36% of patients without meningitis, and 41.2% of those without a diagnosis according to our classification. For the purpose of this study, we therefore chose our own, somewhat more specific case definition for probable tuberculous meningitis.

Data analysis and statistics

Patient characteristics, presented as medians (with interquartile ranges) or proportions as indicated, were compared between HIV-infected and non-infected patients, and subsequent analyses were restricted to HIV-negative patients. Only patients with complete data for the respective variables were included for each analysis, as indicated in the legends of figures and tables. Kaplan-Meier curves were used to illustrate survival over time, with continuous predictors divided in three groups, with cut-offs allowed to deviate slightly from exact tertiles to improve interpretability of results. Glasgow Coma Scale score was treated as a continuous variable to avoid loss of power by stratification. All analyses were performed with RStudio in R 3.3.1. using the R packages ggplot2, reshape2, dplyr, openxlsx, tableone, survminer and Hmisc. Univariate and multivariate Cox regression was performed using the R package survival and hazard ratios as well as the result of log-likelihood ratio tests were reported. CSF cell counts and protein were positively skewed and therefore log-transformed, using a $\log_{10}[x+1]$-transformation to avoid having to exclude patients from regression analysis in whom either CSF cells or CSF protein were zero. Sensitivity analyses were performed excluding culture-negative cases, patients who did not start on corticosteroids, patients who participated in a trial or with known drug-resistant *M. tuberculosis*. Secondary analysis was done to distinguish early and delayed mortality, with early and late definitions based on the median time to death, to assure equal power for both groups. Secondary analysis for the genetic analysis involved a recessive model comparing the *LTA4H* TT genotype against the CC/CT genotypes combined. A correlation matrix was made using the R package corrplot with Spearman ranking, on pairwise-complete observations of all continuous variables. Multivariate analysis was performed as secondary analysis to explore dependence of predictors for clinical, CSF and blood variables separately, entering variables with p values < .1 in univariate analysis in the model.

Results

Clinical presentation and patient mortality

From 1186 patients with clinically suspected meningitis, we excluded 156 patients with incomplete baseline data, 171 with no meningitis or an alternative diagnosis, and 251 with no final diagnosis. This left 608 tuberculous meningitis patients for further analysis, including 55.3% with culture-confirmed tuberculous meningitis and another 11.0% confirmed by in-house PCR or Gene Xpert. Patients generally presented with British Medical Research Counsil tuberculous meningitis Grade II (73.7%) or Grade III (14.5%) tuberculous meningitis; 52.0% had motor abnormalities, and 59.7% cranial nerve palsy. Ninety-three patients (15.3%) were HIV-infected, presenting with severe disease, with available median CD4 counts of 62 per blood (IQR 43-186) in 2014-2016. CSF examination showed typical abnormalities with elevated cell count and protein, and low glucose, especially among HIV-negative patients (**table 5.1**). Follow-up data were complete for 91.5% of patients at one month and 73.2% at one year. One-year mortality of patients with tuberculous meningitis was very high, with values of 60.0% (95% CI 47.8–69.9) for HIV-infected and 40.7% (95% CI 36.1–45.1) for HIV-uninfected patients (HR 1.99, 95% CI: 1.46–2.72, **figure 5.1A**), with a median time to death of 4 and 6 days after start of treatment respectively. As expected, those with the lowest Glasgow Coma Scale had the highest mortality (shown for 447 HIV-negative patients in **figure 5.1B**). We could not analyse an effect of adjuvant corticosteroids, as virtually all patients received corticosteroids (95.1% verified in individual case records). Isoniazid and/or rifampicin resistance (detected in 9 patients) was too infrequent to be analysed separately. The same was true for the use of high dose rifampicin (n=47), or moxifloxacin instead of ethambutol (n=25).

Baseline clinical and laboratory parameters as predictors for death

We restricted further analysis to the 515 HIV-negative patients because of large differences between HIV-infected and noninfected patients in terms of survival and laboratory parameters, and the relatively small number (n=93) of HIV-infected patients. Like Glasgow Coma Scale score, BMRC tuberculous meningitis grade was a very strong predictor of survival (**table 5.2**). Motor abnormalities and increased body temperature (**figure 5.2A**) also predicted mortality; risk estimates for these clinical markers were higher for early (0 - 6 days) compared to late (7 - 365 days) mortality (**supplementary table 5.1**).

Table 5.1 Characteristics of tuberculous meningitis patients, by HIV-status

	HIV-negative (N=515)		HIV-positive (N=93)		P[a]
	Median or %		Median or %		
Clinical					
Sex, male	59.0%		77.4%		< .001
Age, years	29.0	(22.0-37.0)	31.0	(27.0-35.0)	.039
Tuberculous meningitis grade[b]					0.078
I	11.1%		16.5%		
II	75.4%		63.3%		
III	13.6%		20.3%		
Temperature, °C	37.6	(36.8-38.1)	37.2	(36.7-38.2)	.288
Glasgow Coma Scale score	13	(12-15)	13	(11-15)	.509
Seizures present	7.6%		13.1%		.151
Motor abnormalities present	52.0%		52.3%		1
Cranial nerve palsy present	61.1%		51.8%		.133
Abnormal chest radiograph findings	73.8%		56.3%		.001
Cerebrospinal fluid					
Leukocytes, cells/μL	150	(49-326)	48	(11-146)	< .001
Neutrophils, % of total	30	(13-59)	27	(10-60)	.261
Neutrophils, cells/μL	33	(8-109)	8	(2-39)	< .001
Mononuclear cells, % of total	70	(41-87)	72	(40-90)	.274
Mononuclear cells, cells/μL	85	(25-176)	27	(6-111)	< .001
Protein, mg/dL	181	(85-364)	143	(65-245)	.011
CSF to blood glucose ratio	0.19	(0.11-0.32)	0.31	(0.17-0.42)	< .001
M. tuberculosis culture positive	58.6%		40.7%		.002

Blood					
Haemoglobin, g/dL	12.2	(10.5-13.6)	11.5	(9.9-12.7)	.011
Leukocytes, 10^9/L	10.9	(8.1-13.8)	6.0	(4.6-9.6)	< .001
Neutrophils, % of total	85.0	79.0-89.0)	80.0	(71.2-87.8)	.001
Neutrophils, 10^9/L	8.9	(6.8-12.3)	5.2	(3.4-8.6)	< .001
Lymphocytes, % of total	9.0	(6.0-14.5)	13.5	(6.2-20.8)	.001
Lymphocytes, 10^9/L	1.0	(0.6-1.5)	0.8	(0.5-1.1)	.044
Monocytes, % of total	5.0	(2.0-670)	4.0	(3.0-6.8)	.564
Monocytes, 10^9/L	0.5	(0.2-0.8)	0.3	(0.1-0.4)	< .001
Platelets, 10^9/L	300	(215-386)	227	(153-326)	< .001
Genetic					
LTA4H rs17525495 genotype					.487
CC	56.1%		48.4%		
CT	35.5%		40.3%		
TT	8.4%		11.3%		

Data are percentage for categorical variables and median (with interquartile range) for continuous variables. Data is 100% complete for age and sex, ≥ 88% for other clinical parameters, ≥ 95% for inflammatory parameters except for blood differentials (66% complete) and 81% complete for *LTA4H* genotype.
[a] By the $\chi 2$ test, for categorical variables, and Mann-Whitney U test, for continuous variables. Values of <.05 are considered statistically significant.
[b] following the British Medical Research Council grading.

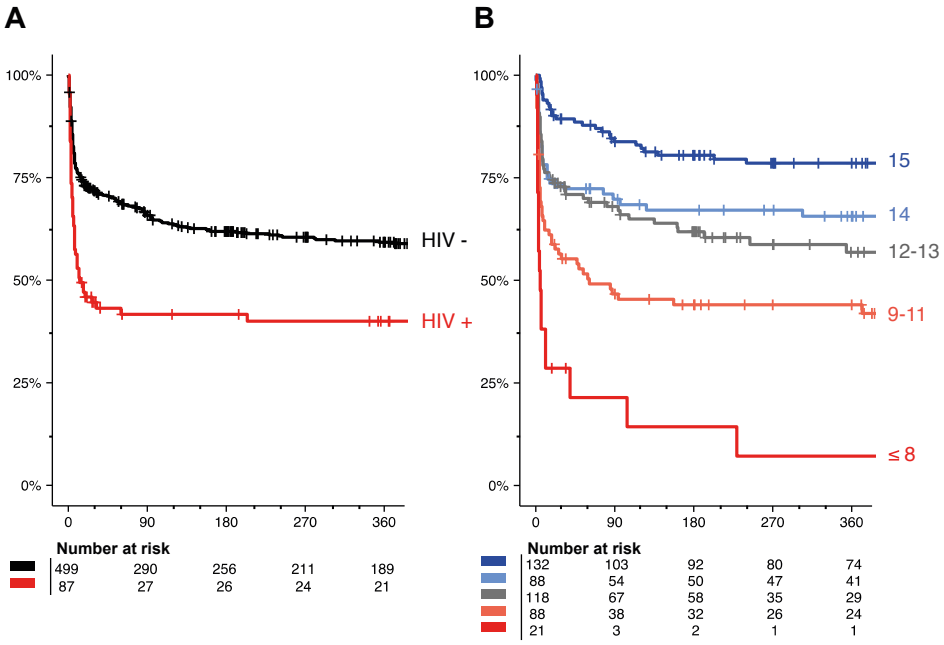

Figure 5.1 Predictors for 365-day mortality due to tuberculous meningitis.

(A) HIV-status in all patients and (B) Glasgow Coma Scale score in HIV-negative patients with survival tables for numbers at risk are shown below the Kaplan-Meier curves.

A focus on CSF characteristics revealed that low CSF to blood glucose ratio (**figure 5.2B**) and elevated protein were associated with death in univariate Cox regression, while the total CSF leukocyte count was not. However, a 10% increase in CSF neutrophil proportion, was associated with a 10% increase in the hazard for mortality. The sensitivity analysis in culture-confirmed cases showed that both neutrophil percentage and count increased risk of mortality. This indicates that neutrophils, rather than a decrease of mononuclear cells are responsible for this effect. Patients with more than 50% CSF neutrophils had a particularly high risk of dying (**figure 5.2C**). Interestingly, a low glucose ratio was more strongly associated with delayed than with early mortality, while CSF neutrophil proportion similarly predicted early and late mortality (**supplementary table 5.1**). Similar or slightly higher risk estimates were found when the analysis was restricted to patients with a positive CSF M. tuberculosis culture (**table 5.2**). By itself, a positive CSF *M. tuberculosis* culture, reflecting a higher bacillary load, was associated with an estimated 1-year mortality of 44.4% (95% CI 35.5–47.3)

compared with 34.8% (95% CI 27.7–41.2) for a CSF culture negative for M. tuberculosis.

Blood neutrophilia (**figure 5.2D**) and corresponding leucocytosis were associated with higher 365-day mortality. In this analysis –still restricted to HIV-uninfected patients– patients with less than 1.3 x 10^9/L lymphocytes, and those with low (< 0.30) or high (≥ 0.60 x 10^9/L) monocytes, showed a higher risk of dying. In secondary analysis, monocyte-lymphocyte ratio (ML-ratio), which has been linked to tuberculosis susceptibility[203], was associated with mortality as well (HR 1.24, 95% CI 1.03–1.51, **supplementary figure 5.1**). Risk estimates for blood markers were similar for early and delayed mortality (**supplementary table 5.1**).

LTA4H genotype

Among 427 HIV-uninfected patients, 56.2% had a CC, 35.6% a CT, and 8.2% a TT rs17525495 *LTA4H* genotype (**table 5.3**). Clinical characteristics were not associated with genotype except for sex, but CSF mononuclear cells were different (median 91 cells/μL in TT vs. 65 cells/μL in TC and 10^9 cells/μL in CC). Total CSF leukocyte count, neutrophils, protein and CSF to blood glucose ratio were not associated with genotype. The percentage culture positivity decreased as a function of the presence of the T allele (p=.013), which is considered to be proinflammatory. *LTA4H* genotype was not associated with a difference in patient survival (**table 5.2**), also in sensitivity analyses excluding 177 patients with negative CSF culture (p=.585), 6 who had not received corticosteroids (p=.845), 9 who had isoniazid and/or rifampicin drug resistant tuberculous meningitis (p=.805) or 85 who participated in a trial (p=.740). In a secondary analysis applying a recessive model, we increased power by combining CC/CT genotypes and compared against the TT genotype: the TT genotype showed a non-significant protective effect (HR 0.91, 95% CI 0.52–1.60), with a similar effect after adjustment for sex and age (HR 0.86, 95% CI 0.49–1.52) and an increased but still not significant effect after adjustment for Glasgow Coma Scale score (HR 0.71, 95% CI 0.38–1.36). Indeed, among 175 patients with milder disease (Glasgow Coma Scale score 14-15) those with the TT genotype showed a trend towards better survival compared to the combined group with the CC or CT genotype (**supplementary figure 5.2**).

Table 5.2 Univariate Cox regression for prediction of 365-day mortality in HIV-negative tuberculous meningitis patients.

	All (N=499)			Culture positive (N=290)		
	HR (95% CI)		p	HR (95% CI)		p
Clinical						
Male sex	1.18	(0.88–1.58)	.258	1.28	(0.88–1.86)	.192
Age, per 10-year increase	1.12	(1.00–1.25)	.048	1.05	(0.90–1.22)	.538
Tuberculous meningitis grade, overall (df = 2)			<.001			<.001
I	1.00			1.00		
II	2.13	(1.12–4.06)	.022	2.72	(1.10–6.73)	.031
III	6.20	(3.11–12.37)	<.001	8.51	(3.29–22.01)	<.001
Body temperature, per 1°C increase	1.28	(1.09–1.50)	.002	1.22	(0.99–1.50)	.067
Glasgow Coma Scale score, per point higher	0.78	(0.74–0.83)	<.001	0.80	(0.75–0.86)	<.001
Seizures present	1.26	(0.74–2.14)	.393	1.20	(0.59–2.47)	.616
Motor abnormalities present	1.90	(1.38–2.61)	<.001	1.92	(1.29–2.85)	.001
Cranial nerve palsy present	1.17	(0.86–1.59)	.319	1.41	(0.94–2.11)	.094
Abnormal chest radiograph findings	1.07	(0.76–1.50)	.706	1.06	(0.68–1.65)	.812
Cerebrospinal fluid						
Leukocytes, per 10-fold increase	1.01	(0.82–1.25)	.894	1.13	(0.84–1.51)	.425
Neutrophils, per 10% increase	1.10	(1.04–1.16)	<.001	1.10	(1.03–1.18)	.004
Neutrophils, per 10-fold increase	1.20	(0.99–1.45)	.057	1.35	(1.03–1.78)	.029
Mononuclear cells, per 10% increase	0.91	(0.86–0.96)	<.001	0.91	(0.85–0.97)	.004
Mononuclear cells, per 10-fold increase	0.90	(0.73–1.12)	.354	1.02	(0.76–1.35)	.909
Protein, per 10-fold increase	1.33	(1.03–1.71)	.027	1.65	(1.14–2.4)	.009
CSF to blood glucose ratio, per 0.10 increase	0.86	(0.77–0.96)	.005	0.85	(0.73–0.98)	.030
M. tuberculosis culture positive	1.37	(1.02–1.84)	.039	n/a (all culture positive)		

Blood						
Haemoglobin, per 1 g/dL increase	1.00	(0.93–1.07)	.902	1.03	(0.94–1.13)	.477
Leukocytes, per 1x10^9/L increase	1.04	(1.02–1.07)	<.001	1.06	(1.02–1.10)	.001
Neutrophils, per 1% increase	1.04	(1.01–1.06)	.004	1.05	(1.02–1.09)	.003
Neutrophils, per 1x10^9/L increase	1.06	(1.03–1.10)	<.001	1.09	(1.05–1.13)	<.001
Lymphocytes, per 1% increase	0.96	(0.93–0.99)	.006	0.95	(0.91–0.99)	.012
Lymphocytes, per 1x10^9/L increase	0.88	(0.68–1.14)	.347	0.81	(0.56–1.17)	.255
Monocytes, per 1% increase	0.96	(0.91–1.02)	.166	0.93	(0.87–1.00)	.055
Monocytes, per 1x10^9/L increase	1.20	(0.83–1.76)	.335	1.01	(0.63–1.61)	.965
Platelets, per 1x10^9/L increase	0.60	(0.20–1.79)	.363	0.76	(0.20–2.90)	.683
Genetic						
LTA4H rs17525495 genotype, overall (df = 2)			.915			.585
CC	1.00			1.00		
CT	0.96	(0.68–1.34)	.795	1.21	(0.80–1.82)	.367
TT	0.89	(0.50–1.60)	.707	0.85	(0.34–2.12)	.728

Data are 100% complete for age and sex, ≥ 88% for other clinical parameters, ≥ 95% for inflammatory parameters except for blood differentials (65% complete) and 83% complete for *LTA4H* genotype. CSF cell counts and protein were analysed after $\log_{10}[x+1]$-transformation. Overall p-values (for tuberculous meningitis grade and *LTA4H* genotype) are results of log-likelihood ratios from Cox regression model. HR = hazard ratio; df = degrees of freedom; CI = confidence interval.

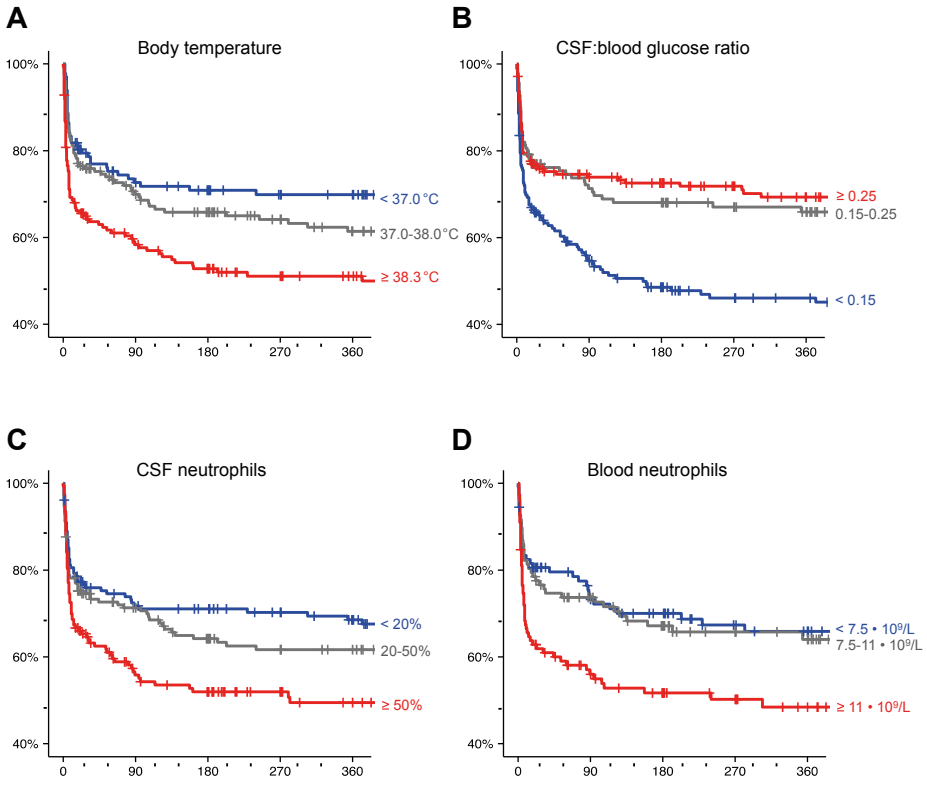

Figure 5.2 Inflammatory markers as predictors for 365-day mortality in HIV– negative patients with tuberculous meningitis.

Kaplan-Meier curves are divided in tertiles with cut-offs rounded to meaningful numbers for (A) body temperature in °C, (B) CSF to blood glucose ratio, (C) CSF neutrophil levels as a percentage of the total CSF leukocyte count, and (D) blood neutrophil counts in 10^9 cells/L.

Prognostic markers - correlation and multivariate Cox regression analysis

We next examined the correlation of clinical, CSF and blood parameters linked with death. Age, fever, Glasgow Coma Scale score and motor abnormalities showed no correlation with one another, and were independently associated with mortality in Cox regression (**figure 5.3, table 5.4**). CSF neutrophil percentage, protein and glucose showed moderate correlation, and independently predicted death in multivariate analysis, while culture positivity did not. CSF markers showed only a weak correlation with blood leukocytes. Blood neutrophil count

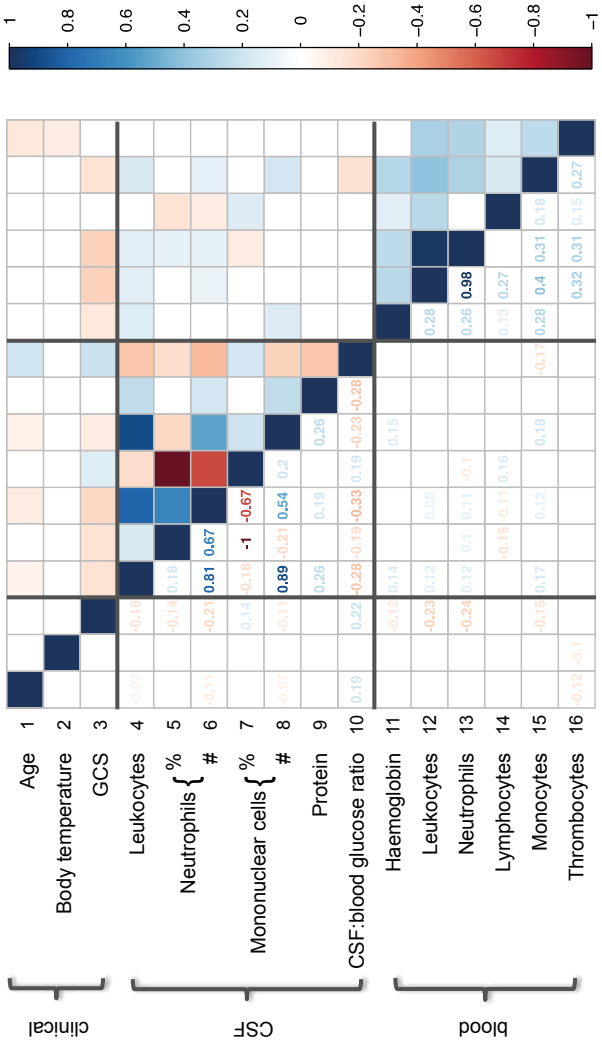

Figure 5.3 Correlation matrix for clinical and inflammatory markers in HIV–negative patients with tuberculous meningitis.

The correlation matrix was made with Spearman ranking, using pair-wise–complete observations. Abbreviation: GCS, Glasgow Coma Scale.

Table 5.3 Characteristics of HIV-negative tuberculous meningitis patients by *LTA4H* rs17525495 genotype.

	CC (N = 240)		CT (N = 152)		TT (N = 35)[a]		
	median or %		median or %		median or %		p[b]
Clinical							
Sex, male	55.0%		54.6%		80.6%		.012
Age, years	28.0	(21.0-37.0)	28.0	(22.0-38.0)	28.0	(21.8-37.2)	.758
Tuberculous meningitis grade[c]							
I	9.9%		8.6%		5.7%		.904
II	77.1%		77.1%		77.1%		
III	13.0%		14.3%		17.1%		
Temperature, °C	37.6	(36.8-38.0)	37.8	(36.8-38.3)	37.0	(36.7-38.0)	
Glasgow Coma Scale score	13	(11-15)	13	(12-15)	13	(11-14)	.139
Seizures present	4.7%		9.0%		6.2%		.211
Motor abnormalities present	56.0%		51.2%		56.2%		.270
Cranial nerve palsy present	63.2%		64.5%		71.4%		.665
Abnormal chest radiograph findings	73.0%		77.7%		64.7%		.641
Cerebrospinal fluid							
Leukocytes, cells/µL	164	(51-351)	138	(49-298)	202	(112-337)	.213
Neutrophils, % of total	34	(14-59)	31	(15-60)	24	(9-47)	.119
Neutrophils, cells/µL	34	(10-124)	32	(9-113)	38	(11-83)	.924
Mononuclear cells, % of total	66	(41-87)	69	(40-85)	76	(52-91)	.144
Mononuclear cells, cells/µL	91	(28-185)	65	(31-158)	109	(75-276)	.031
Protein, mg/dL	180	(112-350)	206	(101-400)	171	(97-383)	.557
CSF to blood glucose ratio	0.19	(0.10-0.29)	0.20	(0.12-0.32)	0.18	(0.13-0.28)	.742
M. tuberculosis culture positive	63.4%		53.6%		40.0%		.013

Blood							
Haemoglobin, g/dL	11.9	(10.5-13.4)	12.2	(10.5-13.7)	13.1	(11.4-14.5)	.046
Leukocytes, 10^9/L	10.6	(8.0-13.5)	10.8	(8.1-14.0)	13.6	(9.9-17.9)	.032
Neutrophils, % of total	85.0	(80.0-89.0)	84.0	(78.2-89.0)	84.5	(80.8-88.3)	.970
Neutrophils, 10^9/L	8.8	(6.6-12.0)	8.4	(6.2-12.5)	10.9	(8.5-15.3)	.147
Lymphocytes, % of total	9.0	(6.0-14.0)	9.0	(5.0-14.5)	10.0	(5.0-11.5)	.848
Lymphocytes, 10^9/L	1.0	(0.6-1.5)	0.9	(0.6-1.4)	1.0	(0.6-1.5)	.683
Monocytes, % of total	5.0	(2.0-7.0)	5.0	(3.0-7.5)	6.0	(4.0-9.2)	.238
Monocytes, 10^9/L	0.5	(0.2-0.8)	0.5	(0.2-0.9)	0.7	(0.4-1.0)	.077
Platelets, 10^9/L	294	(215-373)	281	(217-368)	337	(261-452)	.114

Data are % of patients or median value (interquartile range). Data are 100% complete for age and sex, ≥86% complete for other clinical parameters, and ≥96% complete for inflammatory parameters except for blood differentials (59% complete).

[a] The TT genotype is considered to be proinflammatory and was associated with lower mortality among Vietnamese patients receiving corticosteroids.

[b] By the $\chi 2$ test, for categorical variables, and the Kruskal–Wallis test, for continuous variables. Values of <.05 are considered statistically significant.

[c] following the British Medical Research Council grading.

was the sole blood inflammatory marker independently associated with death in a Cox regression model (neutrophil count correlates strongly with blood total leukocyte count and is the product of total leukocyte count and blood neutrophil percentage, both of which were not included in the model). Correlation matrices were similar for patients who died and those who survived the first year (not shown).

Table 5.4 Multivariate Cox regression for clinical, cerebrospinal fluid and blood variables separately

		365-day mortality		
		HR (95% CI)		p
A	**Clinical**			
	Age, per 10 years increase	1.16	(1.02–1.31)	.015
	Body temperature, per 1 °C increase	1.24	(1.06–1.46)	.009
	Glasgow Coma Scale score, per point higher	0.80	(0.75–0.86)	<.001
	Motor abnormalities present	1.50	(1.06–2.12)	.020
B	**Cerebrospinal fluid**			
	Neutrophils, per 10% increase [a]	1.10	(1.04–1.16)	.012
	Protein, per 10-fold increase	1.42	(1.06–1.90)	.018
	CSF to blood glucose ratio, per 0.10 increase	0.90	(0.80–1.01)	.079
	M. tuberculosis culture positive	1.13	(0.81–1.58)	.455
C	**Blood**			
	Neutrophils, per $1x10^9$/L increase [b]	1.06	(1.03–1.10)	<.001
	Monocyte to lymphocyte ratio, per 0.10 increase	1.20	(0.97–1.47)	.089

Multivariate Cox regression for survival including variables with a p value of < .1 in univariate analysis for 365-day mortality. Three separate models were run: for analysis of clinical variables, 412 patients had complete data; for analysis of CSF inflammatory markers, 464 had complete data; and for analysis of blood inflammatory markers, 327 had complete data available.

[a] CSF neutrophil percentage was used because of its more common use in clinical practice and its stronger association as compared to count.

[b] Blood neutrophil count was used being the multiplication of neutrophil concentration and total leukocyte count (both univariate predictors of mortality) together with the monocyte to lymphocyte ratio (resulting from secondary analysis). CI = confidence interval; HR = hazard ratio.

Discussion

In a prospectively followed cohort of 608 tuberculous meningitis patients in Indonesia, one-year mortality was 43.7%. Mortality was linked with previously reported risk factors (HIV-infection, disease severity, neurological complications, and low CSF glucose) and several newly identified factors including fever, CSF culture-positivity, a predominance of neutrophils in CSF, and a high blood monocyte to lymphocyte ratio. Unlike a previous study in Vietnam we found no relation between the leukotriene A4 Hydrolase (*LTA4H*) promoter polymorphism rs17525495 and outcome.

Tuberculous meningitis is relatively rare, but responsible for a disproportionate number of tuberculosis deaths. Most studies are either relatively small, or compromised by low rates of bacteriological confirmation. Two large clinical trials conducted in Vietnam reported a nine-month mortality of 31.8% [186] and 27.9% [26] for patients who received dexamethasone and standard dose rifampicin. Mortality in our cohort is higher (42.6% at nine months), possibly because 83% of our patients were not included in a clinical trial, or because our patients present with more advanced disease; the proportion of patients with grade I disease is 12.0% in our cohort versus 32.3% and 39.1% in Vietnam. HIV was associated with a two-fold higher risk of death in this study, underlining the importance of early HIV diagnosis and treatment[25].

Because HIV strongly influences inflammatory phenotype and mortality, we concentrated further analysis on HIV-uninfected cases, making it the largest study on predictors of death in this group, with 67% of cases bacteriologically confirmed, and extensive follow-up. Our data clearly show that neurological complications, especially motor abnormalities, are strongly predictive of a poor outcome of tuberculous meningitis. Not unexpectedly, these risk factors weighed strongest for early mortality. Half of deaths in our cohort occurred in the first six days after start of treatment, mostly among those with the most-advanced stage of disease, again reflecting the importance of earlier diagnosis and treatment.
We are the first to report that febrile patients have a higher risk of dying. Fever may reflect damaging inflammation or increased metabolism of a damaged brain, as has been suggested by increased mortality of stroke patients with fever[204]. Further study should determine if aggressive reduction of fever, as advocated in an excellent review on acute care management of tuberculous meningitis[28], can improve outcome of tuberculous meningitis. Of note, mild hypothermia showed no benefit and even seemed harmful in an randomised controlled trial in acute bacterial meningitis patients[205].

Evaluation of CSF markers revealed that high neutrophil numbers strongly predicted mortality, while we did not find a higher fraction of neutrophils in patients with a short duration of disease (data not shown), unlike one earlier case series[32]. Neutrophils are capable of killing *M. tuberculosis* but may also play a detrimental role in tuberculosis[84]. Like in the lung[206], *M. tuberculosis* can also infect neutrophils in the CSF[207]. Interestingly, a higher proportion of CSF neutrophils was associated with CSF culture positivity in studies from Vietnam[208] and Brazil[209], and with the occurrence of IRIS in South Africa[42]. High blood neutrophil counts, which did not correlate with CSF neutrophil counts, also predicted death. The association of a high monocyte to lymphocyte ratio to death provides further support for a possible detrimental role of a disregulated innate immune response in tuberculous meningitis. Of course, we should be careful about inferring a causal role for neutrophils in tuberculous meningitis-associated death, as higher CSF neutrophil counts might also be an epiphenomenon of unfavourable biological processes taking place in tuberculous meningitis. Clearly, the possible detrimental role of neutrophils in tuberculous meningitis needs more study.

We confirmed that a low CSF to blood glucose ratio was associated with mortality, in line with sepsis studies linking cellular metabolism and death[210]. Our study also supports intensified antibiotic treatment as a beneficial strategy, as patients with a CSF culture positive for *M. tuberculosis* had a 37% increased hazard for mortality. In a recent randomized controlled trial, we found that high dose rifampicin administered intravenously, to compensate for poor CSF penetration of rifampicin, was associated with reduced mortality (HR 0.42; 95% CI 0.20–0.91)[29]. A larger randomized controlled trial in Vietnam failed to see an effect of a higher dose oral rifampicin[26], but this may have been due to the modest dose increase in that study[211].

It was recently shown that a polymorphism in *LTA4H* correlated with CSF leukocyte count and survival among 182 Vietnamese tuberculous meningitis patients[191]. This same *LTA4H* genotype was not associated with CSF leukocyte count or with survival in our genotyped cohort of 427 patients, also after correction for possible confounding factors such as disease severity as measured by Glasgow Coma Scale score. Late presentation, which increases mortality, might confound a possible effect of the *LTA4H* genotype and we therefore separately analysed patients with milder disease. Those with the TT genotype showed a trend towards better survival, so an effect in this subgroup cannot be excluded. Unlike the Vietnam study, we could not stratify the effect of *LTA4H* genotype for corticosteroid treatment, as all patients received adjuvant cortico-

steroids according to international guidelines. Our findings suggest that more study is needed to understand the effect of host genetic background on tuberculous meningitis treatment response and outcome, although it will be difficult to examine this specific association outside East-Asia, due to a lower prevalence of the rs17525495 TT *LTA4H* genotype (1000 Genomes Project; available at http://www.internationalgenome.org/).

Our study has several strengths, including its size, high rate of bacteriological confirmation, and complete data and follow-up. We used a somewhat more strict case definition than a consensus definition[202], which still needs evaluation in different settings. Unfortunately, neuroimaging and neurosurgical interventions were not available in this cohort. Also we have no verified treatment adherence. Finally, since our data are observational it is difficult to distinguish causation from association.

In conclusion, this study strengthens the concept that damaging inflammation contributes to the presentation and poor outcome of tuberculous meningitis, and suggests that neutrophils play an important role in this effect. Further immunological, gene expression, metabolic and genetic studies could increase our understanding of immunopathology and help identify targets or genetic markers to guide host-directed therapy in patients with tuberculous meningitis.

Acknowledgements
We thank Pak Hendra, Pak Diyat, Pak Daniel, Feby Purnama, Rani Trisnawati and Shehika Shulda for extending follow-up after discharge; neurology residents for monitoring patients; professor Jelle Goeman for statistical advice; the director of the Hasan Sadikin General Hospital, for accommodating the research.

Author contributions
AvL, SD and CR performed statistical analyses. EH was the field doctor for most of the research period under supervision of SD and ARG. AvL and MSMAD performed the genetic assays. JA and LC led the mycobacteriological laboratory. AvL, SD and RvC performed the literature search and wrote the first complete draft of the report. MGN and BA contributed to the idea of the research and to the manuscript. RvC led the research group and ARG was the Indonesian principal investigator of the cohort. All authors have read and approved the final version.

Supplementary figures

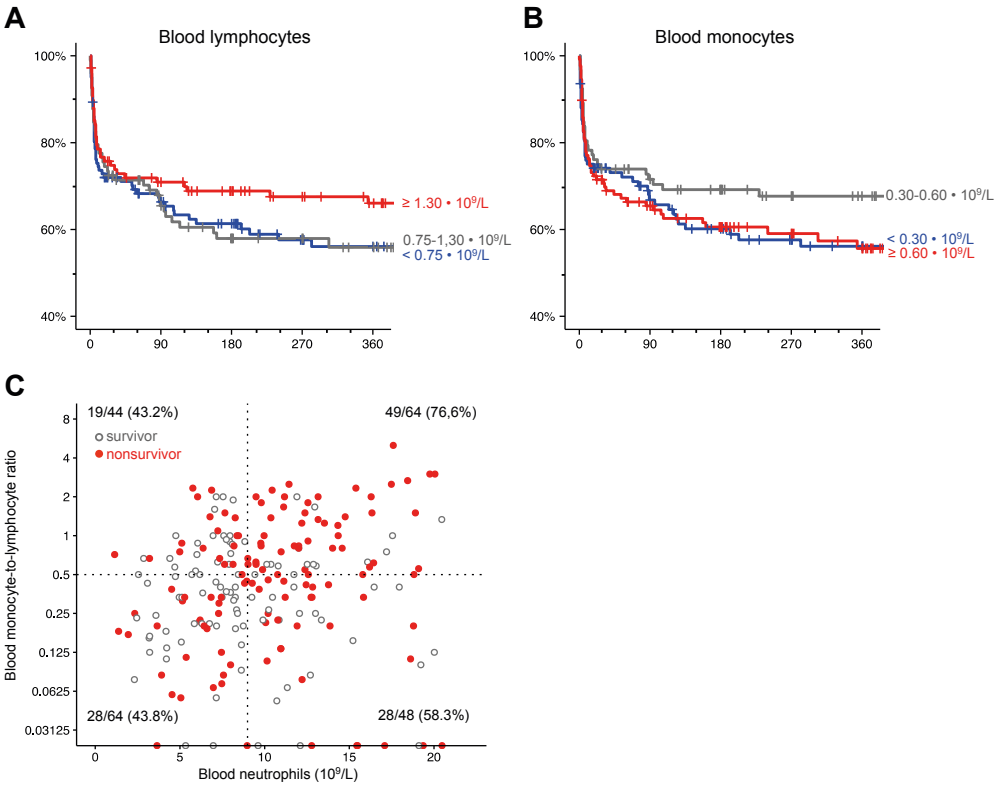

Supplementary figure 5.1 Blood inflammatory markers as predictors for 365-day mortality in HIV-negative tuberculous meningitis patients.

Kaplan Meier curves divided in tertiles with cut-offs rounded to meaningful numbers for blood lymphocytes (A) and monocytes (B) in 10^9 cells/L. C) Blood neutrophils versus blood monocyte-lymphocyte ratio. Individual survivors are indicated by grey open circles and nonsurvivors by red closed circles. Mortality was calculated for each of the four squares, which are divided by the overall medians. Patients with complete follow-up till day 365 are included only, which causes slight overestimation of proportion of nonsurvivors. One outlier (36.9 x 10^9/L neutrophils and ML-ratio of 1) was removed from the graph to improve visibility of the other data points.

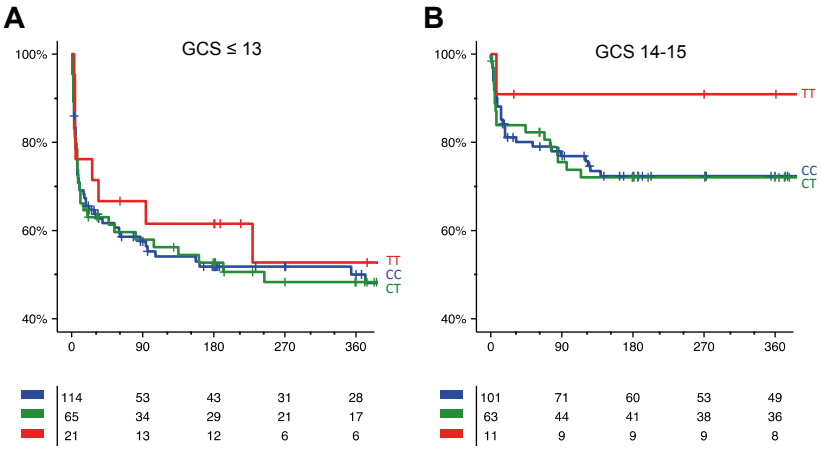

Supplementary figure 5.2 *LTA4H* rs17525495 genotype as predictor for 365-day mortality in HIV-negative tuberculous meningitis patients stratified for disease severity.

Kaplan Meier curves and risk tables for *LTA4H* genotypes CC (blue), CT (green) and TT (red) for patients with (A) severe (Glasgow Coma Scale score ≤ 13) or (B) milder (Glasgow Coma Scale score 14-15) disease. In a recessive model in secondary analysis, TT genotype versus CT/TT combined had a HR 0.81 (95% CI 0.41–1.62, p=.550) in severe and HR 0.31 (95% CI 0.04–2.25, p=.156) in milder disease.

Supplementary table 5.1 Univariate Cox regression for prediction of early (day 0-6) versus late (day 7-365) mortality in HIV-negative tuberculous meningitis patients.

	day 0-6			day 7-365		
	HR (95% CI)		p	HR (95% CI)		p
Clinical						
Male sex	1.19	(0.79–1.8)	.411	1.15	(0.77–1.73)	.494
Age, per 10-year increase	1.13	(0.96–1.31)	.135	1.10	(0.94–1.29)	.249
tuberculous meningitis grade, overall (df = 2)			<.001			.009
I	1.00			1.00		
II	8.20	(1.13–59.3)	.037	1.27	(0.63–2.54)	.507
III	28.7	(3.9–211.31)	.001	3.07	(1.36–6.95)	.007
Body temperature, per 1°C increase	1.36	(1.08–1.71)	.009	1.22	(0.98–1.52)	.074
Glasgow Coma Scale score, per point higher	0.75	(0.70–0.81)	<.001	0.85	(0.77–0.93)	<.001
Seizures present	1.57	(0.78–3.13)	.204	1.04	(0.45–2.39)	.924
Motor abnormalities present	2.00	(1.26–3.20)	.004	1.73	(1.12–2.66)	.013
Cranial nerve palsy present	1.17	(0.75–1.83)	.480	1.09	(0.71–1.67)	.694
Abnormal chest radiograph findings	0.96	(0.59–1.57)	.868	1.16	(0.72–1.88)	.532
Cerebrospinal fluid						
Leukocytes, per 10-fold increase	1.09	(0.81–1.47)	.567	0.92	(0.69–1.24)	.598
Neutrophils, per 10% increase	1.10	(1.02–1.18)	.015	1.09	(1.01–1.18)	.020
Neutrophils, per 10-fold increase	1.30	(1.00–1.69)	.051	1.07	(0.81–1.40)	.644
Mononuclear cells, per 10% increase	0.91	(0.85–0.98)	.016	0.92	(0.85–0.99)	.020
Mononuclear cells, per 10-fold increase	0.96	(0.71–1.30)	.808	0.84	(0.62–1.14)	.259
Protein, per 10-fold increase	1.59	(1.11–2.27)	.011	1.11	(0.77–1.60)	.570
CSF to blood glucose ratio, per 0.10 increase	0.94	(0.83–1.08)	.380	0.77	(0.66–0.91)	.002
M. tuberculosis culture positive	1.29	(0.85–1.96)	.237	1.38	(0.90–2.09)	.136

Blood						
Haemoglobin, per 1 g/dL increase	0.98	(0.89–1.08)	.625	1.00	(0.91–1.11)	.969
Leukocytes, per 1x10^9/L increase	1.04	(1.00–1.07)	.036	1.05	(1.02–1.09)	.005
Neutrophils, per 1% increase	1.03	(1.00–1.07)	.060	1.04	(1.00–1.07)	.042
Neutrophils, per 1x10^9/L increase	1.07	(1.03–1.12)	.001	1.05	(0.99–1.10)	.100
Lymphocytes, per 1% increase	0.96	(0.92–1.01)	.080	0.96	(0.92–1.00)	.067
Lymphocytes, per 1x10^9/L increase	0.87	(0.60–1.27)	.478	0.93	(0.64–1.35)	.709
Monocytes, per 1% increase	0.97	(0.90–1.05)	.414	0.95	(0.89–1.02)	.192
Monocytes, per 1x10^9/L increase	1.13	(0.66–1.92)	.657	1.18	(0.07–2.00)	.539
Platelets, per 1x10^9/L increase	0.22	(0.04–1.07)	.060	1.51	(0.34–6.57)	.586
Genetic						
LTA4H rs17525495 genotype, overall (df = 2)			.988			.865
CC	1.00			1.00		
CT	0.99	(0.61–1.60)	.952	0.97	(0.61–1.53)	.893
TT	1.05	(0.47–2.34)	.901	0.80	(0.34–1.86)	.601

In between day 0 and day 6, 499 patients were at risks and 95 deaths occurred. Of patients still alive at day 7, another 98 patients died between day 7 and day 365. Data is 100% complete for age and sex, ≥ 88% for other clinical parameters, ≥ 95% for inflammatory parameters except for blood differentials (65% complete) and 83% complete for *LTA4H* genotype. CSF cell counts and protein were analysed after $\log_{10}[x+1]$-transformation. HR = hazard ratio; df = degrees of freedom.

6

Immune cell characteristics and cytokine responses in adult HIV-negative tuberculous meningitis: an observational cohort study

Arjan van Laarhoven, Sofiati Dian, Suzanne van Dorp, Feby Purnama, Valerie A.C.M. Koeken, Emira Diandini, Fitria Utami, Resvi Livia, Lika Apriani, Edwin Ardiansyah, Rob ter Horst, Mihai G. Netea, Tri Hanggono Achmad, Philip C. Hill, Rovina Ruslami, Bachti Alisjahbana, James E. Ussher, Agnes Indrati, Ayesha Verrall, Ahmad Rizal Ganiem, Reinout van Crevel

Submitted

Abstract

Rationale
Immunopathology contributes to high mortality in tuberculous meningitis but little is known about the blood and cerebrospinal fluid (CSF) immune response.

Methods
We performed the first in-depth immunophenotyping study combining blood and CSF flow cytometry and ex-vivo cytokine production in tuberculous meningitis patients. We prospectively characterised the immune response of 160 tuberculous meningitis suspects in an Indonesian cohort, including 67 HIV-negative probable or definite tuberculous meningitis cases. Pulmonary tuberculosis patients (n = 26) and healthy controls (n = 27) were recruited from the same site.

Findings
Tuberculous meningitis patients presented with severe disease and 38% died in 6 months. Blood from tuberculous meningitis patients showed lower αβT and γδT cells, NK cells and MAIT cells compared to pulmonary tuberculosis patients (2.4-4-fold, all $p<0.05$) and healthy controls (2.7-7.6-fold, $p<0.001$), but higher neutrophils and classical monocytes (2.3-3.0-fold, $p<0.001$). CSF of tuberculous meningitis patients showed a predominance of αβT cells and NK with higher leukocyte activation compared to blood (1.8-9-fold, $p<0.001$), and CSF αβT and NK cell counts were both associated with better survival ($p<0.05$). Cytokine production in tuberculous meningitis showed a much broader range compared to both control groups ($p<0.001$). Among tuberculous meningitis patients, high ex-vivo production of TNF-α, IL-6 and IL-10 correlated with fever, lymphocyte count and monocyte HLA-DR expression (all $p<0.05$).

Interpretation
Tuberculous meningitis patients show a strong myeloid blood response, with a broad variation in immune function. This may influence the response to adjuvant treatment and should be taken into account in future trials of host-directed therapy.

Introduction

Meningitis is the most severe manifestation of tuberculosis, leaving 30-50% of patients deceased or disabled. Immune pathology is thought to play an important role in the poor outcome of tuberculous meningitis[16]. Adjuvant corticosteroids have shown an overall beneficial effect on survival in HIV-uninfected patients, especially in those with milder disease[44] and are therefore part of routine care. It is conceivable, however, that a hypo-inflammatory subgroup of patients[191] would benefit from withholding corticosteroids as currently examined in HIV-negative patients (NCT02588196), while hyper-inflammatory patients may need additional anti-inflammatory treatment (trial completed, NCT02237365). More detailed information on the local and systemic immune response is needed to rationally select adjuvant agents and patient subgroups for improving host-direct therapy for tuberculous meningitis.

Routine cerebrospinal fluid (CSF) assessment only distinguishes mononuclear from polymorphonuclear cells. The latter, mostly neutrophils, make up on average one third of CSF cells, with higher proportions associated with a worse prognosis (**chapter 5**). Microscopic study of the remaining, mononuclear cells has shown wide variability of cell types and counts[32]. Analysis by flow cytometry has confirmed the presence of αβT and γδT cells, B cells and Natural Killer (NK) cells in CSF of tuberculous meningitis patients[33,212], but these cells have not yet been quantified. NK cells can kill extracellular *M. tuberculosis* and trigger effector mechanisms in macrophages[213]. Other innate lymphocyte populations might also be of importance. Mucosal associated invariant T (MAIT) cells recognize *M. tuberculosis* and are found in the lung in pulmonary tuberculosis[214]. NKT cell number and function are reduced in the blood of tuberculosis patients[215]. Monocytes (myeloid mononuclear cells) recognise *M. tuberculosis*, steer immunity and mature into macrophages with killing capacity[20]. Only one study has examined ex-vivo monocyte responsiveness in tuberculous meningitis[33].

In this study we first characterised and quantified leukocytes in a prospective cohort of tuberculous meningitis patients in blood and CSF. We then established immune phenotype based on ex-vivo whole blood cytokine assays, using pulmonary tuberculosis patients and healthy controls for comparison. We investigated whether separate 'high-responding' and a 'low-responding' immune phenotypes exist and possibly correlate with disease phenotype and outcome.

Methods

Setting and Patients

We prospectively included all patients >14 years of age who presented with suspected tuberculous meningitis (subacute illness including headache, fever or focal neurological symptoms) between December 2014 and July 2016 in the Hasan Sadikin hospital in Bandung, Indonesia. This is a tertiary referral hospital with 966 beds, serving the population of West-Java (43 million). Standardized screening and diagnosis as 'definite tuberculous meningitis' (CSF culture or Gene Xpert positive) or 'probable tuberculous meningitis' (CSF to blood glucose ratio was <0.5 combined with a CSF cell count ≥5 cells/μL), followed the protocols established in **chapter 5**. Follow-up samples (day 2 and 10 for CSF and day 10, 60 and 180 for blood) were done for a subset of patients included in a clinical trial on high-dose rifampicin with inclusion up until November 2016 (NCT02169882). After hospital discharge, patients were followed-up clinically at day 90 and 180. Patients not returning to the hospital were phoned by a social worker. Cause of death, obtained from hospital records or verbal autopsy for those who died after discharge, was classified as: primarily tuberculous meningitis-related (i.e. brain herniation or otherwise increased intracranial pressure); pneumonia or sepsis; other, including non-infection related causes, such as injury, pulmonary embolism and aspiration pneumonia.

Pulmonary tuberculosis patients from the same hospital had chest X-ray abnormalities consistent with pulmonary tuberculosis and 25/26 patients were confirmed by positive sputum culture or smear. Asymptomatic pulmonary tuberculosis household contacts linked to the same study, who had no tuberculosis-suggestive symptoms or X-ray abnormalities and who were Interferon-γ Release Assay (IGRA)-negative were used as controls. HIV-infected patients or controls were excluded from final analysis.

Ethics Statement

Samples for this study were collected as part of three ongoing studies approved by the Ethical Committee of Hasan Sadikin Hospital/Faculty of Medicine of Universitas Padjadjaran, Bandung, Indonesia. Tuberculous meningitis patients were included under the project "Optimization of Diagnosis of Meningitis" (449/UN6.C1.3.3/KEPK/PN/2015). This study sampled only at regular venepunctures and lumbar punctures moments that are part of routine care. Patients, or close relatives of patients who were unconscious therefore gave consent orally. Tuberculous meningitis patients who were part of the high-dose rifampicin study (NCT02169882), gave separate written consent for that study (299/UN6.

C2.1.2/KEPK/PN/2014). Pulmonary tuberculosis patients were part of the TANDEM study[216] (42/UN6.C1.3.2/KEPK/PN/2015) and healthy controls were part of the INFECT study (14/UN6.C2.1.2/KEPK/PN/2014). Pulmonary tuberculosis patients and healthy controls gave written consent for sampling. All samples were handled anonymized.

Flow cytometry

CSF was spun slowly (300 g) for 3 minutes to avoid cell activation, the sediment was resuspended immediately (median 0.8 hours, IQR 0.7-1.0) in 2.5 mL RPMI (ThermoFisher, 22409031) and stored at 4 °C prior to flow cytometry (median 8.7 hours, IQR 4.0-16.2) later. Cell fixation interferes with measurement of activation markers and was therefore not performed. Blood was collected in lithium-heparin tubes and stored at 20-23°C. Blood and CSF samples were processed within 24 hours of collection. Samples were divided in four equal parts, to which a fixed amount (5 μL for CSF, 30 μL for blood) of microparticles (Invitrogen 123count eBeads, 01-1234) was added for quantification, together with fluorochrome-labeled antibodies in four panels: A monocyte/neutrophil panel: CD14 (AF488), CD 16 (PE), HLA-DR (PerCP) and CXCR4 (APC); a NK cell panel: CD3 (AF488), CD16 (PE), CD56 (PerCP) and CD69 (APC); a γδT / NKT cell panel: CD3 (AF488), Va24-Ja18 (PE), Vδ2 (PerCP) and γδ-TCR (APC) and a MAIT cell panel: CD3 (AF488), Vα7.2 (PE), HLA-DR (PerCP) and CD161 (APC). Data were acquired till 1,000,000 events (blood) or a maximum of two minutes (CSF), and were analysed using Kaluza 1.3 (Beckman Coulter) using gating strategies depicted in **supplementary figure 6.1A**. Flow cytometry was started in the seventh month of the study. Routine counts were measured with the Sysmex XN-1000 throughout the study.

Ex-vivo whole blood stimulation assay

Stimuli were prepared in batches at 10 times the final concentration: *M. tuberculosis* H37Rv lysate (final concentration 5 μg/mL), *Streptococcus pneumoniae* lysate (10^6 colony forming units per millilitre, CFU/mL), *Escherichia coli* lysate (10^6 CFU/mL) and *Candida albicans* lysate (10^6 CFU/mL). Live Bacillus Calmette-Guérin (BCG) was resuspended weekly from the vaccine bottle and used at 10^5 CFU/mL. Blood obtained in lithium-heparin tubes (Greiner) was stored at 20-23°C and processed within 24h. Blood was diluted 1:4 with RPMI in a 24-well flat-bottom culture plate and incubated in the presence of the above mentioned stimuli, or left unstimulated, for 24h after which supernatant was stored in two aliquots at -80°C till batch-wise measurement by ELISA: interleukin-1 (IL-1β), IL-1 receptor antagonist (IL-1Ra), tumour necrosis factor alpha (TNF-α) (all from R&D Systems, Minneapolis, MN), and IL-6, IL-10 and interferon-gamma (IFN-γ) (Sanquin, Amsterdam, the Netherlands).

Data analysis

Samples were excluded if they did not meet the technical minimum requirements. For flow cytometry, reasons to exclude were: CSF sample obtained after start of dexamethasone, or not resuspended in medium within 2.5 h, or inadequate fluorochrome staining or inadequate microparticle count in one of four panels. For ex-vivo stimulation exclusion criteria were: blood sample obtained after start of dexamethasone, or processed more than 24h after acquisition, or TNF-α above the detection limit of 90 pg/mL for the unstimulated control.

Analyses were performed in R 3.2.2 (http://www.R-project.org). Non-parametric tests were used for all continuous variables. For principal component analysis (PCA), the covariance matrix was calculated on log-transformed, mean-centered, cytokine data for tuberculous meningitis patients using the R package prcomp. Only stimuli for which data were complete were included. Patients and controls scores were subsequently projected on the principal components using this covariance matrix. A correlation matrix was made using Spearman correlation on pair-wise complete data. Survival analysis was performed using Cox regression with the R packages survival and visualised with survminer. Other packages used were corrplot, dplyr, openxlsx, reshape2 and tableone, and graphs were visualised using ggplot2 enhanced by cowplot.

Results

Patients and quality control

Of 160 patients with suspected tuberculous meningitis who were immunophenotyped, 47 HIV-negative patients did not meet the tuberculous meningitis case definition, and 29 were HIV-positive. After exclusion of samples because of technical issues or because sampling had been performed after the first dose of dexamethasone, 67 HIV-negative tuberculous meningitis patients could be included in the final analysis (**table 6.1**). These 67 patients, 69.0% of whom had culture-confirmed tuberculous meningitis, presented with severe disease, 94.4 % with grade II or III. Tuberculous meningitis patients were slightly younger than pulmonary tuberculosis patients and healthy controls, while sex was similarly distributed (**table 6.1**). Clinical follow-up was complete for all but one tuberculous meningitis patient and 180-day mortality was 40% (**supplementary table 6.1**, **supplementary figure 6.1B**). Cell counts as measured by flow cytometry showed good correlation with routine cell counts (R^2 0.45-0.65 in blood, 0.53-0.70 in CSF, **supplementary figure 6.1C**), although they were systematically lower. The ratio of cell counts using flow cytometry compared to routine counts was 0.73 for

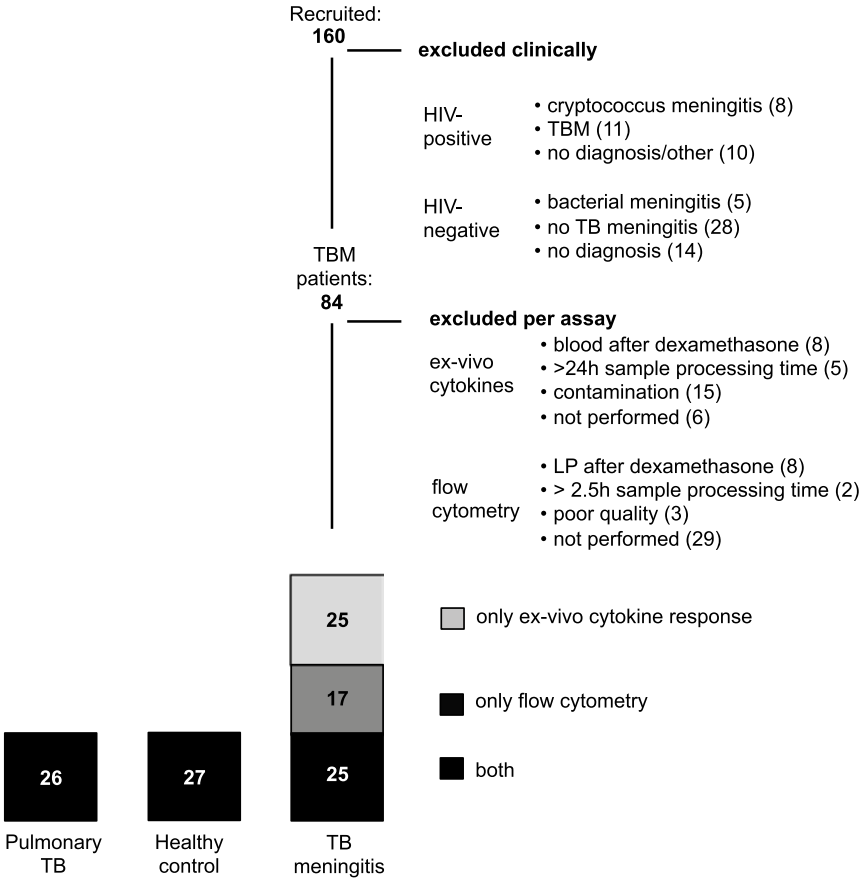

Figure 6.1 Patient inclusion diagram.

Of the 26 patients with pulmonary tuberculosis, one had no ex-vivo cytokine response available. Of the 27 healthy controls, one had no ex-vivo cytokine response and one had no flow cytometry results available. LP = lumbar puncture.

blood neutrophils, 0.76 for blood lymphocytes, 0.42 for blood monocytes, 0.19 for CSF neutrophils and 0.46 for CSF mononuclear cells. These values were not influenced by time from lumbar puncture to resuspension in medium or time to flow cytometric analysis (data not shown). Fifteen patients were excluded from ex-vivo cytokine analysis as result of a batch of contaminated lithium-heparin tubes.

Table 6.1 Comparison of tuberculous meningitis (TBM) patients versus pulmonary tuberculosis (PTB) patients and healthy controls (HC).

Presented are the baseline characteristics of age and sex, routinely obtained cell counts and cell counts by flow cytometry. Comparisons are made by Mann-Whitney U for blood of tuberculous meningitis versus PTB and HC respectively.

		TBM	
		42	
		CSF	blood
sex	N–% male	23 (55%)	
age	year	27 (20–36)	
routine haematology counts			
total leukocytes	× 10^9 cells/L	0.216 (0.136–0.430)	10.1 (8.8–12.0)
neutrophils	× 10^9 cells/L	0.069 (0.026–0.162)	8.6 (7.1–10.2)
lymphocytes	× 10^9 cells/L	0.138 (0.087–0.251)	0.8 (0.4–1.2)
monocytes	× 10^9 cells/L	*	0.7 (0.5–1.0)
thrombocytes	× 10^9 platelets/L	n/a	267 (229–347)
flow cytometry results			
total leukocytes	× 10^6 cells/L	68.4 (33.6–146.9)	7217.5 (5608.5–9258.6)
$CD16^+$ neutrophils	× 10^6 cells/L	12.0 (2.2–47.9)	6000.8 (4254.4–8167.5)
$CD16^{low}$ neutrophils	× 10^6 cells/L	0.5 (0.1–5.1)	113.5 (56.8–268.7)
$CD14^+CD16^-$ monocytes	× 10^6 cells/L	1.3 (0.3–3.0)	300.2 (179.7–395.1)
$CD14^+CD16^+$ monocytes	× 10^6 cells/L	0.2 (0.1–0.5)	7.3 (2.1–15.7)
$CD14^-CD16^+$ monocytes	× 10^6 cells/L	0.1 (0.0–0.3)	1.2 (0.5–1.8)
$CD56^-$ NK cells	× 10^6 cells/L	0.8 (0.3–2.4)	5.8 (2.5–9.4)
$CD56^+$ NK cells	× 10^6 cells/L	2.7 (1.2–7.6)	48.9 (33.7–86.5)
$CD56^{bright}$ NK cells	× 10^6 cells/L	0.5 (0.2–1.3)	1.8 (0.8–3.4)
MAIT cells	× 10^6 cells/L	0.2 (0.1–0.8)	11.2 (7.6–30.7)
NKT cells	× 10^6 cells/L	0.0 (0.0–0.1)	0.4 (0.1–0.8)
$V\delta2^-$ γδT cells	× 10^6 cells/L	0.2 (0.1–0.6)	6.0 (1.9–11.1)
$V\delta2^+$ γδT cells	× 10^6 cells/L	0.4 (0.1–1.5)	6.7 (3.0–15.7)
αβT cells	× 10^6 cells/L	25.9 (17.9–44.4)	315.5 (160.7–689.7)

* CSF mononuclear cells. Routine CSF leukocyte analysis by Sysmex does not differentiate lymphocytes and monocytes. Included in the number of CSF lymphocytes, which are categorized as "mononuclear cells" by Sysmex analysis of CSF.

	PTB	HC	comparison (p)	
	26	26	TBM vs PTB	TBM vs HC
	blood	blood		
	12 (48%)	10 (39%)	0.660	0.290
	31 (24–43)	37 (24–52)	0.042	0.024
	9.1 (7.6–10.7)	6.9 (5.8–7.5)	0.088	<0.001
	6.4 (5.2–8.2)	4.0 (3.3–4.8)	<0.001	<0.001
	1.5 (1.3–1.8)	2.3 (1.8–2.6)	0.005	<0.001
	0.6 (0.5–0.8)	0.4 (0.3–0.5)	0.705	<0.001
	396 (345–480)	285 (240–326)	<0.001	0.562
	6998.1 (5129.2–8629.9)	4052.1 (3757.1–5058.8)	0.276	<0.001
	5011.3 (3434.9–6522.6)	2026.3 (1847.6–2874.9)	0.038	<0.001
	140.7 (100.9–221.6)	237.7 (139.2–265.8)	0.684	0.101
	260.9 (181.1–353.0)	124.8 (94.3–168.2)	0.408	<0.001
	17.9 (13.0–44.8)	11.1 (5.8–18.9)	0.001	0.118
	6.9 (3.5–23.2)	10.2 (2.2–18.0)	<0.001	<0.001
	8.3 (5.5–20.6)	21.8 (14.7–32.7)	0.011	<0.001
	169.6 (94.8–198.8)	164.2 (120.9–198.1)	<0.001	<0.001
	4.9 (3.2–6.9)	5.4 (3.9–7.4)	<0.001	<0.001
	37.6 (12.2–59.4)	85.7 (37.0–134.0)	0.016	<0.001
	0.4 (0.1–1.1)	1.7 (1.3–3.4)	0.969	<0.001
	9.0 (6.4–16.7)	15.2 (7.5–24.8)	0.014	<0.001
	16.7 (11.4–50.3)	29.5 (14.3–60.4)	0.002	<0.001
	817.6 (705.8–1001.2)	1115.4 (950.2–1255.3)	<0.001	<0.001

Tuberculous meningitis is characterised by a predominance of myeloid cells in blood, and αβT cells in CSF

Individual variation was large (**figure 6.2A**), but blood of tuberculous meningitis and pulmonary tuberculosis patients showed a consistently stronger myeloid response compared to healthy controls (**table 6.1**), with increased numbers of mature ($CD16^+$) neutrophils and classical ($CD14^+CD16^-$) monocytes. Intermediate ($CD14^+CD16^+$) and non-classical ($CD14^-CD16^+$) monocytes were lower in tuberculous meningitis compared to both control groups. The lymphoid response showed the opposite: counts of all lymphocyte subsets were lower in tuberculous meningitis patients compared to both pulmonary tuberculosis patients and healthy controls (**figure 6.2B**). In patients who survived past day 10, mature neutrophils showed a further increase while the number of classical monocytes decreased. The CSF cell count of tuberculous meningitis patients also showed a large variation, both in total cell number (median 68/μL, IQR 34-147 as measured by flow cytometry) and in proportions of different cell populations (**figure 6.2C)**. In the lymphoid compartment (median 49/μL, IQR 25-85), αβT cells predominated (57%, IQR 43-73 of lymphocytes), with NK cells as the second largest group (13%, IQR 9-24), with most NK cells $CD56^+$. γδT cells (1.5%, IQR 0.9-3.6) were predominantly $V\delta2^+$, but $V\delta2^-$ cells were also present in all but one patient. Small, but well-defined populations of MAIT cells (0.4%, IQR 0.3-0.8) and NKT cells (0.06%, IQR 0.03-0.12) were found in all but one and three patients, respectively. Monocytes only made up a small proportion (2%) of all CSF cells, but this could be an underestimation because of a larger loss of myeloid cells during sample preparation. Indeed, neutrophils made up 40% of CSF cells in the routine measurement and only 17% by flow cytometry. The large majority (95%) of neutrophils were of the mature ($CD16^+$) phenotype (**figure 5.2D**). Although variable between individuals, all blood lymphocyte subsets remained diminished during follow-up, while in CSF leukocyte counts had dropped by 59% at day 10, with αβT cells remaining the predominant cell type (**supplementary figure 6.2**).

CSF leukocytes are more activated than blood leukocytes

$CD16^+$ neutrophils showed higher expression of the neutrophil activation marker CD69 in CSF compared to blood (MFI 4.3 versus 2.4, $p<0.001$), while there was no difference for the smaller $CD16^{low}$ neutrophil population. CSF monocytes showed higher HLA-DR expression in the classical ($CD14^+CD16^-$, MFI 21.3 versus 7.7, $p<0.001$) and intermediate ($CD14^+CD16^+$, MFI 24.4 versus 17.7, $p=0.043$) subpopulations than in blood (**figure 6.3A**). The difference in activation was even more pronounced in the lymphoid component, with five-fold higher CD69 on NK cells in CSF compared to blood (MFI 10.4 versus 2.0, $p<0.001$)

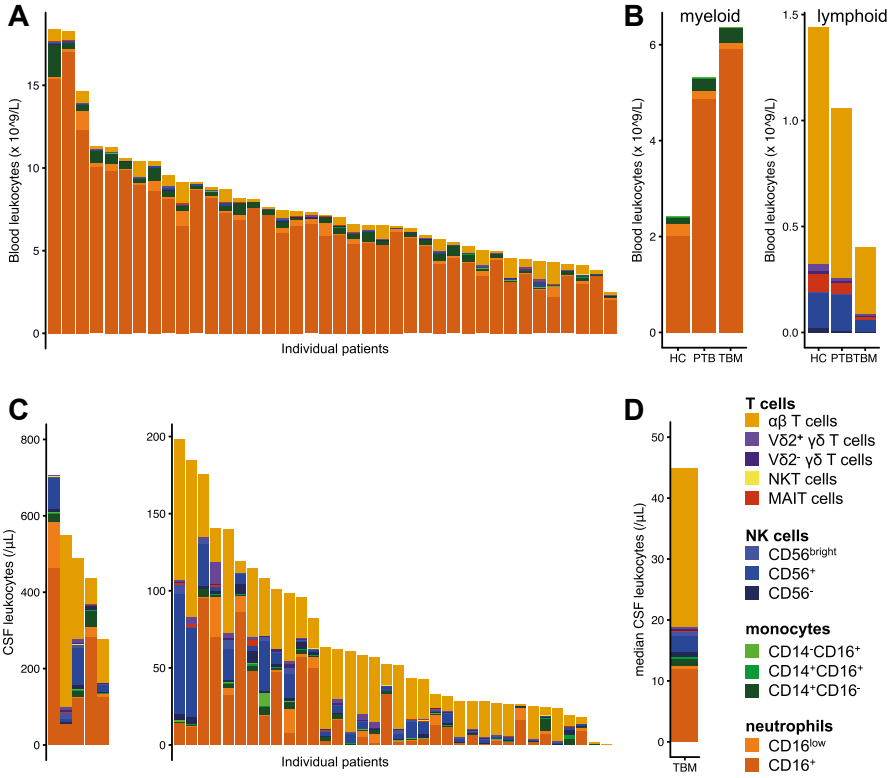

Figure 6.2 Flow cytometry results.

(A) blood flow cytometry results for 40 tuberculous meningitis patients showing concentrations of individual cell types as depicted in the legend. (B) median concentrations in 26 healthy controls, 26 pulmonary tuberculosis and tuberculous meningitis patients for myeloid (left) and lymphoid (right) cell types. (C) CSF flow cytometry results for 41 individual tuberculous meningitis patients. Patients with > 200 leukocytes/µL are displayed in the left subplot and patients with ≤ 200 leukocytes /µL in the right subplot. (D) median CSF cell composition of all tuberculous meningitis patients combined. Note: $CD3^-$ lymphocytes without NK cell markers, most likely B cells (14%, IQR 11-43 of lymphocytes), were not included in the analysis because the flow cytometry panels lacked B-cell markers to formally confirm their phenotype.

and nine-fold higher CD69 on T cells (MFI 10.8 vs. 1.2, p<0.001, **figure 6.3B**). The most activated monocytes were non-classical ($CD14^-CD16^+$) and intermediate ($CD14^+CD16^+$) monocytes that were overrepresented among CSF monocytes compared to blood. Likewise, $CD56^{bright}$ NK cells had the largest proportional presence in CSF compared to blood among NK cells (**supplementary figure 6.3A-B**). During follow-up, a gradual decrease in CSF activation was seen (**supplementary figure 6.3C**).

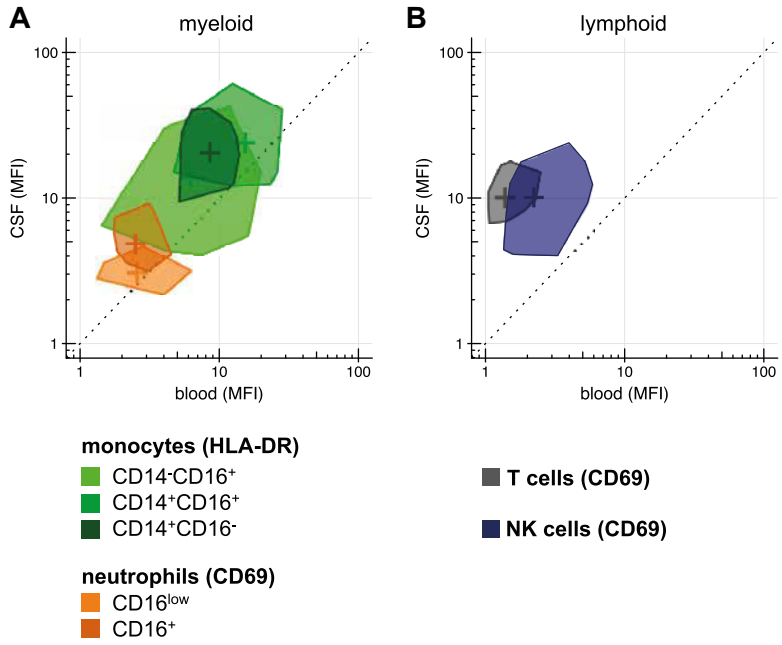

Figure 6.3 Blood versus CSF leukocyte activation.

Median fluorescence intensity of activation markers in blood (x-axis) versus CSF (y-axis) for myeloid (A) and lymphoid (B) cell types. These modified 'bag plots' show the 50% median data-points and can therefore be compared to a two-dimension box plot without whiskers.

Tuberculous meningitis patients show a broad range in ex-vivo cytokine responses

Overall, pulmonary tuberculosis patients had the highest cytokine responses but tuberculous meningitis patients showed the widest range in cytokine production (example for IL-1β in **figure 6.4A**, **table 6.2**). Principal component analysis on the responses to live BCG, *M. tuberculosis* and *S. pneumoniae* lysate for all six cytokines resulted in a first component (PC1, representing 45% of variation) that was largely determined by IL-1β, IL-6, IL-10 and TNF-α in response to all three stimuli (**supplementary figure 6.4A**). Tuberculous meningitis patients showed a much more heterogeneous response compared to pulmonary tuberculosis patients ($p=0.002$, Levene's test for homogeneity) and healthy controls ($p<0.001$), as shown in **figure 6.4B**. The ex-vivo response of tuberculous meningitis patients showed a gradient in the monocyte-derived cytokines TNF-α, IL-1β, IL-6 and IL-10 after stimulation with the specific stimuli,

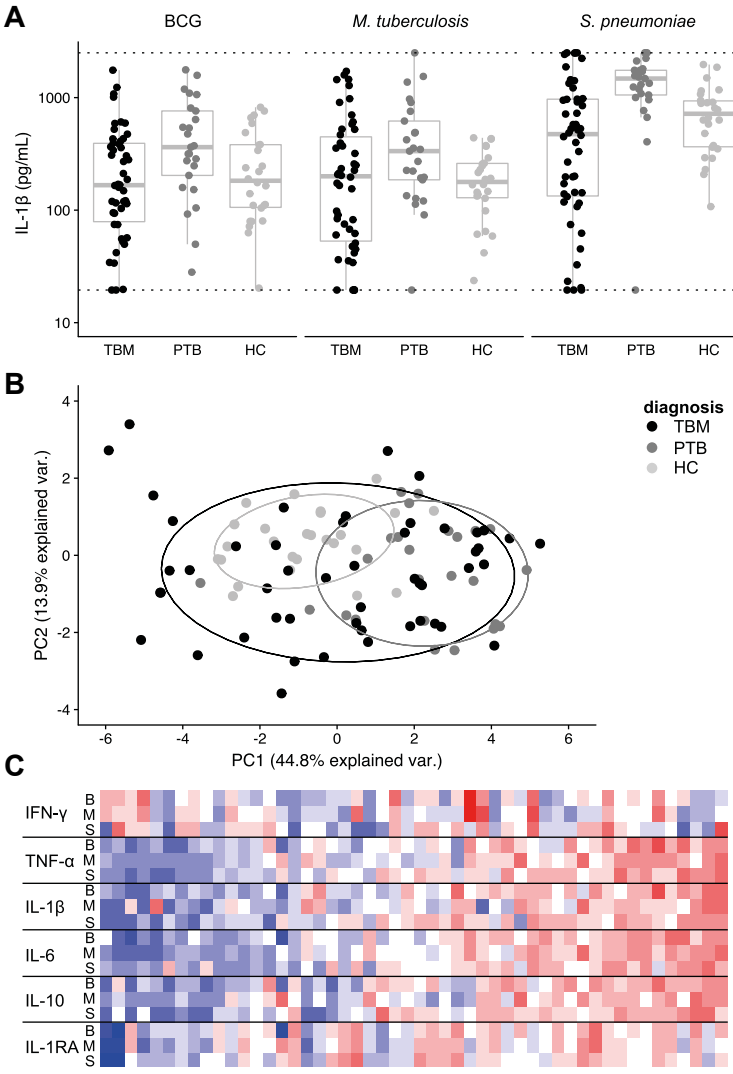

Figure 6.4 Ex-vivo whole blood cytokine results.

(A) IL-1β response after stimulation of whole blood with BCG, *M. tuberculosis* and *S. pneumoniae* for each of the three patient groups tuberculous meningitis (TBM), pulmonary tuberculosis (PTB) and healthy controls (HC). (B) Comparison of these patient groups on principal component (PC) 1 versus PC2 in principal component analysis of all six measured cytokines for the afore-mentioned stimuli for three patients groups. (C) Heatmap showing the combination of six cytokines and three stimuli (y-axis) for all 50 included tuberculous meningitis patients (x-axis) sorted on their score on PC1.

Table 6.2 Whole blood ex-vivo cytokine results at baseline for tuberculous meningitis (TBM) versus pulmonary tuberculosis (PTB) and healthy controls (HC).

	TBM	PTB	HC	p
n	50	25	26	
IFN-γ (pg/mL)				
BCG	18 (10–22)	21 (13–26)	16 (11–29)	0.661
M. tuberculosis	16 (12–24)	16 (12–31)	14 (8–24)	0.403
S. pneumoniae	23 (16–35)	33 (16–47)	24 (15–35)	0.200
E. coli	15 (10–19)	14 (12–18)	16 (10–26)	0.674
C. albicans	12 (9–21)	24 (17–29)	20 (15–32)	0.005
TNF-α (pg/mL)				
BCG	334 (142–847)	930 (538–1530)	252 (128–356)	<0.001
M. tuberculosis	359 (97–803)	466 (215–1036)	83 (50–157)	<0.001
S. pneumoniae	591 (136–1029)	1387 (1125–1668)	369 (202–647)	<0.001
E. coli	365 (104–1242)	915 (333–1569)	391 (206–773)	0.047
C. albicans	122 (52–426)	139 (70–259)	153 (100–217)	0.984
IL-1β (pg/mL)				
BCG	167 (79–393)	363 (204–761)	183 (106–382)	0.030
M. tuberculosis	200 (53–449)	335 (186–619)	178 (129–260)	0.070
S. pneumoniae	474 (134–968)	1477 (1055–1749)	721 (366–935)	<0.001
E. coli	288 (42–473)	760 (486–1037)	667 (195–944)	<0.001
C. albicans	95 (37–193)	106 (53–131)	104 (66–161)	0.723
IL-6 (pg/mL)				
BCG	2838 (1056–5108)	6052 (4477–9882)	2888 (1731–4750)	0.001
M. tuberculosis	2281 (700–6104)	4000 (2986–7269)	1574 (850–2728)	0.001
S. pneumoniae	1635 (573–3114)	2183 (1667–3047)	1530 (971–2160)	0.078
E. coli	2068 (607–3284)	3331 (2379–5149)	2179 (1363–3024)	0.019
C. albicans	1151 (411–2436)	1192 (486–1630)	694 (318–1101)	0.198
IL-10 (pg/mL)				
BCG	39 (12–81)	52 (44–84)	35 (24–53)	0.097
M. tuberculosis	21 (10–59)	36 (17–44)	14 (6–25)	0.023
S. pneumoniae	33 (15–54)	38 (21–55)	24 (13–40)	0.121
E. coli	38 (5–67)	51 (32–89)	61 (28–73)	0.206
C. albicans	6 (5–32)	5 (5–13)	6 (5–9)	0.612

Table 6.2 Continued.

	TBM	PTB	HC	p
n	50	25	26	
IL-1RA (pg/mL)				
BCG	3810 (2020–6132)	4833 (3210–6209)	1597 (1290–2269)	<0.001
M. tuberculosis	3366 (1924–6719)	4651 (2677–5980)	1645 (1325–2067)	<0.001
S. pneumoniae	3948 (1826–5861)	6083 (4499–10546)	1728 (956–2270)	<0.001
E. coli	3902 (1647–6512)	6901 (3789–8459)	2830 (2329–3739)	0.001
C. albicans	1633 (1132–3071)	2334 (1751–3361)	908 (604–1578)	<0.001

Kruskal-Wallis p-values for are shown (df = 2). Data were missing for one pulmonary tuberculosis patient and one healthy control. Data are 100% complete for BCG, *M. tuberculosis* and *S. pneumoniae*, 87% for *E. coli* and 76% for *C. albicans*.

BCG and *M. tuberculosis*, but also with the non-mycobacterial stimulus *S. pneumoniae* (**figure 6.4C**). Data for *C. albicans* (not available for every patient) showed a similar gradient while *E. coli* (also incomplete) did not (data not shown).

During follow-up, cytokine responses showed a decrease from baseline to day 10 (all but two patients had started on corticosteroids), and an increase again at day 60 and 180 (**supplementary figure 6.4B**). The response of tuberculous meningitis patients at day 180 was higher than that of healthy controls for cytokines induced by multiple stimuli: IFN-γ and IL-1RA induced by BCG; TNF-α, IFN-γ, IL-6, IL1-RA induced by *M. tuberculosis*; TNF- α, IFN-γ and IL-1RA induced by *S. pneumoniae*; and IL-1RA induced by *C. albicans* ($p<0.05$ for all, data not shown).

Immune responses correlate to clinical characteristics and survival

Contrary to our hypothesis, we found a broad range in immune responses in tuberculous meningitis patients rather than clearly distinct immune phenotypes ('high' and 'low' responders). We therefore looked for correlations between cell distribution, cell activation and ex-vivo cytokine responses. Myeloid CSF cells correlated with other myeloid cells and lymphoid CSF cells with other lymphoid CSF cells, and the same was true for blood cells. Little or no correlation was seen between the CSF and blood markers (**supplementary figure 6.5**).

We next examined the link between ex-vivo cytokine responses, blood flow cytometry and clinical characteristics. Activation of $CD14^{+}CD16^{-}$ (classical) blood monocytes measured by HLA-DR showed a positive correlation with the

Table 6.3 Immune markers as predictor for 180-day mortality.

Presented are the baseline characteristics of age and sex, routinely obtained cell counts and cell counts by flow cytometry. Comparisons are made by Mann-Whitney U for CSF and blood cell counts and activation markers.

	CSF			Blood		
	Alive (25)	**Dead (16)**	**p**	**Alive (24)**	**Dead (16)**	**p**
Cell counts						
$CD16^+$ neutrophils	12.0 (2.6–47.9)	12.8 (2.0–36.8)	0.769	5641.1 (4076.9–7531.3)	6563.3 (5421.6–8297.8)	0.294
$CD16^{low}$ neutrophils	0.5 (0.1–4.5)	0.8 (0.0–5.6)	0.789	113.5 (82.6–294.9)	102.1 (42.7–259.3)	0.440
$CD14^+CD16^-$ monocytes	1.3 (0.7–3.4)	0.6 (0.3–2.4)	0.149	310.0 (202.8–436.6)	285.7 (179.7–347.9)	0.423
$CD14^+CD16^+$ monocytes	0.2 (0.1–0.6)	0.2 (0.1–0.4)	0.504	7.3 (2.1–18.3)	7.5 (2.5–12.1)	0.956
$CD14^-CD16^+$ monocytes	0.1 (0.0–0.3)	0.1 (0.0–0.3)	0.669	1.1 (0.5–2.2)	1.4 (0.5–1.6)	0.847
$CD56^-$ NK cells	1.0 (0.4–3.5)	0.4 (0.1–1.8)	0.098	6.8 (2.4–9.5)	3.6 (2.7–8.9)	0.508
$CD56^+$ NK cells	5.6 (2.0–15.7)	1.2 (0.8–3.6)	0.016	58.0 (34.7–77.8)	46.4 (28.1–96.7)	0.699
$CD56^{bright}$ NK cells	0.7 (0.4–1.7)	0.4 (0.1–0.6)	0.031	2.0 (0.8–3.4)	1.2 (0.8–3.2)	0.440
MAIT cells	0.3 (0.1–1.1)	0.2 (0.0–0.4)	0.058	12.0 (8.9–35.8)	9.6 (6.6–14.7)	0.116
NKT cells	0.0 (0.0–0.1)	0.0 (0.0–0.0)	0.273	0.4 (0.1–0.8)	0.4 (0.1–0.5)	0.581
$V\delta2^-$ γδT cells	0.3 (0.2–0.7)	0.2 (0.1–0.4)	0.273	7.0 (2.9–11.0)	5.1 (1.9–11.2)	0.912
$V\delta2^+$ γδT cells	0.5 (0.2–1.7)	0.3 (0.1–0.8)	0.229	7.6 (3.0–15.9)	6.2 (3.4–15.2)	0.890
αβT cells	40.2 (20.2–52.7)	21.1 (14.4–27.8)	0.769	420.1 (166.2–723.1)	284.6 (153.8–447.5)	0.269
Cell activation						
$CD16^+$ neutrophils (CD69)	4.2 (3.5–6.4)	4.6 (3.5–7.8)	0.607	2.3 (1.9–3.1)	2.5 (2.2–3.1)	0.699
$CD16^{low}$ neutrophils (CD69)	3.2 (2.5–4.0)	3.4 (2.9–4.2)	0.589	2.9 (1.5–13.1)	1.8 (1.3–3.5)	0.562
$CD14^+CD16^-$ monocytes (HLA-DR)	21.3 (12.8–28.3)	21.3 (15.2–38.3)	0.567	9.5 (6.4–12.6)	7.2 (6.4–8.7)	0.490
$CD14^+CD16^+$ monocytes (HLA-DR)	23.1 (14.4–36.3)	26.0 (14.7–34.6)	0.596	17.7 (12.3–27.3)	14.3 (6.8–25.9)	0.508
$CD14^-CD16^+$ monocytes (HLA-DR)	16.1 (6.5–25.1)	6.8 (4.5–10.2)	0.133	8.8 (4.4–15.4)	5.4 (2.0–13.8)	0.222
NK cells (CD69)	9.7 (5.9–16.6)	12.4 (5.0–15.6)	0.838	2.1 (1.4–3.4)	2.0 (1.6–3.5)	0.847
T cells (CD69)	10.5 (6.9–15.6)	11.5 (9.5–18.4)	0.184	1.2 (1.1–1.9)	1.2 (1.1–1.7)	0.938

Because of the relatively small sample size and skewed distribution, the robust Mann-Whitney U test was chosen. CSF flow cytometry results were missing fore one patient and blood flow cytometry results for two patients.

first principal component of the ex-vivo cytokine response (Spearman rho=0.52, p=0.0089), and this was largely driven by the TNF-α, IL-6 and IL-10 responses across the range of stimuli. Not unexpectedly, the first principal component of the ex-vivo cytokine response also correlated positively to the following routinely collected clinical parameters: temperature (rho=0.33, p=0.0183), blood lymphocytes (rho=0.40, p=0.0048) and blood monocytes (rho=0.34, p=0.0171).

Finally we tested if immune markers predicted patient survival. Neither ex-vivo cytokine responses nor blood count markers showed an association with outcome, while higher levels of the main CSF lymphoid cell types (αβT and NK cells), were associated with better outcome (**table 6.3**).

Discussion

In this prospective cohort of carefully characterised patients in Indonesia, tuberculous meningitis patients showed a strong blood myeloid response compared to healthy controls and pulmonary tuberculosis patients. Within the group of tuberculous meningitis patients, CSF mostly showed a predominance of αβT cells, with highly variable proportions of NK cells and neutrophils, and higher expression of activation markers on CSF monocytes, neutrophils, NK cells and T cells than on these same cell types in blood. Whole blood ex-vivo cytokine responses showed a much wider range in tuberculous meningitis patients compared to pulmonary tuberculosis patients and controls. Rather than distinct immune phenotypes, a gradual scale in the immune response was seen with high cytokine responses correlating with other inflammatory markers.

This study is the first to quantify innate cell population concentrations in blood and CSF of tuberculous meningitis patients in comparison to relevant control groups, adding to previous studies that reported low numbers of αβT cells in blood of tuberculous meningitis patients[217] (probably due to compartmentalisation to CSF[218]), and the presence of γδT and NK cells in CSF[33]. In CSF, besides αβT cells the most abundant cell type were NK cells, an important source of IFN-γ and a critical CSF cytokine in tuberculous meningitis[43]. We also found NKT cells and MAIT cells in CSF, of which the latter have not been described in CSF before. Some patients showed a predominance of neutrophils in CSF, mostly mature, non-apoptotic neutrophils expressing $CD16^{+}$[219]. Monocytes were found in low numbers in CSF, with proportionally more $CD16^{+}$ (macrophage-like) subsets than in blood and with high expression of the activation marker HLA-DR. Leukocyte activation was much higher in CSF than blood, with very

little correlation between compartments, indicating that future studies cannot rely on blood flow cytometry or ex-vivo stimulation assays when aiming to characterise the cerebral immune response.

Whole blood cytokine responses showed a much wider range in tuberculous meningitis patients compared to the two control groups, ranging from non-responsiveness to hyper-responsiveness. This gradient in production of TNF-α, IL-1β, IL-6 and IL-10 was seen in response to the mycobacterial stimuli BCG and *M. tuberculosis* as well as to non-mycobacterial stimuli *S. pneumonia* and *C. albicans*. Ex-vivo cytokine responses showed a positive correlation with blood lymphocyte and monocyte counts and especially with HLA-DR expression on monocytes. Ex-vivo cytokine responses also correlated positively with body temperature, which predicted early mortality in our on routine inflammatory markers in 499 HIV-negative tuberculous meningitis patients presented in **chapter 5**. Other studies have shown that immunoparalytic sepsis patients with low cytokine responses have higher mortality later during the course of disease, possibly because of a higher rate of secondary infection[220], but we could not confirm this in our present study.

At 10 days post admission, a remarkable decrease in CSF myeloid cells and all lymphoid cells except $\alpha\beta$T cells was seen. Different from a Vietnamese study analysing dexamethasone versus placebo that used comparable methodology[33], ex-vivo cytokine responses were strongly down regulated in our patients at day 10. We consider this to be the effect of corticosteroid treatment because the cytokine production was restored after cessation of steroids after 6 weeks (day 60 and 180 measurements). At day 180, proinflammatory cytokine production were even higher than in healthy controls, both in response to mycobacterial stimuli as shown before[221], as well as to unrelated stimuli *C. albicans* and *S. pneumoniae*. Our findings show similarities to HIV-associated cryptococcal meningitis with proportionally overrepresented $CD56^{bright}$ NK cells and $CD14^{+}CD16^{+}$ and $CD14^{-}CD16^{+}$ monocytes in CSF compared to blood[222] and a subgroup of patients with low HLA-DR on monocytes and low ex-vivo TNF-α[223].

Our study has several limitations. Although much larger than previous studies, caution is warranted in its interpretation because of the many comparisons relative to the number of included individuals. Our follow-up was 99% complete, but high early mortality compromised follow-up sampling. Also, CSF leukocytes, especially myeloid cells, show an almost 40% loss from 30 to 60 minutes after lumbar puncture[224]. To limit cell loss, we immediately resuspended CSF cells in culture medium. For the ex-vivo cytokine assay, we chose 24 hours incubation.

This is optimal for measuring for monocyte-derived cytokines[170], but relatively short for IFN-γ. Cytokines in CSF were not measured in this study. The correlations of the ex-vivo cytokine response, require validation in a separate cohort given their number.

What is the clinical relevance of our findings? Besides better supportive care[28] and higher dose rifampicin[29], immunomodulatory therapy may be a third strategy to improve treatment of tuberculous meningitis. In the sepsis field a one-size-fits-all approach has not been successful[225]. Our findings suggest that the same may be true for tuberculous meningitis. There could be a role additional anti-inflammatory therapy, i.e. with aspirin[45](NCT02237365), or interleukin-1 receptor antagonist for patients with a strong inflammatory response. At the same time, patients with a low response might have a better outcome without corticosteroid treatment, or might even benefit from adjuvant IFN-γ therapy to boost their immune response, as has been done successfully in a child with protracted tuberculous meningitis[194]. Preferably, future host-directed trials should include immune markers to allow for post-hoc identification of subgroups benefitting from the initiated therapy. Good candidates are blood monocyte HLD-DR expression, well generalizable to other settings, and ex-vivo cytokine responses. Because of the lack of correlation between blood and CSF compartments, we recommend to also include CSF markers when studying adjuvant therapies.

In conclusion, tuberculous meningitis patients show a previously not appreciated strong myeloid blood response, and an unexpectedly large gradient in the immune response, with little correlation between blood and CSF compartments. We recommend integrating the assessment of the immune response in future randomised clinical trials evaluating host-directed therapy in tuberculous meningitis.

Acknowledgements
We thank the neurology residents and Tiara Pramaesya, Sofia Immaculate, Sri Margi, Rani Trisnawati and Shehika Shulda of the tuberculous meningitis study team for monitoring patients and data management; Witri Indrasari and Leni Lismayanti of the clinical chemistry lab team for facilitating sample flow; Lidya Chaidir and Jessi Annisa for mycobacterial diagnostics; Dwi Febni Ratnangingsih, Inas Kathina, Anbarunik Putri Danthin and Yusandi Sastra Atmaja for performing whole blood stimulation assays and ELISAs; Helga Toenhake-Dijkstra, Heidi Lammers and Intan Mauli for ELISAs; Suharyani and Cor Jacobs for flow cytometry; Jos van der Meer for critical reading of the manuscript and the director of the Hasan Sadikin General Hospital, Bandung, Indonesia, for accommodating the research.

Author contributions

AvL, MGN and RvC designed the study. SD, FP, THA, RR and ARG supervised tuberculous meningitis patient recruitment. AV, LA and PCH supervised recruitment of healthy controls and RL supervised recruitment of pulmonary tuberculosis patients. AI and BA supervised the immunological lab in Bandung. SvD, FU and JU designed and optimized flow cytometry experiments, performed by FU. SvD analysed flow samples. AvL, ED and AV optimized the whole blood cytokine assay, performed by ED. ED and VACMK measured ELISAs. EA and RtH helped with bio-informatic analysis. AvL and RvC wrote the first draft of the manuscript; all other authors provided input to the draft and approved of the final version of the manuscript.

Supplementary figures

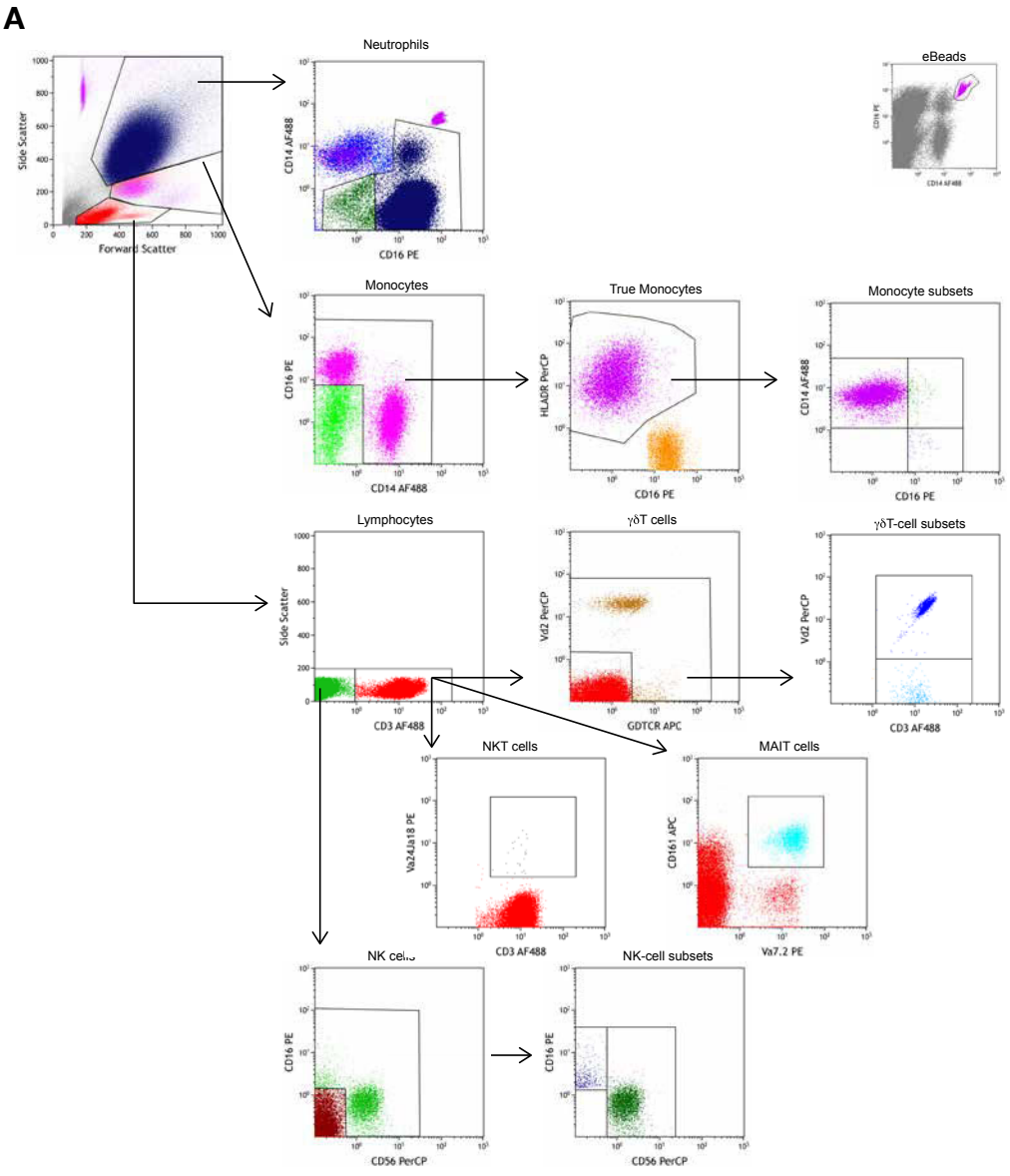

Supplementary figure 6.1

(A) flow cytometry gating strategy. αβT cells are calculated by subtracting NKT cells, γδT cells and MAIT cells from the total number of $CD3^+$ lymphocytes.

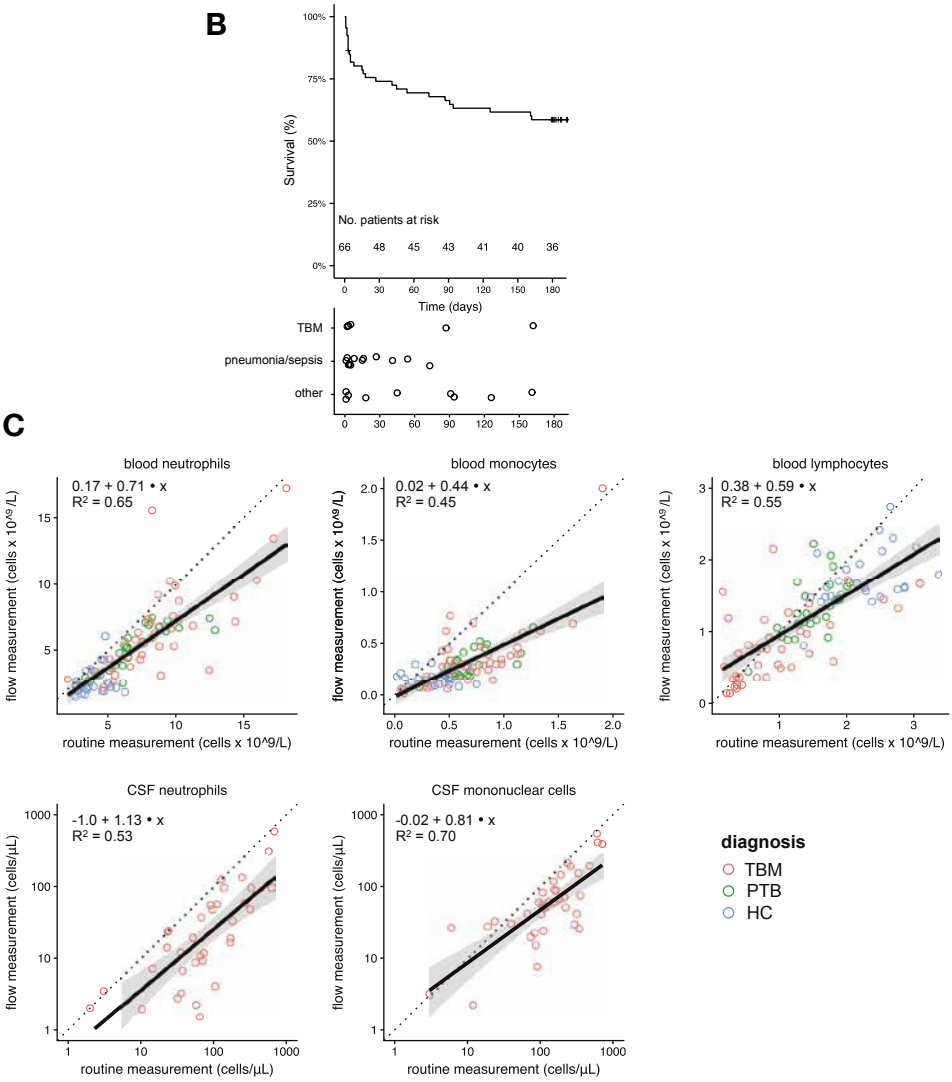

Supplementary figure 6.1 Continued.

(B) Mortality in the first 180 days of follow-up. Outcome data were missing for one patient. Presumptive cause of death is depicted below the Kaplan-Meier graph in three categories: 1) tuberculous meningitis-related causes: 4 because of increased intracranial pressure, 2 because of a paradoxical reaction, 2) pneumonia (8) or sepsis (4), and 3) miscellaneous: 3 aspiration pneumonia, 3 suspected cardiac arrest or pulmonary embolism, 1 head injury, 1 metabolic encephalopathy and 1 with unknown cause. (C) Regression lines with 95% confidence intervals for the correlation between cell counts as measured routinely (x-axis), and with flow cytometry (y-axis) for blood and CSF. Regression formulas and regression coefficients (R^2) are printed on the graphs. Note: CSF cells are plotted on a ^{10}log-axis and regression coefficients are ^{10}log-transformed.

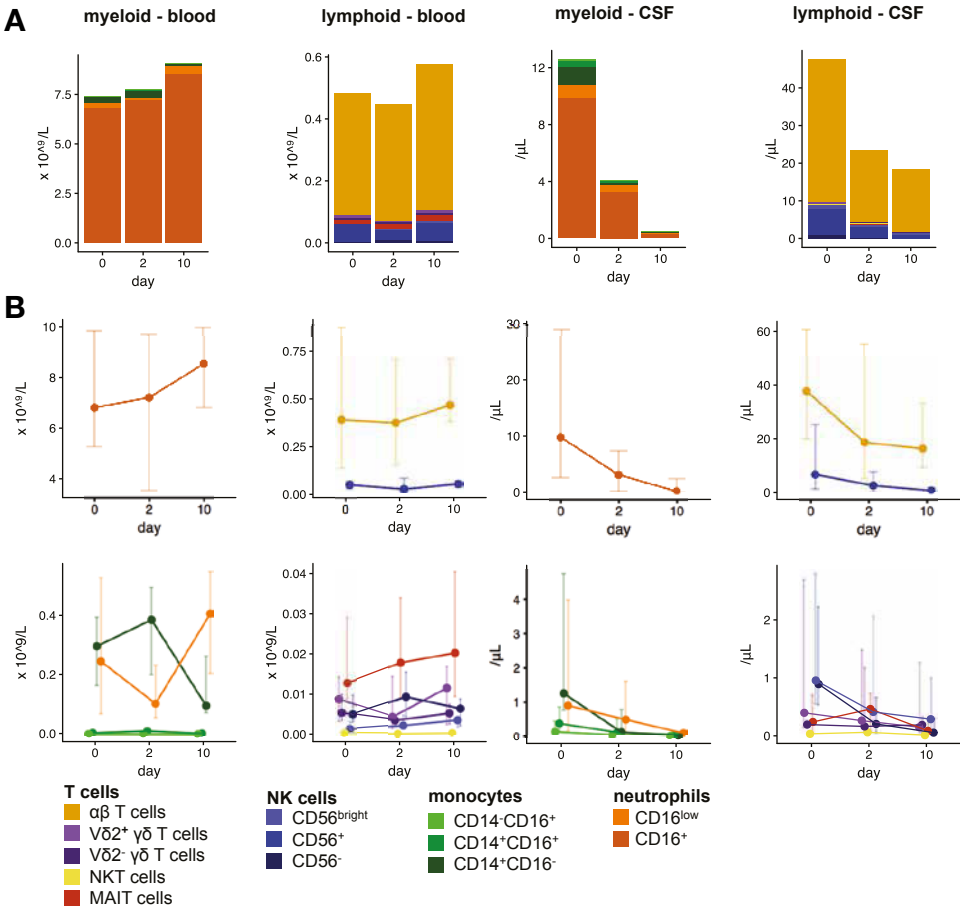

Supplementary figure 6.2

Flow cytometry follow-up results of tuberculous meningitis patients in the follow-up study who survived past day 10 (n = 15). Results show median (A) or median with interquartile range (B) for day 0, 2 and 10 for myeloid and lymphoid cell types separately in blood (left) and CSF (right). Note the different y-axis limits. Data is ≥ 80% complete for all time-points for blood and is ≥ 87% complete for CSF.

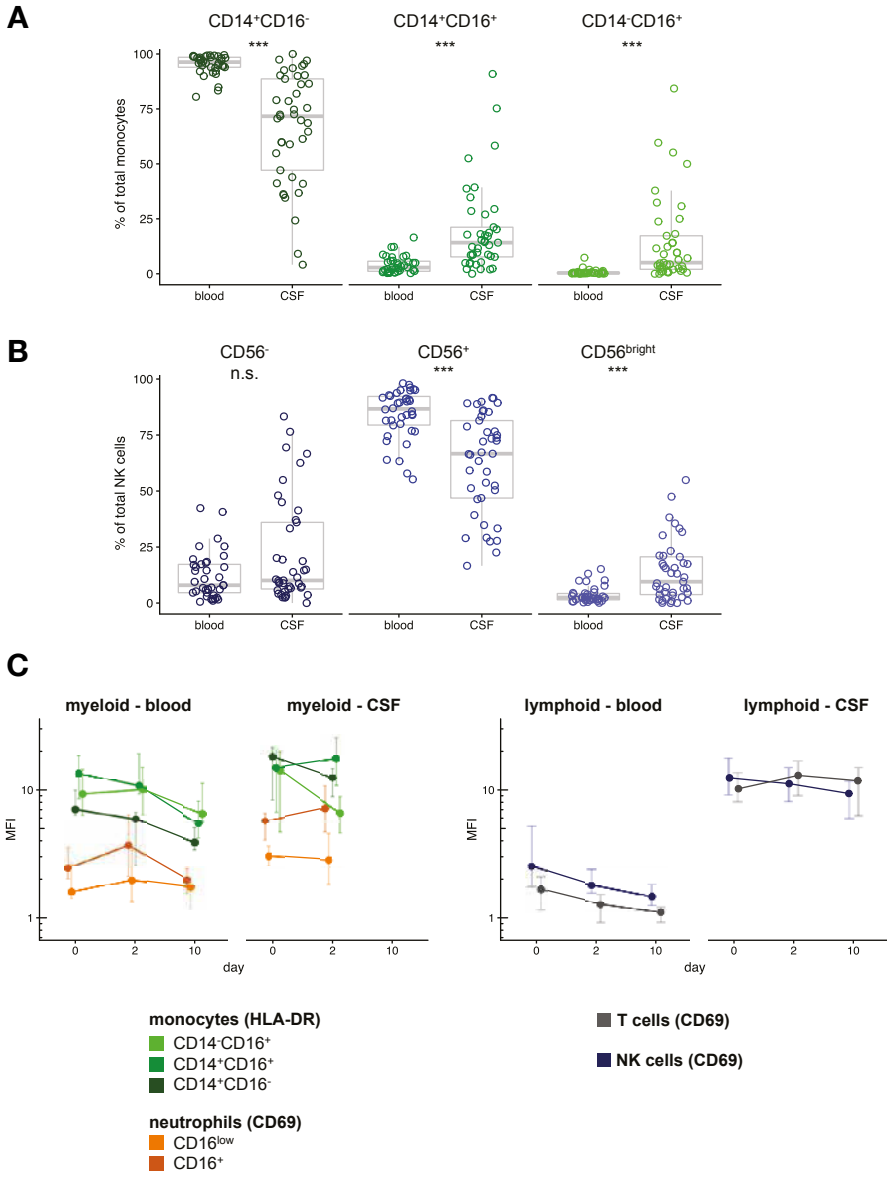

Supplementary figure 6.3

Flow cytometry results of proportions of monocyte (A) and NK cell (B) subtypes in blood versus CSF. *** p<0.001. (C) Activation marker expression by indicated cell populations during follow-up for tuberculous meningitis patients, all of whom survived past day 10 (n = 15). Data is ≥ 80% complete for all time-points for CSF and blood. Note: day 10 myeloid activation markers in CSF could not reliably be measured because of the low cell counts.

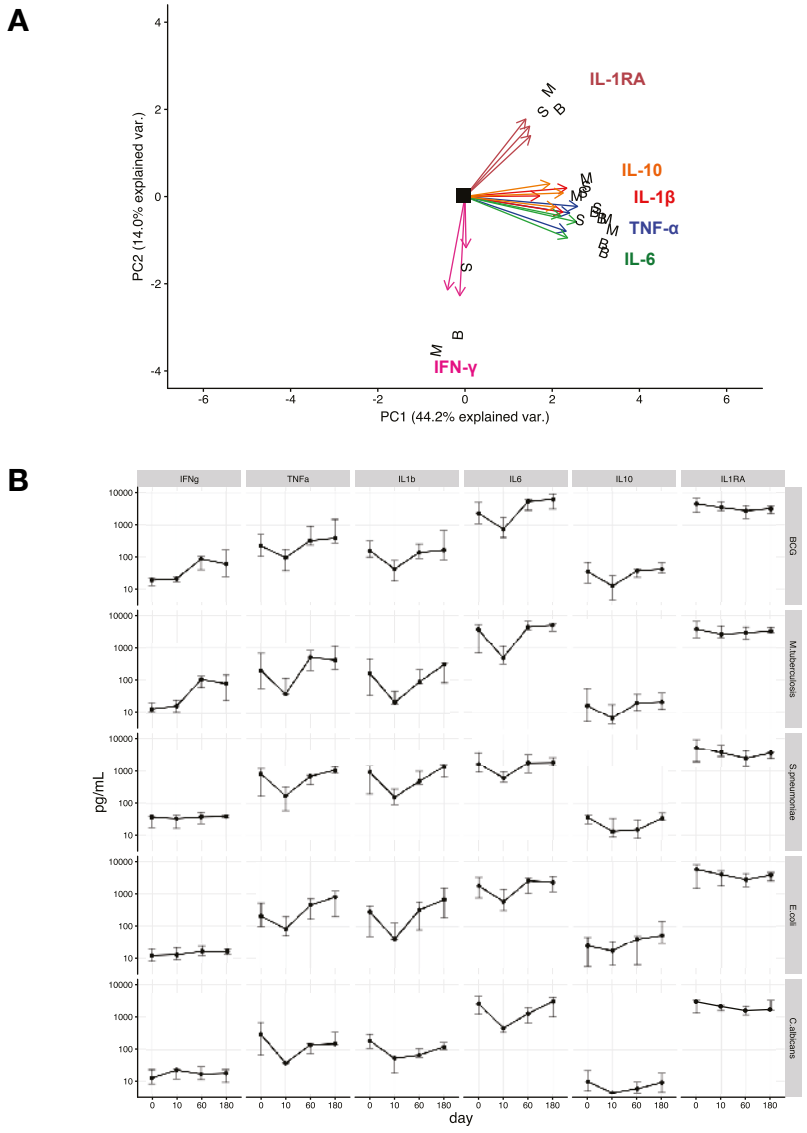

Supplementary figure 6.4

(A) Loadings for principal component analysis on ex-vivo cytokine data. B = BCG, M = *M. tuberculosis* and S = *S. pneumoniae*. (B) Ex-vivo whole blood cytokine results for tuberculous meningitis patients in the follow-up study who survived past day 180 (n = 15). Results show median with interquartile range for all five stimuli (ordered vertically) for all six measured cytokines (horizontally). Patients were selected who had complete data at day 0 and missed maximally one of the follow-up time-points. Data is 93% complete for day 10, 73% for day 60 and 53% for day 180. Missing data were due to technical errors.

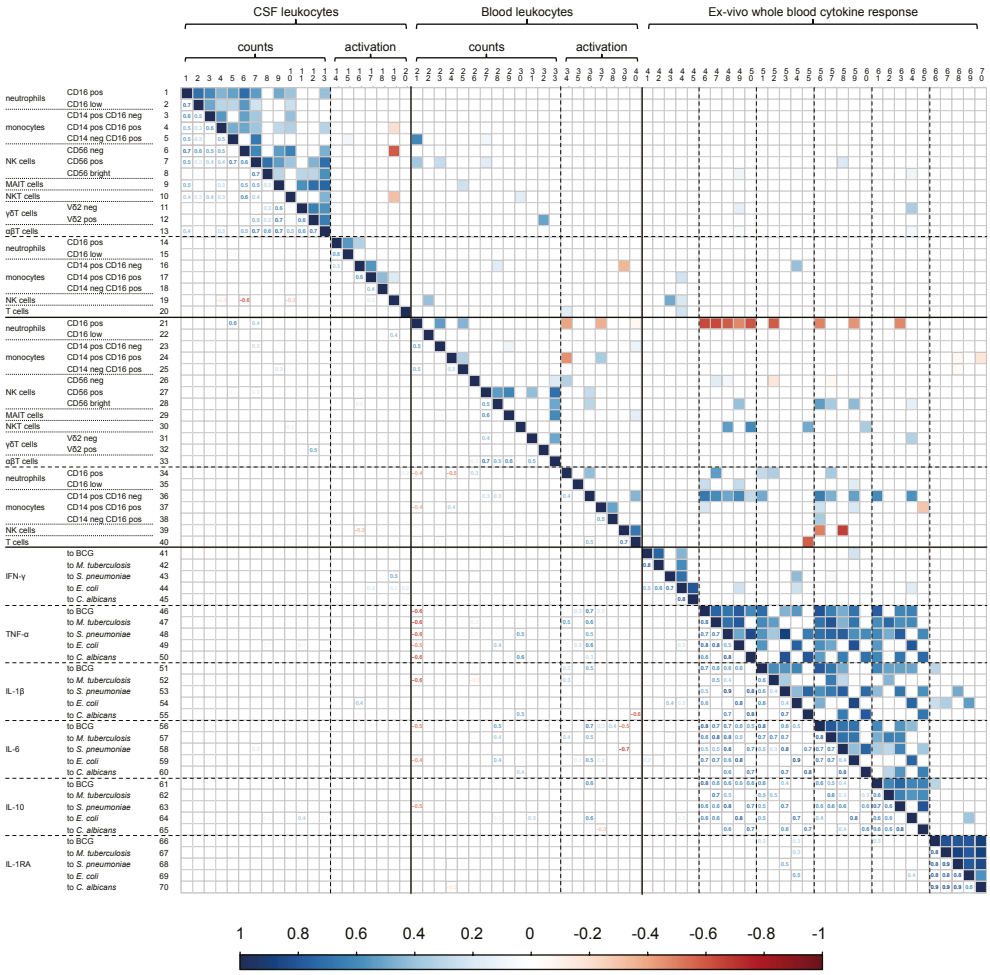

Supplementary figure 6.5

Correlation matrix for CSF and blood cell counts and activation markers, as well as blood ex-vivo whole blood response using Spearman correlation. Pair-wise complete data was included.

Supplementary table 6.1 Clinical, cerebrospinal fluid and blood parameters of tuberculous meningitis patients.

Variable	n/N or median	% or IQR
Clinical features		
Sex	37/67	(56%)
Age	27	(21–38)
Duration of main complaint	4	(2–7)
Duration of the first neurological symptom	14	(7–21)
Tuberculous meningitis grade		
I	2/67	(3%)
II	58/67	(87%)
III	7/67	(10%)
Temperature, °C	37.8	(37.0–38.2)
Glasgow Coma Scale score	13	(11–14)
Seizures present	1/66	(2%)
Motor abnormalities present	38/66	(57%)
Cranial nerve palsy present	51/66	(6%)
Abnormal chest radiograph findings	50/67	(75%)
Cerebrospinal fluid		
CSF to blood glucose ratio	0.14	(0.09–0.20)
Protein, mg/dL	221	(150–386)
Culture, % positive	46/67	(69%)
Blood		
Haemoglobin, g/dL	12.5	(10.5–13.8)
Thrombocytes, x 10^9/L	298	(234–379)
Outcomes		
Length of hospital stay in days	21	(12,23)
Alive at discharge	51/66	(76%)
Outcome at day 180		
Alive	39/71	(58%)
Deceased	27/67	(40%)
Lost to follow-up	1/67	(2%)

Continuous variables are presented as median with interquartile range and categorical variables as number and proportion. IQR = interquartile range. Additional routine inflammatory markers can be found in Table 6.1.

7

Cerebral tryptophan metabolism and outcome of tuberculous meningitis: an observational cohort study

Arjan van Laarhoven, Sofiati Dian, Raúl Aguirre-Gamboa, Julian Avila-Pacheco, Isis Ricaño-Ponce, Carolien Ruesen, Jessi Annisa, Valerie A C M Koeken, Lidya Chaidir, Yang Li, Tri Hanggono Achmad, Leo A.B. Joosten, Richard A. Notebaart, Rovina Ruslami, Mihai G. Netea, Marcel M. Verbeek, Bachti Alisjahbana, Vinod Kumar, Clary B. Clish, Ahmad Ganiem, Reinout van Crevel

The Lancet Infectious Diseases. 2018;18:526–35

Abstract

Rationale
Immunopathology contributes to the high mortality of tuberculous meningitis, but the biological pathways involved are mostly unknown. We aimed to compare cerebrospinal fluid (CSF) and serum metabolomes of patients with tuberculous meningitis with that of controls without tuberculous meningitis, and assess the link between metabolite concentrations and mortality.

Methods
In this observational cohort study at the Hasan Sadikin Hospital (Bandung, Indonesia) we measured 425 metabolites using liquid chromatography-mass spectrometry in CSF and serum from 33 HIV-negative Indonesian patients with confirmed or probable tuberculous meningitis and 22 control participants with complete clinical data between March 12, 2009, and Oct 27, 2013. Associations of metabolite concentrations with survival were validated in a second cohort of 101 patients from the same centre. Genome-wide single nucleotide polymorphism typing was used to identify tryptophan quantitative trait loci, which were used for survival analysis in a third cohort of 285 patients.

Findings
Concentrations of 250 (70%) of 351 metabolites detected in CSF were higher in patients with tuberculous meningitis than in controls, especially in those who died during follow-up. Only five (1%) of the 390 metabolites detected in serum differed between patients with tuberculous meningitis and controls. CSF tryptophan concentrations showed a pattern different from most other CSF metabolites; concentrations were lower in patients who survived compared with patients who died (9-times) and to controls (31-times). The association of low CSF tryptophan with patient survival was confirmed in the validation cohort (hazard ratio 0.73; 95% CI 0.64–0.83; $p<0.0001$; per each halving). 11 genetic loci predictive for CSF tryptophan concentrations in tuberculous meningitis were identified ($p<0.00001$). These quantitative trait loci predicted survival in a third cohort of 285 HIV-negative patients in a prognostic index including age and sex, also after correction for possible confounders ($p=0.0083$).

Interpretation
Cerebral tryptophan metabolism, which is known to affect *M. tuberculosis* growth and central nervous system inflammation, is important for the outcome of tuberculous meningitis. CSF tryptophan concentrations in tuberculous meningitis are under strong genetic influence, probably contributing to the variable outcomes of tuberculous meningitis. Interventions targeting tryptophan metabolism could improve outcomes of tuberculous meningitis.

Introduction

Meningitis is the most severe manifestation of tuberculosis, resulting in death or neurological disability in more than 30% of adult patients (see **chapter 5** and [16,25]). The host immune system contributes to the poor outcome of tuberculous meningitis, either through inadequate killing of *M. tuberculosis*, or through an inappropriate inflammatory response leading to tissue damage (immunopathology)[16]. Studying cellular metabolism can help to determine the function of immune cells, and analysis of cerebrospinal fluid (CSF) metabolites could help unravel underlying biological mechanisms or establish the prognosis of tuberculous meningitis.

Metabolic studies in tuberculosis have examined a small number of metabolites, and most have focused on identification of host or bacterial metabolites as diagnostic markers[226-228]. We aimed to compare CSF and serum metabolomes of patients with tuberculous meningitis with those of controls with negative *M. tuberculosis* culture, and assess the link between metabolite concentrations and mortality.

Methods

Study design and participants

This was a prospective observational cohort study done at the Hasan Sadikin Hospital (Bandung, Indonesia). Study participants were selected from a cohort of patients older than 14 years with suspected meningitis described in **chapter 5**. Eligible patients had definite tuberculous meningitis[229], defined as positive CSF *M. tuberculosis* culture or PCR, or probable tuberculous meningitis, defined as clinically suspected disease with at least five leucocytes per μL of CSF, and a CSF to blood glucose ratio less than 0.5. HIV infection, which strongly affects host cellular responses and increases mortality of tuberculous meningitis, was an exclusion criterion for this study. Oral consent to be included in the study, for storage of surplus sample, and to obtain follow-up data was obtained from patients or close relatives of patients who were unconscious. Control participants were individuals who had a lumbar puncture because of suspected central nervous system infection or subarachnoid bleeding but who showed no abnormalities on routine CSF examination (<5 leucocytes per μL, glucose ratio ≥0.5) and negative *M. tuberculosis* culture.

Ethical approval was obtained from the Ethical Committee of Hasan Sadikin Hospital, Faculty of Medicine of Universitas Padjadjaran, Bandung, Indonesia.

Procedures

We determined the CSF and serum metabolome in a discovery cohort of 33 patients with tuberculous meningitis, of whom 17 died while in hospital and 16 survived during follow-up, and 22 controls without meningitis. Concentrations of metabolites were compared between patients and controls, and (among patients only) linked to survival. A second group of 101 patients with tuberculous meningitis and 17 controls was used for validation of the relationship between the CSF metabolome and survival. Genome-wide single nucleotide polymorphism (SNP) typing was done in 130 patients with tuberculous meningitis from the original discovery and validation cohorts to identify quantitative trait loci for individual CSF metabolites. Associations between identified genetic loci and patient survival were then validated in a third group of 285 tuberculous meningitis patients (the genetic validation cohort).

According to routine care, all patients with suspected meningitis underwent lumbar puncture before starting antimicrobial or corticosteroid treatment. Patients diagnosed with tuberculous meningitis underwent systematic clinical and CSF characterisation at the time of diagnosis, and survival was monitored prospectively for one year.

Gene Xpert MTB/RIF has only been used since 2015 and drug resistance testing was otherwise not routinely available in our study setting. Tuberculous meningitis was treated with a combination of rifampicin (unless otherwise indicated 450 mg, corresponding to about 10 mg/kg), isoniazid (300 mg), ethambutol (750 mg), and pyrazinamide (1500 mg) for 6 months according to Indonesian guidelines. Patients were given adjunctive dexamethasone according to the internationally accepted 6-week tapering regimen, starting at 0.3 mg/kg for grade I and 0.4 mg/kg for grade II or III tuberculous meningitis[186]; patients were switched to an equivalent dose of oral prednisolone in cases of early discharge.

CSF and serum metabolomics

CSF samples were centrifuged at 3000 rpm for 15 min and the supernatant was stored at −80°C. Serum was collected after centrifugation of peripheral blood at 3000 rpm for 15 min. Samples were frozen and thawed once before metabolomics analysis. 425 metabolites were measured in serum and CSF using four liquid chromatography tandem mass spectrometry methods (see **supplementary methods** for more detail)[230,231].

Quantification of CSF tryptophan and CSF and serum albumin

CSF tryptophan in the original and validation cohorts was quantified by ultra-performance liquid chromatography (see Supplementary Methods for more detail). The acquired ultra-performance liquid chromatography data showed good correlation with the original liquid chromatography-mass spectrometry data (Spearman's rho=0.95, p<0.0001). CSF and serum albumin were measured to determine the CSF to serum albumin ratio (normal range 0.005–0.008 for individuals aged 15–60 years[232]; see Supplementary Methods for more detail).

Metabolomic data analysis

Liquid chromatography-mass spectrometry and ultra-performance liquid chromatography data were analysed after log transformation. Values under the lower limit of detection of liquid chromatography-mass spectrometry were replaced with half of the metabolites' lower limit of detection in the specific matrix (CSF or serum). Pathway analysis was done on log-transformed, mean-centred data for metabolites with less than 50% missing values using MetaboAnalyst version 3.0[233], which performs topological analysis with relative betweenness centrality applying the GlobalTest algorithm[234] to test for association of metabolite concentrations with diagnosis. Metabolites discovered in at least one sample were uploaded as a reference metabolome.

All other analyses were done in R version 3.2.2. Visualisation was achieved by principal component analysis on centred unscaled data using the R package prcomp. Comparison of metabolites was done using the R package limma. Figure colour gradients are based on uncorrected p values and tables show false discovery rates after applying the Benjamini-Hochberg procedure to correct for multiple testing. Survival analyses were done using the R package survival and visualised with the R package survminer. Differences between tryptophan strata were evaluated using a log-rank test. Multivariate survival analysis was done using Cox regression after log transformation of skewed continuous variables as indicated. Other R packages used were openxlsx, dplyr, reshape2 (for data handling), and tableone (for data representation), and all graphs were visualised using ggplot2 and enhanced by cowplot. Patients with negative CSF culture, who had received dexamethasone or antituberculosis drugs before lumbar puncture, who were infected with rifampicin-resistant strains, or who had received high-dose rifampicin were excluded from sensitivity analyses.

Transcriptional analyses

The tryptophan pathway was established based on the Kyoto Encyclopaedia of Genes and Genomes (map 00380) and the Small Molecule Pathway Database

(SMP00063), and all genes coding for enzymes in these reactions were included. For brain expression, data were available for five patients with tuberculous meningitis versus four patients deceased because of head injury (GSE23074), all from southern India[235]. Data were quantile-normalised, filtered for positive expression, log transformed, and analysed using the R package limma for association with patient group.

Tryptophan quantitative trait loci mapping and genotype-dependent survival analysis

Genotyping, quality control, and imputation was done as described in the **supplementary methods**. Log-transformed, normalised concentrations of tryptophan were then mapped to the 4,751,257 variants that passed quality control (R^2>0.3 and minor allele frequency ≥0.1) using a linear regression model corrected for age and sex. We defined a threshold for suggestive genome-wide significance ($p<0.00001$). We calculated a prognostic index[236] using the linear component of the Cox model, as in prognostic index=$\beta_1 x_1 + \beta_2 x_2 + \ldots + \beta_p x_p$, where x_1 is the genotype data in dosages and β_1 results from fitting the Cox proportional model. The genetic patient cohort was split into two groups according to the median of the prognostic index (low and high), and patients were evaluated for survival with a log-rank test. Finally, a prognostic index was used as a continuous covariate in multivariate Cox regression including possible confounders.

We used different approaches to examine the role of identified quantitative trait loci. First, identified quantitative trait loci were examined for possible effects on gene expression using the Gtex database. Second, genes neighbouring quantitative trait loci were extracted and expression was examined using Gene Set Enrichment Analysis in different human tissues and cell lines (deposited in the Human tissue compendium[237]). Finally, we used brain gene expression data[235] to assess the differential expression of genes near quantitative trait loci in patients with tuberculous meningitis compared with patients who had died from head injury.

Results

CSF and serum metabolome in tuberculous meningitis patients and controls

For the discovery metabolomics study, we included 33 patients with tuberculous meningitis with positive CSF culture between March 12, 2009, and Oct 27, 2013, including 16 who survived and 17 who died while in hospital. We also included

22 individuals with negative *M. tuberculosis* culture and normal routine CSF characteristics as controls (**supplementary figure 7.1A**).

Patients presented with severe disease, often with lowered consciousness, cranial nerve palsy, or paresis of one or more limbs (**table 7.1**). 425 metabolites were measured in serum and CSF. Quality and coverage of the metabolomics data was high, and routinely measured CSF glucose concentration was correlated with glucose concentration measured by liquid chromatography-mass spectrometry (Spearman's rho=0.986; p<0.0001). The CSF sample of one patient with tuberculous meningitis with aberrant measurements on the hydrophilic interaction chromatography-positive platform was removed from subsequent analyses. Of 425 annotated metabolites, 348 (82%) were detected in CSF and serum, three (1%) in CSF only, and 42 (10%) in serum only (**online supplement**).

Patients with tuberculous meningitis had a distinct CSF metabolome compared with control participants, as shown by principal component analysis (**figure 7.1**). One patient with tuberculous meningitis and miliary tuberculosis who had no leucocytes in CSF clustered with the control group; we did not exclude this patient from the tuberculous meningitis group for the analysis as no technical anomaly was detected. Of 351 metabolites detected in CSF, 250 (71%) were higher and 18 (5%) were lower in patients with tuberculous meningitis than they were in controls (with a false discovery rate threshold of <0.05; **figure 7.1**). Metabolite concentrations showed large variation, but were on average 12-times higher in serum than in CSF (**supplementary figure 7.1B**). The median CSF to serum albumin ratio was 0.050 in patients with tuberculous meningitis, suggesting that the blood-CSF barrier was severely disrupted, compared with 0.0062 in controls (**supplementary figure 7.1C**). The difference in average relative abundance of metabolites between CSF and serum was smaller in patients (6.2-times) than in controls (32.2-times). CSF metabolites across the whole range of quantity and mass showed substantial differences between patients and controls (**supplementary figure 7.1D**), with 58 (97%) of 60 known metabolic pathways being affected (**supplementary table 7.1**). The serum metabolome showed more subtle differences between patients and controls, with only five (1%) of 397 metabolites being significant (false discovery rate <0.05; **figure 7.1**).

CSF metabolome as a predictor for patient survival

We next compared metabolite profiles of patients with tuberculous meningitis who died while in hospital (n=17, median time to death 4 days [IQR 3–7]) and those who were discharged alive (n=15, after exclusion of the sample with aberrant measurements). Patients who survived were discharged after a median

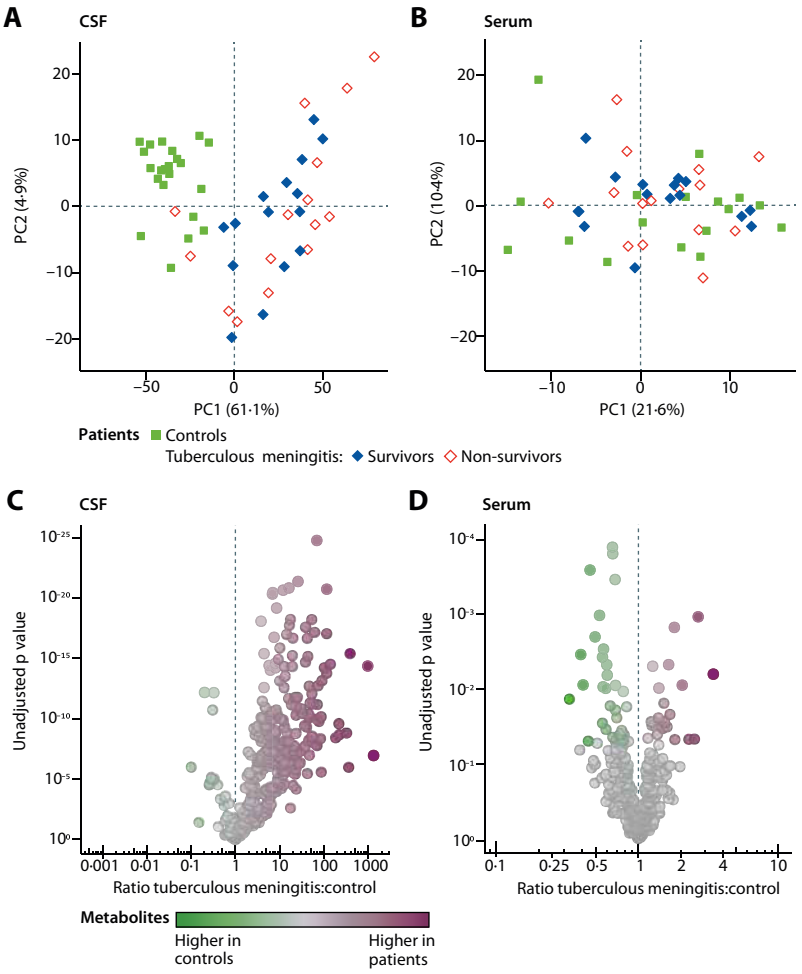

Figure 7.1 CSF and serum metabolome in patients with tuberculous meningitis and controls.

Principal component analysis for CSF (A) and serum (B) with proportion of variance per principal component indicated between brackets. Volcano plots for individual metabolites in CSF (C) and serum (D). Colours indicate strength of association. Metabolites that show no difference between groups (uncorrected p>0.05) are grey. PC = principal component.

of 25 days (IQR 21–29), and one additional outpatient death was recorded at day 89. None of the serum and CSF metabolites reached a false discovery rate threshold of less than 0.05 for comparison between survivors and non-survivors. At an ordinary significance level ($p<0.05$), 33 (8%) of 390 metabolites detected in serum differed between non-surviving and surviving patients with tuberculous meningitis (**supplementary figure 7.2A**), but only one of these (urate) also differed between patients and controls. At an ordinary significance level ($p<0.05$), 28 (8%) of 351 metabolites detected in CSF differed between non-survivors and surviving patients with tuberculous meningitis (**figure 7.2A**). 25 (90%) of 28 metabolites were higher in non-surviving patients than in surviving patients with tuberculous meningitis. Of these 25 CSF metabolites, 13 (52%) were higher in the original comparison of patients with tuberculous meningitis compared to controls. One of these 13 metabolites, the eicosanoid leukotriene B4—a downstream chemoattractant of Leukotriene A4 Hydrolase (*LTA4H*) that has been studied in relation to tuberculous meningitis survival—was lowest in controls, 11-times higher in patients with tuberculous meningitis who survived, and 30-times higher in patients who died. Two metabolites, glucose and inositol, followed the reverse pattern. For example, glucose was highest in controls, 2.5-times lower in patients with tuberculous meningitis who survived, and 4-times lower in those who died. Three CSF metabolites (putrescence, cytidine, and tryptophan) followed a pattern in which survivors had lower concentrations than both controls and non-survivors. CSF tryptophan, which had the largest difference between groups, was 31-times lower in survivors than in controls, and 9-times lower in survivors than non-survivors (unadjusted $p=0.00043$).

Unlike many other metabolites, CSF tryptophan was not associated with CSF to serum albumin ratio (a marker of disruption to the blood–CSF barrier) (Pearson's $r^2=0.015$), CSF polymorphonuclear cell count (Pearson's $r^2=0.058$), or CSF mononuclear cell count (Pearson's $r^2=0.019$), suggesting that CSF tryptophan concentrations instead reflect metabolism in the brain itself (**supplementary figure 7.2B**; for correlations for all other metabolites see **online supplement**). Serum tryptophan concentrations were 1.3-times higher in patients who survived than they were in those who died ($p=0.055$; **online supplement**).

We tested the association between CSF tryptophan concentrations and patient survival in a separate group of 101 consecutively recruited patients with tuberculous meningitis (recruited between July 2, 2014, and April 6, 2016), 67 (66%) of whom were culture-confirmed and 17 control participants (**table 7.1).** The concentration of CSF tryptophan, quantified using ultra-performance liquid

Table 7.1 Patient characteristics.

	Metabolomics discovery cohort		
	Controls (n=22)	Tuberculous meningitis survivors (n=15*)	Tuberculous meningitis non-survivors (n=17)
Clinical features			
Sex			
Male	10 (45%)	11 (73%)	11 (65%)
Female	12 (55%)	4 (27%)	6 (35%)
Age, years	34 (22–25)	27 (25–34)	27 (22–30)
Tuberculous meningitis grade			
I	NA¶	1 (7%)	0/16
II	NA¶	13 (87%)	8/16 (50%)
III	NA¶	1 (7%)	8/16 (50%)
Temperature, °C	37.0 (36.7–37.5)	37.6 (36.9–38.2)	37.6 (37.2–37.9)
Glasgow Coma Scale	14 (13–15)	13 (12–14)	12 (11–13)
Seizures present	4 (18%)	0	2/16 (13%)
Motor abnormalities present	14 (64%)	6 (40%)	9/16 (56%)
Cranial nerve palsy present	13/21 (62%)	8 (53%)	14 (82%)
Cerebrospinal fluid features			
Leucocytes, cells per µL	2 (0–2)	99 (50–306)	54 (15–275)
Neutrophils, cells per µL	0 (0–1)	26 (14–66)	38 (6–171)
Mononuclear cells, cells per µL	1 (0–2)	84 (29–201)	47 (11–118)
Protein, mg/dL	34 (19–47)	291 (126–357)	216 (143–371)
CSF to blood glucose ratio	0.64 (0.56–0.70)	0.21 (0.13–0.29)	0.12 (0.08–0.17)
M. tuberculosis culture positive	0	15 (100%)	17 (100%)
Blood features			
Haemoglobin, g/dL	12.0 (9.40–13.8)	11.9 (10.1–13.8)	12.4 (11.2–13.3)
Leucocytes, x 10^9/L	10.1 (7.6–12.6)	10.0 (8.8–11.3)	12.6 (8.5–15.8)
Thrombocytes, x 10^9/L	278 (136–416)	293 (192–351)	346 (301–400)

	Tryptophan validation cohort		**Genetic validation cohort**
	Controls (n=17)	Tuberculous meningitis (n=101)	Tuberculous meningitis (n=285)
	9 (53%)	62 (61%)	153 (54%)
	8 (47%)	39 (39%)	132 (46%)
	39 (22–39)	30 (21–38)	29 (22–37)
	NA	3/99 (3%)	30/258 (12%)
	NA	82/99 (84%)	195/258 (76%)
	NA	14/99 (14%)	33/258 (13%)
	37.1 (36.8–37.5)	37.8 (37.0–38.3)	37.5 (36.8–38.0)
	15 (14–15)	13 (11–14)	14 (12–15)
	2 (12%)	5/98 (5%)	17/246 (7%)
	8 (47%)	59/99 (60%)	127/241 (53%)
	9 (53%)	69/100 (69%)	161/258 (62%)
	2 (1–2)	236 (124–443)	138 (49–308)
	1 (0–1)	78 (25–186)	27 (8–89)
	1 (1–1)	136 (91–210)	74 (29–165)
	27 (20–33)	173 (125–355)	190 (102–373)
	0.64 (0.56–0.68)	0.17 (0.10–0.25)	0.21 (0.12–0.33)
	0	67 (66%)	138/281 (49%)
	11.0 (9.0–12.8)	12.4 (10.5–13.7)	12.1 (10.5–13.4)
	7.5 (5.2–8.7)	11.0 (8.8–13.7)	11.0 (7.9–14.3)
	254 (168–305)	298 (227–378)	290 (216–377)

Table 7.1 Continued.

	Metabolomics discovery cohort		
	Controls (n=22)	Tuberculous meningitis survivors (n=15*)	Tuberculous meningitis non-survivors (n=17)
Outcomes			
Length of hospital stay, days	16 (12–17)	25 (21–29)	4 (3–7)
Alive at discharge	NA	15 (100%)	0
Outcome at day 30			
Alive	NA	14 (93%)	0
Deceased	NA	0	17 (100%)
Lost to follow-up	NA	1 (7%)	0
Outcome at day 180			
Alive	NA	12 (80%)	0
Deceased	NA	1 (7%)	17 (100%)
Lost to follow-up	NA	2 (13%)	0

Data are n (%) or median (IQR). Quantitative trait loci were identified in the metabolomics discovery and tryptophan validation cohort combined (excluding three patients without genotype data). Data are missing for some patients, as indicated. NA = not applicable. *One patient was excluded from the analysis and table because of aberrant liquid chromatography-mass spectrometry results. ¶Eight control patients in the metabolomics discovery cohort were diagnosed with primary central nervous

chromatography, was 0.20 μM in survivors, 1.11 μM in non-survivors, and 2.08 μM in controls (p<0.0001 for 30-day survival; **supplementary figure 7.2C**). Low CSF tryptophan concentration predicted survival in Cox regression (hazard ratio [HR] for mortality 0.73; 95% CI 0.64–0.83; p<0.0001, for each halving in CSF tryptophan concentration; **figure 7.2B**). The HR was not affected by correction for sex, age, Glasgow Coma Scale, CSF neutrophils, CSF mononuclear cells, and rs17525495 *LTA4H* promotor polymorphism[43,191], either alone or in combination (**table 7.2**). This effect was not different in sensitivity analyses that excluded patients who were not culture-confirmed (n=33), patients who had received treatment before lumbar puncture (nine), patients who had received high-dose rifampicin (n=21), patients who had not received dexamethasone (four), and one patient with rifampicin-resistant tuberculous meningitis (data not shown).

	Tryptophan validation cohort		Genetic validation cohort
	Controls (n=17)	Tuberculous meningitis (n=101)	Tuberculous meningitis (n=285)
11 (4–20)		20 (11–23)	16 (8–22)
NA		72/100 (72%)	187/242 (77%)
NA		69 (68%)	199 (70%)
NA		29 (29%)	74 (26%)
NA		3 (3%)	12 (4%)
NA		52 (51%)	153 (54%)
NA		40 (40%)	99 (35%)
NA		9 (9%)	33 (12%)

system disease (dementia, epilepsy, meningoencephalitis, neurolupus, space-occupying lesions, or stroke), 11 had central nervous system manifestations of systemic disease (active pulmonary or miliary tuberculosis, advanced heart or kidney disease, or metabolic encephalopathy), and three had no final diagnosis.

CSF tryptophan metabolism in tuberculous meningitis

Based on the metabolomic data of the discovery cohort, cerebral tryptophan metabolism appeared to be one of the most upregulated pathways in patients with tuberculous meningitis compared with controls (false discovery rate $<10^{-19}$). Although CSF tryptophan concentrations were lower in patients with tuberculous meningitis compared with controls, downstream metabolites in the kynurenine pathway were 4–60-times higher in CSF samples of patients with tuberculous meningitis than in controls, although none of the downstream metabolites showed a significant association with survival (**supplementary figure 7.3A** and **online supplement**). We analysed publicly available gene expression data from brain autopsies of five patients with tuberculous meningitis and four patients with traumatic brain injury for gene expression[235]. In the kynurenine pathway Indoleamine 2,3-dioxygenase (*IDO1*), which is expressed in astrocytes and neurons[238] and codes for the rate-limiting enzyme that converts tryptophan to L-formylkynurenine, showed greater expression in

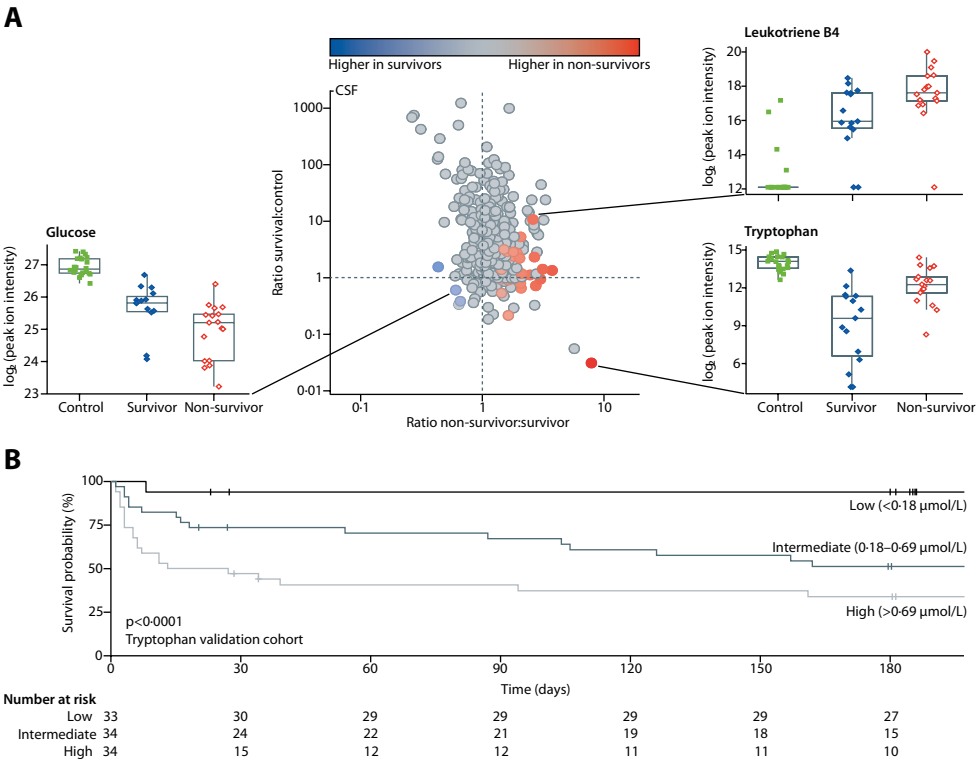

Figure 7.2 CSF metabolome as a determinant of survival in patients with tuberculous meningitis.

(A) Individual metabolites in CSF with ratio between tuberculous meningitis survivors and non-survivors, and ratio between tuberculous meningitis survivors and controls. Colours indicate strength of association; metabolites that do not show differences between groups (uncorrected p>0.05) are grey. The three subplots show metabolite concentrations according to patient category. The y-axis shows the 2-log of the relative abundance of metabolite ions as chromatographic peaks (peak ion intensity). Leukotriene B4, glucose, and tryptophan were chosen as relevant metabolites representing three different quadrants of the plot. (B) Kaplan-Meier plot of patient survival in the tryptophan validation cohort, according to CSF tryptophan concentrations, as divided in the following tertiles: low (<0.18 µmol/L), intermediate (0.18–0.69 µmol/L), and high (>0.69 µmol/L). CSF = cerebrospinal fluid.

patients with tuberculous meningitis than in patients with brain trauma (35-times upregulation, p=0.008; α = 0.05/10 for the ten genes tested; **supplementary figure 7.3B**), suggesting that increased tryptophan metabolism might lead to lower CSF tryptophan in tuberculous meningitis.

Table 7.2 Multivariate Cox regression for 180-day mortality in the tryptophan validation cohort and independent genetic validation cohort.

	Tryptophan validation cohort (n=100)		**Genetic validation cohort (n=235)**	
	HR (95% CI)	p	HR (95% CI)	p
Sex, male	0.86 (0.42–1.72)	0.669	NA*	NA*
Age, per 10-year increase	1.06 (0.80–1.40)	0.691	NA*	NA*
Glasgow Coma Scale, per point increase	0.76 (0.66–0.88)	0.00026	0.80 (0.72–0.88)	<0.0001
CSF neutrophils, per 10-fold increase	1.70 (0.86–3.36)	0.127	1.53 (1.10–2.12)	0.011
CSF mononuclear cells, per 10-fold increase	0.32 (0.14–0.70)	0.0044	0.75 (0.50–1.15)	0.188
LTA4H rs17525495 genotype, CT vs CC	0.76 (0.36–1.59)	0.460	1.06 (0.65–1.71)	0.823
LTA4H rs17525495 genotype, TT vs CC	0.35 (0.07–1.62)	0.177	0.72 (0.30–1.69)	0.446
CSF tryptophan, per each halving	0.74 (0.63–0.87)	0.00033	NA	NA
Prognostic index	NA	NA	NA	0.0083

Patients with complete data were as follows: tryptophan validation cohort (n=100, with 39 events), genetic validation cohort (n=235, with 81 events); for multivariate analysis, one patient was excluded from the tryptophan validation cohort and 50 were excluded from the genetic validation cohort because of missing Glasgow Coma Scale or *LTA4H* genotype data. CSF cell counts were analysed after $\log_{10}[x+1]$ transformation. Prognostic index was included as a continuous variable. HR = hazard ratio. NA = not applicable. CSF = cerebrospinal fluid. *LTA4H* = Leukotriene A4 Hydrolase. *Age and sex were included in the prognostic index together with the 11 tryptophan quantitative trait loci.

The impact of genetic variation on CSF tryptophan levels and patient survival

We mapped quantitative trait loci for CSF tryptophan concentrations using genome-wide SNP genotype data (available for 130 [98%] of 133 patients with available CSF tryptophan concentrations from the discovery and validation cohorts; **supplementary figure 7.1A**) to assess whether host genetic variation plays a part in the regulation of the amount of tryptophan in CSF. No single SNP showed genome-wide significance for CSF tryptophan concentrations, but we identified 11 independent loci that showed suggestive associations with CSF tryptophan levels ($p<0.00001$; **table 7.3**).

These 11 identified quantitative trait loci, along with age and sex, were used to generate a composite prognostic index to predict survival among patients with tuberculous meningitis. As expected, this score strongly predicted survival among the 130 patients we used for identification of the quantitative trait loci (**figure 7.3A**). The relevance of the prognostic index was validated in a separate group of HIV-negative patients with tuberculous meningitis, for whom no CSF tryptophan concentrations were available (**supplementary figure 7.1A**). The prognostic index composed of the 11 tryptophan quantitative trait loci also strongly predicted patient survival in this independent cohort ($p=0.023$ on log-rank test for 180-day survival, $n=285$), and this predictive power was further improved by including age and sex in the model ($p=0.0054$; **figure 7.3B**), although age and sex alone did not predict survival ($p=0.823$). The prognostic index showed a similar effect in sensitivity analysis restricted to 166 bacteriologically confirmed cases ($p=0.021$), and after correction for possible confounders (included in the multivariate analysis presented in **table 7.2**).

Finally, we examined the possible biological relevance of the 11 tryptophan quantitative trait loci. Only one tryptophan quantitative trait locus was known to influence expression of a gene, *WBP4*, the expression of which was affected in skeletal muscle ($p<0.0001$) and tibial nerve ($p=0.0006$). As a second approach to prioritise causal genes at tryptophan quantitative trait loci, we extracted publicly available expression data for annotated genes located within a 1-Mb *cis*-window of the 11 tryptophan quantitative trait loci in different human tissues and cell lines. Unsupervised clustering analysis of the 54 (77%) of 70 annotated genes with data available showed that the tryptophan quantitative trait loci were mainly expressed in immune cells and brain tissues (**supplementary figure 7.4**). In brain autopsy data of patients with tuberculous meningitis[235], 17 (24%) of 70 annotated genes showed differential expression compared to patients who died of head injury (meeting a cut-off of $p<0.05$; **table 7.3**). Pathway analysis for these genes did not reveal enrichment for any one pathway (data not shown), but this selection emphasised the role of immune genes (*TRIL*, *NAP1L1*, and *OSBPL8*), metabolic enzymes (*MAGI1*), and brain-specific genes (*WBP4*, *GAS7*, and *CHN2*) in determining tryptophan concentrations in CSF of patients with tuberculous meningitis.

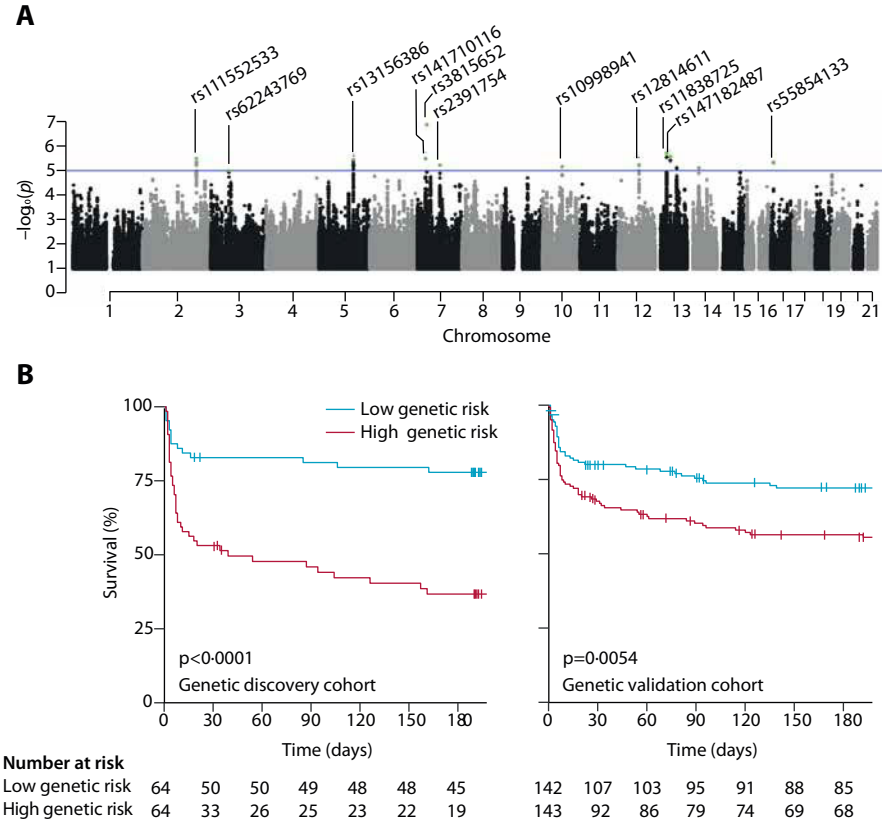

Figure 7.3 Cerebrospinal fluid tryptophan quantitative trait loci in relation to survival of patients with tuberculous meningitis.

(A) Manhattan plot for association of CSF tryptophan concentrations with single nucleotide polymorphisms on 22 somatic chromosomes. The horizontal line depicts the threshold chosen to call suggestive associations ($p<10^{-5}$), with the accession number (rsID) of 11 independent single nucleotide polymorphisms associated with tryptophan concentrations. (B) Kaplan-Meier plots using prognostic index including these 11 tryptophan quantitative trait loci, age, and sex, predicting survival of patients with tuberculous meningitis in the genetic discovery cohort and genetic validation cohort. CSF = cerebrospinal fluid.

Table 7.3 Cerebrospinal fluid tryptophan quantitative trait loci in tuberculous meningitis

	Chr.	Position	Reference allele (A)	Minor allele (a)	In tuberculous meningitis cohort			
					Minor allele frequency	AA	Aa	aa
rs111552533	2	192 996 515	C	T	0.42	47	63	20
rs62243769	3	65 949 227	C	G	0.40	48	60	22
rs13156386	5	123 017 888	A	G	0.27	72	50	8
rs141710116	7	80 867 056	T	C	0.23	72	56	2
rs3815652	7	33 913 404	T	C	0.32	58	63	9
rs2391754	7	29 403 188	T	C	0.20	87	38	5
rs10998941	10	71 495 726	T	G	0.44	39	65	26
rs12814611	12	76 384 849	T	C	0.43	37	74	19
rs11838725	13	41 671 085	T	C	0.21	77	50	3
rs147182487	13	54 547 574	T	C	0.13	36	94	0
rs55854133	17	10 497 745	A	G	0.15	98	29	3

AA, Aa, and aa genotypes are listed, where A represents the major allele and a the minor allele. SNP = single nucleotide polymorphism. *Linear regression analysis was used for quantitative trait loci mapping upon correcting for age and sex. #Based on differential expression analysis in tuberculous meningitis versus brain injury patients data (using data from Kumar and colleagues[235]), genes

Discussion

To our knowledge, this is the first study comparing the CSF and serum metabolome of patients with tuberculous meningitis and controls without meningitis, linking metabolite concentrations to patient mortality. CSF tryptophan concentration was identified as a strong predictor of mortality, and this finding was validated in a second patient cohort. Furthermore, by using genome-wide SNP data we identified 11 quantitative trait loci associated with CSF tryptophan concentrations, and found that these quantitative trait loci were predictive of patient survival in a third cohort of patients with tuberculous meningitis. Collectively, our data showed that cerebral tryptophan metabolism is important for the outcome of tuberculous meningitis.

We also believe this is the first study to examine the outcome of tuberculous meningitis using a combination of metabolomic and genomic approaches. In

In tuberculous meningitis cohort	Association with CSF tryptophan concentration in tuberculous meningitis*		Biological plausibility	
Imputation accuracy (R^2)	p	β	Nearest gene	Genes indicated by differential expression analysis#
0.87	3.21×10^{-6}	1.26	*TMEFF2*	*SDPR*
0.95	9.85×10^{-6}	−1.14	*MAGI1*	*MAGI1*
0.75	3.61×10^{-6}	1.60	*CSNK1G3*	*CEP120*
0.75	5.91×10^{-6}	−1.94	*SEMA3C*	*HGF, SEMA3C*
0.66	1.31×10^{-7}	1.83	*BMPER*	*BMPER, BBS9*
0.47	3.26×10^{-6}	1.73	*CHN2*	*TRIL*
0.87	6.89×10^{-6}	1.22	*COL13A1*	*TYSND1*
0.95	5.61×10^{-6}	1.28	*PHLDA1*	*OSBPL8, BBS10, NAP1L1, PHLDA1*
0.62	1.91×10^{-6}	−1.89	*WBP4*	*RGCC, WBP4, FOXO1*
0.47	2.56×10^{-6}	2.35	*LINC00558*	..
0.70	4.75×10^{-6}	1.87	*MYHAS*	*GAS7*

located within 1 Mb cis window of 11 tryptophan quantitative trait loci (n=70 for the 11 quantitative trait loci) that might contribute to tryptophan concentration in CSF of patients with tuberculous meningitis were identified. Chr = chromosome.

accordance with earlier studies, we found lower CSF glucose and higher lactate concentrations[195], and increased amounts of aminoacids[239] in CSF of patients with tuberculous meningitis compared with controls. We confirmed that glucose was lowest in patients who subsequently died. We focused on tryptophan because of its distinct pattern and biological relevance for tuberculosis. The combination of lower CSF tryptophan concentrations, higher concentrations of downstream kynurenine metabolites, and upregulated *IDO1* in brain autopsy mRNA expression profiles suggests that *M. tuberculosis* brain infection leads to increased cerebral tryptophan metabolism. Based on these findings, we concluded that an individual's genetic makeup determines the response in tryptophan metabolism if *M. tuberculosis* invades the brain to cause meningitis, with lower CSF tryptophan associated with reduced mortality.

Low CSF tryptophan metabolite concentrations have previously been found in bacterial meningitis[240], trypanosomiasis[241], rabies[242] and cerebral malaria[243].

However, to our knowledge, CSF tryptophan has never been reported in relation to survival of patients with central nervous system infection. Several possible explanations exist for how tryptophan and kynurenine metabolism might affect the outcome of tuberculous meningitis. First, activated macrophages could inhibit *M. tuberculosis* growth through activation of *IDO1*, with depletion of tryptophan as an energy source for mycobacteria[244]. Second, tryptophan and its downstream metabolites affect T-cell responses and inflammation. For instance, kynurenine is sensed by the aryl hydrocarbon receptor[245], which is engaged in *M. tuberculosis*-infected macrophages and crucial for several innate immune responses[246]. Finally, certain kynurenine metabolites, such as kynurenic acid and quinolinic acid, are involved in neuroprotective and neurodamaging responses[238]. Therefore, the relative abundance and balance of tryptophan and kynurenine metabolites is likely to affect the outcome of tuberculous meningitis. Notably, compared to tryptophan, individual downstream metabolites showed smaller differences between survivors and non-survivors, probably because tryptophan is metabolised via different pathways.

We found a genetic correlate of CSF tryptophan concentration in tuberculous meningitis that predicted survival in an independent cohort, which suggested the intrinsic ability to upregulate tryptophan metabolism in response to *M. tuberculosis* infection affects the balance between bacterial clearance and immunopathology in tuberculous meningitis. As there are no Indonesian specific SNP reference panels available for imputation we should be cautious about inferring causality of identified variants. Nevertheless, further analysis of CSF tryptophan quantitative trait loci identified several candidate genes with immune, metabolic, or brain-specific functions, which could be targets for further study (e.g., in experimental models). Tryptophan metabolism is an attractive target for adjunctive therapy. Treatment with interferon-α successfully increased peripheral blood but not CSF kynurenine concentrations[247], and ingestion of a 15-aminoacid, tryptophan-free mixture strongly reduced CSF tryptophan concentrations[248].

Strengths of our study are the careful description and prospective follow-up of patients, the combination of metabolomics and genetics, and the validation of findings in two separate patient groups. Limitations of the metabolomic approach include the large but still restricted number of annotated metabolites, which form a fraction of the incompletely characterised human metabolome. Therefore, metabolites other than tryptophan that are not yet annotated could be better predictors for survival. Moreover, the discovery cohort included a relatively small number of culture-confirmed, HIV-negative patients, so further study is needed to discover metabolites with smaller effect sizes and to expand

our findings to HIV-positive patients. We showed a genetic association with tryptophan concentration and mortality, but the observational nature of our study precludes statements on the causative mechanism. Further study is therefore needed to identify specific metabolic steps in cerebral tryptophan metabolism that are linked to immunopathology and patient survival. Also, confirmation of our results in a cohort with a different genetic background could validate the ability of specific quantitative trait loci in their ability to predict CSF tryptophan concentration and survival. Intervention studies should help establish if tryptophan metabolism can be used as a target for adjuvant treatment in tuberculous meningitis.

In summary, a low CSF tryptophan concentration strongly predicted patient survival, and no association was found between serum tryptophan and mortality. CSF tryptophan concentrations in patients with tuberculous meningitis were under genetic influence, and genetic loci correlating with CSF tryptophan concentrations also predicted survival in an independent patient group. Collectively, these data suggest that cerebral tryptophan metabolism is crucial for survival of tuberculous meningitis. Our findings provide possible new strategies for host-directed therapy (e.g., pharmacological induction of tryptophan metabolism) for tuberculous meningitis. Our integrative approach of combining CSF metabolomics and genetics with routine patient characteristics and survival also holds promise for identification of other relevant biological pathways and targets for adjuvant therapy, both in tuberculous meningitis and in other central nervous system infections.

Acknowledgments

We thank the neurology residents and tuberculous meningitis study team for monitoring patients (Hasan Sadikin General Hospital, Bandung, Indonesia); the director of the Hasan Sadikin General Hospital (Bandung, Indonesia) for accommodating the research; Amy Deik, Kerry Pierce, Kevin Bullock, and Justin Scott for processing samples and acquiring liquid chromatography-mass spectrometry data; Jelle Goeman for statistical advice; Corneel Eijsbouts and Rob ter Horst for bioinformatic advice; Ben Geurtz for ultra-performance liquid chromatography measurement of tryptophan and Elma Prudon-Rosmulder for nephelometric analysis of albumin; and Mathieu Platteel for DNA quality control and hybridisation and Lisa van de Wijer for input on tryptophan metabolism.

Author contributions

AvL, CBC, MGN, and RvC designed the study. SD, THA, RR, and ARG supervised patient recruitment. JA, LC, and BA supervised patient sample flow. AvL, CR, and SD did patient data quality control. CBC oversaw metabolomics data acquisition and JA-P and CBC analysed and interpreted these data. MMV supervised ultra-performance liquid chromatography tryptophan measurement. RA-G, IR-P, YL, and VK did the genetic analysis. AvL and VACMK did other bioinformatic analyses. RAN and LABJ contributed to metabolic concepts. AvL and RvC wrote the first draft of the manuscript. All other authors provided input to the draft and approved the final version of the manuscript.

Supplementary Methods

CSF and serum metabolomics

For the hydrophilic interaction chromatography negative ion method, serum and plasma samples were precipitated in 80% methanol containing inosine-^{15}N4, thymine-d4, and glycocholate-d4 internal standards (Cambridge Isotope Laboratories; Andover, MA, USA). Samples were cleared by centrifugation and supernatants injected onto a 150 mm × 2 mm Luna NH2 column (Phenomenex; Torrance, CA, USA).

For the hydrophilic interaction chromatography positive ion method, samples were precipitated with nine volumes of 74.9% acetonitrile, 24.9% methanol, and 0.2% formic acid, by volume containing stable isotope-labelled internal standards (valine-d8; Isotec, Sigma-Aldrich; St Louis, MI, USA; and phenylalanine-d; Cambridge Isotope Laboratories). After centrifugation, supernatants were injected onto a 150 mm × 2 mm Atlantis hydrophilic interaction chromatography column (Waters; Milford, MA, USA)[230].

For measuring compounds of intermediate polarity, serum and plasma samples were extracted in methanol containing PGE2-d4 as an internal standard (Cayman Chemical Company, Ann Arbor, MI, USA), and supernatants of samples were cleared by centrifugation. Extracted CSF samples underwent solid phase extraction with an Oasis HLB Cartridges column (Waters) before injection onto a 150 mm × 2 mm ACQUITY T3 column (Waters). Finally, polar and non-polar lipids were obtained by extracting samples in isopropanol containing 1-dodecanoyl-2-tridecanoyl-sn-glycero-3-phosphocholine as an internal standard (Avanti Polar Lipids; Alabaster, AL, USA). After centrifugation, supernatants were injected directly onto a 100 mm × 2.1 mm ACQUITY BEH C8 column (1.7 μm; Waters)[231].

Targeted data were analysed using MultiQuant software (version 1.1; AB SCIEX, Foster City, CA, USA) for automated peak integration and manual review for quality of integration. Metabolites analysed using non-targeted measurements were manually integrated and inspected using TraceFinder software (version 3.1, Thermo Fisher Scientific; Waltham, MA, USA) and their identities validated by matching measured retention times and masses to mixtures of reference metabolites.

Quantification of CSF tryptophan and CSF to serum albumin ratio

CSF samples were diluted three times with formic acid (0.05%) before injection (25 μL) onto a reverse phase column (ACQUITY UPLC R HSS T3 [1.8 μm, 2.1 × 100 mm]; Waters). The mobile phase (0.3 mL/min) consisted of ammonium acetate buffer (pH 5.4), containing 0.38% methanol. Fluorescence was used for detection (excitation at 278 nm and emission at 325 nm) during a 15 min run.

CSF and serum albumin was measured using routine nephelometry in CSF (Immage; Beckman Coulter, Brea, CA, USA) and photometrically in serum (cobas 6000; Roche Diagnostics, Indianapolis, IN, USA).

Genotyping, quality control and imputation

DNA samples were genotyped using a commercially available SNP chip (HumanOmniExpressExome-8 v1.0; Illumina; San Diego, CA, USA). Genotype calling was performed using Opticall 0.7.0[249] using the default settings. Samples with a call rate less than 0.99 were excluded, as were variants with a Hardy-Weinberg equilibrium $p<0.0001$, and minor allele frequency less than 0.001.

No genetic outliers were detected by visualizing the cohort using multi-dimensional scaling plots. Strands of the remaining 259, 335 variants were aligned and identified against the 1000 Genome reference panel with Genotype Harmonizer.[250] We imputed the samples on the Michigan imputation server,[251] using the Asian population in human reference consortium as reference panel,[252] and then selected variants with an R^2 of at least 0.3[253]. The rs17525495 *LTA4H* promotor polymorphism was genotyped using the TaqMan C__25593629_10 assay on a 7300 ABI real-time PCR system (Applied Biosystems, Foster City, CA, USA).

Supplementary figures

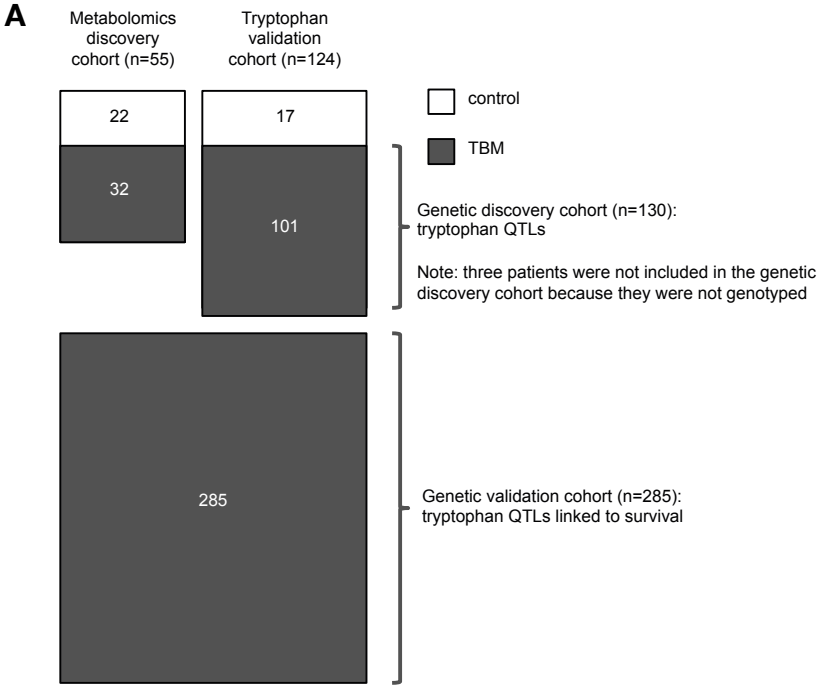

Supplementary figure 7.1

(A) Overview of patients in different parts of the study. All tuberculous meningitis patients (100%) in the metabolomics discovery cohort had a positive CSF culture, and the same was true for 60% of patients in the tryptophan validation cohort and 57% in the genetic validation cohort. (B) Comparison of serum and CSF metabolite concentrations. Correlation between LC-MS obtained values for serum versus CSF. Dotted line: x = y. (C) Differences between patients and controls across the range of metabolites. Serum versus CSF albumin concentration (left) and CSF/serum ratio (right). Mann-Whitney U test for diagnosis (control versus patients): p<0.001. Mann-Whitney U test for outcome (survivor versus non-survivor): p=0.58. Dotted lines indicate the normal range (0.005 to 0.008).[232] (D) Differences between patients and controls across the range of metabolites. Relationship between metabolite m/z and abundance (mean intensity) in CSF and serum. Colours indicate fold difference (margins indicated in the coloured bar) between patients and controls based on uncorrected p-values (as in main text figure 7.1C and 7.1D).

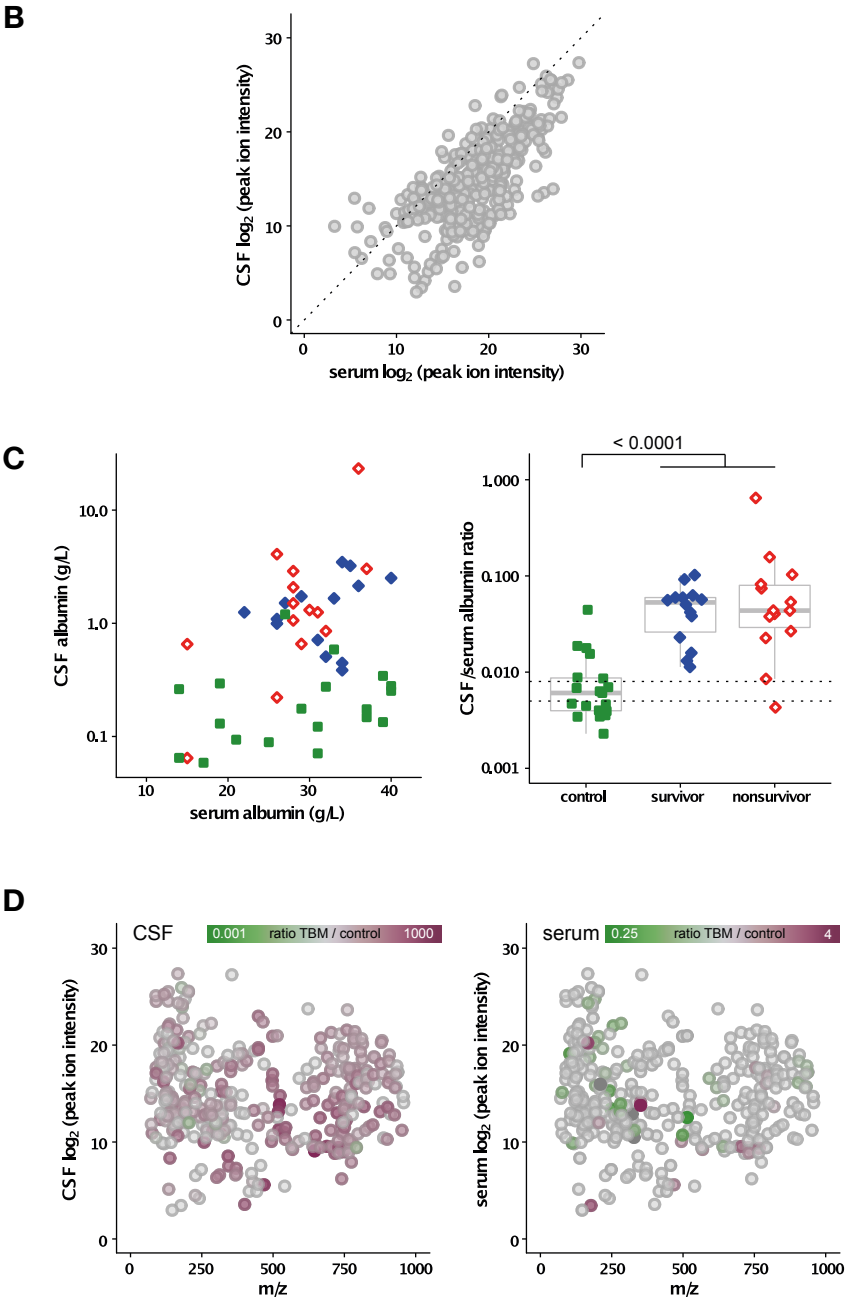

Supplementary figure 7.1 Continued.

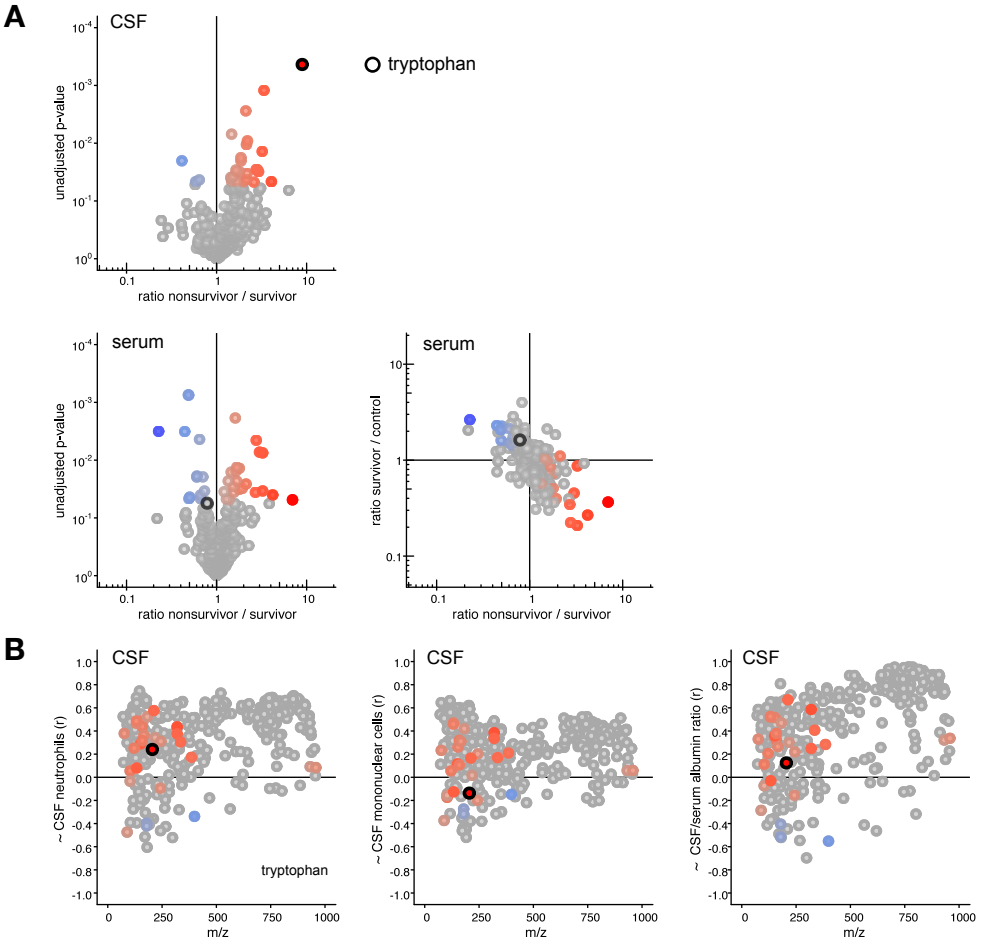

Supplementary figure 7.2 Comparison of CSF and serum metabolites according to survival status.

(A) Volcano plot for individual metabolites in CSF (upper plot) and serum (lower plot), with fold difference between tuberculous meningitis survivors and nonsurvivors (x-axis), and unadjusted p-value (y-axis). The plot on the lower right features the same x-axis, but contrasts against fold difference between tuberculous meningitis survivors and controls (y-axis). Colours indicate strength of association and metabolites without an association (uncorrected p>0.05) are coloured grey. The black circle indicates tryptophan. (B) Correlation of CSF metabolites with CSF neutrophils (left), CSF mononuclear cells (middle) and blood-CSF barrier disruption as measured by CSF-serum albumin gradient in tuberculous meningitis patients. Colours correspond to fold difference between survivors and nonsurvivors. Metabolites without an association (uncorrected p>0.05) are coloured grey (as in Figure 7.2A). The black circle indicates tryptophan. (C) CSF tryptophan measured by ultra-performance liquid chromatography in the discovery and the validation cohort. P-value by Mann-Whitney test for outcome of tuberculous meningitis patients at discharge (discovery cohort) and at 30 days after admission (validation cohort).

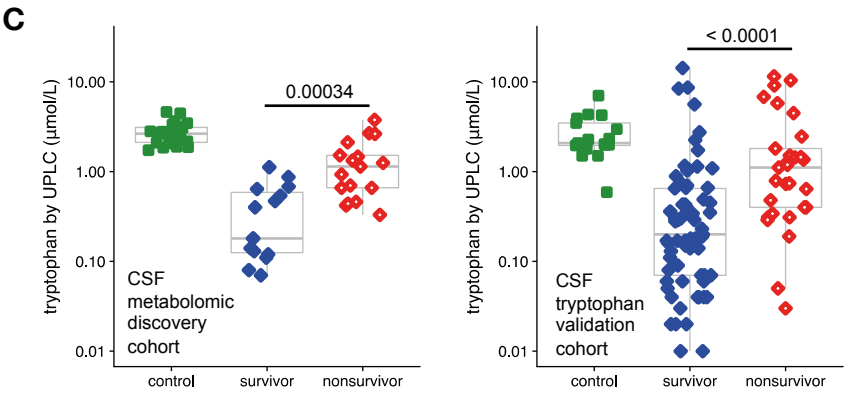

Supplementary figure 7.2 Continued.

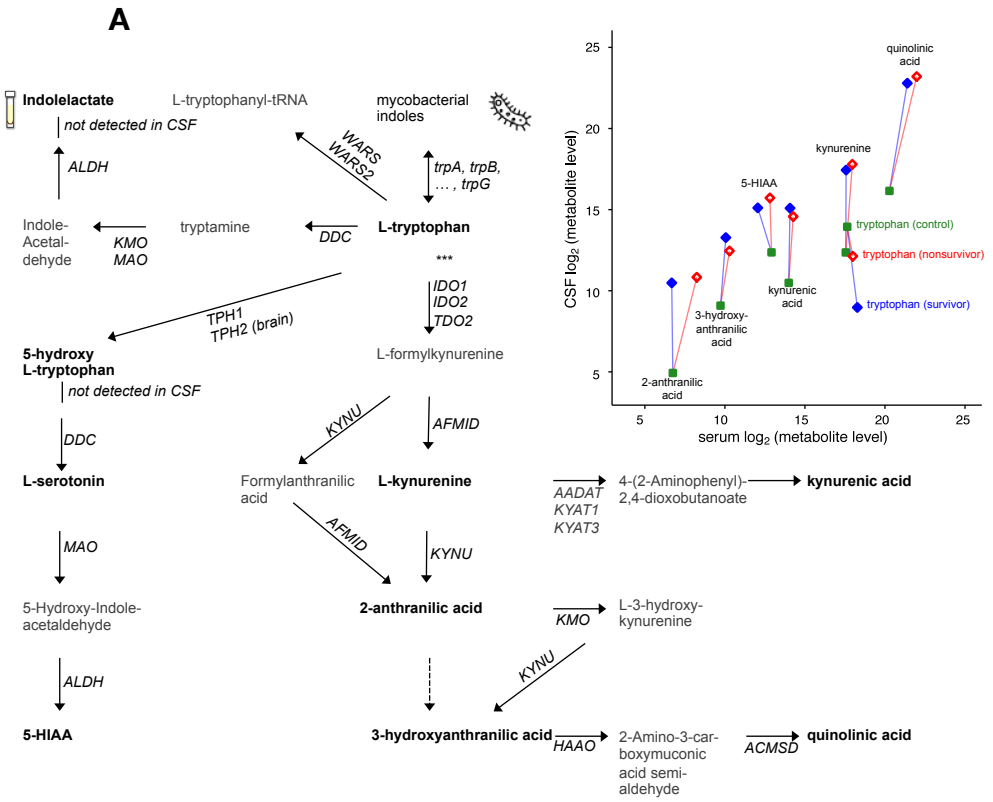

Supplementary figure 7.3

(A) Pathway based on Kyoto Encyclopedia of Genes and Genomes (map 00380; http://www.genome.jp/kegg/pathway/), Virtual Metabolic Human; http://vmh.uni.lu) and the Small Molecule Pathway Database (SMP00063, http://smpdb.ca). Gene symbols: *AADAT*: aminoadipate aminotransferase; *ACMSD*: aminocarboxymuconate semialdehyde decarboxylase; *AFMID*: arylformamidase; *DDC*: DOPA decarboxylase (aromatic L-amino acid decarboxylase); *IDO1* and *IDO2*: indolamine 2,3-dioxygenase 1 and 2; *HAAO*: 3-hydroxyanthranilate 3,4-dioxygenase; *KMO*: kynurenine 3-monooxygenase; *KYAT1* and *KYAT3*: kynurenine aminotransferase 1 and 3; *KYNU*: Kynureninase. *TDO2*: tryptophan 2,3-dioxygenase. *TPH1* and *TPH2*: tryptophan hydroxylase 1/2; *WARS1/2*: tryptophanyl-tRNA synthetase. Other abbreviations: *ALDH*: an aldehyde dehydrogenase; *MAO*: a monoamine oxidase, i.e. MAOA or MAOB. 5-HIAA: 5-hydroxy-indolacetate. Inlay: mean tryptophan pathway metabolite levels in serum versus CSF for controls (green), tuberculous meningitis survivors (blue) and nonsurvivors (red). (B) Volcano plot of brain autopsy mRNA expression with fold difference between five tuberculous meningitis patients and four patients deceased of head-injury (x-axis) with unadjusted p-values (y-axis). Genes involved in the tryptophan pathway are indicated by black circles, against grey circles for all other genes tested by Kumar et al. Differentially expressed genes ($p<0.05$) in the tryptophan pathway are named. Data made publicly available by Kumar et al[235] (GSE23074).

B

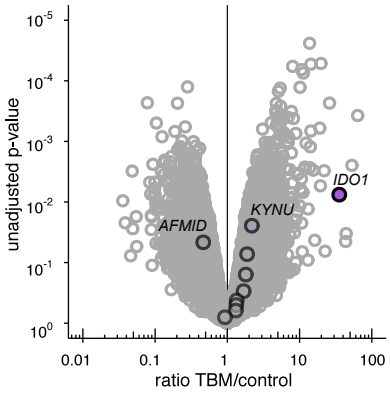

Supplementary figure 7.3 Continued.

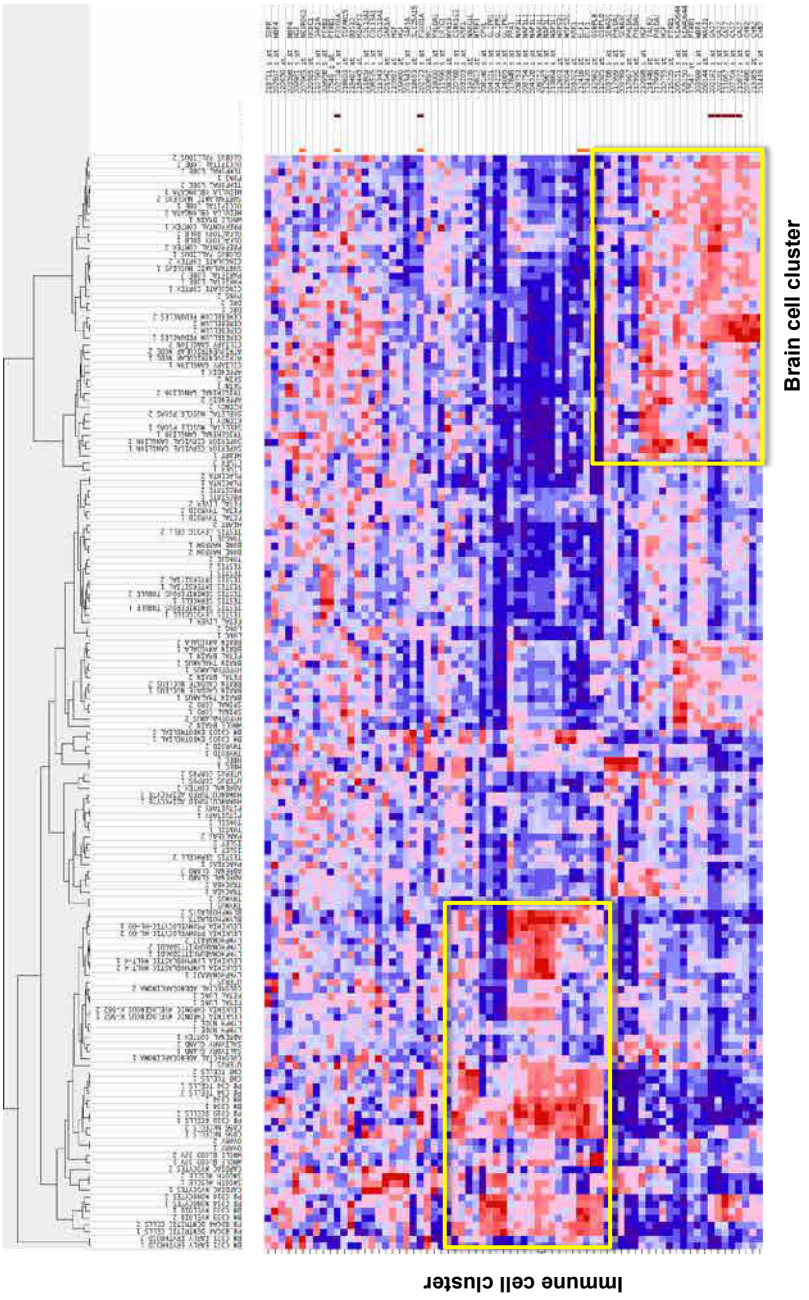

Supplementary figure 7.4 Expression profile of genes linked to tryptophan quantitative trait loci in multiple human tissues.

The expression data could be extracted for 54 of the 70 genes linked to CSF tryptophan quantitative trait loci. Colours indicate relative expression over different tissues (x-axis) from high (red) to low (blue). Some genes are represented by multiple probes (y-axis). Unsupervised clustering analysis identified two main clusters shown as yellow rectangles, one in brain and one in immune cells.

Supplementary table 7.1 Pathway analysis by MetaboAnalyst[254] using the GlobalTest[234] algorithm for metabolites in CSF.

Pathway	Total compounds in pathway	Hits	FDR	Impact
Thiamine metabolism	3	3	1.49×10^{-20}	0.125
Cyanoamino acid metabolism	4	3	2.73×10^{-20}	0.000
Aminoacyl-tRNA biosynthesis	19	18	9.46×10^{-20}	0.169
Tryptophan metabolism	9	5	9.46×10^{-20}	0.264
Methane metabolism	5	4	5.26×10^{-18}	0.018
Glutathione metabolism	9	5	1.10×10^{-17}	0.030
Propanoate metabolism	7	6	1.10×10^{-17}	0.087
Porphyrin and chlorophyll metabolism	4	3	1.19×10^{-17}	0.000
Glycolysis or Gluconeogenesis	5	2	3.83×10^{-17}	0.000
Lysine degradation	5	4	8.65×10^{-17}	0.153
Phenylalanine, tyrosine and tryptophan biosynthesis	7	4	8.65×10^{-16}	0.082
Glycine, serine and threonine metabolism	13	10	1.10×10^{-15}	0.528
Nitrogen metabolism	13	11	1.25×10^{-15}	0.008
Pyruvate metabolism	5	2	1.35×10^{-15}	0.138
Glycerophospholipid metabolism	10	7	6.60×10^{-15}	0.409
Arginine and proline metabolism	18	15	1.33×10^{-14}	0.601
Selenoamino acid metabolism	1	1	4.52×10^{-14}	0.000
Valine, leucine and isoleucine biosynthesis	5	4	3.75×10^{-13}	0.040
Valine, leucine and isoleucine degradation	4	4	5.72×10^{-13}	0.022
Fructose and mannose metabolism	2	1	1.27×10^{-12}	0.009
Pantothenate and CoA biosynthesis	7	5	1.40×10^{-12}	0.291
Ether lipid metabolism	1	1	4.60×10^{-12}	0.000
Nicotinate and nicotinamide metabolism	12	4	4.94×10^{-12}	0.079
Ubiquinone and other terpenoid-quinone biosynthesis	3	1	9.30×10^{-12}	0.000
Pyrimidine metabolism	19	9	2.43×10^{-11}	0.192
Histidine metabolism	8	2	3.18×10^{-11}	0.140
D-Arginine and D-ornithine metabolism	2	2	8.20×10^{-11}	0.000
Lysine biosynthesis	4	1	2.39×10^{-10}	0.100

Biotin metabolism	1	1	2.39×10^{-10}	0.000
Caffeine metabolism	2	2	4.56×10^{-10}	0.031
Arachidonic acid metabolism	8	4	7.09×10^{-10}	0.242
D-Glutamine and D-glutamate metabolism	3	2	1.13×10^{-9}	0.139
Galactose metabolism	7	5	2.28×10^{-9}	0.052
Amino sugar and nucleotide sugar metabolism	5	3	4.36×10^{-9}	0.000
Cysteine and methionine metabolism	11	6	4.40×10^{-9}	0.338
Primary bile acid biosynthesis	8	8	5.09×10^{-9}	0.054
beta-Alanine metabolism	10	6	8.75×10^{-9}	0.302
Glyoxylate and dicarboxylate metabolism	8	6	1.43×10^{-8}	0.185
Alanine, aspartate and glutamate metabolism	11	7	6.51×10^{-8}	0.592
Purine metabolism	21	11	1.71×10^{-7}	0.089
Taurine and hypotaurine metabolism	4	3	6.78×10^{-7}	0.363
Butanoate metabolism	7	5	7.39×10^{-5}	0.051
Glycosylphosphatidylinositol(GPI)-anchor biosynthesis	1	1	7.65×10^{-5}	0.044
Starch and sucrose metabolism	5	3	2.24×10^{-4}	0.077
Pentose and glucuronate interconversions	6	2	2.79×10^{-4}	0.087
Phenylalanine metabolism	8	4	2.88×10^{-4}	0.119
Inositol phosphate metabolism	3	2	3.66×10^{-4}	0.137
Ascorbate and aldarate metabolism	6	2	3.66×10^{-4}	0.033
Tyrosine metabolism	12	3	9.18×10^{-4}	0.047
Citrate cycle (TCA cycle)	9	6	1.96×10^{-3}	0.252
Linoleic acid metabolism	3	1	2.02×10^{-3}	0.000
alpha-Linolenic acid metabolism	1	1	2.02×10^{-3}	0.000
Fatty acid biosynthesis	5	3	3.96×10^{-3}	0.000
Sphingolipid metabolism	6	5	4.60×10^{-3}	0.139
Fatty acid metabolism	2	1	7.88×10^{-3}	0.030
Fatty acid elongation in mitochondria	1	1	7.88×10^{-3}	0.000
Glycerolipid metabolism	4	2	1.05×10^{-2}	0.059
Pentose phosphate pathway	5	2	2.34×10^{-2}	0.098
Sulfur metabolism	1	1	3.13×10^{-1}	0.000
Synthesis and degradation of ketone bodies	1	1	9.89×10^{-1}	0.000

FDR = false discovery rate.

8

Survival of tuberculous meningitis is linked to cerebrospinal fluid vascular endothelial growth factor

Valerie A.C.M. Koeken, Arjan van Laarhoven, Raúl Aguirre-Gamboa, Sofiati Dian, Jessi Annisa, Lidya Chaidir, Robbie Herawan, Rovina Ruslami, Tri Hanggono Ahmad, Mihai G. Netea, Bachti Alisjahbana, Ahmad Ganiem, Vinod Kumar, Reinout van Crevel

In preparation

Abstract

Introduction
Tuberculous meningitis is the most severe form of tuberculosis. Damaging and/or ineffective host immune responses contribute to the high mortality of tuberculous meningitis, but the underlying mechanisms remain largely unknown.

Methods
We included patients with confirmed or probable tuberculous meningitis in a prospective cohort at the Hasan Sadikin Hospital (Bandung, Indonesia). Using a multiplex immunoassay, 94 inflammation-related proteins were measured in cerebrospinal fluid (CSF) samples of 131 tuberculous meningitis patients and 45 control patients without meningitis. Next, genome-wide single nucleotide polymorphism typing was used to identify genetic loci correlating to CSF protein levels. These quantitative trait loci (QTLs) were analysed in a survival analysis in an independent cohort of 299 tuberculous meningitis patients.

Findings
Overall, 77 of 94 proteins detected in at least 25% of the samples were included in the analysis; 69 (92%) of these were significantly different between the tuberculous meningitis patients and the control group (FDR < 0.05), and 66 of 69 markers were higher in tuberculous meningitis patients compared to controls. Four CSF proteins significantly predicted 180-day mortality, including vascular endothelial growth factor (VEGF). Six QTLs for CSF VEGF were identified, including one genome-wide significant QTL (rs3019146; $p=2.17 \times 10^{-8}$). A prognostic index based on these QTLs significantly predicted survival in the discovery cohort (p=0.0088) and an independent validation cohort (p=0.0018).

Interpretation
High CSF concentrations of VEGF show a strong association with increased mortality of tuberculous meningitis, possibly because of its effects on vascular permeability, dysfunction of tight junction proteins, and brain oedema. CSF VEGF concentrations in tuberculous meningitis have a genetic correlate, likely contributing to the variable outcome of tuberculous meningitis.

Introduction

On a global scale, tuberculosis remains a leading cause of death, and approximately one fourth of the world's population is infected with *M. tuberculosis*[1]. Tuberculous meningitis is the most devastating manifestation of tuberculosis, which results in death or severe disability in roughly half of all tuberculous meningitis cases[27]. Understanding and identifying factors that affect mortality is crucial to improve therapeutic strategies.

The host immune system contributes to the poor outcome of tuberculous meningitis, either through inadequate killing of *M. tuberculosis*, or through an inappropriate inflammatory response leading to tissue damage (immunopathology)[16]. Previous studies have identified a low proportion of cerebrospinal fluid (CSF) lymphocytes (**chapter 5**) or a low overall number of CSF leukocytes[43] associated with mortality. Reports on individual inflammatory mediators have not been consistent. For example, in a recent study high CSF IFN-γ was associated with good outcome in HIV-negative patients, but not HIV-positive patients[43], while in an older study IFN-γ was protective only in HIV-positive patients[255].

Therefore, the aim of this study was to obtain a broader characterization of the inflammatory response in CSF in tuberculous meningitis using an unbiased approach, and to link this to mortality. To this purpose we measured a large panel of inflammatory proteins in CSF and linked their concentrations to survival in a prospective cohort of tuberculous meningitis patients. We then searched for single nucleotide polymorphisms (SNPs) that act as quantitative trait loci (QTLs) for CSF proteins associated with survival, and examined whether these QTLs also predicted survival in an independent cohort of tuberculous meningitis patients.

Methods

Study design and participants

Study participants with suspected meningitis were included in a prospective cohort from the Hasan Sadikin Hospital (Bandung, Indonesia) from 31st October 2006 to 16th June 2016 as described in **chapter 5**. HIV co-infection, which strongly affects the immune response and mortality of tuberculous meningitis, was an exclusion criterion for this study. Routine clinical and CSF characterization were performed at the time of diagnosis, and survival was monitored for one year. For the proteomic and genetic analyses, 131 tuberculous meningitis patients and 45 controls were selected from this prospective cohort, and another 299 tuberculous

meningitis patients were selected for genetic validation. Patients were included under the project "Optimization of Diagnosis of Meningitis," approved by the Ethical Committee of Hasan Sadikin Hospital/Faculty of Medicine of Universitas Padjadjaran, Bandung, Indonesia (449/UN6.C1.3.3/KEPK/PN/2015).

Protein analysis

CSF samples were centrifuged for 15 minutes at 3000 x g and the supernatant was stored at -80°C. The commercially available ProSeek Multiplex Inflammation I panel (Olink Proteomics, Uppsala, Sweden) was used to measure a panel of 92 inflammation-related proteins in CSF. The procedure of the multiplex proximity extension assay was performed as previously described[256]. Briefly, proteins are recognized by pairs of antibodies coupled to cDNA strands. These cDNA strands bind when they are in close proximity, after which they extend by a polymerase reaction. After detection and normalization, this results in normalized protein expression values, measured on a $\log_2$-scale. Proteins were excluded from the analysis when the target protein was detected in less than 25% of the samples. Additionally, levels of neuron-specific enolase (NSE), calprotectin (S100A8/A9), and IL-1Ra were measured in these CSF samples using enzyme-linked immunosorbent assays (ELISAs) and were performed according to the manufacturer's protocol (R&D Systems, Minneapolis, Minnesota, USA). ELISA data were log-transformed before analysis. Serum and CSF albumin were measured in a subgroup of patients as described in **chapter 7**.

Protein data analysis and statistics

Data analysis of this study included protein, survival and QTL analysis. All computational analyses were performed in R 3.3.3. Protein levels were compared between tuberculous meningitis patients and controls using two-sample Wilcoxon tests. A false discovery rates (FDR) based on Benjamini-Hochberg procedure of less than 0.05 was considered significant. Proteins levels were then correlated using Spearman's Rank-Order correlation and clustered using average hierarchical clustering using a maximum distance between proteins of 0.3, visualized using the R package 'corrplot'. Each cluster was represented by the protein with the lowest distance to the other proteins in that cluster. Due to high correlation between markers and to avoid the burden of multiple testing corrections, only the representatives were included in further analysis, which enabled us to analyse groups of proteins rather than all markers individually. The protein cluster representatives were correlated to relevant measures of inflammation or brain damage using Spearman correlation, and analysed for survival using Cox regression with R packages survival and survminer. The Bonferroni method was used to correct for multiple testing.

Genome-wide quantitative trait loci mapping

Genotyping and imputation was performed as described in **chapter 7**. Quantitative trait loci (QTLs), genetic variants association with protein levels, were identified using log_2-transformed CSF protein expression values with a threshold for genome-wide significance was of $p<5 \times 10^{-8}$, while $p<1 \times 10^{-5}$ was considered a suggestive association. Finally, to test whether clinical parameters were confounding VEGF or our prognostic index, we performed a multivariate Cox regression including gender, age, Glasgow Coma Scale, and polymorphonuclear and mononuclear cell counts in the CSF.

Results

Inflammation-related proteins in CSF of tuberculous meningitis patients

For the proteomic analysis, 131 tuberculous meningitis patients and 45 controls were included. Of those 131 patients, 97 (74%) had definite tuberculous meningitis, as confirmed by CSF culture or PCR. The patient characteristics of the cohort are summarized in **table 8.1**. Including the proteins measured by ELISA, 94 proteins were measured in CSF (**online supplement**). The quality of the measurement was high, and 99% of the samples passed quality control. Patients with tuberculous meningitis had a distinct CSF proteome compared to controls. Overall, 77 of the 94 (82%) were detected in at least 25% of the tuberculous meningitis patients' CSF samples and therefore included in the analysis. Of these 77 proteins, 71 (92%) differed significantly between the controls and the tuberculous meningitis group, 68 were higher and 3 were lower in tuberculous meningitis patients compared to controls (**figure 8.1**).

Subsequently, we analysed global correlation patterns for CSF proteins in tuberculous meningitis patients. Using Spearman correlations and average hierarchical clustering, we identified 30 clusters of proteins, each represented by one protein with the lowest relative distance to the other proteins in the cluster (**figure 8.2**).

The majority of the protein pairs showed positive correlations, although a number of proteins including CXCL9, CXCL10, and FGF5 mainly showed inverse correlations with the other proteins. None of the CSF protein concentrations correlated well (Spearman's rho>0.5) with CSF mononuclear cell count, and only four (13%) out of 31 correlated with polymorphonuclear cell counts (**figure 8.3**), indicating that CSF leukocytes are not the main source of these proteins. Seven

Table 8.1 Patient characteristics.

	Discovery cohort		Validation cohort
	Tuberculous meningitis (n = 131)	Controls (n = 43)	Tuberculous meningitis (n = 299)
Clinical parameters			
Sex			
Male	82 (63%)	23 (53%)	157 (53%)
Female	49 (37%)	20 (47%)	142 (47%)
Age	29 (22–38)	35 (22–42)	28.5 (22–37)
Tuberculous meningitis grade			
Grade I	6/130 (5%)	NA	31/272 (11%)
Grade II	102/130 (78%)	NA	209/272 (77%)
Grade III	22/130 (17%)	NA	3/272 (1%2)
Temperature, °C	37.7 (37.0–38.2)	37.1 (36.7–37.8)	37.5 (36.8–38.0)
Glasgow Coma Scale	13 (11–14)	15 (14–15)	14 (12–15)
Seizures present	7/126 (6%)	6 (14%)	18/257 (7%)
Motor abnormalities present	73/129 (57%)	24 (56%)	134/253 (53%)
Cranial Nerve Palsy present	90 (69%)	23/42 (55%)	169/270 (63%)
Chest X-ray abnormal	98/129 (76%)	31 (72%)	196/272 (72%)
Cerebrospinal fluid			
Leukocytes, cells/μL	205 (70–368)	2 (1–2)	138 (47–323)
Mononuclear cells, cells/μL	106 (35–188)	1 (0–1)	75 (28–176)
Polymorphonuclear cells, cells/μL	65 (19–173)	0 (0–1)	26 (7–91)
Protein, mg/dL	182 (122–357)	27 (20–38)	190 (106–372)
Neuron-specific enolase, ng/mL	24.7 (15.9–39.9)	15.5 (10.2–21.1)	NA
CSF to blood glucose ratio	0.17 (0.10– 0.24)	0.59 (0.54–0.69)	0.21 (0.11–0.33)
M. tuberculosis culture positive	97 (74%)	0 (0%)	145 (49%)

Blood			
Haemoglobin, g/dL	12.3 (10.5–13.7)	11.3 (8.9–12.8)	12.1 (10.5–13.4)
Leukocytes, x 10^9/L	10.9 (8.8–13.7)	8.2 (7.0–12.3)	11.0 (7.9–14.1)
Thrombocytes, x 10^9/L	302 (229–382)	254 (168–333)	291 (218–380)
Outcomes			
Length of hospitalization, days	19 (7–24)	15 (7–19)	16 (8–22)
Alive at discharge	72/130 (71%)	20 (83%)	198/254 (78%)
Outcome at day 180			
Alive	65 (50%)	NA	165 (55%)
Deceased	57 (44%)	NA	106 (35%)
Lost to follow-up	8 (6%)	NA	28 (9%)

Data are presented as n (%) or median ± IQR. Data are missing for some patients as indicated. NA = not applicable.

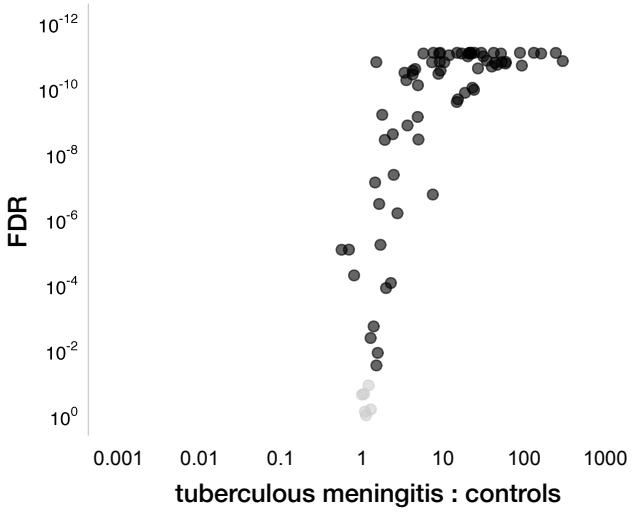

Figure 8.1 Protein levels show large differences between patients and controls in CSF.

Volcano plot for individual proteins in CSF with log-transformed fold change between tuberculous meningitis patients and controls (x-axis), and log-transformed false discovery rate (FDR, y-axis). Proteins significantly different between tuberculous meningitis and controls (FDR < 0.05) are coloured blue.

(23%) protein cluster representatives correlated well with neuron-specific enolase (NSE), a well-established marker for neuronal damage[257]. Correlations were especially high for CSF total protein (11 representatives with rho >0.5). CSF total protein is used as a proxy for blood-CSF barrier disruption, showing an excellent correlation CSF-serum albumin gradient (Pearson $r = 0.95$, $p<0.0001$).

CSF vascular endothelial growth factor concentrations strongly predict patient survival

Among 130 (99%) of the tuberculous meningitis patients with complete follow-up till six months, mortality was 44%. Four protein cluster representatives significantly predicted survival after correction for multiple testing in Cox regression (α=0.05/30 clusters of proteins = 0.0017), all with a hazard ratio above 1, indicating that higher CSF protein concentrations are associated with a higher mortality rate (**table 8.2**). One of the four identified CSF markers was vascular endothelial growth factor (VEGF). Because of its plausible biological role in tuberculous meningitis, we restricted further analysis to VEGF. CSF VEGF levels also

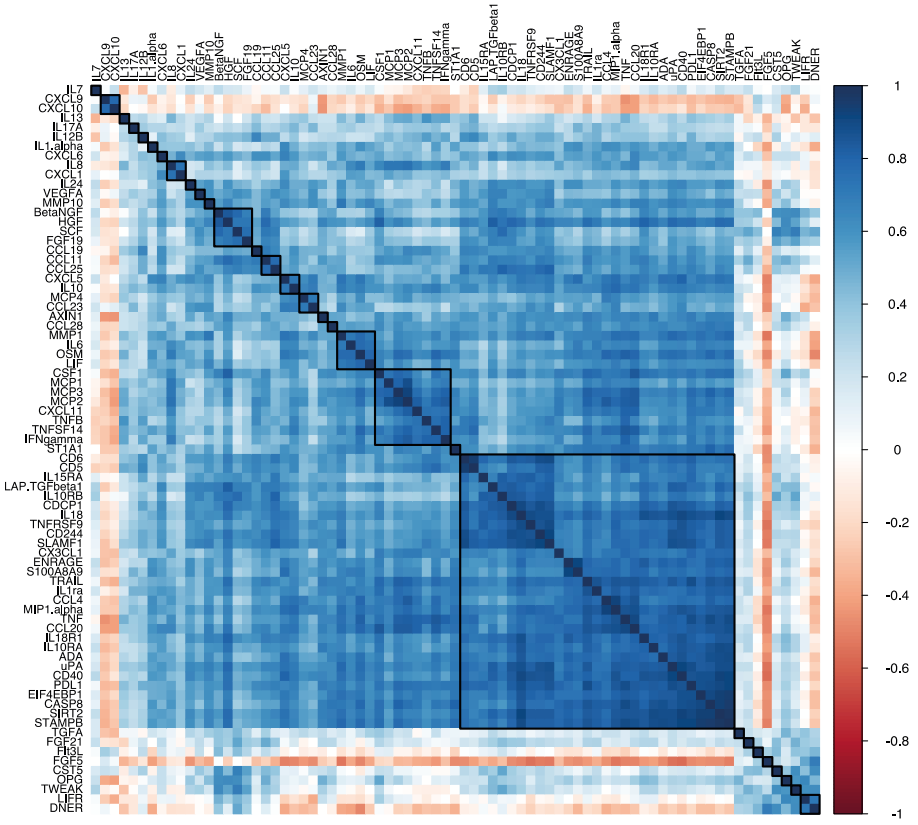

Figure 8.2 High overall correlation between inflammatory proteins.

Correlation matrix with Spearman correlations, in which the proteins are ordered by average hierarchical clustering. The squares define 30 clusters (maximum distance between proteins in the same cluster is 0.3), and the proteins in blue are the representatives for a cluster (the lowest distance to the other proteins in the cluster).

correlated with CSF total protein (Spearman's rho=0.57, p=1.03 x 10^{-12}) and CSF NSE (rho=0.51, p=4.50 x 10^{-8}), and to a lesser extent to CSF polymorphonuclear cell counts (Spearman's rho=0.24, p=0.0069). A two-fold increase in VEGF was associated with a hazard ratio (HR) of 1.57 for 180-day mortality (95% CI 1.24–1.99, p=1.6 x 10^{-4}, **figure 8.4**). This relationship was unchanged in a sensitivity analysis restricted to culture-positive cases (HR 1.54, 95% CI 1.18–2.01) and in multivariate analysis including known risk factors (HR 1.55, 95% CI 1.19–2.01, p=1.2 x 10^{-3}, **table 8.3**).

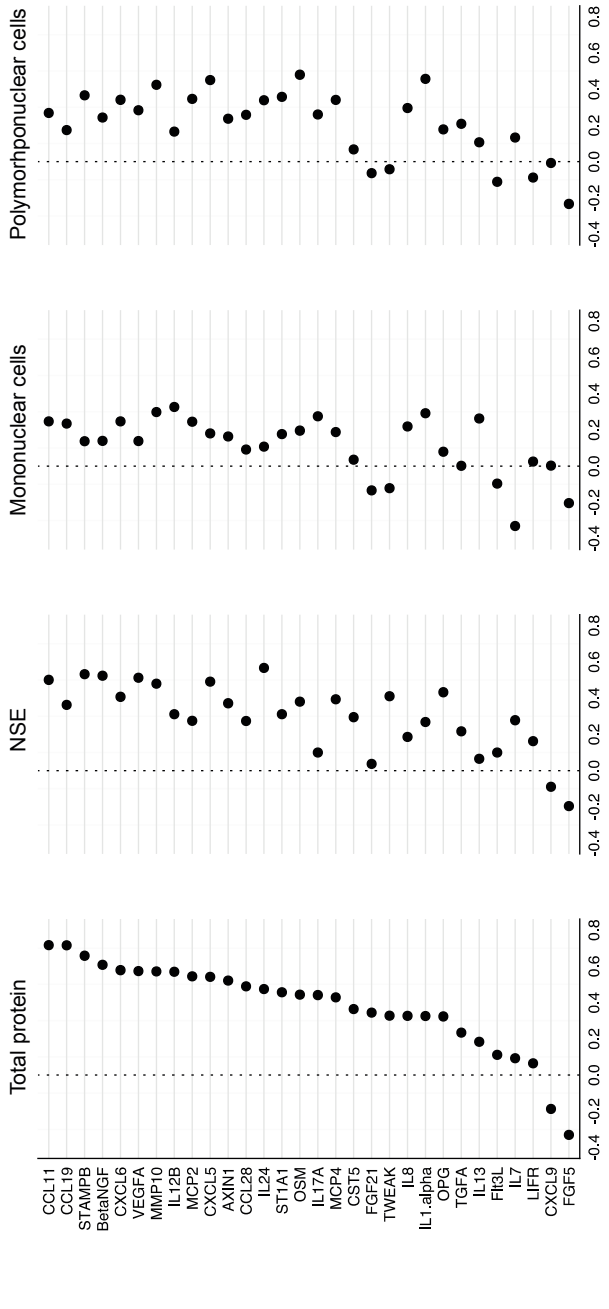

Figure 8.3 CSF proteins (including VEGF) correlate with barrier disruption markers, but poorly with CSF leukocyte counts.

Spearman correlation coefficients (x-axes) of the protein cluster representatives with, CSF total protein, neuron-specific enolase (NSE), mononuclear cell count, polymorphonuclear cell counts.

Table 8.2 Cox regression for 180-day mortality for the 30 protein cluster representatives

Representative	Hazard ratio	+ 95% CI	p	Proteins in the same cluster
IL-24	2.35	(1.59–3.48)	2.00×10^{-5}*	-
TWEAK	1.93	(1.37–2.72)	1.55×10^{-4}*	-
VEGF	1.57	(1.24–1.99)	1.62×10^{-4}*	-
OPG	1.49	(1.18–1.88)	6.85×10^{-4}*	-
IL-7	1.60	(1.16–2.21)	3.92×10^{-3}	-
MMP-10	1.31	(1.08–1.60)	6.11×10^{-3}	-
Beta-NGF	1.91	(1.09–3.33)	2.30×10^{-2}	HGF, SCF, FGF19
CCL11	1.39	(1.05–1.86)	2.36×10^{-2}	CCL25
MCP-4	1.28	(1.03–1.59)	2.51×10^{-2}	CCL23
IL-12B	0.86	(0.74–0.99)	3.55×10^{-2}	-
AXIN1	2.22	(1.05–4.73)	3.80×10^{-2}	-

The hazard ratio is expressed per two-fold increase. The * represents proteins associated with survival after Bonferroni correction ($\alpha = 0.05$; $0.05 / 30 = 0.0017$). N = 130; 57 events.

Genetic variation associated with CSF inflammatory proteins is an independent factor associated with patient survival

To identify a genetic basis for the regulation of CSF VEGF in tuberculous meningitis patients, quantitative trait loci for VEGF were mapped using genome-wide SNP genotype data (**figure 8.5A**). One locus on chromosome 8 (rs3019146 in *RAD54B*) showed a genome-wide significant association with VEGF levels ($p=2.18 \times 10^{-8}$, **figure 8.5B-C**). This SNP has a known function in influencing the expression of *RAD54B*, which is involved in DNA repair and mitotic recombination. Five other loci showed a suggestive association with VEGF levels ($p<1 \times 10^{-5}$, **table 8.4**).

These six identified quantitative loci were used to generate a prognostic index, and study participants were divided into two groups, low and high risk, based on the median of the prognostic index. As expected, this predicted survival in the 128 (98%) tuberculous meningitis patients used for QTL mapping (log-rank test for 180-days survival, p=0.0088, **figure 8.5D**). This finding was validated in a second group of 299 tuberculous meningitis patients (49% culture-confirmed) with complete six-month follow-up for 171 (91%) with 106 (35%) recorded deaths (**table 8.1**). Similar to the discovery cohort, the prognostic index including QTLs

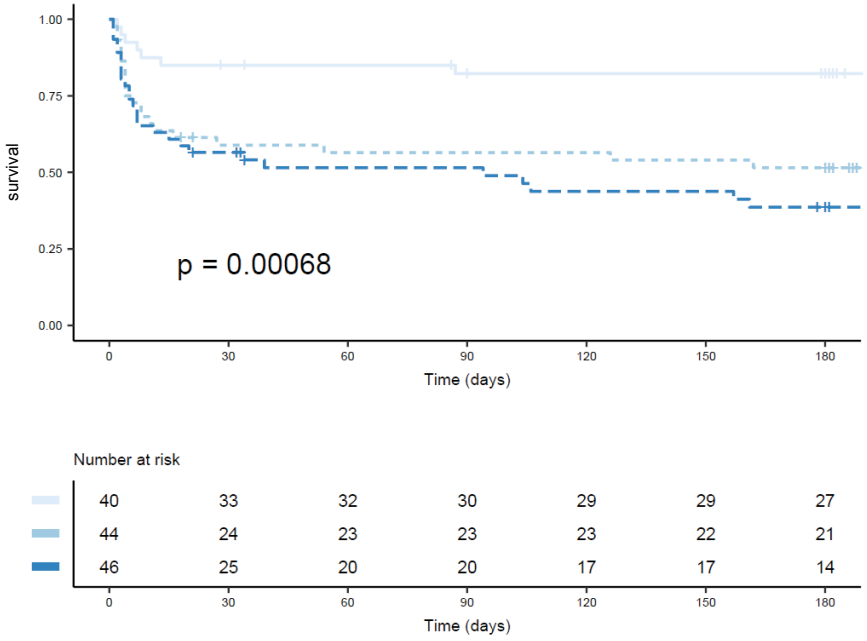

Figure 8.4 CSF VEGF concentrations predict survival in tuberculous meningitis.

Kaplan-Meier graph with survival table for patients (n=130) based on CSF VEGF concentrations divided in tertiles. The VEGF concentrations are expressed as normalized protein expression (NPX) and groups were defined by the following cut-offs: low (NPX < 9.80), middle (NPX 9.80 – 10.87) and high (NPX > 10.87).

for CSF VEGF predicted survival in this second group of 299 tuberculous meningitis patients (p=0.0018, **figure 8.5E**), also in multivariate analysis correcting for possible confounders (**table 8.3**).

Table 8.3 Multivariate Cox regression for 180-day mortality in the proteome validation cohort and independent genetic validation cohort

	VEGF discovery cohort (n = 127)		Genetic validation cohort (n = 249)	
	HR (95% CI)	p	HR (95% CI)	p
Sex, male	0.74 (0.42–1.31)	0.307	1.18 (0.77–1.82)	0.451
Age, per 10-year increase	1.26 (1.03–1.54)	0.0224	1.15 (0.98–1.35)	0.0886
Glasgow Coma Scale, per point increase	0.80 (0.72–0.90)	0.00011	0.79 (0.71–0.87)	1.52×10^{-6}
CSF PMNs, per ten-fold increase	1.32 (0.76–2.30)	0.328	1.46 (1.07–1.20)	0.0164
CSF MNs, per ten-fold increase	0.53 (0.30–0.95)	0.0316	0.83 (0.55–1.25)	0.384
VEGF, per two-fold increase	1.55 (1.19–2.01)	0.0012	NA	NA
Prognostic index	NA	NA	NA	0.0263

For this multivariate analysis, four patients were excluded from the VEGF discovery cohort and 50 were excluded from the genetic validation cohort because of missing Glasgow Coma Scale. CSF cell counts were analysed after $\log_{10}[x+1]$ transformation. Prognostic index was included as a continuous variable. HR = hazard ratio; NA = not applicable; CSF = cerebrospinal fluid; PMNs = polymorphonuclear cells; MNs = mononuclear cells.

Table 8.4 CSF VEGF quantitative trait loci in tuberculous meningitis

SNP	Chr	Position	Ref allele	Minor allele	β	p	Nearest gene	Expression QTL	
								Gene	Tissue
rs4354149	6	47334825	G	A	-1.07	1.39×10^{-7}	TNFRSF21	CD2AP	Fibroblasts
rs73100092	7	33826648	G	A	-1.31	7.25×10^{-6}	RP11-89N17.4		
rs3019146	8	95414106	T	C	0.79	2.18×10^{-8}	RAD54B (intronic)	RAD54B	Whole blood
rs9423705	10	3200155	C	G	0.84	1.33×10^{-6}	PITRM1 (intronic)	PFKP, PITRM1	Whole blood, skin
rs79640016	12	127650445	A	T	-0.77	3.87×10^{-6}	AC079949.1		
rs734950	22	29541447	A	G	-0.69	8.47×10^{-6}	KREMEN1 (3′-UTR)	KREMEN1	Adipose, Heart, Thyroid

Quantitative trait loci (QTLs) were tested for association with gene expression (expression QTL) using publicly available data sources. References for expression QTL data: rs4354149, rs9423705 and rs734950 (23); rs3019146 (24). Chr = chromosome; Ref allele = Reference allele.

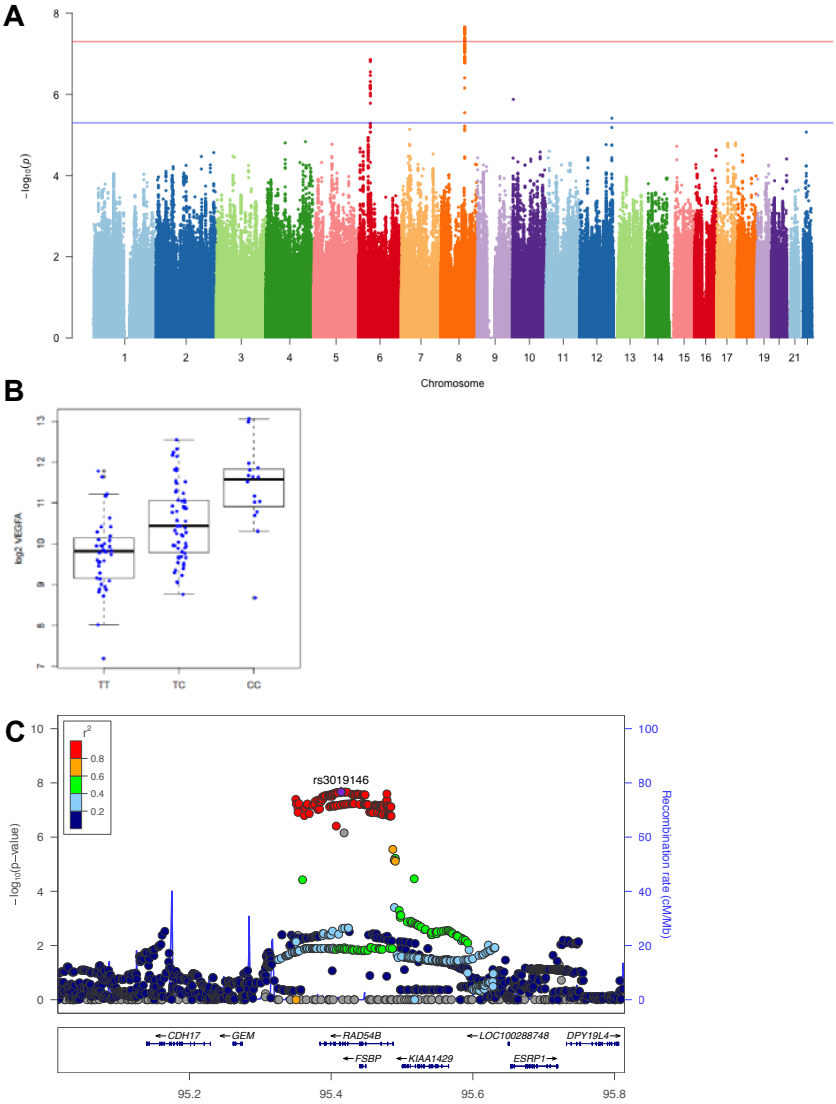

Figure 8.5 Genetic traits predict VEGF levels in CSF from tuberculous meningitis patients.

(A) Manhattan plot showing the genome-wide QTL mapping results for CSF VEGF levels in tuberculous meningitis patients. Horizontal dashed lines correspond to $p<5 \times 10^{-7}$ and $p<1 \times 10^{-5}$. (B) Boxplot showing the VEGF levels distributed across the three genotypes of the genome-wide QTL rs2291439. (C) Regional plot for genome-wide QTL rs2291439. (D) Kaplan-Meier graph of prognostic index predicting survival in 128 individuals with available genetic and follow-up data from the discovery cohort. (E) Kaplan-Meier graph of prognostic index predicting survival in 299 individuals with available genetic and follow-up data from the validation cohort.

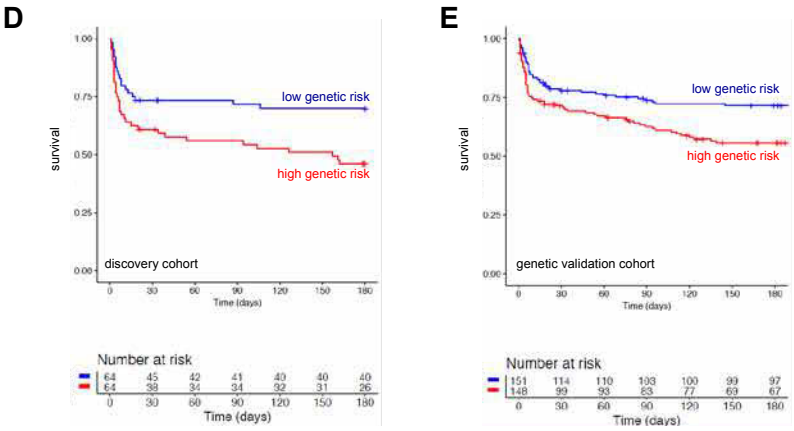

Figure 8.5 Continued.

Discussion

Damaging or ineffective host immune responses contribute to the high mortality of tuberculous meningitis, but the underlying mechanisms remain largely unknown. We studied the inflammatory proteome in CSF of tuberculous meningitis patients and its correlation to CSF leukocytes and markers of damage to the brain and blood-CSF barrier. Four proteins showed an independent association with mortality, including vascular endothelial growth factor (VEGF). We identified six genetic loci associated with CSF VEGF concentrations in tuberculous meningitis patients, including one locus with genome-wide significance. A prognostic index based on these loci predicted survival in an independent validation cohort.

VEGF induces a potent angiogenic response, but is also known as a vascular permeability factor, based on its ability to induce vascular leakage[258]. One of the most critical triggers of angiogenesis is hypoxia, which activates hypoxia-inducible factor (HIF) proteins, HIF-1 and HIF-2, leading to an increased VEGF release. Although hypoxia is considered to be the main driver of angiogenesis, inflammation also makes important contributions to this process, e.g. TNF-α is also able to induce VEGF production[259]. Due to cerebral vasculitis and stroke, both cerebral hypoxia and inflammation are often present in tuberculous meningitis patients.

To our knowledge, this study is the first to link VEGF levels in CSF to survival in tuberculous meningitis patients and to describe a genetic basis for VEGF levels in CSF in tuberculous meningitis. In a pulmonary tuberculosis rabbit model, anti-VEGF treatment reduced the formation of immature and hyperpermeable vessels and hypoxia in tuberculous granuloma's, thereby increasing anti-tuberculous drug efficacy[260]. Increased VEGF could also play a causal role in tuberculous meningitis immunopathology, in which case anti-VEGF treatment might reduce this 'collateral damage'. Tuberculous meningitis is characterized by disruption of the blood-brain barrier, cerebral oedema and increased intracranial pressure[16]. As mentioned, VEGF is a potent vascular permeability factor, which induces dysfunction of tight junction proteins, and is a mediator of brain oedema[261]. Therefore, targeting this pathway may help to reduce the dysfunction of tight junctions, which is characteristic of tuberculous meningitis disease, and improve outcome.

This is not the first study showing VEGF is increased in tuberculous meningitis. Children with tuberculous meningitis, who all received anti-tuberculous and adjuvant corticosteroid therapy, had significantly higher CSF VEGF concentrations compared to controls[262]. Compared to bacterial, fungal, and viral meningitis, tuberculous meningitis patients had higher serum and CSF VEGF levels, especially in those with hydrocephalus[263]. In adult tuberculous meningitis patients in India, higher serum VEGF was associated with infarction on MRI[264].

It has not yet been established whether CSF VEGF originates from the inflammatory infiltrate or the brain parenchyma. In HIV-associated cryptococcal meningitis, VEGF was thought to result from local production based on CSF-serum indices[265]. In an immunohistochemical brain autopsy study in bacterial meningitis, VEGF was found in the neutrophil and monocyte infiltrate, as well in brain endothelium and epithelium[266]. In paediatric tuberculous meningitis, CSF VEGF correlated with CSF-serum barrier disruption[262]. We found that CSF VEGF correlated with NSE, as a marker of neuronal damage, as with CSF total protein concentration used as a proxy for blood-CSF barrier disruption.

Our study has several limitations. We did not include serum measurements in our study, as in our previous metabolomic study in **chapter 7** the CSF metabolome was much more informative than the plasma metabolome. Also, we could not examine brain tissue to establish the source of detrimental VEGF production, because brain autopsy is not performed in Indonesia. In addition, examining HIV-infected patients could give further insights, noting that previous studies have found associations between serum VEGF and immune reconstitution

syndrome in HIV-associated cryptococcal meningitis[267]. Although we validated our genetic risk factors findings in a second cohort, no validation of proteomic data or QTLs was done in patients from a different setting or genetic background. Finally, although the genetic correlate suggests a causal role for VEGF in tuberculous meningitis immunopathogenesis, it is also possible that it is a bystander effect of hypoxia caused by another pathway.

In conclusion, CSF concentrations of VEGF show a strong association with increased mortality of tuberculous meningitis, possibly because of its effects on vascular permeability, dysfunction of tight junction proteins, and brain oedema. CSF VEGF concentrations in tuberculous meningitis are under strong genetic influence, likely contributing to the variable outcome of tuberculous meningitis. Future studies should examine if monoclonal antibodies against VEGF improve outcome of tuberculous meningitis patients. Combined with timely diagnosis, appropriate supportive treatment[28], and intensified antibiotic treatment[29,30], such strategies to limit immunopathology or boost host defence against *M. tuberculosis* may help improve outcome of this most deadly manifestation of tuberculosis.

Acknowledgements

We thank the neurology residents and tuberculous meningitis study team for monitoring patients; the director of the Hasan Sadikin General Hospital (Bandung, Indonesia) for accommodating the research; Elma Prudon-Rosmulder for nephelometric analysis of albumin; Rob ter Horst for bioinformatic advice; and Mathieu Platteel for DNA quality control and hybridization.

Author contributions

VACMK, AvL, and RvC designed the study. SD, THA, RR, and ARG supervised patient recruitment. JA, LC, and BA supervised patient sample flow. VACMK performed the ELISAs. AvL and SD did patient data quality control. VACMK, RA-G, and VK did the genetic analysis, and VACMK performed other analysis. MGN contributed to immunological concepts. VACMK, AvL and RvC wrote the first draft of the manuscript. All other authors provided input to the draft and approved the final version of the manuscript.

9

Summary and general discussion

Summary and general discussion

Much has been learned on human immunology in the past decades, but so far this has hardly led to better tools to prevent or treat tuberculosis. One reason may be that we need to study the immunology of tuberculosis in its specific context, as much as possible linking epidemiology, clinical manifestations and laboratory sciences. That is what I have aimed for in this thesis, combining patient studies with genetics and in-vitro experimental models, in order to improve understanding of factors determining tuberculosis susceptibility, transmission and outcome (graphically summarised in **figure 9.1**).

Summary of research findings

Tuberculosis susceptibility and transmission

The first part of this thesis focussed on susceptibility to tuberculosis and on transmission of *M. tuberculosis.*

Since the C-type lectin receptor CLEC4D was recently shown to recognize components of *M. tuberculosis,* we investigated its role in the development of active disease in **chapter 2**. We showed that mice without functioning Clec4d have higher pulmonary bacterial burden and higher mortality upon infection with *M. tuberculosis.* In humans, we found increased *CLEC4D* expression in pulmonary tuberculosis in five publicly available gene expression data sets. This is most outspoken in monocytes and granulocytes and reverses with successful treatment. We then found that one allele of a nonsynynomous *CLEC4D* polymorphism is more common in pulmonary tuberculosis patients than controls. CLEC4D is therefore likely to play a role in the development of active pulmonary tuberculosis.

Hypothesising that the early immune response to different *M. tuberculosis* strains partly explains their widely varying prevalence, we studied the immune response evoked by different *M. tuberculosis* strains in blood monocytes, lymphocytes and neutrophils of healthy volunteers in **chapter 3** and **4**. In **chapter 3** it was shown that strains of the evolutionary successful modern Beijing genotype family evoke a less profound proinflammatory cytokine response compared to ancient Beijing strains. Variation between strains was large also within the modern strains, but on average they induced lower amounts of IL-1β, IFN-γ and IL-22 in leukocytes of healthy volunteers.

In **chapter 4** we used a more refined starting point for the selection of strains: the ability of individual strains to cause secondary cases. Based on the Dutch tuberculosis database, which includes >13,000 *M. tuberculosis* strains, we selected isolates with contrasting abilities in causing secondary cases. Strains that clustered among cases without risk factors for transmission, i.e. among elderly female patients, were considered to be highly transmissible. Strains that did not cause a secondary case, even though they were isolated from a patient with many risk factors for clustering, i.e. a homeless young male, were considered to be minimally transmissible. Through whole-genome sequencing of 100 of these strains, variation in five mycobacterial genes was associated with clustering. Four of these genes were confirmed in a second dataset of 143 isolates from a different geographical background. We then selected 19 representative *M. tuberculosis* strains that did or did not carry a mutation in these five genes and linked different cytokine responses to the presence or absence of mutations in three of these genes. One of these genes was associated with a difference in

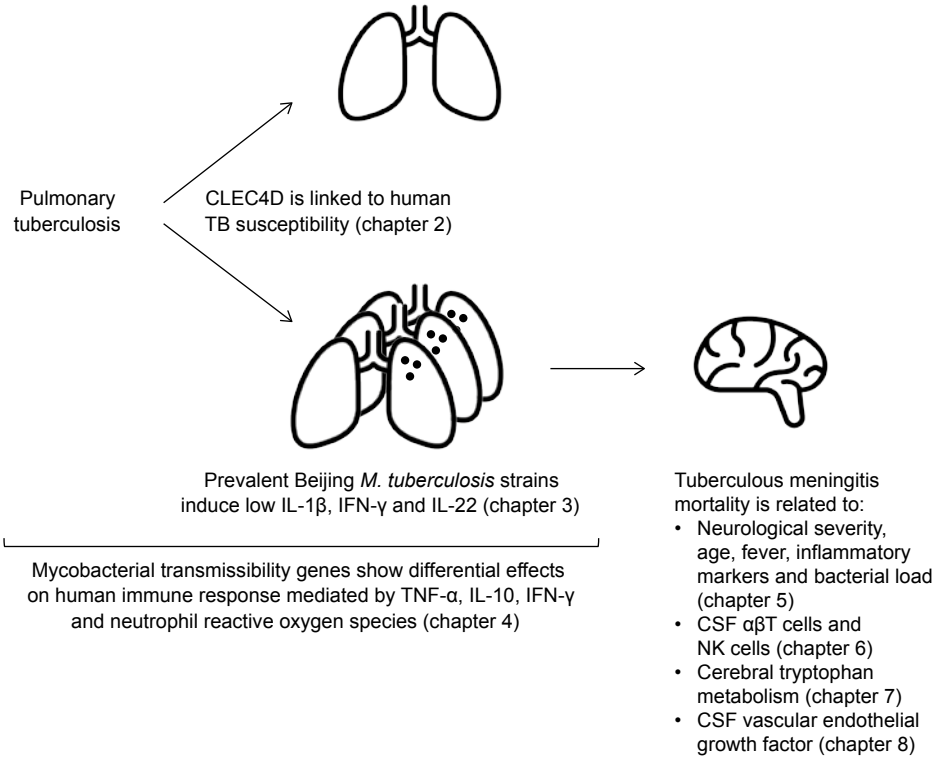

Figure 9.1 Summary of the main findings of this thesis.

neutrophil responses, important in of the first line of defence against *M. tuberculosis*. Together, chapter 3 and 4 provide evidence for interaction between *M. tuberculosis* genotype and the human immune response in establishing transmission and disease.

Outcome of tuberculous meningitis

The second part of this thesis focussed on tuberculous meningitis and more specifically on factors determining the poor prognosis of this manifestation of tuberculosis.

To identify patient groups in highest need of adjunctive treatment, we identified routine prognostic factors for outcome of tuberculous meningitis in a large prospective cohort in Indonesia in **chapter 5**. In line with other studies we identified HIV co-infection, low Glasgow Coma Scale (indicating severe disease), and a low cerebrospinal fluid (CSF)-blood glucose ratio as important predictors for mortality. Additional clinical parameters predictive for mortality were high body temperature and paresis of extremities, inflammatory markers including high CSF and blood neutrophil counts, and high CSF protein and a positive CSF *M. tuberculosis* culture as a marker for bacterial load.

New host-directed therapies are proposed as adjunct to antibiotics to improve the prognosis of tuberculous meningitis. The immune response in tuberculous meningitis shows large variation between patients in terms of body temperature, inflammation on neuroimaging, or CSF inflammatory markers. Therefore, some patients might need strong immunosuppressive therapy, while others are more likely to benefit from immune stimulatory therapy. In **chapter 6** we therefore explored the immune response in tuberculous meningitis in detail. We found a strong myeloid immune response in blood compared to pulmonary tuberculosis patients and healthy controls, while lymphocytes, including the innate γδT cells, MAIT cells, NKT cells and NK cells, were decreased in number. In contrast, lymphoid cells dominated CSF in 70% of patients, again with all innate subsets present. The cytokine response that was determined *ex vivo* by stimulating blood with specific (BCG, *M. tuberculosis*) and aspecific (*S. pneumoniae, C. albicans*) stimuli, showed a much broader range in tuberculous meningitis than in pulmonary tuberculosis patients and controls. A high ex-vivo blood cytokine response correlated to fever, higher blood lymphocyte counts and higher monocyte activation. Low CSF αβT and γδT cells were associated with increased mortality. In future trials investigating immunomodulatory therapy, adequate immunophenotyping will be important to identify patient groups benefitting from the studied intervention.

Since metabolism is important for an efficient immune response, we measured over 400 metabolites in both CSF and serum of both patients and controls from the same cohort in Indonesia in **chapter 7**. Low CSF tryptophan was a strong predictor for survival of tuberculous meningitis. CSF tryptophan was lower in patients than controls, something that is known from other cerebral infections, but especially low in patients who survived. The ability to modulate tryptophan concentrations is partially genetically determined, and polymorphisms that predicted CSF tryptophan, also predicted survival in another group of tuberculous meningitis patients. Cerebral tryptophan metabolism could affect outcome of tuberculous meningitis through food-deprivation of *M. tuberculosis*, or because of the immunomodulatory properties of downstream tryptophan metabolites.

Studies on individual cytokines have shown a high and sustained cytokine response in tuberculous meningitis, but without clear relation to patient outcome. In **chapter 8** we choose a more comprehensive approach examining almost examining almost 100 cytokines and other inflammatory proteins. Most of the 100 studied leukocyte or brain-derived inflammatory messenger molecules showed a strong increase in CSF of tuberculosis meningitis patients compared to controls. These proteins showed strong clustering and 4 of 30 clusters correlated to increased mortality. Vascular endothelial growth factor (VEGF) showed a strong relation with mortality. It correlated with measures of neuronal damage and blood-CSF barrier disruption. The VEGF concentrations had a genetic correlate, which predicted survival in a second group of tuberculous meningitis patients.
Together, chapters 5 to 8 identified an important and partially genetically determined role for the immune response in the outcome of tuberculous meningitis. These findings strengthen the basis for rational host-directed therapy in the treatment of tuberculous meningitis.

General discussion

The two parts of this thesis are discussed separately, followed by a discussion of the employed integrative approach and how this can be used in the improvement host-directed therapy of tuberculosis.

Susceptibility and transmission

Susceptibility to tuberculosis can be viewed only in relationship to particular tuberculosis phenotypes. In other words, biological mechanisms responsible for establishing infection may be different from those causing progression to active pulmonary tuberculosis or tuberculous meningitis. The first part of this thesis shows that precise patient phenotyping and *M. tuberculosis* strains classification helps advancing insight in susceptibility and transmission.

The estimated extent to which tuberculosis susceptibility is heritable is high, based on old twin studies that find much higher concordance rate for monozygotic twins (32-65%) than dizygotic twins (13-25%)[268]. In contrast, the yield of present-day genetic association studies is relatively modest: few loci have been identified, each only linked to a relatively small proportions of increased risk (odds ratio) for pulmonary disease compared to controls. The two largest studies so far found an odds ratio of 1.19 (95% CI 1.13–1.27, n=7,501) in 18q11.2[269] and 1.10–1.30 (overall $p=2.57 \times 10^{-11}$, n=13,859) in 11p13[23] respectively, and our study on the *CLEC4D* polymorphism in chapter 2 found a similar effect with an odds ratio of 1.33 (95% CI 1.02–1.73). In contrast to twins, who grew up in very homogenous circumstances and were exposed to the same *M. tuberculosis* strains and in the same amount, present-day genetic studies are performed in large cohorts of unrelated individuals. Of our present-day 'healthy controls', we do not know their exposure level or infection status (**figure 9.2**). This means that in our case, the rs4304840 in variant in *CLEC4D* confers increased susceptibility to 1) infection; 2) primary progression to active tuberculosis; 3) secondary progression to active tuberculosis; 4) to a combination of each of these; or 5) - theoretically - is protective at one stage and harmful at another. A positive example of a study employing sophisticated phenotyping is the INFECT study in Bandung[12] that follows exposed individuals overtime and records infection later on. INFECT will increase our knowledge on the susceptibility to infection itself, but will also provide well-phenotyped control groups for studying susceptibility to pulmonary tuberculosis.

Imprecise phenotyping probably contributes to the lack of successful replication studies in other populations. Other problems involved are a lower frequency

of causative genetic variants, or differences in prevalence of different polymorphisms and linkage disequilibrium between populations: an identified polymorphism is linked to the causative – unknown – polymorphism in one, but not another population. Additionally, the *M. tuberculosis* strains in the replication area might be different, decreasing statistical power in these studies.

Including mycobacterial genotyping may increase power to find human susceptibility loci for pulmonary tuberculosis, as shown in three previous studies. An *ALOX5* polymorphism was linked to increased susceptibility especially for patients infected with *M. africanum*[270] and a Toll-like receptor 2 (*TLR2*) variant was especially linked to tuberculosis caused by Beijing strains[85]. Like a third study, linking an *NRAMP1* polymorphism to Beijing strains[271], these associations were found under 'optimal conditions': large proportions (≥ 29%) of the mycobacterial genotype that showed an association; few human polymorphisms (2-3) tested or reported; and all with reasonably high minor allele frequencies (8% or higher). Even these studies, published 8-10 years ago, with odd ratios of 1.7-2.5, still await replication. To decipher the meaning of the SNP identified in chapter 2, we would ideally first compare uninfected controls, infected individuals and patients with active tuberculosis disease in a replication

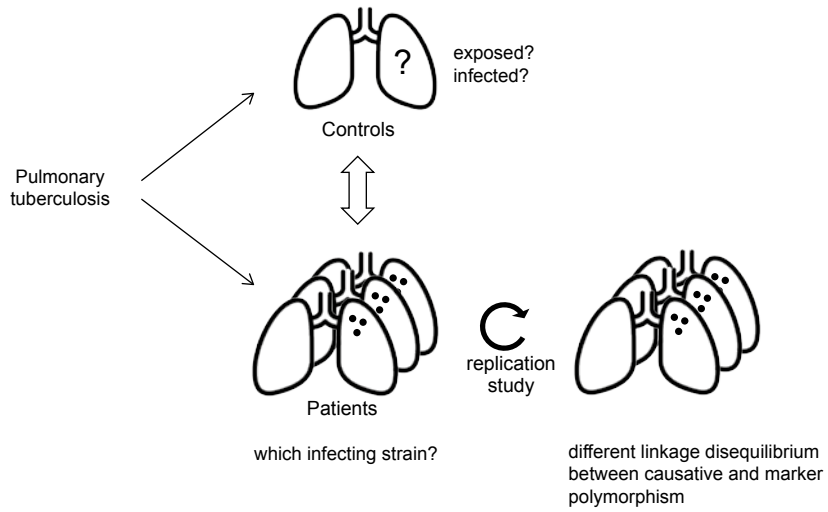

Figure 9.2 Imprecise patient and control phenotyping decrease the power of genetic association studies.

study in the same geographical area. This can help define the association as important for either infection, or progression to active disease, possibly restricted to one specific mycobacterial lineage. More precisely establishing the role of the genetic variation would significantly increase the chances of successful replication in other populations.

Also in immunological association studies, more detailed *M. tuberculosis* genotyping is important. In chapter 3 we found a lower induction of proinflammatory cytokines (i.e. IL-1β) in four out of seven modern Beijing strains included. Another group replicated our findings with 13 out of 20 modern Beijing strains they selected[168]. This shows that more precise genotyping than 'modern' versus 'ancient' is necessary to identify the driving genetic difference because not all modern Beijing strains behave in the same way. Further accuracy can also be gained by more precise phenotypic definition of relevant mycobacterial strains, like in chapter 4 that took the ability to cause secondary cases as starting point, before identifying relevant mycobacterial genetics and immunological consequences. This study however also shows that the sheer number of identified genetic variants becomes larger than the statistical power of immunological studies allows. We therefore aggregated these mycobacterial loci at a gene level and analysed host responses at the level of cell types instead of cytokines. This increases the robustness of the findings at the expense of the level of detail. At a methodological level, it would be good to test whether our identified associations can be confirmed in an experimental model with live mycobacteria.

Based on the studies in this thesis and those of others, I think we can only increase our understanding of tuberculosis susceptibility and transmission by precise characterisation of human subjects, and by including mycobacterial genotypes into the equation. An important methodological challenge is to decide about the optimal resolution to use when comparing different 'phenotypes' given the vast amount data. As some associations identified will be a result of trial-and-error with multiple testing issues, solid confirmatory studies will be needed, ultimately in settings with a different human and mycobacterial genotype distribution.

Outcome of tuberculous meningitis

The second part of this thesis focuses on outcome of tuberculous meningitis. Its extremely high mortality is associated to severe disease at the moment of presentation in the hospital, which is often late. This leaves time for *M. tuberculosis*, but also for the immune response, to cause damage.

Table 9.1 Possible intervention strategies in tuberculous meningitis.

Example (mechanism)	Clinical study	N	Success	Comment
Dexamethasone (immune suppression)	RCTs	337	Yes	RR 0.75 (0.65-0.87) in the first two years[44]
Thalidomide (immune suppression)	RCT	47	No	Increased mortality when applied at 24mg/kg/day in children[193]
Aspirin (immune suppression and platelet inhibition)	RCTs	60	Yes	Unblinded Indian study showed reduced mortality with 150mg aspirin daily[45]
		120	Result pending	Vietnamese pilot study underway evaluating 81 and 1000mg aspirin (NCT02237365)

Strategies to improve patient outcome once in the hospital include better supportive care[28], which is not yet studied systematically, and better antibiotic-delivery to the brain. Interesting in this regard, intrathecal injection has been used in individual cases from 1946 [272] to 2017 [273]. Larger studies have been performed with increased dosing of the cornerstone drug rifampicin, administered either orally[26] or intravenously, of which the latter strategy has shown promising results in a phase IIb-study[29]. Other possible strategies, improving blood-brain penetration or inhibiting drug efflux pumps[274], have not yet been applied clinically. Given the strong influence of the immune response on outcome of tuberculous meningitis as exemplified in chapter 5 to 8, alternative strategies can be formulated, involving modulation of the host immune response, some of which have been tried (**table 9.1**).

Studying the local immune response in tuberculous meningitis is facilitated by the access to lumbar or even ventricular[275] CSF, which contains waste products of the brain and is therefore indicative of local metabolism and inflammation. As summarised in the General introduction (**table 1.1 and 1.2**), data on the immune response in tuberculous meningitis are limited and sometimes contradictory. For example, in a recent study a higher IFN-γ and other Th1 as well as Th2 cytokines were protective in HIV-negative patients but not HIV-positive patients[43], while a in an older study IFN-γ was protective in HIV-positive but not HIV-negative patients[255] and also in our study in chapter 8, CSF IFN-γ did not predict mortality in HIV-negative patients.

We identified CSF VEGF as an important determinant for tuberculous meningitis mortality in chapter 8 and this moves the focus to hypoxia as a possible, and potentially modifiable, pathway. The interpretation of levels of cytokines and other circulating mediators remains challenging. We infer the meaning of signals from other in-vitro models or other diseases, like pulmonary tuberculosis, and it is hard to interpret the origins of the signals considering that either the CSF leukocytes or brain astrocytes or microglia as producers of these molecules. The brain is likely to play an active role in the immunopathogenesis of tuberculous meningitis, as brain cells of deceased tuberculous meningitis patients have shown, with >1,000 genes at least two-fold upregulated compared to patients who died of an accident[235]. A similar study using CSF leukocytes would be very interesting, but is technically difficult because of the small amount of RNA involved, and the difference in CSF cell number and composition in control subjects. Including CSF metabolites in the analysis has the advantage of the elaborate existing knowledge on their interdependence and (enzymatic) regulation. Moreover, host genetics can be added to further pinpoint regulatory mechanisms.

It is yet unknown what immunomodulatory treatment is most promising, and for whom. Chapter 7 showed that a low CSF tryptophan is associated with better survival, and it should be investigated whether this has therapeutic potential. Decreasing CSF tryptophan supply is possible within a day by a tryptophan-depleted diet[248], but given the brain-protecting effects of some downstream tryptophan metabolites a strategy that increases CSF tryptophan metabolism, for example by employing IFN-γ, may be preferred[247]. This is most likely to be effective in the group of patients that naturally have the least active tryptophan metabolism (i.e. the tertile with the highest CSF tryptophan levels in **figure 6.4**), while the patients with the lowest CSF tryptophan already have such a low 6-month mortality (5%) in our study that side effects might outweigh benefits.

Another selection criterion for immunomodulatory therapy could be the immune response as studied in chapter 6. Patients with a high ex-vivo response and more activated monocytes might benefit from extra immunosuppressive therapy such as IL-1 receptor antagonist (anakinra). The group with low responses however, might benefit from other interventions including adjunctive IFN-γ therapy, or simply withholding corticosteroids that are now routinely administered[276]. A genotype-based trial (NCT03100786) currently randomises patients with CC or CT *LTA4H* rs1725495 genotypes to dexamethasone or placebo. Even if the primary outcome is not met, this study can improve our understanding of the disease.

In the field of sepsis, over 100 phase II and III trials have been performed testing different adjuvant strategies, all without success[225]. We should learn from this experience. Future host-directed trials in tuberculous meningitis could be improved by adhering to the following criteria: 1) the proposed intervention should be expected to be beneficial to a larger number of patients than it is expected to harm; and 2) the design should allow answering pathophysiological questions through collection of genetic and immune phenotypic data for post-hoc identification of patient subgroups for whom the intervention showed benefit, no effect or harm. For example, when studying adjunctive IFN-γ, it will be key to assess downstream tryptophan metabolites, but also the number and activation of regulatory T cells in CSF, as well as mycobacterial counts. Ideally, readily available markers will be included that will allow upfront stratification in a follow-up trial. It is challenging to perform these immunological measures in low- or middle-income countries, but the studies in this thesis and others[33] have shown its feasibility.

I think that a major remaining question is how the different clinical, metabolic, inflammatory prognostic factors should be integrated, not just to better predict outcome, but especially to improve our understanding of the processes involved.

Future perspectives, using an integrative approach

Tuberculosis is an old foe, and continues to be a challenging disease. Vaccine development is hampered by the absence of known immunological correlates of protection against infection[277] and even natural immunity only partially protects from active disease[278]. Common genetic variations conferring high level of protection against tuberculosis, like sickle cell trait protects against malaria[279], would have been detected by conducted genome-wide association studies[269] by now already. A 'vector-based approach', like targeting the *Aedes* mosquito in dengue, will not be feasible because of the rare, but severe side-effects in the treatment of latent tuberculosis combined with the large pool (1.7 billion people!) of latently infected individuals[1].

Will there be 'Mountains beyond Mountains'[280] in the quest for better treatment of tuberculosis? Possibly, but there is reason for optimism when it comes to better understanding of the disease. Promising, and increasingly affordable, techniques now include live functional imaging in both pre-clinical[191] and clinical[281] models. Also, RNA-sequencing techniques requiring small RNA concentrations[282] allows transcriptomics of tissues closer to the infection than blood, like CSF leukocytes or lung or brain tissue obtained by biopsy. Lastly, the combination of genetics with other platforms is a powerful way to identify the

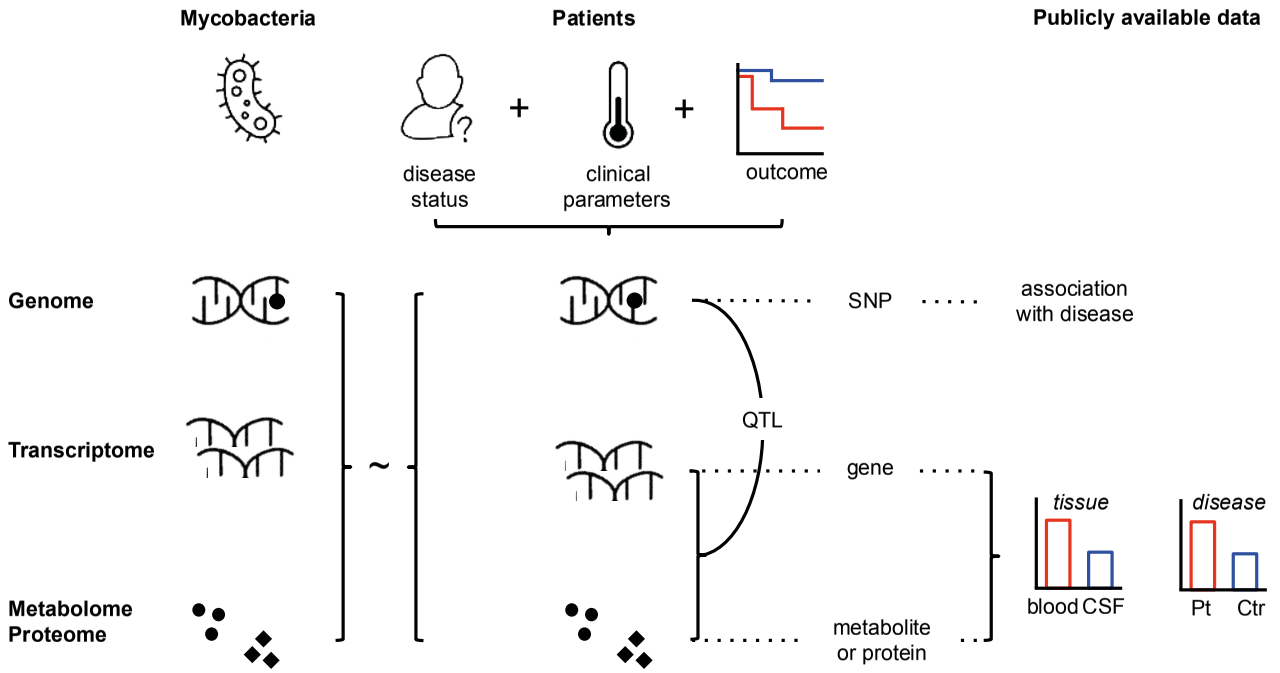

Figure 9.3 The possibilities of the integrative approach used in this thesis.

Pt = patient, Ctr = control, SNP = single nucleotide polymorphism. QTL = quantitative treat locus.

effect of polymorphisms on a quantitative measurement such as gene expression in a certain condition. These response quantitative trait loci (QTLs)[21,283] were determined *in vitro* and need to be confirmed in patient studies. As an example, the difference in metabolites before and after dexamethasone administration is likely to depend on certain genetic traits that can next be used to predict which patients benefit most from this intervention.

Another reason for optimism is the increasing power of computational biology integrating different data sources. 'Systems biology' cannot be expected to produce new biological insights just by itself[284], but it can help identifying new biological concepts. This thesis propagates an integrative approach, most often starting with a clinical observation (**figure 9.3**), such as higher mortality in patients with fever and a higher proportion of CSF neutrophils. Rather than performing large studies using one modality, such as genetics, that need confirmation by even larger studies, we combined analytical platforms with high-quality patient phenotyping in relatively small cohorts. The tuberculous meningitis patient data itself is rich and layered, so that genetic polymorphisms can be searched to predict the patient phenotype, but also the associated gene expression, metabolite or protein levels. We next used publicly available data (**table 9.2**) to sharpen hypotheses.

This requires the definition of certain 'keys': a genetic polymorphism (SNP), or a gene or metabolite name. Additionally, hypotheses arising from this approach can be further refined using mycobacterial data. If for example a certain metabolite is identified as important, mycobacterial genetics focussing on the specific pathway can be associated to patient outcomes. This thesis shows that the starting-points can be an association between mycobacterial genotype and transmission or human immune response (chapter 3 and 4), or a gene identified in an animal model (chapter 2), or an association between a metabolite or protein level and patient outcome (chapter 7 and 8). The association between clinical parameters or immune response and survival (chapter 5 and 6), asks for further exploration to other levels of this model.
Because these types of studies are exploratory in nature, external validation is needed. A biologically driven and specific hypothesis, supported by multiple data sources, can be confirmed by testing specific metabolites or genetic loci in relatively small patient cohorts of hundreds. We think that the limited funds available for tuberculosis research (0.7 billion US$ annually)[2] ask for an integrative, iterative approach to answer clinical questions using new technologies as close as possible to the side of disease. I think that intervention studies will be needed to move from correlation to causation. The power to identify meaningful differences

Table 9.2 Publicly available data relevant to tuberculosis research.

Subject	Example
Mycobacterial	
Genetics	TB Database
Proteomics	Peptide Atlas
Human genetics	
Function	NCBI
SNP prevalence	1000 genomes
SNP linkage	Broad institute
Gene expression	
Comparing disease status	Expression in blood of pulmonary tuberculosis patients versus controls[72]; expression in brain of tuberculous meningitis patients versus head-injury controls[235]
Comparing human issues	BioGPS; GTEx portal
Quantitative trait loci	
Comparing gene expression depending on the presence of a SNP	GTEx portal
Comparing gene expression in response to in-vitro manipulation in response to a SNP	Stimulation of dendritic cells by *M. tuberculosis*[283]
Pathway analysis	
Gene expression	WebGestalt, DAVID
Metabolites	MetaboAnalyst

might be increased by careful serial clinical and immunological phenotyping, which could be aided by studying brain biopsies or using functional brain imaging in the case of tuberculous meningitis.

Tuberculosis is a devastating disease with a fascinating immunopathogenesis. I hope that this thesis will contribute to identification of effective host-directed therapy to brighten the outlook for future patients.

Abbreviations
References

Abbreviations

BCG = *M. bovis* Bacille Calmette-Guérin
CFU = colony forming units
CI = confidence interval
CLR = C-type lectin receptor
CSF = cerebrospinal fluid
CPP = cluster propensity to propagate
GFP = green fluorescent protein
HR = hazard ratio
IL = interleukin
IFN = interferon
LTA4H = Leukotriene A4 Hydrolase
MN = mononuclear cell
PBMC = peripheral blood mononuclear cells
PC = principal component
PMN = polymorphonuclear cell
QTL = quantitative trait locus
SNP = single nucleotide polymorphism
TDM = trehalose- 6,6-dimycolate
TIM = target of independent mutation
TNF = tumour necrosis factor

References

1. Houben RMGJ, Dodd PJ. The Global Burden of Latent Tuberculosis Infection: A Re-estimation Using Mathematical Modelling. PLoS Med. 2016 Oct;13(10):e1002152.
2. WHO. Global tuberculosis report 2017. 2017 Oct pp. 1–262.
3. Ramakrishnan L. Revisiting the role of the granuloma in tuberculosis. Nat Rev Immunol. 2012 Apr 20;12(5):352–66
4. Comas I, Chakravartti J, Small PM, Galagan J, Niemann S, Kremer K, Ernst JD, Gagneux S. Human T cell epitopes of *Mycobacterium tuberculosis* are evolutionarily hyperconserved. *Nat Genet*. 2010 Jun;42(6):498–503..
5. Comas I, Coscolla M, Luo T, Borrell S, Holt KE, Kato-Maeda M, Parkhill J, Malla B, Berg S, Thwaites G, Yeboah-Manu D, Bothamley G, Mei J, Wei L, Bentley S, Harris SR, Niemann S, Diel R, Aseffa A, Gao Q, Young D, Gagneux S. Out-of-Africa migration and Neolithic coexpansion of *Mycobacterium tuberculosis* with modern humans. *Nat Genet*. 2013 Oct;45(10):1176–82.
6. Brosch R, Gordon SV, Marmiesse M, Brodin P, Buchrieser C, Eiglmeier K, Garnier T, Gutierrez C, Hewinson G, Kremer K, Parsons LM, Pym AS, Samper S, van Soolingen D, Cole ST. A new evolutionary scenario for the *Mycobacterium tuberculosis* complex. Proc Natl Acad Sci USA. 2002 Mar 19;99(6):3684–9.
7. Bos KI, Harkins KM, Herbig A, Coscolla M, Weber N, Comas I, Forrest SA, Bryant JM, Harris SR, Schuenemann VJ, Campbell TJ, Majander K, Wilbur AK, Guichon RA, Wolfe Steadman DL, Cook DC, Niemann S, Behr MA, Zumarraga M, Bastida R, Huson D, Nieselt K, Young D, Parkhill J, Buikstra JE, Gagneux S, Stone AC, Krause J. Pre-Columbian mycobacterial genomes reveal seals as a source of New World human tuberculosis. Nature. 2014 Aug 20.
8. Williams, Dunbar R. Big Brains, Meat, Tuberculosis, and the Nicotinamide Switches: Co-Evolutionary Relationships with Modern Repercussions? IJTR. 2013 Oct;:73–16.
9. de Jong BC, Hill PC, Aiken A, Awine T, Antonio M, Adetifa IM, Jackson Sillah DJ, Fox A, DeRiemer K, Gagneux S, Borgdorff MW, McAdam KPWJ, Corrah T, Small PM, Adegbola RA. Progression to Active Tuberculosis, but Not Transmission, Varies by *Mycobacterium tuberculosis*Lineage in The Gambia. J INFECT DIS. 2008 Oct;198(7):1037–43.
10. Gagneux S, Small PM. Global phylogeography of *Mycobacterium tuberculosis* and implications for tuberculosis product development. The Lancet Infectious Diseases. 2007 May;7(5):328–37.
11. Merker M, Blin C, Mona S, Duforet-Frebourg N, Lecher S, Willery E, Blum MGB, (…), Wirth T. Evolutionary history and global spread of the *Mycobacterium tuberculosis* Beijing lineage. Nat Genet. 2015 Jan 19;47(3):242–9.
12. Verrall AJ, G Netea M, Alisjahbana B, Hill PC, van Crevel R. Early clearance of *Mycobacterium tuberculosis*: a new frontier in prevention. Immunology. 2014 Mar 11;141(4):506–13.
13. World Health Organization. Global tuberculosis report 2016. 2016.
14. Comstock GW, Livesay VT, Woolpert SF. The prognosis of a positive tuberculin reaction in childhood and adolescence. Am J Epidemiol. 1974 Feb;99(2):131–8.
15. Horsburgh CR. Priorities for the treatment of latent tuberculosis infection in the United States. N Engl J Med. 2004 May 13;350(20):2060–7.
16. Wilkinson RJ, Rohlwink U, Misra UK, van Crevel R, Mai NTH, Dooley KE, Caws M, Figaji A, Savic R, Solomons R, Thwaites GE, Tuberculous Meningitis International Research Consortium. Tuberculous meningitis. Nat Rev Neurol. 2017 Oct;13(10):581–98.
17. Rich AR, McCordock HA. The Pathogenesis of Tuberculous Meningitis. Bull Johns Hopkins Hosp. 1933 Feb 7;52:2–37.
18. Thwaites GE, Tran TH. Tuberculous meningitis: many questions, too few answers. Lancet Neurol. 2005 Mar;4(3):160–70.
19. Kleinnijenhuis J, Oosting M, Joosten LAB, Netea MG, van Crevel R. Innate Immune Recognition of *Mycobacterium tuberculosis*. Clinical and Developmental Immunology. 2011;2011:1–12.

20. O'Garra A, Redford PS, McNab FW, Bloom CI, Wilkinson RJ, Berry MPR. The Immune Response in Tuberculosis. Annu Rev Immunol. 2013 Mar 21;31(1):475–527.
21. Li Y, Oosting M, Smeekens SP, Jaeger M, Aguirre-Gamboa R, Le KTT, Deelen P, Ricaño-Ponce I, Schoffelen T, Jansen AFM, Swertz MA, Withoff S, van de Vosse E, van Deuren M, van de Veerdonk F, Zhernakova A, van der Meer JWM, Xavier RJ, Franke L, Joosten LAB, Wijmenga C, Kumar V, Netea MG. A Functional Genomics Approach to Understand Variation in Cytokine Production in Humans. Cell. 2016 Nov 3;167(4):1099–1102.e14.
22. Cobat A, Gallant CJ, Simkin L, Black GF, Stanley K, Hughes J, Doherty TM, Hanekom WA, Eley B, Jaïs J-P, Boland-Auge A, van Helden P, Casanova J-L, Abel L, Hoal EG, Schurr E, Alcaïs A. Two loci control tuberculin skin test reactivity in an area hyperendemic for tuberculosis. Journal of Experimental Medicine. 2009 Nov 23;206(12):2583–91.
23. Thye T, Owusu-Dabo E, Vannberg FO, van Crevel R, Curtis J, Sahiratmadja E, Balabanova Y, Ehmen C, Muntau B, Ruge G, Sievertsen J, Gyapong J, Nikolayevskyy V, Hill PC, Sirugo G, Drobniewski F, van de Vosse E, Newport M, Alisjahbana B, Nejentsev S, Ottenhoff THM, Hill AVS, Horstmann RD, Meyer CG. Common variants at 11p13 are associated with susceptibility to tuberculosis. Nat Genet. 2012 Feb 5;44(3):257–9.
24. Hill AVS. Evolution, revolution and heresy in the genetics of infectious disease susceptibility. Philosophical Transactions of the Royal Society B: Biological Sciences. 2012 Feb 6;367(1590):840–9.
25. Ganiem AR, Parwati I, Wisaksana R, van der Zanden A, van de Beek D, Sturm P, van der Ven A, Alisjahbana B, Brouwer A-M, Kurniani N, de Gans J, van Crevel R. The effect of HIV infection on adult meningitis in Indonesia: a prospective cohort study. AIDS. 2009 Nov 13;23(17):2309–16.
26. Heemskerk AD, Bang ND, Mai NTH, Chau TTH, Phu NH, Loc PP, Chau NVV, Hien TT, Dung NH, Lan NTN, Lan NH, Lan NN, Phong LT, Vien NN, Hien NQ, Yen NTB, Ha DTM, Day JN, Caws M, Merson L, Thinh TTV, Wolbers M, Thwaites GE, Farrar JJ. Intensified Antituberculosis Therapy in Adults with Tuberculous Meningitis. N Engl J Med. 2016 Jan 14;374(2):124–34.
27. Thwaites GE, van toorn MBChB R, Schoeman J. Tuberculous meningitis: more questions, still too few answers. Lancet Neurol. 2013 Aug 22;:1–12.
28. Figaji AA, Fieggen AG. The neurosurgical and acute care management of tuberculous meningitis: evidence and current practice. Tuberculosis 2010 Oct 11;90(6):393–400.
29. Ruslami R, Ganiem AR, Dian S, Apriani L, Achmad TH, van der Ven AJ, Borm G, Aarnoutse RE, van Crevel R. Intensified regimen containing rifampicin and moxifloxacin for tuberculous meningitis: an open-label, randomised controlled phase 2 trial. The Lancet Infectious Diseases. 2013 Jan;13(1):27–35.
30. Brake Te L, Dian S, Ganiem AR, Ruesen C, Burger D, Donders R, Ruslami R, van Crevel R, Aarnoutse R. Pharmacokinetic/pharmacodynamic analysis of an intensified regimen containing rifampicin and moxifloxacin for tuberculous meningitis. Int J Antimicrob Agents. 2015 May;45(5):496–503.
31. Hektoen L. The Fate of the Giant Cells in Healing Tuberculous Tissue, as Observed in a Case of Healing Tuberculous Meningitis. J Exp Med. 1898 Jan 1;3(1):21–52.
32. Jeren T, Beus I. Characteristics of cerebrospinal fluid in tuberculous meningitis. 1982 Sep 1;26(5):678–80.
33. Simmons CP, Thwaites GE, Quyen NTH, Chau TTH, Mai PP, Dung NT, Stepniewska K, White NJ, Hien TT, Farrar J. The clinical benefit of adjunctive dexamethasone in tuberculous meningitis is not associated with measurable attenuation of peripheral or local immune responses. 2005 Jul 1;175(1):579–90.
34. Fleischer B, Bogdahn U. Growth of antigen specific, HLA restricted T lymphocyte clones from cerebrospinal fluid. Clin Exp Immunol. 1983 Apr;52(1):38–44.
35. Plouffe JF, Silva J, Fekety R, Baird I. Cerebrospinal fluid lymphocyte transformations in meningitis. 1979 Feb 1;139(2):191–4.
36. Kim S-H, Cho O-H, Park S-J, Lee EM, Kim M-N, Lee S-O, Choi S-H, Kim YS, Woo JH, Lee S-A, Kang JK. Rapid diagnosis of tuberculous meningitis by T cell-based assays on peripheral blood and cerebrospinal fluid mononuclear cells. Clin Infect Dis. 2010 May 15;50(10):1349–58.

37. Pan L, Liu F, Zhang J, Yang X, Zheng S, Li J, Jia H, Chen X, Gao M, Zhang Z. Interferon-Gamma Release Assay Performance of Cerebrospinal Fluid and Peripheral Blood in Tuberculous Meningitis in China. BioMed Research International. Hindawi Publishing Corporation; 2017;2017(3):8198505–10.
38. Park K-H, Lee MS, Kim S-M, Park S-J, Chong YP, Lee S-O, Choi S-H, Kim YS, Woo JH, Kang JK, Lee S-A, Kim S-H. Diagnostic usefulness of T-cell based assays for tuberculous meningitis in HIV-uninfected patients. J Infect. 2016 Apr;72(4):486–97.
39. Baig SM. Anti-purified protein derivative cell-enzyme-linked immunosorbent assay, a sensitive method for early diagnosis of tuberculous meningitis. Journal of Clinical Microbiology. 1995 Nov;33(11):3040–1.
40. Sunbul M, Atilla A, Esen S, Eroglu C, Leblebicioglu H. Thwaites' diagnostic scoring and the prediction of tuberculous meningitis. Med Princ Pract. 2005 May;14(3):151–4.
41. Karstaedt AS, Valtchanova S, Barriere R, Crewe-Brown HH. Tuberculous meningitis in South African urban adults. 1998 Nov 1;91(11):743–7.
42. Marais S, Wilkinson KA, Lesosky M, Coussens AK, Deffur A, Pepper DJ, Schutz C, Ismail Z, Meintjes G, Wilkinson RJ. Neutrophil-Associated Central Nervous System Inflammation in Tuberculous Meningitis Immune Reconstitution Inflammatory Syndrome. Clin Infect Dis. 2014 Aug 8.
43. Thuong NTT, Heemskerk D, Tram TTB, Thao LTP, Ramakrishnan L, Ha VTN, Bang ND, Chau TTH, Lan NH, Caws M, Dunstan SJ, Chau NVV, Wolbers M, Mai NTH, Thwaites GE. Leukotriene A4 Hydrolase Genotype and HIV Infection Influence Intracerebral Inflammation and Survival From Tuberculous Meningitis. Journal of Infectious Diseases. 2017 Apr 1;215(7):1020–8.
44. Prasad K, Singh MB, Ryan H. Corticosteroids for managing tuberculous meningitis. Cochrane Database Syst Rev. John Wiley & Sons, Ltd; 2016 Apr 28;4:CD002244.
45. Misra UK, Kalita J, Nair PP. Role of aspirin in tuberculous meningitis: A randomized open label placebo controlled trial. Journal of the Neurological Sciences 2010 Jun 15;293(1-2):12–7.
46. Nagesh Babu G, Kumar A, Kalita J, Misra UK. Proinflammatory cytokine levels in the serum and cerebrospinal fluid of tuberculous meningitis patients. Neuroscience Letters. 2008 May 2;436(1):48–51.
47. Yadav A, Chaudhary C, Keshavan AH, Agarwal A, Verma S, Prasad KN, Rathore RKS, Trivedi R, Gupta RK. Correlation of CSF proinflammatory cytokines with MRI in tuberculous meningitis. Acad Radiol. 2010 Feb;17(2):194–200.
48. Misra UK, Kalita J, Srivastava R, Nair PP, Mishra MK, Basu A. A study of cytokines in tuberculous meningitis: Clinical and MRI correlation. Neuroscience Letters 2010 Oct 8;483(1):6–10.
49. Sharma S, Goyal MK, Sharma K, Modi M, Sharma M, Khandelwal N, Prabhakar S, Sharma N, R S, Gairolla J, Jain A, Lal V. Cytokines do play a role in pathogenesis of tuberculous meningitis: A prospective study from a tertiary care center in India. Journal of the Neurological Sciences 2017 Aug 15;379(C):131–6.
50. Akalin H, Akdiş AC, Mistik R, Helvaci S, Kiliçturgay K. Cerebrospinal fluid interleukin-1 beta/interleukin-1 receptor antagonist balance and tumor necrosis factor-alpha concentrations in tuberculous, viral and acute bacterial meningitis. Scand J Infect Dis. 1994;26(6):667–74.
51. Mastroianni CM, Paoletti F, Lichtner M, D'Agostino C, Vullo V, Delia S. Cerebrospinal fluid cytokines in patients with tuberculous meningitis. Clin Immunol Immunopathol. 1997 Aug;84(2):171–6.
52. Patel VB, Bhigjee AI, Bill PLA, Connolly CA. Cytokine profiles in HIV seropositive patients with tuberculous meningitis. J Neurol Neurosurg Psychiatr. 2002 Nov;73(5):598–9.
53. Kashyap RS, Deshpande PS, Ramteke SR, Panchbhai MS, Purohit HJ, Taori GM, Daginawala HF. Changes in cerebrospinal fluid cytokine expression in tuberculous meningitis patients with treatment. Neuroimmunomodulation. 2010;17(5):333–9.
54. Mansour AM, Frenck RW, Darville T, Nakhla IA, Wierzba TF, Sultan Y, Bassiouny MI, McCarthy K, Jacobs RF. Relationship between intracranial granulomas and cerebrospinal fluid levels of gamma interferon and interleukin-10 in patients with tuberculous meningitis. Clin Diagn Lab Immunol. 2005 Feb;12(2):363–5.

55. Mastroianni CM, Paoletti F, Rivosecchi RM, Lancella L, Ticca F, Vullo V, Delia S. Cerebrospinal fluid interleukin 8 in children with purulent bacterial and tuberculous meningitis. Pediatr Infect Dis J. 1994 Nov;13(11):1008–10.
56. Yilmaz E, Gürgöze MK, Ilhan N, Doğan Y, Aydinoğlu H. Interleukin-8 levels in children with bacterial, tuberculous and aseptic meningitis. Indian J Pediatr. 2002 Mar;69(3):219–21.
57. Yang Q, Cai Y, Zhao W, Wu F, Zhang M, Luo K, Zhang Y, Liu H, Zhou B, Kornfeld H, Chen X. IP-10 and MIG are compartmentalized at the site of disease during pleural and meningeal tuberculosis and are decreased after anti-tuberculosis treatment. Clin Vaccine Immunol. American Society for Microbiology; 2014 Oct 1;21(12):1635–44.
58. Chaidir L, Ganiem AR, vander Zanden A, Muhsinin S, Kusumaningrum T, Kusumadewi I, van der Ven A, Alisjahbana B, Parwati I, van Crevel R. Comparison of real time IS6110-PCR, microscopy, and culture for diagnosis of tuberculous meningitis in a cohort of adult patients in Indonesia. PLoS ONE. 2012;7(12):e52001.
59. Ruslami R, Nijland H, Aarnoutse R, Alisjahbana B, Soeroto AY, Ewalds S, van Crevel R. Evaluation of high- versus standard-dose rifampin in Indonesian patients with pulmonary tuberculosis. Antimicrobial Agents and Chemotherapy. 2006 Feb;50(2):822–3.
60. Png E, Alisjahbana B, Sahiratmadja E, Marzuki S, Nelwan R, Balabanova Y, Nikolayevskyy V, Drobniewski F, Nejentsev S, Adnan I, van de Vosse E, Hibberd ML, van Crevel R, Ottenhoff TH, Seielstad M. A genome wide association study of pulmonary tuberculosis susceptibility in Indonesians. BioMed Central Ltd; 2012 Jan 13;13(1):5.
61. Parwati I, Alisjahbana B, Apriani L, Soetikno RD, Ottenhoff TH, van der Zanden AGM, van der Meer J, van Soolingen D, van Crevel R. *Mycobacterium tuberculosis* Beijing genotype is an independent risk factor for tuberculosis treatment failure in Indonesia. Journal of Infectious Diseases. 2010 Feb 15;201(4):553–7.
62. Marakalala MJ, Graham LM, Brown GD. The role of Syk/CARD9-coupled C-type lectin receptors in immunity to *Mycobacterium tuberculosis* infections. Clinical and Developmental Immunology. 2010;2010(6):567571–9.
63. Fremond CM, Togbe D, Doz E, Rose S, Vasseur V, Maillet I, Jacobs M, Ryffel B, Quesniaux VFJ. IL-1 receptor-mediated signal is an essential component of MyD88-dependent innate response to *Mycobacterium tuberculosis* infection. J Immunol. 2007 Jul 15;179(2):1178–89.
64. Dorhoi A, Desel C, Yeremeev V, Pradl L, Brinkmann V, Mollenkopf H-J, Hanke K, Gross O, Ruland J, Kaufmann SHE. The adaptor molecule CARD9 is essential for tuberculosis control. Journal of Experimental Medicine. 2010 Apr 12;207(4):777–92.
65. Ishikawa E, Ishikawa T, Morita YS, Toyonaga K, Yamada H, Takeuchi O, Kinoshita T, Akira S, Yoshikai Y, Yamasaki S. Direct recognition of the mycobacterial glycolipid, trehalose dimycolate, by C-type lectin Mincle. Journal of Experimental Medicine. 2009 Dec 21;206(13):2879–88.
66. Schoenen H, Bodendorfer B, Hitchens K, Manzanero S, Werninghaus K, Nimmerjahn F, Agger EM, Stenger S, Andersen P, Ruland J, Brown GD, Wells C, Lang R. Cutting edge: Mincle is essential for recognition and adjuvanticity of the mycobacterial cord factor and its synthetic analog trehalose-dibehenate. The Journal of Immunology. 2010 Mar 15;184(6):2756–60.
67. Behler F, Steinwede K, Balboa L, Ueberberg B, Maus R, Kirchhof G, Yamasaki S, Welte T, Maus UA. Role of Mincle in alveolar macrophage-dependent innate immunity against mycobacterial infections in mice. The Journal of Immunology. 2012 Sep 15;189(6):3121–9.
68. Heitmann L, Schoenen H, Ehlers S, Lang R, Hölscher C. Mincle is not essential for controlling *Mycobacterium tuberculosis* infection. Immunobiology. 2013 Apr;218(4):506–16.
69. Yonekawa A, Saijo S, Hoshino Y, Miyake Y, Ishikawa E, Suzukawa M, Inoue H, Tanaka M, Yoneyama M, Oh-Hora M, Akashi K, Yamasaki S. Dectin-2 is a direct receptor for mannose-capped lipoarabinomannan of mycobacteria. Immunity. 2014 Sep 18;41(3):402–13.
70. Graham LM, Gupta V, Schafer G, Reid DM, Kimberg M, Dennehy KM, Hornsell WG, Guler R, Campanero-Rhodes MA, Palma AS, Feizi T, Kim SK, Sobieszczuk P, Willment JA, Brown GD. The C-type lectin receptor CLECSF8 (CLEC4D) is expressed by myeloid cells and triggers cellular activation through Syk kinase. J Biol Chem. 2012 Jul 27;287(31):25964–74.

71. Miyake Y, Toyonaga K, Mori D, Kakuta S, Hoshino Y, Oyamada A, Yamada H, Ono K-I, Suyama M, Iwakura Y, Yoshikai Y, Yamasaki S. C-type lectin MCL is an FcRγ-coupled receptor that mediates the adjuvanticity of mycobacterial cord factor. Immunity. 2013 May 23;38(5):1050–62.
72. Berry MPR, Graham CM, McNab FW, Xu Z, Bloch SAA, Oni T, Wilkinson KA, Banchereau R, Skinner J, Wilkinson RJ, Quinn C, Blankenship D, Dhawan R, Cush JJ, Mejias A, Ramilo O, Kon OM, Pascual V, Banchereau J, Chaussabel D, O'Garra A. An interferon-inducible neutrophil-driven blood transcriptional signature in human tuberculosis. Nature. 2010 Aug 10;466(7309):973–7.
73. Maertzdorf J, Weiner J, Mollenkopf H-J, TBornotTB Network, Bauer T, Prasse A, Müller-Quernheim J, Kaufmann SHE. Common patterns and disease-related signatures in tuberculosis and sarcoidosis. Proc Natl Acad Sci USA. 2012 May 15;109(20):7853–8.
74. Ottenhoff THM, Dass RH, Yang N, Zhang MM, Wong HEE, Sahiratmadja E, Khor CC, Alisjahbana B, van Crevel R, Marzuki S, Seielstad M, van de Vosse E, Hibberd ML. Genome-Wide Expression Profiling Identifies Type 1 Interferon Response Pathways in Active Tuberculosis. PLoS ONE. 2012 Sep 21;7(9):e45839.
75. Anderson ST, Kaforou M, Brent AJ, Wright VJ, Banwell CM, Chagaluka G, Crampin AC, Dockrell HM, French N, Hamilton MS, Hibberd ML, Kern F, Langford PR, Ling L, Mlotha R, Ottenhoff THM, Pienaar S, Pillay V, Scott JAG, Twahir H, Wilkinson RJ, Coin LJ, Heyderman RS, Levin M, Eley B. Diagnosis of Childhood Tuberculosis and Host RNA Expression in Africa. N Engl J Med. 2014 May;370(18):1712–23.
76. Westra H-J, Peters MJ, Esko T, Yaghootkar H, Schurmann C, Kettunen J, (…), Franke L. Systematic identification of trans eQTLs as putative drivers of known disease associations. Nat Genet. 2013 Oct;45(10):1238–43.
77. GTEx Consortium. The Genotype-Tissue Expression (GTEx) project. Nat Genet. 2013 Jun;45(6):580–5.
78. Barrett JC, Fry B, Maller J, Daly MJ. Haploview: analysis and visualization of LD and haplotype maps. Bioinformatics. 2005 Jan 15;21(2):263–5.
79. Songane M, Kleinnijenhuis J, Alisjahbana B, Sahiratmadja E, Parwati I, Oosting M, Plantinga TS, Joosten LAB, Netea MG, Ottenhoff THM, van de Vosse E, van Crevel R. Polymorphisms in Autophagy Genes and Susceptibility to Tuberculosis. PLoS ONE. 2012 Aug 6;7(8):e41618.
80. Zhu L-L, Zhao X-Q, Jiang C, You Y, Chen X-P, Jiang Y-Y, Jia X-M, Lin X. C-type lectin receptors Dectin-3 and Dectin-2 form a heterodimeric pattern-recognition receptor for host defense against fungal infection. Immunity. 2013 Aug 22;39(2):324–34.
81. Steichen AL, Binstock BJ, Mishra BB, Sharma J. C-type lectin receptor Clec4d plays a protective role in resolution of Gram-negative pneumonia. Journal of Leukocyte Biology. 2013 Sep;94(3):393–8.
82. Philips JA, Ernst JD. Tuberculosis pathogenesis and immunity. Annu Rev Pathol. 2012;7:353–84.
83. Lobato-Pascual A, Saether PC, Fossum S, Dissen E, Daws MR. Mincle, the receptor for mycobacterial cord factor, forms a functional receptor complex with MCL and FcεRI-γ. Eur J Immunol. 2013 Dec;43(12):3167–74.
84. Lowe DM, Redford PS, Wilkinson RJ, O'Garra A, Martineau AR. Neutrophils in tuberculosis: friend or foe? Trends in Immunology 2012 Jan 1;33(1):14–25.
85. Caws M, Thwaites G, Dunstan S, Hawn TR, Thi Ngoc Lan N, Thuong NTT, Stepniewska K, Huyen MNT, Bang ND, Huu Loc T, Gagneux S, van Soolingen D, Kremer K, van der Sande M, Small P, Thi Hoang Anh P, Chinh NT, Thi Quy H, Thi Hong Duyen N, Quang Tho D, Hieu NT, Torok E, Hien TT, Dung NH, Thi Quynh Nhu N, Duy PM, van Vinh Chau N, Farrar J. The Influence of Host and Bacterial Genotype on the Development of Disseminated Disease with *Mycobacterium tuberculosis*. PLoS Pathogens. 2008 Mar 28;4(3):e1000034.
86. Tamassia N, Zimmermann M, Castellucci M, Ostuni R, Bruderek K, Schilling B, Brandau S, Bazzoni F, Natoli G, Cassatella MA. Cutting edge: An inactive chromatin configuration at the IL-10 locus in human neutrophils. The Journal of Immunology. 2013 Mar 1;190(5):1921–5.
87. Schafer G, Guler R, Murray G, Brombacher F, Brown GD. The role of scavenger receptor B1 in infection with *Mycobacterium tuberculosis* in a murine model. PLoS ONE. 2009 Dec 24;4(12):e8448.

88. Herre J, Marshall ASJ, Caron E, Edwards AD, Williams DL, Schweighoffer E, Tybulewicz V, Reis e Sousa C, Gordon S, Brown GD. Dectin-1 uses novel mechanisms for yeast phagocytosis in macrophages. Blood. 2004 Dec 15;104(13):4038–45.
89. Graham LM, Tsoni SV, Willment JA, Williams DL, Taylor PR, Gordon S, Dennehy K, Brown GD. Soluble Dectin-1 as a tool to detect beta-glucans. Journal of Immunological Methods. 2006 Jul 31;314(1-2):164–9.
90. Pyż E, Brown GD. Screening for ligands of C-type lectin-like receptors. Methods Mol Biol. Totowa, NJ: Humana Press; 2011;748(Chapter 1):1–19.
91. van Soolingen D, Qian L, de Haas PE, Douglas JT, Traore H, Portaels F, Qing HZ, Enkhsaikan D, Nymadawa P, van Embden JD. Predominance of a single genotype of *Mycobacterium tuberculosis* in countries of east Asia. Journal of Clinical Microbiology. 1995 Dec;33(12):3234–8.
92. Hershberg R, Lipatov M, Small PM, Sheffer H, Niemann S, Homolka S, Roach JC, Kremer K, Petrov DA, Feldman MW, Gagneux S. High Functional Diversity in *Mycobacterium tuberculosis* Driven by Genetic Drift and Human Demography. Plos Biol. 2008;6(12):e311.
93. Parwati I, van Crevel R, van Soolingen D. Possible underlying mechanisms for successful emergence of the *Mycobacterium tuberculosis* Beijing genotype strains. The Lancet Infectious Diseases 2010 Feb 1;10(2):103–11.
94. Cobelens F. Relative reproductive fitness of the W-Beijing genotype. int j tuberc lung dis. 2012; 16(3):287.
95. Mokrousov I, Narvskaya O, Otten T, Vyazovaya A, Limeschenko E, Steklova L, Vyshnevskyi B. Phylogenetic reconstruction within *Mycobacterium tuberculosis* Beijing genotype in northwestern Russia. Res Microbiol. 2002 Dec;153(10):629–37.
96. Schürch AC, Kremer K, Warren RM, Hung NV, Zhao Y, Wan K, Boeree MJ, Siezen RJ, Smith NH, van Soolingen D. Mutations in the regulatory network underlie the recent clonal expansion of a dominant subclone of the *Mycobacterium tuberculosis* Beijing genotype. Infection, Genetics and Evolution 2011 Apr 1;11(3):587–97.
97. Kremer K. Vaccine-induced Immunity Circumvented by Typical *Mycobacterium tuberculosis* Beijing Strains. Emerg Infect Dis. 2009 Feb;15(2):335–9.
98. Mokrousov I, Jiao WW, Valcheva V, Vyazovaya A, Otten T, Ly HM, Lan NN, Limeschenko E, Markova N, Vyshnevskiy B, Shen AD, Narvskaya O. Rapid Detection of the *Mycobacterium tuberculosis* Beijing Genotype and Its Ancient and Modern Sublineages by IS6110-Based Inverse PCR. Journal of Clinical Microbiology. 2006 Aug 4;44(8):2851–6.
99. Dou H-Y, Tseng F-C, Lin C-W, Chang J-R, Sun J-R, Tsai W-S, Lee S-Y, Su I-J, Lu J-J. Molecular epidemiology and evolutionary genetics of *Mycobacterium tuberculosis* in Taipei. BMC Infectious Diseases. 2008;8(1):170.
100. Strauss OJ, Warren RM, Jordaan A, Streicher EM, Hanekom M, Falmer AA, Albert H, Trollip A, Hoosain E, van Helden PD, Victor TC. Spread of a Low-Fitness Drug-Resistant *Mycobacterium tuberculosis* Strain in a Setting of High Human Immunodeficiency Virus Prevalence. Journal of Clinical Microbiology. 2008 Apr 2;46(4):1514–6.
101. Kato-Maeda M, Kim EY, Flores L, Jarlsberg LG, Osmond D, Hopewell PC. Differences among sublineages of the East-Asian lineage of *Mycobacterium tuberculosis* in genotypic clustering. int j tuberc lung dis. 2010 May;14(5):538–44.
102. Iwamoto T, Fujiyama R, Yoshida S, Wada T, Shirai C, Kawakami Y. Population Structure Dynamics of *Mycobacterium tuberculosis* Beijing Strains during Past Decades in Japan. Journal of Clinical Microbiology. 2009 Sep 30;47(10):3340–3.
103. Wada T, Fujihara S, Shimouchi A, Harada M, Ogura H, Matsumoto S, Hase A. High transmissibility of the modern Beijing *Mycobacterium tuberculosis* in homeless patients of Japan. Tuberculosis 2009 Jul 1;89(4):252–5.
104. Ioerger TR, Feng Y, Chen X, Dobos KM, Victor TC, Streicher EM, Warren RM, van Pittius NCG, van Helden PD, Sacchettini JC. The non-clonality of drug resistance in Beijing-genotype isolates of *Mycobacterium tuberculosis* from the Western Cape of South Africa. BMC Genomics. BioMed Central Ltd; 2010 Nov 26;11(1):670.

105. Mokrousov I, Jiao W-W, Sun G-Z, Liu J-W, Valcheva V, Li M, Narvskaya O, Shen A-D. Evolution of drug resistance in different sublineages of *Mycobacterium tuberculosis* Beijing genotype. Antimicrobial Agents and Chemotherapy. 2006 Aug;50(8):2820–3.
106. Jiao W-W, Mokrousov I, Sun G-Z, Li M, Liu J-W, Narvskaya O, Shen A-D. Molecular characteristics of rifampin and isoniazid resistant *Mycobacterium tuberculosis* strains from Beijing, China. Chin Med J. 2007 May 5;120(9):814–9.
107. Plikaytis BB, Marden JL, Crawford JT, Woodley CL, Butler WR, Shinnick TM. Multiplex PCR assay specific for the multidrug-resistant strain W of *Mycobacterium tuberculosis*. Journal of Clinical Microbiology. 1994 Jun;32(6):1542–6.
108. Dysvik B, Jonassen I. J-Express: exploring gene expression data using Java. Bioinformatics. 2001 Apr;17(4):369–70.
109. Cooper AM, Mayer-Barber KD, Sher A. Role of innate cytokines in mycobacterial infection. Mucosal Immunol. 2011 Mar 23;4(3):252–60.
110. van Crevel R, Ottenhoff THM, van der Meer JWM. Innate immunity to *Mycobacterium tuberculosis*. Clinical Microbiology Reviews. 2002 Apr;15(2):294–309.
111. Ottenhoff THM, Verreck FAW, Lichtenauer-Kaligis EGR, Hoeve MA, Sanal O, van Dissel JT. Genetics, cytokines and human infectious disease: lessons from weakly pathogenic mycobacteria and salmonellae. Nat Genet. 2002 Sep;32(1):97–105.
112. Ottenhoff THM. New pathways of protective and pathological host defense to mycobacteria. Trends in Microbiology. 2012 Jul 9.
113. Keane J, Gershon S, Wise RP, Mirabile-Levens E, Kasznica J, Schwieterman WD, Siegel JN, Braun MM. Tuberculosis associated with infliximab, a tumor necrosis factor alpha-neutralizing agent. N Engl J Med. 2001 Oct 11;345(15):1098–104.
114. Miller EA, Ernst JD. Illuminating the black box of TNF action in tuberculous granulomas. Immunity. 2008 Aug 15;29(2):175–7.
115. Flynn JL, Chan J, Lin PL. Macrophages and control of granulomatous inflammation in tuberculosis. Mucosal Immunol. 2011 May;4(3):271–8.
116. Torrado E, Cooper AM. IL-17 and Th17 cells in tuberculosis. Cytokine Growth Factor Rev. 2010 Dec;21(6):455–62..
117. Davis JM, Ramakrishnan L. The Role of the Granuloma in Expansion and Dissemination of Early Tuberculous Infection. Cell. 2009 Jan 9;136(1):37–49.
118. Glader P, Smith ME, Malmhäll C, Balder B, Sjöstrand M, Qvarfordt I, Lindén A. Interleukin-17-producing T-helper cells and related cytokines in human airways exposed to endotoxin. Eur Respir J. 2010 Nov;36(5):1155–64.
119. Sonnenberg GF, Fouser LA, Artis D. Border patrol: regulation of immunity, inflammation and tissue homeostasis at barrier surfaces by IL-22. Nat Immunol. 2011 May;12(5):383–90.
120. Portevin D, Gagneux S, Comas I, Young D. Human Macrophage Responses to Clinical Isolates from the *Mycobacterium tuberculosis* Complex Discriminate between Ancient and Modern Lineages. PLoS Pathogens. 2011 Mar 3;7(3):e1001307.
121. Coscolla M, Gagneux S. Does *M. tuberculosis* genomic diversity explain disease diversity? Drug Discovery Today: Disease Mechanisms. 2010 Mar;7(1):e43–e59.
122. Wang C, Peyron P, Mestre O, Kaplan G, van Soolingen D, Gao Q, Gicquel B, Neyrolles O. Innate Immune Response to *Mycobacterium tuberculosis* Beijing and Other Genotypes. PLoS ONE. 2010 Oct 25;5(10):e13594.
123. Chacón-Salinas R, Serafín-López J, Ramos-Payán R, Méndez-Aragón P, HERNANDEZ-PANDO R, van Soolingen D, Flores-Romo L, Estrada-Parra S, Estrada-García I. Differential pattern of cytokine expression by macrophages infected in vitro with different *Mycobacterium tuberculosis* genotypes. Clin Exp Immunol. 2005 Jun;140(3):443–9.
124. Cappelli G, Volpe P, Sanduzzi A, Sacchi A, Colizzi V, Mariani F. Human macrophage gamma interferon decreases gene expression but not replication of *Mycobacterium tuberculosis*: analysis of the host-pathogen reciprocal influence on transcription in a comparison of strains H37Rv and CMT97. Infection and Immunity. 2001 Dec;69(12):7262–70.

125. Krishnan N, Malaga W, Constant P, Caws M, Thi Hoang Chau T, Salmons J, Thi Ngoc Lan N, Bang ND, Daffé M, Young DB, Robertson BD, Guilhot C, Thwaites GE. *Mycobacterium tuberculosis* Lineage Influences Innate Immune Response and Virulence and Is Associated with Distinct Cell Envelope Lipid Profiles. PLoS ONE. 2011 Sep 8;6(9):e23870.
126. Kato-Maeda M, Shanley CA, Ackart D, Jarlsberg LG, Shang S, Obregon-Henao A, Harton M, Basaraba RJ, Henao-Tamayo M, Barrozo JC, Rose J, Kawamura LM, Coscolla M, Fofanov VY, Koshinsky H, Gagneux S, Hopewell PC, Ordway DJ, Orme IM. Beijing sublineages of *Mycobacterium tuberculosis* differ in pathogenicity in the guinea pig. Clin Vaccine Immunol. 2012 Jun 20.
127. Mihret A, Bekele Y, Loxton AG, Aseffa A, Howe R, Walzl G. Plasma Level of IL-4 Differs in Patients Infected with Different Modern Lineages of *M. tuberculosis*. J Trop Med. 2012;2012:518564.
128. WHO. World Health Organization (2012) Global tuberculosis control: WHO Report 2012. Geneva; 2012 Nov 29;:1–100.
129. Kik SV, Verver S, van Soolingen D, de Haas PEW, Cobelens FG, Kremer K, van Deutekom H, Borgdorff MW. Tuberculosis Outbreaks Predicted by Characteristics of First Patients in a DNA Fingerprint Cluster. Am J Respir Crit Care Med. 2008 Jul;178(1):96–104.
130. Kong Y, Cave MD, Zhang L, Foxman B, Marrs CF, Bates JH, Yang ZH. Population-based study of deletions in five different genomic regions of *Mycobacterium tuberculosis* and possible clinical relevance of the deletions. Journal of Clinical Microbiology. 2006 Nov;44(11):3940–6.
131. Albanna AS, Reed MB, Kotar KV, Fallow A, McIntosh FA, Behr MA, Menzies D. Reduced Transmissibility of East African Indian Strains of *Mycobacterium tuberculosis*. PLoS ONE. 2011 Sep 19;6(9):e25075.
132. Romero MM, Balboa L, Basile JI, López B, Ritacco V, la Barrera de SS, Sasiain MC, Barrera L, Alemán M. Clinical Isolates of *Mycobacterium tuberculosis* Differ in Their Ability to Induce Respiratory Burst and Apoptosis in Neutrophils as a Possible Mechanism of Immune Escape. Clinical and Developmental Immunology. 2012;2012:1–11.
133. Rakotosamimanana N, Raharimanga V, Andriamandimby SF, Soares JL, Doherty TM, Ratsitorahina M, Ramarokoto H, Zumla A, Huggett J, Rook G, Richard V, Gicquel B, Rasolofo-Razanamparany V, the VACSEL/VACSIS Study Group. Variation in Gamma Interferon Responses to Different Infecting Strains of *Mycobacterium tuberculosis* in Acid-Fast Bacillus Smear-Positive Patients and Household Contacts in Antananarivo, Madagascar. Clinical and Vaccine Immunology. 2010 Jul 2;17(7):1094–103.
134. Manca C, Tsenova L, Bergtold A, Freeman S, Tovey M, Musser JM, Barry CE, Freedman VH, Kaplan G. Virulence of a *Mycobacterium tuberculosis* clinical isolate in mice is determined by failure to induce Th1 type immunity and is associated with induction of IFN-alpha /beta. Proc Natl Acad Sci USA. 2001 May 8;98(10):5752–7.
135. López B, Aguilar D, Orozco H, Burger M, Espitia C, Ritacco V, Barrera L, Kremer K, Hernandez-Pando R, Huygen K, van Soolingen D. A marked difference in pathogenesis and immune response induced by different *Mycobacterium tuberculosis* genotypes. Clin Exp Immunol. 2003 Jul;133(1):30–7.
136. Aguilar León D, Hanekom M, Mata D, van Pittius NCG, van Helden PD, Warren RM, Hernandez-Pando R. *Mycobacterium tuberculosis* strains with the Beijing genotype demonstrate variability in virulence associated with transmission. Tuberculosis. 2010 Sep 1;90(5):319–25.
137. Jones-López EC, Kim S, Fregona G, Marques-Rodrigues P, Hadad DJ, Molina LPD, Vinhas S, Reilly N, Moine S, Chakravorty S, Gaeddert M, Ribeiro-Rodrigues R, Salgame P, Palaci M, Alland D, Ellner JJ, Dietze R. Importance of cough and *M. tuberculosis* strain type as risks for increased transmission within households. PLoS ONE. 2014;9(7):e100984.
138. Shin D-M, Jeon BY, Lee H-M, Jin HS, Yuk J-M, Song C-H, Lee S-H, Lee Z-W, Cho S-N, Kim J-M, Friedman RL, Jo E-K. *Mycobacterium tuberculosis* eis regulates autophagy, inflammation, and cell death through redox-dependent signaling. PLoS Pathogens. 2010;6(12):e1001230.
139. Nebenzahl-Guimaraes H, Borgdorff MW, Murray MB, van Soolingen D. A novel approach - the propensity to propagate (PTP) method for controlling for host factors in studying the transmission of *Mycobacterium tuberculosis*. PLoS ONE. 2014;9(5):e97816.

140. Small PM, Hopewell PC, Singh SP, Paz A, Parsonnet J, Ruston DC, Schecter GF, Daley CL, Schoolnik GK. The epidemiology of tuberculosis in San Francisco. A population-based study using conventional and molecular methods. N Engl J Med. 1994 Jun 16;330(24):1703–9.
141. Alland D, Kalkut GE, Moss AR, McAdam RA, Hahn JA, Bosworth W, Drucker E, Bloom BR. Transmission of tuberculosis in New York City. An analysis by DNA fingerprinting and conventional epidemiologic methods. N Engl J Med. 1994 Jun 16;330(24):1710–6.
142. Farhat MR, Shapiro BJ, Sheppard SK, Colijn C, Murray M. A phylogeny-based sampling strategy and power calculator informs genome-wide associations study design for microbial pathogens. Genome Medicine. 2014 Dec 2;6(101):1–14.
143. Read TD, Massey RC. Characterizing the genetic basis of bacterial phenotypes using genome-wide association studies: a new direction for bacteriology. 2014 Nov 20;:1–11.
144. Rengarajan J, Bloom BR, Rubin EJ. Genome-wide requirements for *Mycobacterium tuberculosis* adaptation and survival in macrophages. Proc Natl Acad Sci USA. 2005 Jun 7;102(23):8327–32.
145. Sassetti CM, Boyd DH, Rubin EJ. Genes required for mycobacterial growth defined by high density mutagenesis. Mol Microbiol. 2003 Apr;48(1):77–84.
146. Fortune SM, Jaeger A, Sarracino DA, Chase MR, Sassetti CM, Sherman DR, Bloom BR, Rubin EJ. Mutually dependent secretion of proteins required for mycobacterial virulence. Proc Natl Acad Sci USA. 2005 Jul 26;102(30):10676–81.
147. Gehre F, Otu J, DeRiemer K, de Sessions PF, Hibberd ML, Mulders W, Corrah T, de Jong BC, Antonio M. Deciphering the Growth Behaviour of Mycobacterium africanum. PLoS Negl Trop Dis. 2013 May 16;7(5):e2220.
148. de Jong BC, Hill PC, Brookes RH, Gagneux S, Jeffries DJ, Otu JK, Donkor SA, Fox A, McAdam KPWJ, Small PM, Adegbola RA. Mycobacterium africanum elicits an attenuated T cell response to early secreted antigenic target, 6 kDa, in patients with tuberculosis and their household contacts. J INFECT DIS. 2006 May 1;193(9):1279–86.
149. Tientcheu LD, Sutherland JS, de Jong BC, Kampmann B, Jafali J, Adetifa IM, Antonio M, Dockrell HM, Ota MO. Differences in T-cell responses between *Mycobacterium tuberculosis* and Mycobacterium africanum-infected patients. Eur J Immunol. 2014 May;44(5):1387–98.
150. Talarico S, Ijaz K, Zhang X, Mukasa LN, Zhang L, Marrs CF, Cave MD, Bates JH, Yang Z. Tuberculosis 2011 May 1;91(3):244–9.
151. Yesilkaya H, Forbes KJ, Shafi J, Smith R, Dale JW, Rajakumar K, Barer MR, Andrew PW. The genetic portrait of an outbreak strain. Tuberculosis. 2006 Sep;86(5):357–62.
152. Reiling N, Homolka S, Walter K, Brandenburg J, Niwinski L, Ernst M, Herzmann C, Lange C, Diel R, Ehlers S, Niemann S. Clade-Specific Virulence Patterns of *Mycobacterium tuberculosis* Complex Strains in Human Primary Macrophages and Aerogenically Infected Mice. mBio. 2013 Jun 25;4(4):e00250–13–e00250–13.
153. Yang C-T, Cambier CJ, Davis JM, Hall CJ, Crosier PS, Ramakrishnan L. Neutrophils exert protection in the early tuberculous granuloma by oxidative killing of mycobacteria phagocytosed from infected macrophages. Cell Host and Microbe. 2012 Sep 13;12(3):301–12.
154. Lee PPW, Chan K-W, Jiang L, Chen T, Li C, Lee T-L, Mak PHS, Fok SFS, Yang X, Lau Y-L. Susceptibility to mycobacterial infections in children with X-linked chronic granulomatous disease: a review of 17 patients living in a region endemic for tuberculosis. Pediatr Infect Dis J. 2008 Mar;27(3):224–30.
155. Arnold A, Witney AA, Vergnano S, Roche A, Cosgrove CA, Houston A, Gould KA, Hinds J, Riley P, Macallan D, Butcher PD, Harrison TS. XDR-TB transmission in London: Case management and contact tracing investigation assisted by early whole genome sequencing. J Infect. 2016 Sep;73(3):210–8.
156. Xu P, Wu J, Yang C, Luo T, Shen X, Zhang Y, Nsofor CA, Zhu G, Gicquel B, Gao Q. Prevalence and transmission of pyrazinamide resistant *Mycobacterium tuberculosis* in China. Tuberculosis (Edinb). 2016 May;98:56–61.
157. Luciani F, Sisson SA, Jiang H, Francis AR, Tanaka MM. The epidemiological fitness cost of drug resistance in *Mycobacterium tuberculosis*. Proc Natl Acad Sci USA. 2009 Aug 25;106(34):14711–5.

158. Li Q-J, Jiao W-W, Yin Q-Q, Xu F, Li J-Q, Sun L, Xiao J, Li Y-J, Mokrousov I, Huang H-R, Shen A-D. Compensatory Mutations of Rifampin Resistance Are Associated with Transmission of Multidrug-Resistant *Mycobacterium tuberculosis* Beijing Genotype Strains in China. Antimicrobial Agents and Chemotherapy. 2016 May;60(5):2807–12.
159. Salvatore PP, Becerra MC, Abel zur Wiesch P, Hinkley T, Kaur D, Sloutsky A, Cohen T. Fitness Costs of Drug Resistance Mutations in Multidrug-Resistant *Mycobacterium tuberculosis*: A Household-Based Case-Control Study. Journal of Infectious Diseases. 2016 Jan 1;213(1):149–55.
160. van Soolingen D, de Haas PE, Hermans PW, Groenen PM, van Embden JD. Comparison of various repetitive DNA elements as genetic markers for strain differentiation and epidemiology of *Mycobacterium tuberculosis*. Journal of Clinical Microbiology. 1993 Aug;31(8):1987–95.
161. Barrick JE, Yu DS, Yoon SH, Jeong H, Oh TK, Schneider D, Lenski RE, Kim JF. Genome evolution and adaptation in a long-term experiment with Escherichia coli. Nature. 2009 Oct 29;461(7268):1243–7.
162. Guerra-Assunção JA, Houben RMGJ, Crampin AC, Mzembe T, Mallard K, Coll F, Khan P, Banda L, Chiwaya A, Pereira RPA, McNerney R, Harris D, Parkhill J, Clark TG, Glynn JR. Recurrence due to relapse or reinfection with *Mycobacterium tuberculosis*: a whole-genome sequencing approach in a large, population-based cohort with a high HIV infection prevalence and active follow-up. Journal of Infectious Diseases. 2015 Apr 1;211(7):1154–63.
163. Farhat MR, Shapiro BJ, Kieser KJ, Sultana R, Jacobson KR, Victor TC, Warren RM, Streicher EM, Calver A, Sloutsky A, Kaur D, Posey JE, Plikaytis B, Oggioni MR, Gardy JL, Johnston JC, Rodrigues M, Tang PKC, Kato-Maeda M, Borowsky ML, Muddukrishna B, Kreiswirth BN, Kurepina N, Galagan J, Gagneux S, Birren B, Rubin EJ, Lander ES, Sabeti PC, Murray M. Genomic analysis identifies targets of convergent positive selection in drug-resistant *Mycobacterium tuberculosis*. Nat Genet. 2013 Sep 1;:1–9.
164. Ashkenazy H, Penn O, Doron-Faigenboim A, Cohen O, Cannarozzi G, Zomer O, Pupko T. FastML: a web server for probabilistic reconstruction of ancestral sequences. Nucleic Acids Research. 2012 Jun 27;40(W1):W580–4.
165. Schubert OT, Ludwig C, Kogadeeva M, Zimmermann M, Rosenberger G, Gengenbacher M, Gillet LC, Ben C Collins, Röst HL, Kaufmann SHE, Sauer U, Aebersold R. Absolute Proteome Composition and Dynamics during Dormancy and Resuscitation of *Mycobacterium tuberculosis*. Cell Host and Microbe. 2015 Jul 8;18(1):96–108.
166. Mawuenyega KG, Forst CV, Dobos KM, Belisle JT, Chen J, Bradbury EM, Bradbury ARM, Chen X. *Mycobacterium tuberculosis* functional network analysis by global subcellular protein profiling. Mol Biol Cell. 2005 Jan;16(1):396–404.
167. Coscolla M, Gagneux S. Consequences of genomic diversity in *Mycobacterium tuberculosis*. Semin Immunol. 2014 Dec 1;26(6):431–44.
168. Chen Y-Y, Chang J-R, Huang W-F, Hsu S-C, Kuo S-C, Sun J-R, Dou H-Y. The pattern of cytokine production in vitro induced by ancient and modern Beijing *Mycobacterium tuberculosis* strains. PLoS ONE. 2014;9(4):e94296.
169. Netea MG, Drenth JP, De Bont N, Hijmans A, Keuter M, Dharmana E, Demacker PN, van der Meer JW. A semi-quantitative reverse transcriptase polymerase chain reaction method for measurement of MRNA for TNF-alpha and IL-1 beta in whole blood cultures: its application in typhoid fever and exentric exercise. Cytokine. 1996 Sep;8(9):739–44.
170. van Crevel R, van der Ven-Jongekrijg J, Netea MG, de Lange W, Kullberg BJ, van der Meer JW. Disease-specific ex vivo stimulation of whole blood for cytokine production: applications in the study of tuberculosis. Journal of Immunological Methods. 1999 Jan 1;222(1-2):145–53.
171. Galluzzi L, Aaronson SA, Abrams J, Alnemri ES, Andrews DW, Baehrecke EH, (…), Kroemer G. Guidelines for the use and interpretation of assays for monitoring cell death in higher eukaryotes. 2009 Apr 17;16(8):1093–107.
172. Goeman JJ, Finos L. The inheritance procedure: multiple testing of tree-structured hypotheses. Stat Appl Genet Mol Biol. 2012 Jan 21;11(1):Article11.

173. Borgdorff MW, van den Hof S, Kremer K, Verhagen L, Kalisvaart N, Erkens C, van Soolingen D. Progress towards tuberculosis elimination: secular trend, immigration and transmission. Eur Respir J. 2010 Aug;36(2):339–47.
174. Nava-Aguilera E, Andersson N, Harris E, Mitchell S, Hamel C, Shea B, López-Vidal Y, Villegas-Arrizón A, Morales-Pérez A. Risk factors associated with recent transmission of tuberculosis: systematic review and meta-analysis. int j tuberc lung dis. 2009 Jan;13(1):17–26.
175. Horton KC, MacPherson P, Houben RMGJ, White RG, Corbett EL. Sex Differences in Tuberculosis Burden and Notifications in Low- and Middle-Income Countries: A Systematic Review and Meta-analysis. PLoS Med. 2016 Sep;13(9):e1002119.
176. Hamblion EL, Le Menach A, Anderson LF, Lalor MK, Brown T, Abubakar I, Anderson C, Maguire H, Anderson SR, Public Health England Strain Typing Project Board. Recent TB transmission, clustering and predictors of large clusters in London, 2010-2012: results from first 3 years of universal MIRU-VNTR strain typing. Thorax. 2016 Aug;71(8):749–56.
177. Pagaoa MA, Royce RA, Chen MP, Golub JE, Davidow AL, Hirsch-Moverman Y, Marks SM, Teeter LD, Thickstun PM, Katz DJ, Tuberculosis Epidemiologic Studies Consortium. Risk factors for transmission of tuberculosis among United States-born African Americans and Whites. int j tuberc lung dis. 2015 Dec;19(12):1485–92.
178. Fok A, Numata Y, Schulzer M, FitzGerald MJ. Risk factors for clustering of tuberculosis cases: a systematic review of population-based molecular epidemiology studies. int j tuberc lung dis. 2008 May;12(5):480–92.
179. Lobato MN, Hopewell PC. *Mycobacterium tuberculosis* infection after travel to or contact with visitors from countries with a high prevalence of tuberculosis. Am J Respir Crit Care Med. 1998 Dec;158(6):1871–5.
180. Jung P, Banks RH. Tuberculosis risk in US Peace Corps Volunteers, 1996 to 2005. J Travel Med. 2008 Mar;15(2):87–94.
181. Mancuso JD, Tobler SK, Eick AA, Keep LW. Active Tuberculosis and Recent Overseas Deployment in the U.S. Military. Am J Prev Med. 2016 Sep 20;39(2):157–63.
182. Bryant JM, Schürch ACS, van Deutekom H, Harris SR, de Beer JL, de Jager V, Kremer K, van Hijum SAFT, Siezen RJ, Borgdorff M, Bentley SD, Parkhill J, van Soolingen D. Inferring patient to patient transmission of *Mycobacterium tuberculosis* from whole genomesequencing data. BMC Infectious Diseases. BMC Infectious Diseases; 2013 Feb 27;13(1):1–1.
183. Kruh NA, Troudt J, Izzo A, Prenni J, Dobos KM. Portrait of a Pathogen: The *Mycobacterium tuberculosis* Proteome In Vivo. PLoS ONE. 2010 Nov 11;5(11):e13938.
184. Williams M, Mizrahi V, Kana BD. Molybdenum cofactor: A key component of *Mycobacterium tuberculosis*pathogenesis? Critical Reviews in Microbiology. 2014 Feb;40(1):18–29.
185. Schuessler DL, Cortes T, Fivian-Hughes AS, Lougheed KEA, Harvey E, Buxton RS, Davis EO, Young DB. Induced ectopic expression of HigB toxin in *Mycobacterium tuberculosis*results in growth inhibition, reduced abundance of a subset of mRNAs and cleavage of tmRNA. Mol Microbiol. 2013 Aug 23.
186. Thwaites GE, Nguyen DB, Nguyen HD, Hoang TQ, Do TTO, Nguyen TCT, Nguyen QH, Nguyen TT, Nguyen NH, Nguyen TNL, Nguyen NL, Nguyen HD, Vu NT, Cao HH, Tran THC, Pham PM, Nguyen TD, Stepniewska K, White NJ, Tran TH, Farrar JJ. Dexamethasone for the treatment of tuberculous meningitis in adolescents and adults. N Engl J Med. 2004 Oct 21;351(17):1741–51.
187. Tho DQ, Torok ME, Yen NTB, Bang ND, Lan NTN, Kiet VS, van Vinh Chau N, Dung NH, Day J, Farrar J, Wolbers M, Caws M. Influence of Antituberculosis Drug Resistance and *Mycobacterium tuberculosis* Lineage on Outcome in HIV-Associated Tuberculous Meningitis. Antimicrobial Agents and Chemotherapy. 2012 May 12;56(6):3074–9.
188. Erdem H, Ozturk-Engin D, Tireli H, Kilicoglu G, Defres S, Gulsun S, (…), Elaldi N, Deveci O, Ozkaya HD, Karabay O, Senbayrak S, Agalar C, Vahaboglu H. Hamsi scoring in the prediction of unfavorable outcomes from tuberculous meningitis: results of Haydarpasa-II study. J Neurol. 2015;262(4):890–8.

189. Gu J, Xiao H, Wu F, Ge Y, Ma J, Sun W. Prognostic factors of tuberculous meningitis: a single-center study. Int J Clin Exp Med. 2015;8(3):4487–93.
190. Marais S, Pepper DJ, Schutz C, Wilkinson RJ, Meintjes G. Presentation and outcome of tuberculous meningitis in a high HIV prevalence setting. PLoS ONE. 2011;6(5):e20077.
191. Tobin DM, Roca FJ, Oh SF, McFarland R, Vickery TW, Ray JP, Ko DC, Zou Y, Bang ND, Chau TTH, Vary JC, Hawn TR, Dunstan SJ, Farrar JJ, Thwaites GE, King M-C, Serhan CN, Ramakrishnan L. Host Genotype-Specific Therapies Can Optimize the Inflammatory Response to Mycobacterial Infections. Cell. 2012 Feb 3;148(3):434–46.
192. Zumla A, Rao M, Parida SK, Keshavjee S, Cassell G, Wallis R, Axelsson-Robertsson R, Doherty M, Andersson J, Maeurer M. Inflammation and tuberculosis: host-directed therapies. J Intern Med. 2015 Apr;277(4):373–87.
193. Schoeman JF, Springer P, van Rensburg AJ, Swanevelder S, Hanekom WA, Haslett PAJ, Kaplan G. Adjunctive thalidomide therapy for childhood tuberculous meningitis: results of a randomized study. 2004 Apr 1;19(4):250–7.
194. Coulter JBS, Baretto RL, Mallucci CL, Romano MI, Abernethy LJ, Isherwood DM, Kumararatne DS, Lammas DA. Tuberculous meningitis: protracted course and clinical response to interferon-gamma. The Lancet Infectious Diseases. 2007 Mar;7(3):225–32.
195. Thwaites GE, Simmons CP, Than Ha Quyen N, Thi Hong Chau T, Phuong Mai P, Thi Dung N, Hoan Phu N, White NP, Tinh Hien T, Farrar JJ. Pathophysiology and prognosis in Vietnamese adults with tuberculous meningitis. J INFECT DIS. 2003 Oct 15;188(8):1105–15.
196. Yunivita V, Dian S, Ganiem AR, Hayati E, Hanggono Achmad T, Purnama Dewi A, Teulen M, Meijerhof-Jager P, van Crevel R, Aarnoutse R, Ruslami R. Pharmacokinetics and safety/tolerability of higher oral and intravenous doses of rifampicin in adult tuberculous meningitis patients. Int J Antimicrob Agents. 2016 Oct;48(4):415–21.
197. Chaidir L, Annisa J, Dian S, Moore AJ. MODS culture for primary diagnosis of tuberculous meningitis and HIV-associated pulmonary tuberculosis in Indonesia. Int J Trop Dis Health. 2013;3(4):346–54.
198. Ganiem AR, Dian S, Indriati A, Chaidir L, Wisaksana R, Sturm P, Melchers W, van der Ven A, Parwati I, van Crevel R. Cerebral toxoplasmosis mimicking subacute meningitis in HIV-infected patients; a cohort study from Indonesia. PLoS Negl Trop Dis. 2013;7(1):e1994.
199. Yunivita V, Dian S, Ganiem AR, Hayati E, Hanggono Achmad T, Purnama Dewi A, Teulen M, Meijerhof-Jager P, van Crevel R, Aarnoutse R, Ruslami R. Pharmacokinetics and safety/tolerability of higher oral and intravenous doses of rifampicin in adult tuberculous meningitis patients. Int J Antimicrob Agents. 2016 Oct;48(4):415–21.
200. Török ME, Yen NTB, Chau TTH, Mai NTH, Phu NH, Mai PP, Dung NT, Chau NVV, Bang ND, Tien NA, Minh NH, Hien NQ, Thai PVK, Dong DT, Anh DTT, Thoa NTC, Hai NN, Lan NN, Lan NTN, Quy HT, Dung NH, Hien TT, Chinh NT, Simmons CP, de Jong M, Wolbers M, Farrar JJ. Timing of initiation of antiretroviral therapy in human immunodeficiency virus (HIV)--associated tuberculous meningitis. Clin Infect Dis. 2011 Jun;52(11):1374–83.
201. Ganiem AR, Indrati AR, Wisaksana R, Meijerink H, van der Ven A, Alisjahbana B, van Crevel R. Asymptomatic cryptococcal antigenemia is associated with mortality among HIV-positive patients in Indonesia. J Int AIDS Soc. 2014;17:18821.
202. Marais S, Thwaites G, Schoeman JF, Török ME, Misra UK, Prasad K, Donald PR, Wilkinson RJ, Marais BJ. Tuberculous meningitis: a uniform case definition for use in clinical research. 2010. pp. 803–12.
203. Naranbhai V, Hill AVS, Abdool Karim SS, Naidoo K, Abdool Karim Q, Warimwe GM, McShane H, Fletcher H. Ratio of monocytes to lymphocytes in peripheral blood identifies adults at risk of incident tuberculosis among HIV-infected adults initiating antiretroviral therapy. Journal of Infectious Diseases. 2014 Feb 15;209(4):500–9.
204. Nkoke C, Lekoubou A, Balti E, Kengne AP. Stroke mortality and its determinants in a resource-limited setting: A prospective cohort study in Yaounde, Cameroon. Journal of the Neurological Sciences. 2015 Nov 15;358(1-2):113–7.

205. Mourvillier B, Tubach F, van de Beek D, Garot D, Pichon N, Georges H, (…), Wolff M. Induced Hypothermia in Severe Bacterial Meningitis. JAMA. 2013 Nov 27;310(20):2174–10.
206. Eum S-Y, Kong J-H, Hong M-S, Lee Y-J, Kim J-H, Hwang S-H, Cho S-N, Via LE, Barry CE. Neutrophils are the predominant infected phagocytic cells in the airways of patients with active pulmonary TB. Chest. 2010 Jan;137(1):122–8.
207. Chen P, Shi M, Feng G-D, Liu J-Y, Wang B-J, Shi X-D, Ma L, Liu X-D, Yang Y-N, Dai W, Liu T-T, He Y, Li J-G, Hao X-K, Zhao G. A highly efficient Ziehl-Neelsen stain: identifying de novo intracellular *Mycobacterium tuberculosis* and improving detection of extracellular *M. tuberculosis* in cerebrospinal fluid. Journal of Clinical Microbiology. 2012 Apr;50(4):1166–70.
208. Thwaites GE, Chau TTH, Farrar JJ. Improving the bacteriological diagnosis of tuberculous meningitis. Journal of Clinical Microbiology. 2004 Jan;42(1):378–9.
209. Puccioni-Sohler M, Brandão CO. Factors associated to the positive cerebrospinal fluid culture in the tuberculous meningitis. Arq Neuropsiquiatr. 2007 Mar;65(1):48–53.
210. Cheng S-C, Scicluna BP, Arts RJW, Gresnigt MS, Lachmandas E, Giamarellos-Bourboulis EJ, Kox M, Manjeri GR, Wagenaars JAL, Cremer OL, Leentjens J, van der Meer AJ, van de Veerdonk FL, Bonten MJ, Schultz MJ, Willems PHGM, Pickkers P, Joosten LAB, van der Poll T, Netea MG. Broad defects in the energy metabolism of leukocytes underlie immunoparalysis in sepsis. Nat Immunol. 2016 Mar 7;17(4):406–13.
211. van Crevel R, Ruslami R, Aarnoutse R. Therapy for Tuberculous Meningitis. N Engl J Med. 2016 Jun 2;374(22):2187.
212. Dieli F, Sireci G, Di Sano C, Champagne E, Fourniè JJ, Salerno JI. Predominance of Vgamma9/Vdelta2 T lymphocytes in the cerebrospinal fluid of children with tuberculous meningitis: reversal after chemotherapy. Mol Med. 1999 May;5(5):301–12.
213. Allen M, Bailey C, Cahatol I, Dodge L, Yim J, Kassissa C, Luong J, Kasko S, Pandya S, Venketaraman V. Mechanisms of Control of *Mycobacterium tuberculosis* by NK Cells: Role of Glutathione. Front Immunol. 2015 Oct 5;6.
214. Gold MC, Cerri S, Smyk-Pearson S, Cansler ME, Vogt TM, Delepine J, Winata E, Swarbrick GM, Chua W-J, Yu YYL, Lantz O, Cook MS, Null MD, Jacoby DB, Harriff MJ, Lewinsohn DA, Hansen TH, Lewinsohn DM. Human mucosal associated invariant T cells detect bacterially infected cells. Plos Biol. 2010;8(6):e1000407.
215. Kee SJ, Kwon YS, Park YW, Cho YN, Lee SJ, Kim TJ, Lee SS, Jang HC, Shin MG, Shin JH, Suh SP, Ryang DW. Dysfunction of Natural Killer T Cells in Patients with Active *Mycobacterium tuberculosis* Infection. Infection and Immunity. 2012 May 11;80(6):2100–8.
216. van Crevel R, Dockrell HM, TANDEM Consortium. TANDEM: understanding diabetes and tuberculosis. The Lancet Diabetes & Endocrinology. 2014 Apr;2(4):270–2.
217. Davoudi S, Rasoolinegad M, Younesian M, Hajiabdolbaghi M, Soudbakhsh A, Jafari S, EmadiKouchak H, Mehrpouya M, Lotfi H. CD4+ cell counts in patients with different clinical manifestations of tuberculosis. Braz J Infect Dis. 2008 Dec;12(6):483–6.
218. Caccamo N, Meraviglia S, La Mendola C, Guggino G, Dieli F, Salerno A. Phenotypical and functional analysis of memory and effector human CD8 T cells specific for mycobacterial antigens. J Immunol. 2006 Aug 1;177(3):1780–5.
219. Hübl W, Andert S, Thum G, Ortner S, Bayer PM. Value of neutrophil CD16 expression for detection of left shift and acute-phase response. Am J Clin Pathol. 1997 Feb;107(2):187–96.
220. Timmermans K, Kox M, Vaneker M, van den Berg M, John A, van Laarhoven A, van der Hoeven H, Scheffer GJ, Pickkers P. Plasma levels of danger-associated molecular patterns are associated with immune suppression in trauma patients. Intensive Care Med. 2016 Feb 24;42(4):551–61.
221. Antas PRZ, Ding L, Hackman J, Reeves-Hammock L, Shintani AK, Schiffer J, Holland SM, Sterling TR. Decreased CD4+ lymphocytes and innate immune responses in adults with previous extrapulmonary tuberculosis. J Allergy Clin Immunol. 2006 Apr;117(4):916–23.
222. Naranbhai V, Chang CC, Durgiah R, Omarjee S, Lim A, Moosa M-YS, Elliot JH, Ndung'u T, Lewin SR, French MA, Carr WH. Compartmentalization of innate immune responses in the central nervous system during cryptococcal meningitis/HIV coinfection. AIDS. 2014 Mar;28(5):657–66.

223. Scriven JE, Graham LM, Schutz C, Scriba TJ, Wilkinson KA, Wilkinson RJ, Boulware DR, Urban BC, Lalloo DG, Meintjes G. A Glucuronoxylomannan-Associated Immune Signature, Characterized by Monocyte Deactivation and an Increased Interleukin 10 Level, Is a Predictor of Death in Cryptococcal Meningitis. J INFECT DIS. 2016 May 4;213(11):1725–34.
224. Graaf MT, Broek PDM, Kraan J, Luitwieler RL, Bent MJ, Boonstra JG, Schmitz PIM, Gratama JW, Sillevis Smitt PAE. Addition of serum-containing medium to cerebrospinal fluid prevents cellular loss over time. J Neurol. 2011 Mar 12;258(8):1507–12.
225. Cohen J, Vincent J-L, Adhikari NKJ, Machado FR, Angus DC, Calandra T, Jaton K, Giulieri S, Delaloye J, Opal S, Tracey K, van der Poll T, Pelfrene E. Sepsis: a roadmap for future research. The Lancet Infectious Diseases. 2015 May;15(5):581–614.
226. Haas CT, Roe JK, Pollara G, Mehta M, Noursadeghi M. Diagnostic "omics" for active tuberculosis. BMC Medicine. BMC Medicine; 2016 Jun 30;:1–19.
227. Li Z, Du B, Li J, Zhang J, Zheng X, Jia H, Xing A, Sun Q, Liu F, Zhang Z. Cerebrospinal fluid metabolomic profiling in tuberculous and viral meningitis: Screening potential markers for differential diagnosis. Clinica Chimica Acta. 2017 Mar 1;466(C):38–45.
228. Mu J, Yang Y, Chen J, Cheng K, Li Q, Wei Y, Zhu D, Shao W, Zheng P, Xie P. Elevated host lipid metabolism revealed by iTRAQ-based quantitative proteomic analysis of cerebrospinal fluid of tuberculous meningitis patients. Biochemical and Biophysical Research Communications 2015 Oct 30;466(4):689–95.
229. Chaidir L, Annisa J, Dian S, Parwati I, Alisjahbana A, Purnama F, van der Zanden A, Ganiem AR, van Crevel R. Microbiological diagnosis of adult tuberculous meningitis in a ten-year cohort in Indonesia. Diagn Microbiol Infect Dis. 2018 Jan 9.
230. Bao XR, Ong S-E, Goldberger O, Peng J, Sharma R, Thompson DA, Vafai SB, Cox AG, Marutani E, Ichinose F, Goessling W, Regev A, Carr SA, Clish CB, Mootha VK. Mitochondrial dysfunction remodels one-carbon metabolism in human cells. Elife (Cambridge). 2016;5.
231. Pirhaji L, Milani P, Leidl M, Curran T, Avila-Pacheco J, Clish CB, White FM, Saghatelian A, Fraenkel E. Revealing disease-associated pathways by network integration of untargeted metabolomics. Nat Methods. 2016 Aug 1.
232. Deisenhammer F, Sellebjerg F, Teunissen C, Tumani H. Cerebrospinal Fluid in Clinical Neurology. 2015.
233. Xia J, Sinelnikov IV, Han B, Wishart DS. MetaboAnalyst 3.0--making metabolomics more meaningful. Nucleic Acids Research. 2015 Jul 1;43(W1):W251–7.
234. Goeman JJ, van de Geer SA, de Kort F, van Houwelingen HC. A global test for groups of genes: testing association with a clinical outcome. Bioinformatics. 2004 Jan 1;20(1):93–9.
235. Kumar GS, K Venugopal A, N Selvan LD, Marimuthu A, Keerthikumar S. Gene Expression Profiling of Tuberculous Meningitis. JPB. 2011;04(05).
236. Collett D. Modelling Survival Data in Medical Research. Vol. 3. 2003. 1 p.
237. Su AI, Wiltshire T, Batalov S, Lapp H, Ching KA, Block D, Zhang J, Soden R, Hayakawa M, Kreiman G, Cooke MP, Walker JR, Hogenesch JB. A gene atlas of the mouse and human protein-encoding transcriptomes. Proc Natl Acad Sci USA. National Academy of Sciences; 2004 Apr 20;101(16):6062–7.
238. Lovelace MD, Varney B, Sundaram G, Lennon MJ, Lim CK, Jacobs K, Guillemin GJ, Brew BJ. Recent evidence for an expanded role of the kynurenine pathway of tryptophan metabolism in neurological diseases. Neuropharmacology. 2017 Jan;112:373–88.
239. Mason S, van Furth AM, Mienie LJ, Engelke UFH, Wevers RA, Solomons R, Reinecke CJ. A hypothetical astrocyte-microglia lactate shuttle derived from a (1)H NMR metabolomics analysis of cerebrospinal fluid from a cohort of South African children with tuberculous meningitis. Metabolomics. 2015;11(4):822–37.
240. Coutinho LG, Christen S, Bellac CL, Fontes FCL, de Souza FRS, Grandgirard D, Leib SL, Agnez-Lima LF. The kynurenine pathway is involved in bacterial meningitis. 2015 Mar 15;11(1):1–8.
241. Sternberg JM, Forrest CM, Dalton RN, Turner C, Rodgers J, Stone TW, Kennedy PG. Kynurenine Pathway Activation in Human African Trypanosomiasis. J INFECT DIS. 2016 Dec 24;:jiw623–7.

242. O'Sullivan A, Willoughby RE, Mishchuk D, Alcarraz B, Cabezas-Sanchez C, Condori RE, David D, Encarnacion R, Fatteh N, Fernandez J, Franka R, Hedderwick S, McCaughey C, Ondrush J, Paez-Martinez A, Rupprecht C, Velasco-Villa A, Slupsky CM. Metabolomics of cerebrospinal fluid from humans treated for rabies. J Proteome Res. 2013 Jan 4;12(1):481–90.
243. Medana IM, Day NPJ, Salahifar-Sabet H, Stocker R, Smythe G, Bwanaisa L, Njobvu A, Kayira K, Turner GDH, Taylor TE, Hunt NH. Metabolites of the kynurenine pathway of tryptophan metabolism in the cerebrospinal fluid of Malawian children with malaria. J INFECT DIS. 2003 Sep 15;188(6):844–9.
244. Zhang YJ, Reddy MC, Ioerger TR, Rothchild AC, Dartois V, Schuster BM, Trauner A, Wallis D, Galaviz S, Huttenhower C, Sacchettini JC, Behar SM, Rubin EJ. Tryptophan Biosynthesis Protects Mycobacteria from CD4 T-Cell-Mediated Killing. Cell. 2013 Dec 5;155(6):1296–308.
245. Mezrich JD, Fechner JH, Zhang X, Johnson BP, Burlingham WJ, Bradfield CA. An interaction between kynurenine and the aryl hydrocarbon receptor can generate regulatory T cells. The Journal of Immunology. 2010 Sep 15;185(6):3190–8.
246. Memari B, Bouttier M, Dimitrov V, Ouellette M, Behr MA, Fritz JH, White JH. Engagement of the Aryl Hydrocarbon Receptor in *Mycobacterium tuberculosis*-Infected Macrophages Has Pleiotropic Effects on Innate Immune Signaling. The Journal of Immunology. 2015 Nov 1;195(9):4479–91.
247. Raison CL, Dantzer R, Kelley KW, Lawson MA, Woolwine BJ, Vogt G, Spivey JR, Saito K, Miller AH. CSF concentrations of brain tryptophan and kynurenines during immune stimulation with IFN-alpha: relationship to CNS immune responses and depression. Mol Psychiatry. 2010 Apr;15(4):393–403.
248. Moreno FA, Parkinson D, Palmer C, Castro WL, Misiaszek J, Khoury El A, Mathé AA, Wright R, Delgado PL. CSF neurochemicals during tryptophan depletion in individuals with remitted depression and healthy controls. Eur Neuropsychopharmacol. 2010 Jan;20(1):18–24.
249. Shah TS, Liu JZ, Floyd JAB, Morris JA, Wirth N, Barrett JC, Anderson CA. optiCall: a robust genotype-calling algorithm for rare, low-frequency and common variants. Bioinformatics. Oxford University Press; 2012 Jun 15;28(12):1598–603.
250. Deelen P, Bonder MJ, van der Velde KJ, Westra H-J, Winder E, Hendriksen D, Franke L, Swertz MA. Genotype harmonizer: automatic strand alignment and format conversion for genotype data integration. BMC Res Notes. BioMed Central; 2014 Dec 11;7(1):901.
251. Das S, Forer L, Schönherr S, Sidore C, Locke AE, Kwong A, Vrieze SI, Chew EY, Levy S, McGue M, Schlessinger D, Stambolian D, Loh P-R, Iacono WG, Swaroop A, Scott LJ, Cucca F, Kronenberg F, Boehnke M, Abecasis GR, Fuchsberger C. Next-generation genotype imputation service and methods. Nat Genet. 2016 Oct;48(10):1284–7.
252. McCarthy S, Das S, Kretzschmar W, and others of the Haplotype Reference Consortium. A reference panel of 64,976 haplotypes for genotype imputation. Nat Genet. 2016 Oct;48(10):1279–83.
253. Howie B, Fuchsberger C, Stephens M, Marchini J, Abecasis GR. Fast and accurate genotype imputation in genome-wide association studies through pre-phasing. Nat Genet. 2012 Aug;44(8):955–9.
254. Xia J, Wishart DS. Web-based inference of biological patterns,functions and pathways from metabolomic datausing MetaboAnalyst. Nat Protoc. 2011 May 5;6(6):743–60.
255. Simmons CP, Thwaites GE, Quyen NTH, Torok E, Hoang DM, Chau TTH, Mai PP, Lan NTN, Dung NH, Quy HT, Bang ND, Hien TT, Farrar J. Pretreatment intracerebral and peripheral blood immune responses in Vietnamese adults with tuberculous meningitis: diagnostic value and relationship to disease severity and outcome. J Immunol. 2006 Feb 1;176(3):2007–14.
256. Assarsson E, Lundberg M, Holmquist G, Björkesten J, Thorsen SB, Ekman D, Eriksson A, Rennel Dickens E, Ohlsson S, Edfeldt G, Andersson A-C, Lindstedt P, Stenvang J, Gullberg M, Fredriksson S. Homogenous 96-plex PEA immunoassay exhibiting high sensitivity, specificity, and excellent scalability. PLoS ONE. 2014;9(4):e95192.
257. Rohlwink UK, Figaji AA. Biomarkers of Brain Injury in Cerebral Infections. Clin Chem. 2014 May 28;60(6):823–34.
258. Ferrara N, Gerber H-P, LeCouter J. The biology of VEGF and its receptors. Nat Med. 2003 Jun;9(6):669–76.

259. Tas SW, Maracle CX, Balogh E, Szekanecz Z. Targeting of proangiogenic signalling pathways in chronic inflammation. Nat Rev Rheumatol. 2016 Feb;12(2):111–22.
260. Datta M, Via LE, Kamoun WS, Liu C, Chen W, Seano G, Weiner DM, Schimel D, England K, Martin JD, Gao X, Xu L, Barry CE III, Jain RK. Anti-vascular endothelial growth factor treatment normalizes tuberculosis granuloma vasculature and improves small molecule delivery. Proc Natl Acad Sci USA. 2015 Feb 10;112(6):1827–32.
261. Kaal ECA, Vecht CJ. The management of brain edema in brain tumors. Curr Opin Oncol. 2004 Nov;16(6):593–600.
262. van der Flier M, Hoppenreijs S, van Rensburg AJ, Ruyken M, Kolk AHJ, Springer P, Hoepelman AIM, Geelen SPM, Kimpen JLL, Schoeman JF. Vascular endothelial growth factor and blood-brain barrier disruption in tuberculous meningitis. Pediatr Infect Dis J. 2004 Jul;23(7):608–13.
263. Matsuyama W, Hashiguchi T, Umehara F, Matsuura E, Kawabata M, Arimura K, Maruyama I, Osame M. Expression of vascular endothelial growth factor in tuberculous meningitis. Journal of the Neurological Sciences 2001 May 1;186(1-2):75–9.
264. Misra UK, Kalita J, Singh AP, Prasad S. Vascular endothelial growth factor in tuberculous meningitis. Int J Neurosci. 2013 Feb;123(2):128–32.
265. Coenjaerts FEJ, van der Flier M, Mwinzi PNM, Brouwer AE, Scharringa J, Chaka WS, Aarts M, Rajanuwong A, van de Vijver DA, Harrison TS, Hoepelman AIM. Intrathecal production and secretion of vascular endothelial growth factor during Cryptococcal Meningitis. J INFECT DIS. 2004 Oct 1;190(7):1310–7.
266. van der Flier M, Stockhammer G, Vonk GJ, Nikkels PG, van Diemen-Steenvoorde RA, van der Vlist GJ, Rupert SW, Schmutzhard E, Gunsilius E, Gastl G, Hoepelman AI, Kimpen JL, Geelen SP. Vascular endothelial growth factor in bacterial meningitis: detection in cerebrospinal fluid and localization in postmortem brain. J INFECT DIS. 2001 Jan 1;183(1):149–53.
267. Boulware DR, Meya DB, Bergemann TL, Wiesner DL, Rhein J, Musubire A, Lee SJ, Kambugu A, Janoff EN, Bohjanen PR. Clinical features and serum biomarkers in HIV immune reconstitution inflammatory syndrome after cryptococcal meningitis: a prospective cohort study. PLoS Med. Public Library of Science; 2010 Dec 21;7(12):e1000384.
268. Schurr E. The contribution of host genetics to tuberculosis pathogenesis. Kekkaku. 2011 Jan;86(1): 17–28.
269. Thye T, Vannberg FO, Wong SH, and others of Wellcome Trust Case Control Consortium, Hill AVS. Genome-wide association analyses identifies a susceptibility locus for tuberculosis on chromosome 18q11.2. Nat Genet. 2010 Sep;42(9):739–41.
270. Herb F, Thye T, Niemann S, Browne ENL, Chinbuah MA, Gyapong J, Osei I, Owusu-Dabo E, Werz O, Rusch-Gerdes S, Horstmann RD, Meyer CG. ALOX5 variants associated with susceptibility to human pulmonary tuberculosis. Human Molecular Genetics. 2007 Dec 7;17(7):1052–60.
271. van Crevel R, Parwati I, Sahiratmadja E, Marzuki S, Ottenhoff THM, Netea MG, van der Ven A, Nelwan RH, van der Meer JW, Alisjahbana B, van de Vosse E. Infection with *Mycobacterium tuberculosis* Beijing genotype strains is associated with polymorphisms in SLC11A1/NRAMP1 in Indonesian patients with tuberculosis. Journal of Infectious Diseases. 2009 Dec 1;200(11):1671–4.
272. Cairns H, Duthie ES. Intrathecal streptomycin in meningitis; clinical trial in tuberculous, coliform, and other infections. The Lancet. 1946 Aug 3;2(6414):153–5.
273. Nakatani Y, Suto Y, Fukuma K, Yamawaki M, Sakata R, Takahashi S, Nakayasu H, Nakashima K. Intrathecal Isoniazid for Refractory Tuberculous Meningitis with Cerebral Infarction. Intern Med. 2017;56(8):953–7.
274. Brake te LHM, de Knegt GJ, de Steenwinkel JE, van Dam TJP, Burger DM, Russel FGM, van Crevel R, Koenderink JB, Aarnoutse RE. The Role of Efflux Pumps in Tuberculosis Treatment and Their Promise as a Target in Drug Development: Unraveling the Black Box. Annu Rev Pharmacol Toxicol. 2018 Jan 6;58:271–91.
275. Rohlwink UK, Mauff K, Wilkinson KA, Enslin N, Wegoye E, Wilkinson RJ, Figaji AA. Biomarkers of cerebral injury and inflammation in pediatric tuberculous meningitis. Clin Infect Dis. 2017 Jun 9;65(8):1298–307.

276. Török ME, Bang ND, Chau TTH, Yen NTB, Thwaites GE, Thi Quy H, Dung NH, Hien TT, Chinh NT, Thi Thanh Hoang H, Wolbers M, Farrar JJ. Dexamethasone and Long-Term Outcome of Tuberculous Meningitis in Vietnamese Adults and Adolescents. PLoS ONE. 2011 Dec 8;6(12):e27821.
277. Bhatt K, Verma S, Ellner JJ, Salgame P. Quest for Correlates of Protection against Tuberculosis. Clinical and Vaccine Immunology. 2015 Feb 25;22(3):258–66.
278. Andrews JR, Noubary F, Walensky RP, Cerda R, Losina E, Horsburgh CR. Risk of Progression to Active Tuberculosis Following Reinfection With *Mycobacterium tuberculosis*. Clin Infect Dis. 2012 Feb 22;54(6):784–91.
279. Allison AC. Protection afforded by sickle-cell trait against subtertian malareal infection. Br Med J. BMJ Publishing Group; 1954 Feb 6;1(4857):290–4.
280. Kidder T. Mountains Beyond Mountains. Profile Books; 2003. 1 p.
281. Chen RY, Dodd LE, Lee M, Paripati P, Hammoud DA, Mountz JM, Jeon D, Zia N, Zahiri H, Coleman MT, Carroll MW, Lee JD, Jeong YJ, Herscovitch P, Lahouar S, Tartakovsky M, Rosenthal A, Somaiyya S, Lee S, Goldfeder LC, Cai Y, Via LE, Park S-K, Cho S-N, Barry CE. PET/CT imaging correlates with treatment outcome in patients with multidrug-resistant tuberculosis. Science Translational Medicine. 2014 Dec 3;6(265):265ra166.
282. Hashimshony T, Wagner F, Sher N, Yanai I. CEL-Seq: Single-Cell RNA-Seq by Multiplexed Linear Amplification. CellReports. The Authors; 2012 Sep 27;2(3):666–73.
283. Barreiro LB, Tailleux L, Pai AA. Deciphering the genetic architecture of variation in the immune response to *Mycobacterium tuberculosis* infection. 2012.
284. Rappuoli R, Aderem A. A 2020 vision for vaccines against HIV, tuberculosis and malaria. Nature. 2011 May 26;473(7348):463–9.

Appendix

Nederlands samenvatting
Contributing authors
Funding and Permissions
List of publications
Dankwoord
Curriculum vitae

Nederlands samenvatting

Tuberculose

Een hoestende tuberculosepatiënt verspreidt *Mycobacterium tuberculosis* door de lucht. Als iemand anders deze bacterie vervolgens inademt, zijn er verschillende uitkomsten mogelijk: een vooralsnog onbekend deel van de blootgestelde individuen ruimt *M. tuberculosis* op, nog voordat het afweersysteem geheugen opbouwt. Een kleine minderheid wordt direct en vaak ernstig ziek, terwijl de meerderheid niets van de besmetting merkt omdat de infectie beperkt blijft tot een klein stukje van de long. Als in de loop van het leven het afweersysteem verzwakt, kan zich alsnog actieve tuberculose ontwikkelen. Dat gebeurt bij ongeveer een op de tien besmette personen. Actieve tuberculose manifesteert zich doorgaans in de long maar het kan ook in de botten, in de lymfeklieren, in de organen van de buik en zelfs in de hersenen voorkomen.

Deel 1: tuberculose gevoeligheid en transmissie

Tuberculose is een oeroude ziekte. Naar schatting 70.000 jaar geleden evolueerde *M. tuberculosis* uit het geslacht van Mycobacteriae, bacteriën die ook nu nog in de bodem gevonden worden. Mensen leefden toen in kleine, geïsoleerde gemeenschappen, geen ideale omstandigheden voor een besmettelijke ziekte. *M. tuberculosis* kon tóch persisteren door de combinatie van een lange incubatie-periode die jaren kan duren, een lange periode waarin iemand besmettelijk is en het feit dat slechts een deel van de besmette individuen op jonge leeftijd overlijdt. De bacterie is vervolgens met de mens mee gemigreerd vanuit Afrika, door het Arabisch Schiereiland naar Europa en Azië, en door kolonisatie verder over de wereld verspreid. Doordat de populatiedichtheid van de mens toenam, kregen ook modernere, epidemische ziektekiemen zoals de pest of Zika een kans. Deze leiden vrijwel direct tot ziekte in een groot deel van de besmette personen, met een hoge sterfte tot gevolg. Toch is de 'strategie' van tuberculose nog steeds succesvol te noemen: naar schatting zijn 1,7 biljoen wereldburgers besmet met *M. tuberculosis* en krijgen jaarlijks 10,4 miljoen patiënten actieve tuberculose, met 1,7 miljoen sterfgevallen tot gevolg.

In **hoofdstuk 2** onderzoeken we een aspect van de menselijke gevoeligheid voor tuberculose. Het slijmvlies van onze luchtwegen en de macrofagen die daar aanwezig zijn vormen de eerste afweer tegen zwevende ziektekiemen. Deze macrofagen en andere witte bloedcellen gebruiken 'receptoren' (eiwitten op hun oppervlakte) om typische bacteriële structuren te herkennen. Deze receptoren vallen in een aantal groepen uiteen en een daarvan is de groep van de 'C-type lectins' (CLECs). Van receptor *CLEC subtype 4D* was bekend dat het

M. tuberculosis kon herkennen. In dit hoofdstuk toonden we aan dat muizen die deze receptor missen, een hevige ontsteking krijgen als ze besmet worden met *M. tuberculosis*. De sterfte aan de infectie is hoger dan bij muizen mét de receptor. We gebruikten vervolgens gepubliceerde studies met openbare data om te onderzoeken wat er bij de mens gebeurt gedurende het ziekteproces. Het blijkt dat het gen dat codeert voor de receptor *CLEC4D* veel sterker tot expressie wordt gebracht bij zieke patiënten met longtuberculose dan bij gezonde individuen. Deze expressie neemt weer af gedurende de behandeling. Vervolgens onderzochten we of genetische variatie in de code van dit gen geassocieerd is met de kans op het krijgen van longtuberculose. In het DNA van meer dan duizend longtuberculosepatiënten uit het Hasan Sadikin ziekenhuis in Bandung in Indonesië hebben we gekeken naar drie plaatsen in het gen *CLEC4D* waarvan bekend is dat er in Azië verschil is tussen individuen. Op een van de drie locaties kwam een bepaalde variant vaker voor bij patiënten dan gezonde invidiuen. Dit vormt een aanwijzing dat *CLEC4D* van belang is bij de ontwikkeling van longtuberculose. Een makke bij veel genetische associatiestudies, waaronder de onze, is dat we van deze 'controles' niet weten in welke mate zij óók zijn blootgesteld aan tuberculose, en of ze besmet zijn geraakt. We weten daarom nog niet of deze genetische variatie slechts een verhoogd risico geeft op besmetting of ook op het daadwerkelijk ziek worden. Daarnaast is vooralsnog onduidelijk of de bevindingen ook van toepassing zijn op patiënten met een andere genetische achtergrond.

Hoofdstuk 3 gaat in op de Beijing 'familie' van *M. tuberculosis* binnen de Oost-Aziatische hoofdgroep van de bacterie. Binnen de Beijing familie komen de modernere stammen steeds vaker voor dan hun oudere familieleden. Mogelijk zijn ze beter overdraagbaar, of hebben ze zich beter aangepast aan de huidige hoge populatiedichtheid door sneller tot ziekte te leiden. We gebruikten een extract van zeven moderne en zeven oude Beijing *M. tuberculosis*-stammen om witte bloedcellen van gezonde vrijwilligers mee te stimuleren. Nadat deze witte bloedcellen de bacterie herkenden, maakten ze in de daaropvolgende dagen zoals verwacht signaalstoffen aan. Enkele van deze zogeheten cytokines die helpen de afweerreactie op gang te brengen en te houden, kwamen na stimulatie met de moderne stammen in lagere concentratie voor dan na stimulatie met hun evolutionair oudere verwanten. Dit wijst op een minder efficiënte herkenning door de witte bloedcellen en dit kan mogelijk bijdragen aan het succes van de moderne Beijing *M. tuberculosis* stammen.

In **hoofdstuk 4** gebruikten we ook de afweerreactie van witte bloedcellen van gezonde vrijwilligers om het succes van *M. tuberculosis* stammen mee te verklaren, maar de selectie van de stammen was gebaseerd op hun bewezen vermogen om nieuwe gevallen van tuberculose te veroorzaken. Het Rijksinstituut voor de Volksgezondheid en Milieu weet van meer dan 10.000 tuberculosepatienten uit de periode 1993-2014 in Nederland door welke stam ze besmet zijn geraakt (inmiddels is het aantal tuberculosegevallen in Nederland gedaald tot <1000/jaar). We zochten eerst stammen die voorkwamen in een cluster mensen die door dezelfde bron besmet geraakt waren. We zochten daarbij specifiek naar clusters van mensen die a-priori een laag risico hadden om tot een cluster te behoren, dat zijn bijvoorbeeld oudere vrouwen die gebruikelijk met name tuberculose krijgen door reactivatie van stammen opgelopen in het verleden. Als stammen in deze groep tóch veel nieuwe gevallen veroorzaken, zijn het blijkbaar wel erg goed overdraagbare stammen, zo redeneerden we. Daarna zochten we naar stammen die voorkwamen bij individuen die juist veel risico hadden om tot een cluster te behoren, zoals jonge dakloze mannen die alcohol en drugs gebruikten. Door de hoge mate van blootstelling, en een verzwakte afweerrespons, worden zij juist relatief vaak snel ziek na een besmetting. Als een stam slechts in één individu met deze kenmerken ziekte had veroorzaakt, was het blijkbaar een weinig besmettelijke stam. Van 100 patiënten uit deze twee groepen vergeleken we vervolgens het complete genoom. We konden daarmee vijf *M. tuberculosis* genen identificeren die geassocieerd waren met het veroorzaken van nieuwe gevallen. De variatie in drie van die genen leidde ook daadwerkelijk tot een andere afweerrespons in de witte bloedcellen van gezonde vrijwilligers. Dit vormt een extra bevestiging van het belang van de afweerrespons in het verklaren van het succes van sommige tuberculosestammen ten opzichte van andere stammen.

Deel 2: de uitkomst van tuberculeuze meningitis

Het tweede deel van dit proefschrift behandelt hersenvliesontsteking (meningitis) als specifieke verschijningsvorm van tuberculose. Deze ziekte kenmerkt zich door een langzaam progressief beloop, waarin patiënten aanvankelijk aspecifieke symptomen hebben zoals hoofdpijn. Tuberculeuze meningitis wordt dan meestal nog niet als zodanig herkend. In de dagen of meestal weken die volgen, kan het bewustzijn afnemen en kunnen uitvalsverschijnselen optreden. Zo kunnen herseninfarcten of beklemming van hersenzenuwen in een dikke laag pus verlamming van ledematen of uitval van gelaatsfuncties veroorzaken. Jonge kinderen en met HIV geïnfecteerde patiënten hebben de grootste kans op uitgezaaide tuberculose. Meningitis is hiervan de ernstigste verschijningsvorm en leidt bij 30-50% van de aangedane patiënten tot

invaliditeit of de dood. We denken dat deze percentages verkleind kunnen worden door snellere herkenning van de ziekte, betere ondersteunende therapie zoals bloeddrukregulatie en zuurstoftoediening en toediening van hogere doses van antibiotica zodat die beter in het hersenvocht doordringen. Momenteel krijgen alle patiënten met tuberculeuze meningitis behalve antibiotica ook afweerremmende medicijnen (corticosteroïden) en dit verlaagt de sterfte enigszins, maar alleen bij de minst zieke patiënten. Het is onbekend hoe de ontstekingsmechanismen in tuberculeuze meningitis precies werken en daarop gaat dit tweede deel in.

In **hoofdstuk 5** geven we een overzicht van voorspellers van sterfte door tuberculeuze meningitis. We gebruikten hiervoor de data die in het Hasan Sadikin ziekenhuis in Bandung, Indonesië vanaf 2006 systematisch verzameld zijn samen met het Radboud Universitair Medisch Centrum. Het Hasan Sadikin is een tertiair verwijzingscentrum met een afferentiegebied voor 43 miljoen mensen uit West-Java. We konden bevestigen dat HIV-infectie een sterke voorspeller is van sterfte door meningitis en beperkten vervolgens de analyse tot de 499 HIV-negatieve patiënten. Hieruit kwamen verschillende onafhankelijke klinische voorspellers van een hogere mortaliteit één jaar na diagnose: ernstige ziekte-ernst, hogere leeftijd, verlamming van een of meer ledematen, en ook een hogere temperatuur bij binnenkomst. Dit laatste wijst al op een rol voor ontstekingscellen, die ook de lichaamstemperatuur beïnvloeden. Voor de diagnostiek van tuberculeuze meningitis wordt het hersenvocht, de liquor cerebrospinalis, middels een lumbaalpunctie afgetapt. Metingen aan de liquor lieten zien dat de verhouding tussen neutrofiele en lymfoïde witte bloedcellen een belangrijke voorspeller is van sterfte. Neutrofiele witte bloedcellen kunnen potentieel *M. tuberculosis* doden, maar kunnen door de vorming van vrije zuurstofradicalen ook veel schade veroorzaken. Ook in bloed waren hogere neutrofielen geassocieerd met hogere sterfte. We deden in dit cohort verder een replicatiestudie van genetische variatie die in Vietnamees onderzoek voorspellend bleek te zijn voor sterfte. Deze associatie konden we niet bevestigen voor de Indonesische patiënten met tuberculeuze meningitis.

Hoofdstuk 6 gaat dieper in op de ontsteking in zowel liquor cerebrospinalis als het bloed. We categoriseerden de subtypen van witte bloedcellen preciezer door antistoffen te gebruiken die zich binden verschillende eiwitten op het oppervlakte van de witte bloedcellen. In het bloed van patiënten met tuberculeuze meningitis waren meer neutrofielen en monocyten maar minder lymfocyten dan bij longtuberculosepatiënten en gezonde controles. In de liquor cerebrospinalis van patiënten met tuberculeuze meningitis vonden we deze

lymfocyten weer terug en deze bleken niet alleen te bestaan uit de eerder beschreven αβT-cellen van het adaptieve deel van het immuunsysteem, maar ook uit meerdere type witte bloedcellen van het aangeboren immuunsysteem: γδT-cellen, NKT-cellen, NK-cellen en MAIT-cellen. Deze cellen waren bijna zonder uitzondering veel sterker geactiveerd in liquor dan in bloed. Het bloed van de patiënten hebben we daarnaast in het laboratorium gestimuleerd met verschillende bacteriën om te zien welke cytokines deze aanmaakten, analoog aan de methode van hoofdstuk 3 en 4. De witte bloedcellen van patiënten met tuberculeuze meningitis lieten een groot bereik zien in hun reactievermogen. Dit liep van lager dan de gezonde controles, tot aan hoger dan de longtuberculosepatiënten. De patiënten met de meeste cytokinerespons, hadden daarbij ook de hoogste lichaamstemperatuur. Bij het optimaliseren van de afweerbeïnvloedende therapie bij tuberculose meningitis, lijkt het dan ook waarschijnlijk dat rekening gehouden moet worden met de individuele immuunrespons.

In **hoofdstuk 7** bestudeerden we het metabolisme (de stofwisseling) in bloed en liquor cerebrospinalis van patiënten met tuberculeuze meningitis. We gebruikten hierbij vloeistofchromatografie gecombineerd met massaspectrometrie waardoor het mogelijk was om in zeer kleine volumes toch meer dan 400 metabolieten te onderscheiden. We vonden grote verschillen in liquor tussen de 32 patiënten en 22 controles, maar niet in bloed. Binnen de patiëntengroep verschilden enkele metabolieten in liquor ook tussen hen die het overleefden en hen die al in het ziekenhuis overleden. De laatste groep had vaak een meer uitgesproken respons: de metabolieten die hoger waren bij patiënten dan controles, waren bij hen extra hoog en vice versa. Tryptofaan liet als enige metaboliet een uitgesproken afwijkende respons zien: het was lager in patiënten dan controles, en bijzonder laag in hen die het overleefden. Tryptofaan is een essentieel aminozuur voor de mens, dat wil zeggen dat we het alleen door voeding tot ons kunnen nemen. We kunnen van tryptofaan wel andere metabolieten maken. De waardes hiervan waren juist hoger in patiënten, wat wijst op actieve omzetting van tryptofaan. In een grotere groep van 101 patiënten konden we de relatie van tryptofaan met overleving bevestigen. Vervolgens zochten we naar genetische variatie die samenhing met de tryptofaanrespons en we vonden 11 plaatsen in het DNA die hiervoor goed voorspellend waren. Gecombineerd voorspelde deze genetische informatie zoals verwacht ook de overleving van deze patiënten. Interessant is dat het ook de overleving voorspelde in een derde groep van 285 tuberculeuze meningitis patiënten. Het is dus goed mogelijk dat individuen verschillen in hun aanleg om tryptofaan te metaboliseren als ze tuberculeuze meningitis krijgen. Vervolgonderzoek kan uitwijzen hoe een gunstige omzetting van tryptofaan gestimuleerd zou kunnen worden.

In **hoofdstuk 8** onderzoeken we de cytokinerespons in tuberculeuze meningitis. We gebruikten hiervoor een techniek die in een kleine hoeveelheid liquor cerebrospinalis bijna honderd signaalstoffen (cytokines) kan meten. Zoals verwacht, waren de concentraties van bijna alle cytokines hoger in patiënten dan in controles. Veel cytokines vertoonden een hoge mate van correlatie, dat wil zeggen dat als ze in één patiënt omhoog gingen, ze dat ook in een tweede patiënt deden. We verdeelden de cytokines in 30 clusters op basis van hun onderlinge correlatie en testten van elk cluster één cytokine op relatie met overleving. Vijf clusters waren sterk voorspellend voor overleving tot na 180 dagen. Een hiervan is 'vascular endothelial growth factor' (VEGF), een eiwit dat vaatgroei stimuleert. Dit kan gebeuren in respons op zuurstofgebrek. Het verbreekt daarbij mogelijk ook de verbindingen van de bloed-hersenbarrière en de bloed-liquorbarrière. Analoog aan hoofdstuk 7 zochten we naar genetische variatie die de VEGF respons voorspelde. Zes plaatsen in het DNA van de patiënten bleken hiermee geassocieerd. Samen voorspelden deze de overleving van patiënten in zowel het oorspronkelijke cohort als in 299 patiënten uit een tweede groep patiënten.

Slot: onderzoeksaanpak van complexe ziekten

Tuberculose is een oeroude, fascinerende en verwoestende ziekte. De complexiteit van het ziektebeeld noopt tot het combineren van verschillende methoden om haar te onderzoeken. Gezien het grote aantal variabelen dat tegelijkertijd gemeten wordt bij moderne meetmethoden, zijn er volgens de maatstaven van klassieke statistiek heel grote patiëntenaantallen nodig om robuuste verschillen te vinden. De beperkte middelen en infrastructuur in de landen waar de meerderheid van de patiënten zich bevindt, staan deze grote aantallen echter niet toe. Dit proefschrift laat zien dat door integratie van verschillende methoden in patiëntencohorten van slechts honderden patiënten toch betekenisvolle resultaten gevonden kunnen worden. Dit zal hopelijk bijdragen aan het identificeren van effectieve aanvullende behandeling en het verbeteren van de overlevingskansen van toekomstige tuberculosepatiënten.

Contributing authors

I am very grateful for the pleasant collaboration with his co-authors, which are listed here under their main affiliation at the time of the research.

Radboud University Medical Center (Nijmegen, the Netherlands)
Aldert Zomer
Carolien Ruesen
Edwin Ardiansyah
Ekta Lachmandas
Johanneke Kleinnijenhuis
Leo Joosten
Marcel Verbeek
Michelle Damen
Mihai Netea
Reinout van Crevel
Richard Notebaart
Rob ter Horst
Sacha van Hijum
Suzanne van Dorp
Theo Plantinga
Valerie Koeken

Universitas Padjadjaran & Hasan Sadikin Hospital (Bandung, Indonesia)
Agnes Indrati
Ahmad Rizal Ganiem
Bachti Alisjahbana
Ela Hayati
Emira Diandini
Feby Purnama
Fitria Utami
Jessi Annisa
Lidya Chaidir
Lika Apriani
Resvi Livia
Robbie Herawan
Rovina Ruslami
Sofiati Dian
Tri Hanggono Achmad

University Medical Centre Groningen (Groningen, The Netherlands)
Isis Ricaño-Ponce
Li Yang
Raúl Aguirre-Gamboa
Vinod Kumar

Leiden University Medical Center (Leiden, the Netherlands)
Tom Ottenhoff
Esther van de Vosse

National Institute for Public Health and the Environment (Bilthoven, The Netherlands)
Hanna Nebenzahl-Guimaraes
Mimount Enaimi
Dick van Soolingen

University of Utrecht
Jornt Mandemakers

University of Otago (Dunedin, New Zealand)
Ayesha Verrall
James Ussher
Philip Hill

The Broad Institute of MIT and Harvard (Boston, USA)
Clary Clish
Julian Avila-Pacheco

Harvard Medical School (Boston, USA)
Maha R. Farhat
Megan Murray

University of Aberdeen (Aberdeen, United Kingdom)
Bernhard Kerscher
Delyth M Reid
Gillian Wilson
Gordon Brown
Janet Willment
Rebecca Drummond

University of Birmingham (Birmingham, United Kingdom)
Gurdyal S. Besra

University of Cape Town (Cape Town, South-Africa)
Dhirendra Govender
Jennifer Hoving
Mohlopheni Marakalala
Muazzam Jacobs
Roanne Keeton

Kyushu University (Fukuoka, Japan)
Sho Yamasaki

Funding

I am grateful to the following funders who financially supported the research in this thesis:

- Radboud University fellowships [to the author, to Sofiati Dian, to Ahmad Rizal Ganiem, to Lidya Chaidir and to Bachti Alisjahbana].
- The Netherlands Organisation for Scientific Research with a Veni grant [to Theo S. Plantinga], a Vidi grant [017.106.310 to Reinout van Crevel], a Vici grant [918.10.610 to Mihai G. Netea] and a Spinoza Prize [to Mihai G. Netea].
- The European Commission [Consolidator Grant #310372 to Mihai G. Netea; EC FP7 projects NEWTBVAC, 41745 and ADITEC, 280873 to Tom H.M. Ottenhoff],
- The Netherlands' Royal Academy of Arts and Sciences [09-PD-14 to Reinout van Crevel; to Tom H.M. Ottenhoff]
- The Netherlands Leprosy Relief Foundation [702.02.72 to Tom H.M. Ottenhoff]
- Direktorat Jendral Pendidikan Tinggi, Indonesia [BPPLN fellowship to Sofiati Dian]
- Ministry of Research, Technology, and Higher Education, Indonesia [PKSLN grant to Rovina Ruslami, Sofiati Dian and Tri Hanggono Achmad]
- The Medical Research Counsil United Kingdom & Wellcome Trust (Gordon D. Brown),
- United States Agency for International Development [PEER Health grant to Rovina Ruslami and Ahmad Rizal Ganiem].
- Medical Research Counsil South-Africa and Sydney Brenner Fellowship (MJM),
- Carrnegie Corporation and CIDRI (Jennifer C. Hoving), and the University of Aberdeen (Bernhard Kerscher).
- The Portuguese Foundation for Science and Technology (FCT) [SFRH/BD/33902/2009 to Hanna Nebenzahl-Guimaraes]
- Publication of this thesis was financially supported by KNCV Tuberculosis Foundation.

The funders had no role in study design, data collection, data analysis, data interpretation, or writing of any of the studies.

Permissions

Chapters 2 (doi: 10.1016/j.chom.2015.01.004) and chapter 7 (doi: 10.1016/S1473-3099(18)30053-7) were reproduced with permission of Elsevier Ltd.

Chapter 3 (doi: 10.1128/IAI.00282-13) was reproduced with permission of the American Society for Microbiology

Chapter 4 (doi 10.1164/rccm.201605-1042OC) was reproduced with permission of the American Thoracic Society.

Chapter 5 (doi: 10.1093/infdis/jix051) was reproduced with permission of the Infectious Diseases Society of America.

The drawing of the microscopy observations by Ludvig Hektoen (1863-1951) at page 113 was reproduced with permission of the Rockefeller University Press.

List of publications

Research articles

Ruesen C, Chaidir L, **van Laarhoven A**, Dian S, Ganiem AR, Nebenzahl-Guimaraes H, Huynen MA, Alisjahbana B, Dutilh BE, van Crevel R. Large-scale genomic analysis shows association between homoplastic genetic variation in Mycobacterium tuberculosis genes and meningeal or pulmonary tuberculosis. *BMC Genomics*. 2018;19(1):122.

van Laarhoven A, Dian S, Aguirre-Gamboa R, Avila-Pacheco J, Ricaño-Ponce I, Ruesen C, Annisa J, Koeken VACM, Chaidir L, Li Y, Achmad TH, Joosten LAB, Notebaart RA, Ruslami R, Netea MG, Verbeek MM, Alisjahbana B, Kumar V, Clish CB, Ganiem AR, van Crevel R. Cerebral tryptophan metabolism and outcome of tuberculous meningitis: an observational cohort study. *The Lancet Infectious Diseases*. 2018;18:526–35.

Nebenzahl-Guimaraes H*, **van Laarhoven A***, Farhat MR*, Koeken VACM, Mandemakers JJ, Zomer A, van Hijum SAFT, Netea MG, Murray M, van Crevel R, van Soolingen D. Transmissible Mycobacterium tuberculosis Strains Share Genetic Markers and Immune Phenotypes. *Am J Respir Crit Care Med*. 2017; 195(11):1519–27.

van Laarhoven A*, Dian S*, Ruesen C, Hayati E, Damen MSMA, Annisa J, Chaidir L, Ruslami R, Achmad TH, Netea MG, Alisjahbana B, Rizal Ganiem A, van Crevel R. Clinical Parameters, Routine Inflammatory Markers, and LTA4H Genotype as Predictors of Mortality Among 608 Patients With Tuberculous Meningitis in Indonesia. *Journal of Infectious Diseases*. 2017;215(7):1029–39.

Arts RJW, Novakovic B, Horst ter R, Carvalho A, Bekkering S, Lachmandas E, Rodrigues F, Silvestre R, Cheng S-C, Wang S-Y, Habibi E, Gonçalves LG, Mesquita I, Cunha C, **van Laarhoven A**, van de Veerdonk FL, Williams DL, van der Meer JWM, Logie C, O'Neill LA, Dinarello CA, Riksen NP, van Crevel R, Clish C, Notebaart RA, Joosten LAB, Stunnenberg HG, Xavier RJ, Netea MG. Glutaminolysis and Fumarate Accumulation Integrate Immunometabolic and Epigenetic Programs in Trained Immunity. *Cell Metabolism*. 2016;24(6):807-19.

Lachmandas E, Beigier-Bompadre M, Cheng S-C, Kumar V, **van Laarhoven A**, Wang X, Ammerdorffer A, Boutens L, De Jong D, Kanneganti T-D, Gresnigt MS, Ottenhoff THM, Joosten LAB, Stienstra R, Wijmenga C, Kauffman SHE, van Crevel R, Netea MG. Rewiring cellular metabolism via the AKT/mTOR pathway contributes to host defence against Mycobacterium tuberculosis in human and murine cells. *Eur J Immunol*. 2016;46(11):2574–86.

Timmermans K, Kox M, Vaneker M, van den Berg M, John A, **van Laarhoven A**, van der Hoeven H, Scheffer GJ, Pickkers P. Plasma levels of danger-associated molecular patterns are associated with immune suppression in trauma patients. *Intensive Care Med*. 2016;42(4):551–61.

Wilson GJ*, Marakalala MJ*, Hoving JC*, **van Laarhoven A***, Drummond RA, Kerscher B, Keeton R, van de Vosse E, Ottenhoff THM, Plantinga TS, Alisjahbana B, Govender D, Besra GS, Netea MG, Reid DM, Willment JA, Jacobs M, Yamasaki S, van Crevel R, Brown GD. The C-Type Lectin Receptor CLECSF8/CLEC4D Is a Key Component of Anti-Mycobacterial Immunity. *Cell Host and Microbe*. 2015; 17(2):252–9.

Pingen M, Nijhuis M, Mudrikova T, **van Laarhoven A**, Langebeek N, Richter C, Boucher CAB, Wensing AMJ. Infection with the frequently transmitted HIV-1 M41L variant has no influence on selection of tenofovir resistance. *Journal of Antimicrobial Chemotherapy*. 2015;70(2):573–80.

van Laarhoven A, Mandemakers JJ, Kleinnijenhuis J, Enaimi M, Lachmandas E, Joosten LAB, Ottenhoff THM, Netea MG, van Soolingen D, van Crevel R. Low Induction of Proinflammatory Cytokines Parallels Evolutionary Success of Modern Strains within the Mycobacterium tuberculosis Beijing Genotype. *Infection and Immunity*. 2013;81(10):3750–6.

Mullarkey CE, Boyd A, **van Laarhoven** A, Lefevre EA, Carr BV, Baratelli M, Molesti E, Temperton NJ, Butter C, Charleston B, Lambe T, Gilbert SC. Improved adjuvanting of seasonal influenza vaccines: Pre-clinical studies of MVA-NP+M1 co-administration with inactivated influenza vaccine. *Eur J Immunol*. 2013; 43(7):1940–52.

Lambe T, Carey JB, Li Y, Spencer AJ, **van Laarhoven A**, Mullarkey CE, Vrdoljak A, Moore AC, Gilbert SC. Immunity against heterosubtypic influenza virus induced by adenovirus and MVA expressing nucleoprotein and matrix protein-1. *Sci Rep*. 2013;3:1443.

Reviews

van Laarhoven A, Kaan JA, Schippers HM, Mager HJ, van Soolingen D, van der Meulen MFG. Twee patiënten met tuberculeuze meningitis; denk ook aan *M. bovis* als verwekker. *Nederlands Tijdschrift voor Medische Microbiologie*. 2010; 18(2):18–21.

van Laarhoven A. Vingertopafwijkingen bij verschillende systeemziekten. *Nederlands tijdschrift voor geneeskunde Studenteneditie*. 2008;11(3):49–51.

Correspondence

van Laarhoven A*, Valerie ACM Koeken*, Dian S, Ganiem AR, van Crevel R. Neuromarker levels also predict mortality in adult tuberculous meningitis. *Clinical Infectious Diseases*. 2018 Mar 30

van Laarhoven A, Dian S, Ganiem AR, van Crevel R. Reply to Neeradi et al and Dhawan and Sankhyan. *Journal of Infectious Diseases*. 2017;216(3):395–6.

van Laarhoven A, Kaan JA, Schippers HM, Mager JJ, van der Meulen MFG. [Three patients with tuberculous meningitis: treatment started at tentative diagnosis]. *Nederlands tijdschrift voor geneeskunde*. 2008;152(25):1445–6.

* shared first authorship

Dankwoord

Dank aan iedereen die me tegemoet kwam op weg naar de voltooiing van dit proefschrift. Door jullie werd het een inspirerende tocht. Dank ook aan het Nederlandse onderwijssysteem dat de voorwaarden schiep en specifiek aan de St. Fredericusschool in Velp, het Stedelijk Gymnasium Arnhem en de Universiteit van Utrecht.

Veel dank aan mijn promotores die zo prachtig combineren: Reinout van Crevel, die leidt in een tomeloze hoeveelheid energie, met een goed oog voor de karakters die hij om zich heen verzameld heeft. Door niet alleen veel te vragen van zijn promovendi, maar hun ook veel te geven, is er een enorme stroom ontwikkeling op gang gekomen. Dat heeft in Nijmegen, maar ook in Bandung veel moois tot stand gebracht. Mihai Netea's inspiratie door de biologie neemt jonge onderzoekers mee en zijn bescheidenheid is voor mij een voorbeeld. Jullie heetten me hartelijk welkom en vervolgens was er veel ruimte binnen het lab en nog meer ruimte om naar buiten te treden. Aan ideeën en ook uitvoerbare plannen nooit een gebrek. Ik had geen idee dat dit proefschrift het resultaat zou zijn. Jullie waarschijnlijk ook niet. Dank voor het vertrouwen vanaf de start en nu nog steeds.

Dank aan Robert Sauerwein, Irma Joosten en Jaap van Dissel die als manuscriptcommissie dit proefschrift kritisch hebben bezien.

Anderen gingen mijn promoteren als mentor vooraf: Kees van Gastel was altijd stimulerend als het ging om wetenschap en geneeskunde. Anne Wensing nam me enthousiast onder haar hoede in het Utrechtse HIV-onderzoek. Joep Lange gaf me de mogelijkheid om voor PharmAccess naar Tanzania te gaan. Teresa Lambe was an excellent mentor in the animal and immunological labs of the Jenner Institute and showed how good science, a good laugh and holding the door open for others go hand in hand.

Wetenschap is soms een eenzaam bedrijf, maar brengt ook een hoop plezier door samenwerking. Het lab van de Experimentele Interne Geneeskunde is daarvoor een fijne uitvalsbasis. Leo Joosten neemt je mee in het plezier van het bedrijven en organiseren van wetenschap, met als gevolg een fijne samenwerking op het lab. Jos van der Meer, dank voor het delen van inzichten en ervaring op verschillende momenten. Tegen de tijdsgeest in zou ik graag pleiten voor meer analisten in vaste dienst, want het collectief geheugen van Anneke Hijmans, Cor Jacobs, Heidi Lemmers, Helga Toenhake, Ineke Verschueren, Kiki Schraa,

Liesbeth Jacobs en Trees Jansen is van onschatbare waarde, net als de getalenteerde post-docs uit wiens kennis ik mocht putten: Bas Heijnhuis, James Cheng, Janna van Diepen, Jessica Quintin, Marije Oosting, Mark Gresnigt, Richard Notebaart, Rinke Stienstra, Sanne Smeekens en Theo Plantinga. Veel dank aan het steeds veranderende, uitdijende en blijvend leuke team van medepromovendi, voor de gezelligheid en het heel fijne samenwerken: Ajeng Tunjungputri, Andreea Mirea, Anne Ammerdorfer, Anne Jansen, Anouk Jansen, Bas Blok, Berenice Rösler, Charlotte de Bree, Charlotte de Bruijn, Charlotte van der Heijden, Diana RosentulAmram, Daniela Ifrim, Duby Ballak, Floor Aleva, Hanne Rooijackers, Hedwig Vrijmouth, Hinta Meierink, Inge van den Munckhof, Jaap ten Oever, Jacqueline Ratter, Jessica Dos Santos, Johanneke Kleinnijenhuis, Jorge Dominguez Andres, Katharina Gößling, Kathrin Buffen, Kathrin Thiem, Khutso Mothapo, Laszlo Groh, Lilly Boutens, Lisa van de Wijer, Maartje Cleophas, Mariska Kerstholt, Mark Stappers, Marlies Noz, Martin Jäger, Meta Michels, Michelle Damen, Monique Stoffels, Rob Arts, Rob ter Horst, Ruud Raijmakers, Simone Moorlag, Siroon Bekkering, Tania Crisan, Teske Schoffelen, Thalijn Wolters, Vesla Kullaya, Wouter van der Heijden en Yvette Sloot.

Valerie Koeken was als student en later als collega een schot in de roos, met een combinatie van inzet en relativeringsvermogen, enthousiasme en nuchterheid. It has also been a big pleasure and an honour to work with the other fellow tuberculosis PhD students Anca Riza, Carolien Ruesen, Ekta Lachmandas, Lidya Chaidir, Lindsey te Brake and Sofiati Dian. Van de ijver, humor en inzet van de Nijmeegse club internist-infectiologen heb ik al een fijn voorproefje gehad. Ook bij hen loopt niets soepel zonder de secretariële ondersteuning van Mieke Daalderop en Jeanine van der Wijst, die niet alleen voor de internationale studenten maar ook voor ons een baken van licht en gezelligheid zijn.

More than a quarter of my PhD time was spent in Bandung, were all the work in the TB-HIV working group starts with the laugh and twinkling eyes of Dr Bachti Alisjahbana. He takes pride in extending good care to everyone in his study team, whom he enables to excel in the studies performed. *Terima kasih untuk semua teman2 kantor, untuk keramahan, kesabaran dan kebaikan Anda. Senang sekali bekerja bersama Anda semua.* Thanks to my roommates Alit Koesoemadinata, Misheilla Maryam, Resvi Livia, Sue McAllister and Sofia Imaculata for all the good company, and lunches at Sederhana and Sederhana baru. Shared experiences made it so nice to chat with the other PhD students Annissa Rahmalia, Merrin Rutherford, Meta Michels, Silvita Riswari and Vycke Yunivita. A great place to be and work was Dr Agnes Indrati's lab immuno, where Emira Diandini, Fitria Utami, Suharyani, Dwi Febni Ratnaningsih, Inas Kathina,

Nana Rasnawati and Yusandi Sastra Atmaja, worked with great optimism and dedication. It was a great joy to do the Immunology Classes with you. I'm very glad to have met Intan Mauli there, who pursues her own passion, while remaining understanding to others. I'm happy to have you as my paranimf on the side, and our whole family is glad that you brought Edwin and Fadlan to the Netherlands.

The tuberculous meningitis clinical team took care of excellent clinical phenotyping, led by Dr Ahmad Rizal Ganiem with whom one can discuss TBM, photography and history. Dr Sofiati Dian was in the daily lead, stood up for her team and was in for a good laugh. She is a hard worker who has given so much of herself in the research in Bandung, and abroad. It was a big pleasure to work with Ela Hayati, Feby Purnama, Tiara Pramaesya, Sofia Imaculata, Sri Margi, Rani Trisnawati and Shehika Shulda. Thanks also to Witri Indrasari and Dr Leni Lismayanti of the clinical chemistry lab team for arranging a flow for quick blood and cerebrospinal fluid processing out-of-office hours that would have been impossible in many other settings. All of the clinical work would have been of lesser quality without the mycobacterial lab in Bandung. Lidya Chaidir has put tremendous effort not only in techniques and machines but also in her colleagues who provide high-quality diagnostics. Jessi Annisa worked tirelessly in overseeing the big sample flows and other managerial tasks. Arlisa Alisjahbana is always keen to learn new techniques, just as the rest of the team that does a tremendous job. Prof Rovina Ruslami has been not only a welcoming host, but also as counterpart and sparring partner from the first time in Bandung. Prof Philip Hill, thank you for showing your ways of performing excellent research in Bandung and enabling others to shine (and for a joke or two). Ayesha Verrall thanks for the discussions we had from the first moment onwards and the optimistic long-term collaboration, and to you and Alice for your hospitality. Lika Apriani and INFECT-team, your efforts reaching out to the household are tremendous, and thanks to part of the team and others for the nice evenings of indoor soccer. Rudi Wisaksana and Yovita Hartantri welcomed me on the instructive Friday morning clinical rounds. Like everywhere, nothing in the TB-HIV working group starts without the help of the secretarial team of Ria Windyani and her team, which took care of guests, packages, forms, reminders and a smile. We would not have been able to give the best of ourselves without the support of Ibu Zaimah and Pak Dudu at our home in Cipaku. Thanks to our biking friends for their help in keeping body and mind healthy too.

I'm very grateful for the welcome I received at other places where the research took me: thanks to Arnout Mulder, Jessica de Beer, Miramda Kamst, Petra de Haas and Tridia van der Laan for the selection and culturing of many strains at the RIVM; thanks to Jakko van Ingen, Melanie Wattenberg and Nicole Aalders for not only discussing mycobacteria, but also showing how to handle them; to Tom Otterhof and Esther van der Vosse in Leiden for showing the first steps in genetics; for the friendly welcome by Adrian Hill and Vivek Naranbhai, who patiently guided me through basic computational genetics in Oxford. Many thanks for the enthusiastic discussions with Vinod Kumar in Groningen and the reception by Mathieu Plateel and the collaboration with Yang Li, Isis Ricaño-Ponce and Raúl Aguirre-Gamboa. A big thank you for the hospitality of Julian Avila-Pacheco, and the science-pursuing open mindedness of Clary Clish who has a great team of co-workers Amy Deik, Kerry Pierce, Kevin Bullock, and Justin Scott at the Broad Institute in Boston.

I have enjoyed meeting inspiring co-workers and colleagues some of whom are co-writers of the manuscripts in this thesis or who were keen to discussing tuberculosis in all its aspects: Ayesha Verrall, Darma Imram, Dick van Soolingen, Gillian Wilson, Gordon Brown, Guy Thwaites, Hanna Guimaraes, James Ussher, Jelle Goeman, Jeroen de Keijzer, Megan Murray, Philip Hill and Suzaan Marais. Lucas Kaaij's ultimate enthusiasm for science has been inspirational. Dank aan prof. dr. Daan den Hengst en dr. Joost van Neer, voor het verhelderen van de oorsprong van de citaten van respectievelijk Gilbert Cousin en Augustinus. Ook veel dank aan mijn voormalige collega's uit het Rijnstate voor de gezelligheid op de fiets en in de trein, en de onwijs fijne sfeer tijdens het werk.

Lieve vrienden, jullie zijn een bijzonder stel. Dank voor alle gezelligheid en warmte, en voor het brengen van relativering door jullie onbegrip voor medische streberigheid. Bas, Coen en paranimf Jornt hebben hierin een hoofdrol gehad. Lieve vrienden die toevallig ook nog dokter zijn, voor jullie geldt hetzelfde, min dat stuk over de streberigheid dan. Afstand speelt nauwelijks een rol, en we zien jullie overal, zelfs in Nijmegen. Het is een genoegen ook daar fijne mensen te ontdekken. Dank ook aan de lieve mensen die ik eerder tegen ben gekomen en een positieve rol in mijn ontwikkeling hebben gehad, in het bijzonder Willemijn en familie. Siebren en familie, heel fijn om je ook na drieëndertig jaar er weer bij te hebben.

Dank aan mijn lieve schoonfamilie Yvonne & Harry, Chris & Doreen, Alice & Lynn, voor de gezelligheid, discussies, en onophoudelijke stroom leestips en grappen.

Ik ben blij met mijn warme en diverse familie in bredere zin en ben in het bijzonder dankbaar voor de voorbeelden die mijn vier grootouders zijn geweest, met elk hun eigen eigenschappen: interesse in de mens, liefde voor onderwijs en het helpen van anderen, verzet en sociale betrokkenheid, bedachtzaamheid en reflectie, leeslust, reislust en levenslust.

Mijn lieve ouders hebben Marlou, Kasper en mij alle ruimte en veiligheid geboden om wat te brouwen van de mix van eigenschappen die we van ze hebben gekregen. Deze thuishaven blijft een fijne plek, en fijner nog door coole kant Jibbe. Zonder jullie was dit proefschrift er zeker niet geweest, was ik niet geweest wie ik ben en had ik me zeker nooit door zo'n prachtige vrouw kunnen laten schaken. Lieve Suzanne, de zeven heerlijk vette jaren die we achter ons liggen doen me enorm verheugen op de rest.

Curriculum Vitae

Arjan van Laarhoven was born in Nijmegen on the 23rd of November in 1984, and grew up in Velp with his parents and two siblings. He graduated *cum laude* from the Stedelijk Gymnasium Arnhem. At Utrecht University, he studied Medicine, and a bit of Physics and Philosophy. Arjan went to Nagercoil, India and Dar es Salaam, Tanzania for clinical internships. He participated in the Honours programme for Medical Humanities and Research. In the Jenner Institute in Oxford he gained his first immunological lab experience working on a universal influenza vaccine supervised by Dr Teresa Lambe. He obtained his medical degree in 2010, and then started his clinical career in Internal Medicine in the St Antonius hospital supervised by Dr Tom Geers, and worked as a registrar in Rijnstate Hospital supervised by Dr Vera Mattijssen, Dr Louis Reichert and Dr Arianne van Bon, alternating between clinical work and research. Based in the lab of Experimental Internal Medicine in Nijmegen under supervision of Prof Reinout van Crevel and Prof Mihai Netea, his PhD-project brought him to work at the National Institute for Public Health and the Environment in Bilthoven, Leiden University, Groningen University, Oxford University and the Broad Institute in Boston. Especially rewardingly, he spent almost a year in the TB-HIV working group led by Dr Bachti Alisjahbana of Universitas Padjadjaran in Bandung, Indonesia. Here he helped setting up immunological assays to strengthen the ongoing cohort of tuberculous meningitis patients. Arjan is married to his beloved Suzanne and together they have two children.

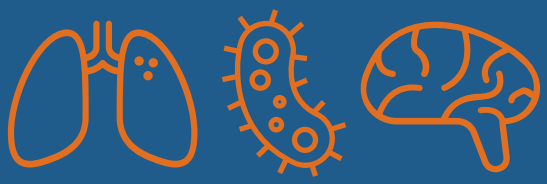

Tuberculosis has plagued humankind since prehistoric times. Coughing tuberculosis patients disperse the bacterium *Mycobacterium tuberculosis* through the air. Inhalation of this bacterium does not always lead to an infection, and only one in ten infected individuals becomes ill. In most cases, tuberculosis is contained to the lungs, but the infection can also spread to lymph nodes, bones and even the brain. Over the last century, higher standards of living and the development of antibiotics have significantly reduced the disease burden but still, each year, 1.7 million people die because of tuberculosis globally.

This thesis examines the role of the human immune system in tuberculosis. The first part assesses tuberculosis susceptibility and transmission by studying the interaction between white blood cells and various tuberculosis strains. The second part focuses on the high mortality rates associated with tuberculous meningitis by studying cells, proteins and metabolites in blood and cerebrospinal fluid of infected patients. The research in this thesis aims to advance a customized and more effective treatment for this ancient, but still highly relevant disease.